Selective oxidation reactions catalysed by gold

Peter Miedziak

ProQuest LLC
789 East Eisenhower Parkway
P.O. Box 1346
Ann Arbor, MI 48106-1346

DECLARATION

This work has not previously been accepted in substance for any degree and is not concurrently submitted in candidature for any degree.

Signed ..... (Candidate) Date .....

STATEMENT 1

This thesis is being submitted in partial fulfillment of the requirements for the degree of PhD

Signed ..... (Candidate) Date .....

STATEMENT 2

This thesis is the result of my own independent work/investigation, except where otherwise stated. Other sources are acknowledged by explicit references.

Signed ..... (Candidate) Date .....

STATEMENT 3

I hereby give consent for my thesis, if accepted, to be available for photocopying and for inter-library loan, and for the title and summary to be made available to outside organizations.

Signed ..... (Candidate) Date .....

STATEMENT 4: PREVIOUSLY APPROVED BAR ON ACCESS

I hereby give consent for my thesis, if accepted, to be available for photocopying and for inter-library loans **after expiry of a bar on access previously approved by the Graduate Development Committee.**

Signed ..... (Candidate) Date .....

Abstract

The oxidation of benzyl alcohol over supported gold, palladium and gold palladium catalysts was studied in a high-pressure stirred autoclave. Reaction conditions such as oxygen pressure and reaction temperature were varied to obtain optimum conditions for catalyst screening. Gold palladium catalysts supported on various oxides were prepared and screened with titania supported catalysts proving to be the most active. Different preparation methodologies were used to prepare titania supported bi-metallic catalysts, co-deposition precipitation methodology was found to give the most active and stable catalyst.

Further gold, palladium and gold palladium catalysts were prepared supported on ceria that had been obtained from the calcination of cerium acetylacetate that had been precipitated into a supercritical carbon dioxide antisolvent. These catalysts proved to be significantly more active than those supported on the ceria form the simple calcination of the precursor. Reuse experiments showed that the supercritically prepared ceria precursor catalyst increased in activity with use, despite significant leaching of the metals, an effect not observed for the non-supercritically prepared ceria precursor catalyst. The ceria catalysts prepared by the supercritical antisolvent method displayed very high turn over frequencies for the oxidation of 1-octen-3-ol, 2-octen-1-ol and cinnamyl alcohol.

Gold and gold palladium catalysts supported on titania and graphite were used for the oxidation of 2,5-dimethyl furan to form hex-3-ene-2,5-dione. The effect of temperature, pressure and radical initiator were investigated and the highest selectivity was achieved at the lowest oxygen pressure. The oxidation of α-pinene to verbenone investigated, the reaction proceeded with highest conversion at high oxygen pressure with catalyst not required for the reaction to proceed.

Gold palladium catalysts were used for the oxidation of isophorone and valencene using the optimized conditions established for the α-pinene reaction system. 2,6-lutidene, 2-picoline and 3-picoline were found to be poisons for gold palladium catalysts.

Acknowledgements

I would like to thank my supervisors, Graham Hutchings, Stuart Taylor, Albert Carley and Dave Knight for their input, help and support during the course of my studies.

Dan Enache and Jennifer Edwards, my post docs, for training me and filtering out the more ridiculous ideas from the marginally insane.

I would also like to thank my industrial supervisor Brian Tarbit from Vertellus Chemicals for his support, knowledge of organic chemistry and suggestions of new reaction systems.

Furthermore I would like to thank the department technical staff for all their assistance with special mention to Alun Davies for his ability to repair exploded reactors and Rob Jenkins for his help with the analysis equipment.

I would like to thank all my friends in labs 1.88, 1.86 and 0.90 who made the three years of study an enjoyable experience with a special mention for Cat who knew how to use Microsoft Word.

Finally I would like to thank my parents for the help they have given me over the course of my education.

Table of Contents

Abstract

The oxidation of benzyl alcohol over supported gold, palladium and gold palladium catalysts was studied in a high-pressure stirred autoclave. Reaction conditions such as oxygen pressure and reaction temperature were varied to obtain optimum conditions for catalyst screening. Gold palladium catalysts supported on various oxides were prepared and screened with titania supported catalysts proving to be the most active. Different preparation methodologies were used to prepare titania supported bi-metallic catalysts, co-deposition precipitation methodology was found to give the most active and stable catalyst.

Further gold, palladium and gold palladium catalysts were prepared supported on ceria that had been obtained from the calcination of cerium acetylacetate that had been precipitated into a supercritical carbon dioxide antisolvent. These catalysts proved to be significantly more active than those supported on the ceria form the simple calcination of the precursor. Reuse experiments showed that the supercritically prepared ceria precursor catalyst increased in activity with use, despite significant leaching of the metals, an effect not observed for the non-supercritically prepared ceria precursor catalyst. The ceria catalysts prepared by the supercritical antisolvent method displayed very high turn over frequencies for the oxidation of 1-octen-3-ol, 2-octen-1-ol and cinnamyl alcohol.

Gold and gold palladium catalysts supported on titania and graphite were used for the oxidation of 2,5-dimethyl furan to form hex-3-ene-2,5-dione. The effect of temperature, pressure and radical initiator were investigated and the highest selectivity was achieved at the lowest oxygen pressure. The oxidation of α-pinene to verbenone investigated, the reaction proceeded with highest conversion at high oxygen pressure with catalyst not required for the reaction to proceed.

Gold palladium catalysts were used for the oxidation of isophorone and valencene using the optimized conditions established for the α-pinene reaction system. 2,6-lutidene, 2-picoline and 3-picoline were found to be poisons for gold palladium catalysts.

Chapter One

1. Introduction

1.1 Catalysis

Berzelius first used the term catalysis in 1836[1] to explain the effect of porous platinum on the combustion of hydrogen and oxygen at ambient temperatures. He noted that certain compounds could speed up the reaction whilst remaining unchanged themselves. In 1825 Faraday explained the activity of the platinum was due to a process of adsorption. Further work led to further definitions with Ostwald in 1902 defining catalysts as "agents which accelerate chemical reactions without affecting the chemical equilibrium"

Catalysis operates by lowering the amount of energy required to form one or more transition states between the reactant and the product (figure 1.1), this lowers the activation energy of the reaction. However the thermodynamics and the products of the reaction remain the same.

Catalysis can be defined by there different groups, homogeneous, heterogeneous and enzymatic. Homogeneous catalysts are catalysts that function in the same phase as the reactants, heterogeneous catalysts function in a different phase from the reactants, typically a solid catalyst operating with liquid or gas phase reactants. The reaction with a heterogeneous catalyst takes place on the phase boundary. Heterogeneous catalysts are often metals supported on a secondary material, such as metal oxides, with the secondary material enhancing the activity of the catalyst. Enzymes are biomolecules and are present in the metabolic pathway of most living creatures.

Catalysis is currently used in about nine tenths of chemical manufacturing processes, with the current desire for green technology and processes the demand for new catalysts and catalytic processes has lead to significant research into the field.

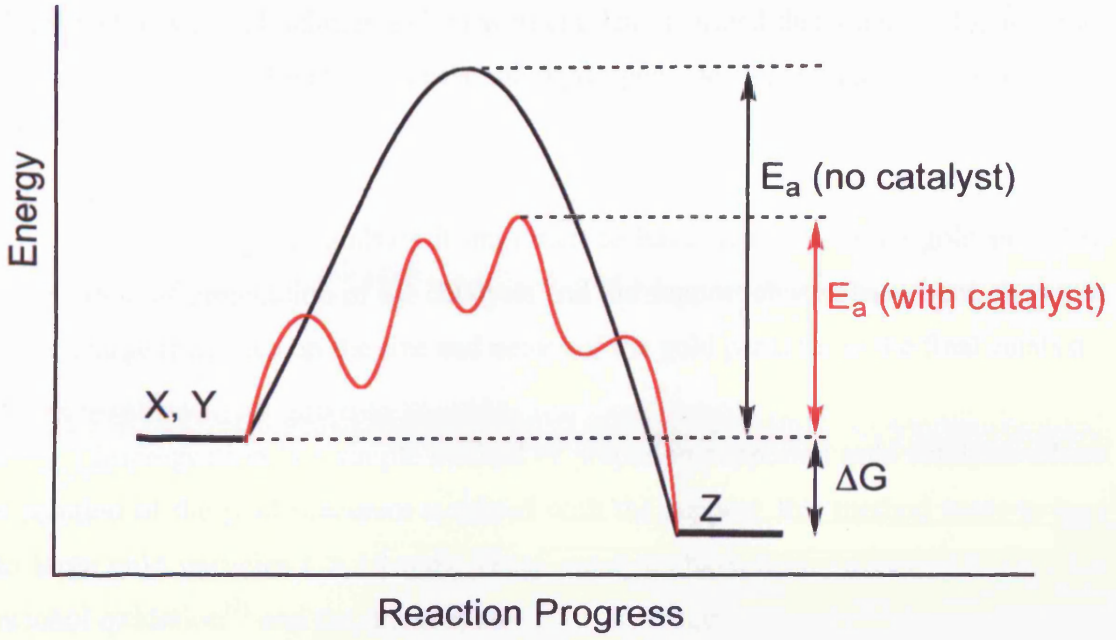

Figure 1.1: A potential energy diagram showing an exothermic reaction of X and Y to give Z. The peaks on the diagram represent transition states, by forming one or more lower energy transition state the catalyst (red line) is able to lower the activation energy of the reaction making the reaction more facile[2].

1.2 Gold catalysis

Until relatively recently gold had been considered catalytically inactive, Bond *et al*[3] were the first to use supported gold, prepared by impregnation of $HAuCl_4$, which was dried and reduced in hydrogen and gave a catalyst that was suitable for the hydrogenation of olefins. Later, Haruta[4] demonstrated that gold was the most effective catalyst for the low temperature oxidation of CO and Hutchings[5] demonstrated it was the most effective catalyst for the hydrochlorination of ethyne to vinyl chloride. Initial catalysts prepared by Haruta *et al*[4] for the oxidation of CO were supported on iron oxide, and it was found the preparation method significantly affected the size of the gold particles which was vital to the activity of the catalyst. Subsequent work by Haruta and co-workers[6] demonstrated that gold supported on titania could be used for the selective oxidation of propene to propene oxide. A further significant development of the use of gold catalysts was the demonstration of the selective oxidation of alcohols with molecular oxygen as first demonstrated by

Pratti and Rossi[7]. Hutchings and co-workers demonstrated that supported gold could be used for the direct synthesis of hydrogen peroxide under non-explosive conditions[8].

For active gold catalysts it important to have nanoparticulate gold particles, the method of preparation of the catalysts and the support chosen have been shown to have a large influence on the size and nature of the gold particles in the final catalyst.

Impregnation is a simple method of preparing supported gold catalysts where a solution of the gold precursor is stirred with the support, this method tends to lead to large gold particles (> 10 nm). These catalysts have been successfully used for alcohol oxidation[9] and the direct synthesis of hydrogen peroxide[10], but are inactive for the oxidation of CO. This lead to the development by Haruta[11] of the deposition precipitation method of catalyst preparation, where by the support is stirred in a solution of the metal precursor and the pH value of the solution is varied by the addition of base at elevated temperatures. This method leads to small gold particles but the nature of the catalyst produced is dependant on several factors[3]:

- The concentration of the metal precursor solution
- The ratio of the precursor solutions volume and concentration to the mass of support.
- The base used.
- The temperature of the solution.
- The final pH of the solution.
- The time allowed for the deposition to occur.
- The method of filtration.
- The method of drying.
- The calcination conditions.

A further method, co-precipitation has been used to prepare supported gold catalysts with small particle size[12]. A solution of the metal precursor and the metal oxide precursor, typically the metal nitrate, are heated and adjusted to the appropriate pH where precipitation occurs. The solution is then filtered, washed, dried and

calcined, the influence of parameters on this preparation method is similar to those described for deposition precipitation[3].

1.3 The Development of gold catalysts for selective oxidations:

1.3.1 Direct synthesis of H_2O_2

Hydrogen peroxide is a simple molecule with many uses, both in the home, in bleaches and hair dyes and industrially, in large scale processes such as the bleaching of paper[13]. Hydrogen peroxide is also considered a green oxidant as the only by-product from the oxidations is water. It can be used in place of bulky stoichometeric oxygen donors such as sodium perorbate, sodium chromate or sodium percarbonate which have serious toxicity issues associated with them[14, 15].

Hydrogen peroxide is currently produced by the anthraquinone cycle; the global production of hydrogen peroxide is about 1.9×10^6 tonnes per annum[16]. The process is only economical when it is carried out on the large scale and when hydrogen peroxide is produced at high concentrations, often higher than the desired concentration at the point of use. The development of a direct oxidation process for the synthesis of hydrogen peroxide from hydrogen and oxygen under non explosive conditions would be desirable. Significant research has been carried out into this reaction, recently excellent results have been achieved using gold monometallic and gold palladium bimetallic catalysts.

The first group to show that supported gold catalysts could be effective for this reaction was Hutchings and co workers[17] who carried out the direct synthesis of hydrogen peroxide using gold catalysts supported on alumina. Previous studies on this reaction had been carried out using supported palladium catalysts and it was also discovered that the alloying of gold and palladium gave a significant increase in the productivity of the reaction[17] (table 1.1). The additional productivity of the bi-metallic catalyst was attributed to greater selectivity. Selectivity is the major problem in this reaction as the conditions that promote the formation of hydrogen peroxide also promote its decomposition and hydrogenation. Further studies into the same

catalytic system[18] by Hutchings and co-workers used x-ray photoelectron spectroscopy to show that the supported nanocrystals are core shell by nature with a palladium rich shell surrounding an gold rich centre.

Table 1.1: The direct formation of H_2O_2 using gold, palladium and gold+palladium supported on Al_2O_3 as reported by Hutchings *et al*[17] at 2°C with CH_3OH/H_2O solvent.

Catalyst	H_2 conversion (%)	H_2O_2 (wt%)	H_2O_2 Selectivity	H_2O_2 production rate mol h^{-1} kg $(cat)^{-1}$ x 10^{-3}
Au/Al_2O_3	6	0.031	53	1530
Pd/Al_2O_3	80	0.0008	1	370
$Pd\text{-}Au(1:1)/Al_2O_3$	63	0.090	14	4460

Fe_2O_3 which has also been shown to be an effective support for the low temperature oxidation of CO[19] was subsequently tested for hydrogen peroxide synthesis by Hutchings and co-workers[20] the Fe_2O_3 catalysts were also shown to exhibit a core shell nature but did not show a significant improvement in activity over the alumina supported catalysts.

Subsequent work by Ishihara *et al*[21] studied gold supported on a range of oxide and zoelite supports including silica, alumina, gallia, H-ZMS-5 and H-Y zeolite, in this case silica was found to be the best support and they also found that the addition of palladium to the catalysts presented an improvement in the rate of formation (Table 1.2).

Hutchings *et al*[10] later investigated titania as a support for this reaction, the rates of formation achieved using this support were superior to those achieved when using alumina as a support. Again the bimetallic catalysts proved more effective than the monometallic with a Au:Pd ratio of 4:1 and 1:1 ratio catalysts prepared, the productivity of the 1:1 metal ratio catalyst was shown to be twice that of the 4:1 ratio catalyst (Table 1.3). The preparation method for gold supported on titania catalyst

was also studied, supported gold catalysts prepared by the deposition precipitation method have been shown to be considerably more active for the oxidation of CO[22]. However these catalysts were considerably less active for the formation of hydrogen peroxide than those prepared by the impregnation method. The effect of calcination was also studied, the most active catalysts was dried at 100 °C followed by the catalyst calcined at 200 °C and the lowest activity was shown by the catalyst calcined at 400 °C (Table 1.4). The dried catalyst and the catalyst calcined at 200 °C however were not stable when reused, with significant leaching of the active metals observed. The catalyst calcined at 400 °C was shown to be stable for 3 uses of the catalyst.

Table 1.2: the formation of H_2O_2 using various catalysts as reported by Ishihara *et al*[21] at 283 K, metal loading 1%.

Catalyst	H_2 conversion (%)	H_2O_2 formation rate (μmol/min)	H_2O_2 Selectivity (%)
Ag/SiO_2	1.9	0	0
Pt/SiO_2	3.9	0	0
Pd/SiO_2	2.0	0	0
Au/SiO_2	2.3	0.069	2.07
H-ZSM-5 Zeolite (Si/Al = 20)	1.4	0.031	1.04
H-Y Zeolite (Si/Al = 50)	2.3	0.029	0.91
Cu_2O	2.3	0.062	1.91
SiO_2-Al_2O_3	2.5	0	0
ZrO_2	2.3	0.031	1.04
Bi_2O_3	2.2	0	0
Al_2O_3	2.1	0	0
Ga_2O_3	1.4	0	0
ZnO	2.1	0	0
MgO	1.96	0	0

Table 1.3: Comparison of hydrogen peroxide productivity and CO conversion for catalysts prepared by deposition–precipitation (DP) and impregnation (I) as reported by Hutchings *et al*[10].

Catalyst	Catalyst mass (mg)	Preparation method	Pre-treatment	H_2O_2 production rate mol h^{-1} kg $(cat)^{-1}$	H_2O_2 (wt%)	CO Conversion (%)
5%Au/TiO_2	50	DP	Air, 25 °C	0.229	0.002	85
5%Au/TiO_2	50	DP	Air, 120 °C	0.482	0.005	76
5%Au/TiO_2	50	DP	Air, 400 °C	0.388	0.004	40
5%Au/TiO_2	50	I	Air, 400 °C	7.1	0.014	< 1
4%Au/1%Pd/TiO_2	10	I	Air, 400 °C	28	0.057	< 1
2.5%Au/2.5%Pd/TiO$_2$	10	I	Air, 400 °C	64	0.128	< 1
5%Pd/TiO_2	10	I	Air, 400 °C	31	0.061	< 1

Table 1.4: the effect of calcination on the productivity of hydrogen peroxide as reported by Hutchings *et al*[10], reaction time 30 mins with 10 mg catalyst; nd = not determined

Catalyst	Pre-treatment	H_2O_2 Productivity mol h^{-1} kg_{cat}^{-1}	H_2O_2 (wt%)	H_2 conversion (%)	H_2O_2 Selectivity (%)
2.5%Pd/TiO_2	Air, 25 °C	90	0.180	38	48
5%Pd/TiO_2	Air, 25 °C	173	0.346	86	40
2.5%Au-2.5%Pd/TiO_2	Air, 25 °C	202	0.404	46	89
5%Pd/TiO_2	Air, 200 °C, 3h	99	0.198	42	47
2.5%Au-2.5%Pd/TiO_2	Air, 200 °C, 3h	124	0.248	34	73
2.5%Pd/TiO_2	Air, 400 °C, 3h	24	0.048	19	25
5%Pd/TiO_2	Air, 400 °C, 3h	31	0.062	29	21
2.5%Au-2.5%Pd/TiO_2	Air, 400 °C, 3h	64	0.128	21	61
2.5%Au-2.5%Pd/TiO_2	Air, 400 °C, 3h + H2 500 °C	32	0.064	nd	nd

Work by Li et al[23] used zeolite supported catalysts for the oxidation, with HZMS-5, zeolite Y, zeolite beta and TS1 tested as supports. Again impregnation was shown to be a superior preparation method when compared to deposition precipitation for this reaction. A range of metals supported on the zeolites were also tested with Pd being the most active followed by Au and Pt and with Cu, Ag, Rh and Ru catalysts showing low activity. Further work by the same authors[24] on zeolite Y and ZMS-5 again found that the addition of palladium to the gold catalysts had a synergic effect on the rate of hydrogen peroxide formation. Other bimetallic catalysts were prepared with no synergic effect observed with the addition of Ru or Rh to the gold catalyst. There was a synergic effect with the addition of Pt to the gold catalyst but it was not a significant as that observed with the addition of Pd.

A further investigation by Edwards *et al*[25] found that using G60 carbon as a support yields an even more active catalyst than previously observed. The authors also ranked the previously used supports in terms of their activity as follows; Carbon > Titania > Silica > Alumina > Iron Oxide. A subsequent study on the same reaction system[26] has shown that the carbon supported catalyst are not core shell in nature and instead exhibits homogeneous alloy natured bimetallic particles.

1.3.2 Epoxidation reactions

Gold supported on titania or titania silicates have been shown to be very active for the epoxidation of propene to propene oxide. These reactions however only take place when a sacrificial reductant, typically hydrogen is present [27, 28]. Hutchings and co-workers[29] investigated the oxidation of cyclohexene using 1%Au/C catalysts with a solvent and molecular oxygen as the oxidant. It was found that in the presence of polar solvents no C_6 products were observed, even under mild conditions (60-80 °C, 4-24h). The experiment was subsequently repeated in the absence of solvent and 2-cyclohexene-1-one and 2-cyclohexen-1-ol were observed as products, when apolar solvents were tested C_6 selectivity was observed (table 1.5). Deuterated solvents were also used to test whether the solvent was acting as a sacrificial source of hydrogen but there was no incorporation of deuterium into the products.

Table 1.5: The effect of solvent on the selectivity of the products of the oxidation of cyclohexene by 1%Au/C as reported by Hutchings et al[29]. Reaction conditions: 1% Au/C (0.22g), 0.012 mol C_6H_{10}, 80 °C, 24h, 20 ml solvent, 5 mol% *tert*-butyl hydroperoxide based on C_6H_{10} added when apolar solvents used.

Solvent	Conversion (%)	Epoxycyclohexane Selectivity (%)	2-cyclohexene-1-one Selectivity (%)	2-cyclohexene-1-ol Selectivity (%)	1,2-cyclohexanedione Selectivity (%)
Water	100	0	0	0	0
Methanol	27.1	0	0	0	0
THF	5.8	0	0	0	0
Hexane	26.1	tr	tr	Tr	0
Toluene	29.1	tr	35.1	25.1	0
1,4-Dimethylnenzene	53.5	0	12	0	43.5
1,3,5-Trimethylbenzene	8	tr	78.1	Tr	0
1,2,3,5-Tetramethylbenzne	29.7	50.2	26.3	0	0
1,2,4,5-Tetramethylbenzne -1,4-Dimethylbenzene	23.1	26	42	9.1	0
Quinoline	33.2	0	10.5	0	0
1,4-Diflourobenzene	29.1	0	47.1	26.8	0
Hexaflourobenzene	15.8	8.9	36.1	2.5	0

Further to this work the authors investigated the oxidation of cis-cyclooctene under solvent free conditions[30] and it was found that with the addition of a small amount of peroxide initiator high selectivities to the epoxide could be achieved (table 1.6)

Subsequently Caps *et al*[31] have shown that supported gold catalysts can be used to convert trans-stilbene into trans-stilbene oxide in the presence of molecular oxygen with selectivity of 88% achieved when using gold supported on titania and

methylcyclohexane as a solvent. The titania supported catalyst was found to be better than an Au/C catalyst for this reaction.

Table 1.6: The oxidation of cis-cyclooctene with molecular oxygen in the absence of solvent as reported by Hutchings et al[30]. Reaction conditions: 0.12g catalyst, 10 cm^3 *cis*-cyclooctene, 80 °C, 24 h, 3 bar O_2, TBHP = *tert*-butylhydroperoxide.

Catalyst	TBHP (g)	Conversion (%)	Cyclooctane Epoxide Selectivity (%)	2-cycloocten-1-ol Selectivity (%)	2-cycloocten-1-one Selectivity (%)	1,2-cyclooctane dione Selectivity (%)
1% Au/Graphite	0.12	7.9	81.2	9.3	4.1	0.5
1% Au/Graphite	0.02	7.1	79.2	6.8	3.0	0.5
1% Au/Graphite	0.002	1.3	86.2	7.4	2.1	0.6
No Catalyst	0.008	2.0	Trace	0	0	0
Graphite	0.008	2.3	Trace	0	0	0

1.3 Alcohol oxidations

The oxidation of primary alcohols to aldehydes is an important laboratory and commercial procedure[32]. Aldehydes are valuable both as intermediates and as high value components for the perfume industry. Often oxidations of this type are carried out using stoichiometric oxygen donors such as chromate or permanganate, but these reagents are expensive and have serious toxicity and environmental issues associated with them. Given these limitations, there is substantial interest in the development of heterogeneous catalysts that use molecular O_2 as the oxidant. Gold nanocrystals have been shown to be highly effective for the oxidation of alcohols with O_2 in an aqueous base, in particular diols and triols; although under these conditions, the product is the corresponding mono-acid, not the aldehyde[7]. However, gold in the absence of base has recently been shown to be highly effective for the oxidation of alcohols[33].

1.4.1 Benzyl alcohol oxidation

Benzaldehyde is an important intermediate in the perfumery and pharmaceutical industries. It can be produced from the hydrolysis of benzyl chloride,

however this will contain traces of chlorine. The oxidation of benzyl alcohol to benzaldehyde has been investigated in the gas phase but it is difficult to prevent over-oxidation to carbon oxide products[34]. The liquid phase oxidation of benzyl alcohol presents a solution to this problem and work by Choudhary and co-workers[35] investigated a range of non-noble transition metal containing hydrotalcite-like solid catalysts under solvent free conditions. The metals investigated were Co-Al, Ni-Al, Cu-Al, Zn-Cu, Mg-Fe, Co-Fe, Ni-Fe, Mn-Cr, Co-Cr, Ni-Cr, Zn-Cr and Cu-Cr, all of the catalysts tested showed some conversion of benzyl alcohol however the reactions were carried out at a relatively high temperature (210 °C). The Cu or Mn containing catalysts were found to be the most active but the selectivity towards benzaldehyde was low.

Huctchings *et al*[36] showed that supported gold catalysts could be used for this reaction, using a range of supports and different preparation methods for the catalysts. The highest conversion for supported gold catalysts prepared by the co-precipitation technique was observed for an iron oxide supported catalyst. Supported gold prepared by impregnation to give the titania supported catalyst showed the highest selectivity to benzaldehyde.

Further work by Choudhary and co-workers[37] then prepared a wide range of supported gold catalysts and tested them for benzyl alcohol oxidation (table 1.7). When considered in terms of the TOF (turn over frequency) the most effective supports were found to be ZrO_2, MnO_2, Sm_2O_3 and Al_2O_3.

Enache *et al*[36] investigated the synergic effect of adding palladium to the gold catalysts. In the case of the impregnation prepared titania supported catalysts the initial activity of the bimetallic catalysts was higher than the that of the gold monometallic catalyst but lower than the palladium monometallic catalyst. However over the duration of the reaction the bimetallic catalyst displayed the highest conversion of benzyl alcohol (74.5% for the bimetallic catalyst compared to 60.1% for supported Pd catalyst) and significantly higher selectivity towards benzaldehyde (91.6% for the bimetallic catalyst compared to 51.3% for supported Pd catalyst). Several different supports were used for the bimetallic catalysts prepared by co-

impregnation of the metals and alumina and titania were found to be superior to silica, iron oxide and carbon.

Table 1.7: The oxidation of benzyl alcohol to benzaldehyde by a range of metal oxide suppoted gold catalysts as reported by Choudhary *et al*[37].

Catalyst	Conversion (%)	Benzaldehyde Selectivity (%)	Benzylbenzoate Selectivity (%)	Benzaldehyde Yeild	TOF/mol $g(Au)^{-1}h^{-1}$
7.5%Au/MgO	51.0	86.0	14.0	43.9	0.34
4.7%Au/CaO	33.3	91.3	8.6	30.4	0.38
5.3%Au/BaO	43.5	81.5	18.5	35.5	0.39
6.4%Au/Al_2O_3	68.9	65.0	35.0	44.8	.041
3%Au/ZrO_2	50.7	87.0	13.0	44.1	0.85
6.5%Au/La_2O_3	51.6	68.8	31.3	35.5	0.32
4.2%Au/Sm_2O_3	44.4	75.0	25.0	33.3	0.46
6.6%Au/Eu_2O_3	37.5	87.5	12.5	32.4	0.29
8%Au/U_3O_8	53.0	95.0	5.0	50.4	0.37
4.1%AuMnO_2	39.7	88.8	11.1	34.5	0.49
6.1%Au/Fe_2O_3	16.2	100	-	16.2	0.15
7.1%Au/CoO	28.3	95.2	4.8	26.7	0.22
6.2%Au/NiO	32.0	78.0	22.0	25.0	0.23
6.8%Au/CuO	27.0	69.0	31.0	18.6	0.16
6.6%Au/ZnO	40.5	92.8	7.2	37.6	0.33

A subsequent more detailed investigation by Choudhary *et al*[38] focused on the U_3O_8 support and investigated the different methods of gold deposition, the gold loading and gold particle size. The deposition precipitation method proved to be more active than analogous catalysts prepared by the co-precipitation method and the impregnation method provided the least active catalyst. For a 8wt%Au/U_3O_8 calcined at different temperatures the conversion of benzyl alcohol initially increased with

increasing calcination temperature, peaking at 400 °C before subsequently dropping (figure 1.1). The authors also demonstrated that the reaction was most effective in the absence of solvent but the reaction would proceed in toluene and DMF and that the conversion of benzyl alcohol increased almost linearly with metal loading.

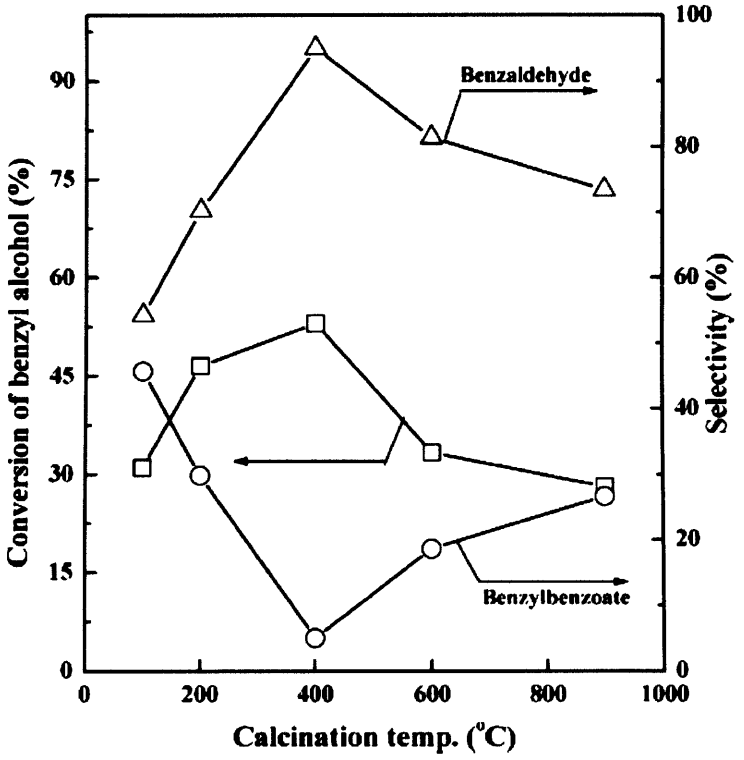

Figure 1.1. The effect of calcinations temperature on the conversion of benzyl alcohol by 8%Au/U_3O_8 as reported by Choudhary *et al*[38].

Smaller gold particles can be useful for this reaction as was demonstrated by Richards *et al*[39] who used gold nano-particles confined in the walls of mesoporous silica to oxidise benzyl alcohol, again an almost linear improvement was observed with an increase in the gold loading up to 2.5wt%Au. A 10 wt%Au catalyst was also tested however this did not display a proportional improvement when compared to the 2.5wt% catalyst. It was further demonstrated that the reactions could be carried out using toluene as a solvent and under these conditions the catalyst was shown to be stable for 3 uses.

Dimitratos *et al*[40] used a sol immobilization technique to create gold nano-particles with a small particle size and a narrow particle size distribution. These

catalysts could be made at low metal loadings (1%) and displayed turn over frequencies that were superior to those reported for catalysts prepared by impregnation of the gold. In this work the authors investigated the effect of different gases during the calcinations step of the catalyst preparation. The catalysts treated under air showed significantly higher initial activity than catalysts treated under nitrogen or hydrogen.

Enache *et al*[41] carried out a detailed study into the Au:Pd ratio for catalysts supported on titania. The authors showed that the addition of palladium to gold does not follow a linear trend in terms of the initial activity of the catalysts (table 1.8). The highest activity was displayed by the Pd monometallic catalyst, but the 2.5wt%Au+2.5wt%Pd catalyst displayed the highest activity of the bimetallic catalysts. In contrast to this the highest benzaldehyde selectivity at iso-conversion was observed for the gold monometallic catalyst. The selectivies towards benzaldehyde by the bimetallic catalysts was reasonably similar to the monometallic gold catalyst with the palladium monometallic catalyst displaying the lowest selectivity towards benzaldehyde of all the catalysts tested.

Table 1.8: The effect of Au:Pd ratio on the oxidation of benzyl alcohol by titania supported catalysts as reported by Enache *et al*[41].

Catalyst	TOF (h^{-1}) (at 0.5h reaction time) Au-Pd catalysts	TOF (h^{-1}) (at 0.5h reaction time) Au-Pd physical mixtures
5%Au/TiO_2	33700	33700
4%Au-1%Pd/TiO_2	47600	42300
3%Au-2%Pd/TiO_2	48700	50800
2.5%Au-2.5%Pd/TiO_2	65400	55100
2%Au-3%Pd/TiO_2	65100	59400
1%Au-4%Pd/TiO_2	64000	67900
5%Pd/TiO_2	76500	76500

Su and co-workers[42] carried out oxidations of benzyl alcohol using gold supported on the polymorphs of gallia and found these catalysts to be more active and

to show higher selectivity towards benzaldehyde than analogous catalysts prepared on titania, ceria or iron oxide (table 1.9)

Table 1.9: The solvent free oxidation of benzyl alcohol by various gold catalysts as reported by Fu *et al*[42]. Reaction conditions: 20 cm^3 benzyl alcohol, 0.2g catalyst, 130 °C, 5 bar O_2, 5h.

Catalyst	S_{BET} (m^2g^{-1})	Conversion (%)	Benzaldehyde Selectivity (%)	Benzylbenzoate Selectivity (%)	Benzoic Acid Selectivity (%)
2.3%Au/α-Ga_2O_3	40	7.6	99.4	0.6	-
2.4%Au/β-Ga_2O_3	71	23.2	97.8	2.2	-
2.5%Au/ γ-Ga_2O_3	133	40.0	97.7	2.3	-
2.5%Au/CeO_2	76	16.5	95.1	1.5	3.4
1.4%Au/TiO_2	48	6.0	93.2	2.3	4.5
4.4%Au/Fe_2O_3	35	2.1	89.9	4.1	6.0

A recent study by Hutchings and co-workers[43] prepared gold palladium bi-metallic catalysts by the sol immobilisation method. These catalysts were found to be more active than catalysts prepared by impregnation. The authors also prepared bimetallic catalysts in a 1:1 molar ratio and compared them to the 1:1 weight ratio catalysts. The 1:1 weight ration proved to be the more active catalyst under the reaction conditions tested and showed greater selectivity towards benzaldehyde at iso-conversion.

1.4.2 1-octen-3-ol oxidation

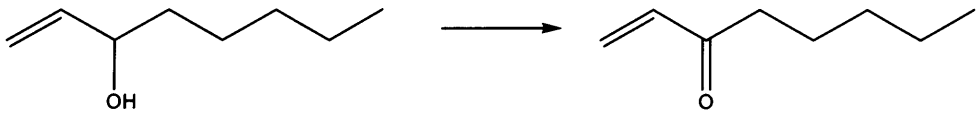

Scheme 1.1: The oxidation of 1-octen-3-ol

1-octen-3-one is a flavour and fragrance compound with a strong mushroom smell; it can be obtained from the oxidation of 1-octen-3-ol. Sheldon *et al*[44] showed

this oxidation could be achieved using a water soluble bathophensnthroline disulfonate palladium complex as a catalyst. They achieved conversion of 98% and a selectivity towards 1-octen-3-one of 80% using 30 bar air as the oxidant at 100 °C.

Corma and co-workers[45] were the first group to demonstrate that supported gold could be used for this selective oxidation. They demonstrated the use of gold supported nanocrystalline ceria could lead to an 80% conversion of the 1-octen-3-ol after a period of 3.5 hours using 0.5mol%Au/CeO_2 catalyst at 80 °C. They subsequently demonstrated that at atmospheric pressure aerobic oxidation of 1-octen-3-ol could be achieved using Dean-Stark apparatus at 120 °C[46]. Gold supported on ceria, palladium supported on ceria and palladium supported on apatite catalysts were tested and while all three catalysts achieved a conversion of above 99% after 3 hours the selectivity towards 1-octen-3-one achieved with the gold catalysts was considerably higher than the palladium catalysts (93%, 58% and 23% respectively) as the palladium catalysts tended to lead to the isomerisation product.

Hutchings and co-workers[47] demonstrated that good turn over frequencies could be achieved using a 2.5wt%Au + 2.5wt%Pd/TiO_2 catalyst. 1-octen-3-ol was oxidised at 160 °C using molecular oxygen as the oxidant and a TOF of 12600 was recorded after half an hour of reaction.

Further work by Corma and co-workers[46] compared the activity of Au+Pd/CeO_2, Au+Pd/TiO_2 and Au/TiO_2 catalysts and found that the conversion for all catalysts was above 99% but again the selectivity towards 1-octen-3-one was superior when using the gold monometallic catalyst. Subsequent work by the same authors has shown that the reaction can also be carried out using atmospheric air as the oxidant and toluene as the solvent[48] with conversion above 99% and selectivity towards 1-octen-3-one above 90% at 90 °C.

1.4.3 2-octen-1-ol oxidation

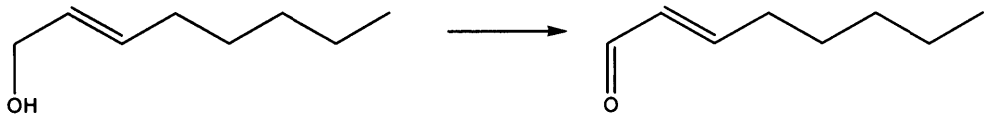

Scheme 2: The oxidation of 2-octen-1-ol

2-octen-1-al is another flavour and fragrance compound that has a fruity smell and can be obtained from the oxidation of 2-octen-1-ol. Kaneda et al[49] showed that oxidation of 2-octen-1-ol to form 2-octen-1-al could be achieved using a $ZrO(OAc)_2$ catalyst. 0.5 mmol of 2-octen-1-ol was oxidised by 0.025 mmol $ZrO(OAc)_2$ with the addition of 1.5 mmol *tert*-butyl hydroperoxide in 5 ml Chloroform refluxing under nitrogen for 6h. A yield of 71% 2-octen-1-al was obtained.

Corma and co-workers[46] were again the first to use a gold supported on ceria catalysts, for the solvent free oxidation of 2-octen-1-ol achieving 56% conversion and 72% selectivity, this catalyst showed almost equal conversion to a $Au+Pd/TiO_2$ catalyst also tested (54%) but much higher selectivity towards 2-octen-1-al (33%). When the reaction was performed using toluene as a solvent and 12.5 times the amount of catalyst the Au/CeO_2 and $Au+Pd/CeO_2$ catalysts again showed good conversion (90% and 95% respectively) but the selectivity towards 2-octen-1-al was superior for the gold monometallic catalyst (91% for Au/CeO_2 compared to 73% for $Au+Pd/CeO_2$). Under these conditions the $Au+Pd/TiO_2$ catalysts displayed very low conversion (17% with 60% selectivity towards 2-octen-1-al).

Prati and co-workers[50] investigated carbon supported catalysts, and found that the alloying of gold and palladium led to a significant increase in the activity of the catalyst. The monometallic gold catalyst displayed no conversion after 2h of reaction at 50 °C with 3 bar O_2 as the oxidant, the monometallic palladium catalyst converted 3% of the 2-octen-1-ol and the bimetallic gold palladium catalysts converted 97% of the 2-octen-1-ol after 2h. A bimetallic gold platinum catalyst was also tested and this also showed a synergistic effect with a Pt/C catalysts converting

1% of the 2-octen-1-ol, the bimetallic gold platinum catalysts converted 8% of the 2-octen-1-ol after 2h.

1.4.4 Cinnamyl alcohol oxidation

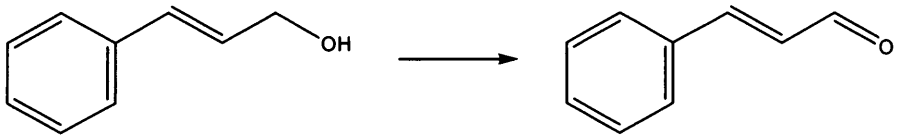

Scheme 1.3: Cinnamyl alcohol oxidation.

Cinnamyl alcohol is a white crystalline solid at room temperature with the odor of hyacinth and is used in the perfumery industry and as a deodorant; it can be oxidized to form Phenylacetaldehyde which has a floral odour. Shelodon et al[51] used a palladium(II) bathophenanthroline complex for the oxidation of cinnamyl alcohol with sodium acetate in water with 30 bar air. They achieved a conversion of 100% and selectivity of 99% to the aldehyde product at 80 °C.

Corma and coworkers[45] demonstrated that cinnamyl alcohol could be oxidised by gold supported on ceria using 1 atm O_2, after 7 hours 66% conversion was achieved with a 73% selectivity towards cinnamylaldehyde.

Hutchings and coworkers[47] oxidised cinnamyl alcohol using toluene as a solvent with 2.5%Au+2.5%Pd/TiO_2 at 190 °C and observed a TOF of 97 mol kg^{-1} h^{-1} with 1 atm O_2.

Corma et al[46] in subsequent work used Au/CeO_2, Au+Pd/CeO_2 and Au+Pd/TiO_2 to perform the oxidation at 120 °C with 1 bar O_2, using toluene as a solvent, the conversion was above 95% for all three catalysts although the ceria supported catalysts showed the best selectivity, 99% for the monometallic and 93% for the bimetallic.

1.5 Alkene oxidations

1.5.1 2,5-dimethyl furan oxidation

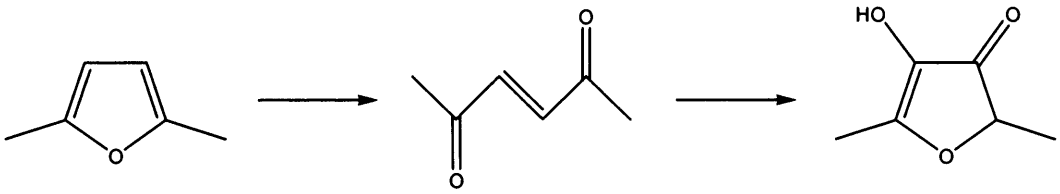

Scheme 1.4: The sequential oxidation of 2,5-dimethyl furan.

The initial oxidation of 2,5-dimethylfuran to form hex-3-ene-2,5-dione has reported through several different methods. One of the most successful was reported by Adgar *et al*[52] who used dimethyldioxirane as an oxidant at room temperature using acetone as a solvent. With one equivalent of dimethyldioxirane quantitative yield of hex-3-ene-2,5-dione was obtained.

Finlay *et al*[53] found that methytrioxoruthenium in combination with urea hydrogen peroxide could also be used to ring open furan systems. The reaction was carried out at room temperature with a yield of 97% of hex-3-ene-2,5-dione was achieved.

Massa *et al*[54] used a $Mo(CO)_6$/cumyl hydroperoxide system to oxidise 2,5-dimethyl furan. They converted 2 mmol of 2,5-dimethyl furan using 0.2 mmol $Mo(CO)_6$, 2 mmol cumyl hydroperoxide in chloroform at 50 °C stirred for 24h with a yield of 94%.

Wahlen et al[55] used titanium silicate (TS-1) and hydrogen peroxide to oxidise various furan derivatives. They achieved 94% conversion of 10 mmol 2,5-dimethylfuran by 0.1 g TS-1, 12.5 mmol hydrogen peroxide in 10 ml acetonitrile at 25 °C after 3h with a selectivity of 85% to hex-3-ene-2,5-dione.

The further oxidation of hex-3-ene-2,5-dione could lead to 3,4-dihydroxyhexane-2,5-dione. Briggs *et al*[56] have shown that 3,4-dihydroxyhexane-

2,5-dione can be converted into furaneol, by refluxing the aqueous solution for 7 days with piperidinium they formed furaneol with a 48% yield.

1.5.2 α-pinene oxidation

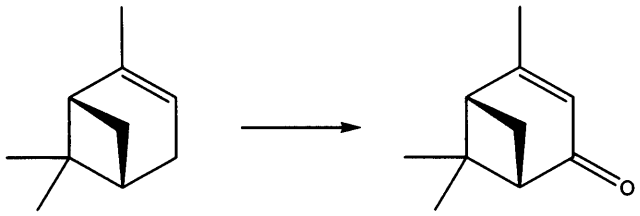

Scheme 1.5: the oxidation of α-pinene

α-pinene is the main component of turpentine which is a by-product of cellulose production. The target for the oxidation of α-pinene is verbenone, which can be used to obtain one of the rings of taxol[57], it is also a flavour and fragrance compound.

The oxidation of α-pinene to verbenone is a reaction that has been studied quite extensively, with Moore *et al*[58] reporting on the autoxidation in 1955. In their work α-pinene was autoxidesed in the dark at 100 °C, after 160 mins 65% of the α-pinene had been converted, the majority products were verbenol and α-pinene epoxide with 9% selectivity to verbenone.

More recently Lajunen *et al*[59] used several Co (II) complexes to oxidise α-pinene in air. The oxidation was carried out in solvent free conditions at 68 °C with bubbling air. The complex that gave the best conversion of α-pinene was [Co(4-Me(C_5H_4N)$_2$$Br_2$]. They found that on short reaction runs the major product was verbenol but on longer reaction runs this was converted into verbenone with a selectivity of 76% after 7 days. In a further study by Lajunen[60] using Co (II) complexes as catalysts and air as an oxidant the author found [Co(pyridine)$_2$$Br_2$] to be an effective catalyst for the oxidation. The author found the addition of hydrogen peroxide increased the conversion under mild conditions and raising the temperature did not significantly increase the yield of verbenone. It was noted that the use of dichloromethane or acetonitrile as a reaction solvent considerably retarded the

reaction. A 40% yield of verbenone was achieved at 100 °C with α-pinene conversion of about 80%. It was also noted that at 100 °C with no catalyst present there was a reaction after 23h with a 22% selectivity towards verbenone.

Work by Hutchings and co workers[61] used a commercial silica-titania co-gel catalyst and *tert*-butyl hydrogenperoxide as an oxidant .Using methanol as a solvent they acheieved a conversion of 32% after a period of 8h at 80 °C and a selectivity towards verbenone of 63%. Under these conditions in the absence of a catalyst there was only an 8% conversion of the α-pinene.

Allal *et al*[62] carried out the oxidation of α-pinene using various catalytic conditions. Under conditions of 70 °C, with 7.3 mmol of α-pinene, 0.073 mmol of catalyst, 44 mmol of *t*-buOOH in 6 ml acetonitrile with O_2 bubbling 100% conversion could be achieved after 12h with 78% selectivity towards verbenone (table 1.10). The authors also carried out the oxidation using analogous conditions but with a $Pd(acac)_2$ catalyst and hydrogen peroxide and found this gave a selectivity towards verbenol of 30%.

Table 1.10: The oxidation of α-pinene by various catalysts as reported by Allal *et al*[62]. Reaction conditions: α-pinene; 7.3 mmol, catalyst; 0.073 mmol, *t*-BuOOH; 44 mmol, MeCN; 6 cm^3, O_2 bubbling.

Catalyst	Time (h)	Conversion (%)	Verbenol Selectivity (%)	Verbenone Seleectivity (%)
CuI	11	100	tr	70
CuCl	12	98	1	45
$CuCl_2$	12	100	3	78
$Cu(OAc)_2$	17	100	tr	60
$Co(OAc)_2$	12	98	2	43
$Mn(OAc)_2$	46	100	tr	48
$Pd(OAc)_2$	26	92	7	26
$Pd(acac)_2$	22	94	10	30

Ancel *et al*[63] investigated the effect of pressure and temperature on the oxidation. They found that an increase in pressure led to an increase in the conversion up to 2 bars, however between 2 bar and 6 bar they found no effect. The increase in temperature between 70 and 120 °C resulted in an increase in the rate of α-pinene conversion and a small difference in the product distribution.

Romanenko *et al*[64] used iron supported on alumina silicates as a catalyst and *tert*-butyl hydro peroxide as an oxidant. Carrying out the reaction at 40 °C using 1.47 mmol of α-pinene and 2.98 mmol of *tert*-butyl hydro peroxide in 2 ml of dichloromethane under an argon atmosphere they achieved 100% conversion of α-pinene with a selectivity towards verbenone of 84.2% after 80h of reaction.

Kuznetsova *et al*[65] tested various metal catalysts supported on carbon. Under conditions of 6.3 mmol α-pinene, 50 mg catalysts 5% metal supported on carbon, 10 mg tetrahexylammonium chloride, 90°C and 2h the highest conversion of α-pinene was achieved by a Rh catalysts followed by Ir, Ru and Pt. however the total selectivity towards verbenol and verbenone did not exceed 56%.

1.5.2 Valenecene oxidation

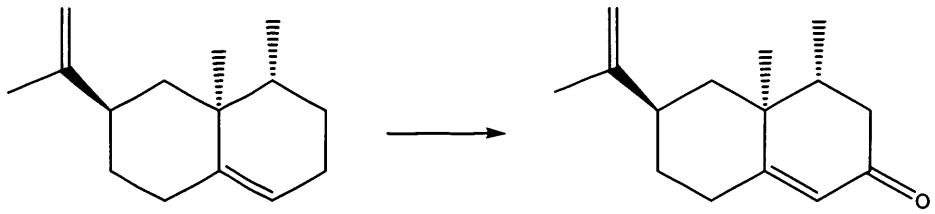

Scheme1.6: The oxidation of valencene

Valencene is a natural constituent of citrus oils that is used as a flavour and fragrance compound. The oxidation of valencene to yield nootkatone would be useful as nootkatone is a high value product. It is a flavouring that is added to many commercial soft drinks. It is currently extracted form citrus pulp and rind a direct oxidation of valencene to nootkatone would be cheaper and more efficient. Chappell *et al*[66] have isolated and purified a nucleic acid sequence to produce an enzyme that is capable of catalysing the oxidation.

The synthesis of nootkatone from valencene has been reported as early a 1978 by Wilson[67] the author formed nootkatone with an overall yield of 47% by oxidising valencene *tert*-butyl peracetate forming the β-acetate product. The acetate product was subsequently converted to the alcohol by treatment with lithium aluminium hydride which was subsequently oxidised to nootkatone using chromic acid.

A further example of biotransformation was reported by Silvestre *et al*[68], mutated forms of the P450 enzyme achieved a 20% yield of product with a selectivity towards nootkatone of 47% after 48 hours. Sakamaki *et al*[69] also used a biotransformation to form nootkatone using a series of plant cultured cells (table 1.11). The best result achieved by the authors was a 72% yield of nootkatone using the *G.pentaphyllum* plant cultered cell from 90 mg of valencene after 20 days. A further biotranformation was demonstrated by Furusawa *et al*[70] who used the green algae Chlorella species they found that *C. vulgaris* converted 100% of 20mg of valencene over 25 days with a selectivity of 100% towards nootkatone.

Table 1.11 the conversion of valencene by various plant cultured cells as reported by[69].

Cultured Cells	Time (days)	Yeild Nootkatone (%)	Yeild Nootkatol (%)	Yeild Epinookatol (%)
C.chamlagu	15	12	2	1
C.chamlagu	20	25	4	2
H.cannabinus	15	14	2	1
H.cannabinus	20	28	3	1
G.pentaphylham	15	37	8	4
G.pentaphylham	20	72	11	5

Salvador *et al*[71] used a $Co(OAc)_2/SiO_2$ catalyst (0.06g) in acetonitrile (15 ml) under an atmosphere of nitrogen with *tert*-butyl hydroperoxide (2.4 cm^3) at 55 °C. After 24 hours of reaction a yield of 75% nootkatone was achieved. Further work by the same author[68] used a bismuth (III) salt as a catalyst and this achieved a yield of

35% nootkatone under more harsh reaction conditions (70 °C, 16 mg catalyst, 16 mg valencene, 3 ml acetonitrile, 0.9 cm^3 *tert*-butyl hydro peroxide, 20h). A further experiment by the same authors[72] used sodium chlorite with *tert*-butyl hydro peroxide and N-hydroxyphthalimide as a catalyst achieved a 38% yield of nootkatone using 0.35 mmol valencene, 1.35 mmol *tert*-butyl hydro peroxide, 0.3 mmol sodium chlorite, in 3 ml 3:1 by volume acetonitrile:water soltutuion at 50 °C for 18h.

1.5.3 Isophrone oxidation

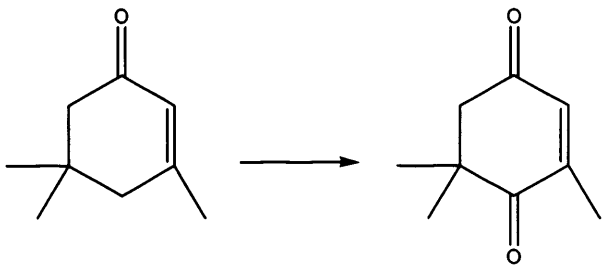

Scheme 1.7: The oxidation of isophorone.

The oxidation of isophorone to ketoisophorone represents a value added process that could be useful industrially. There are several examples in the literature of the oxidation of isophorone. Halligudi *et al*[73] have oxidised β-isophorone using [LMn(III)(Cl)] where L = bis-salicylaldehydeethylenedi-imine as a catalyst. They found there was a linear relationship between the amount of catalyst and the rate of reaction, they also found a half order dependence on the rate of reaction with respect to oxygen concentration. At high conversions (> 90%) they achieved a selectivity of around 60% to ketoisophorone.

Daniele *et al*[74] made a iron tetrasulfohtalocyanine supported on titania nanocrystals catalyst and used it for the oxidation of β-isophorone. Using conditions of 0.1 mmol β-isophorone, 15 mg (1 mol%) catalyst and 2 bar O_2 they achieved a conversion of 99% and a selectivity towards ketoisophorone of 57% after 24h at 60 °C

Li *et al*[75] oxidised β-isophorone to ketoisophorone using Schiff base complexes, the most successful of theses was the oxidation by the catalyst shown in

figure 1.2, using 0.1g of catalysts 50g β-isophorone in 20 ml pyridine were stirred in a glass reactor at 48 °C with air flowing through the solution they achieved a 99.3% conversion with a selectivity towards ketoisophorone of 85%.

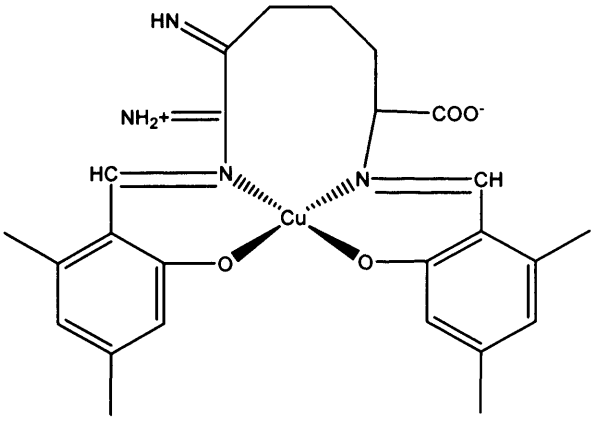

Figure 1.2: the Schiff base catalysed used in the oxidation of β-isophorone by Li et al[75]

Table 1.12: the effect of temperature upon the oxidation of isophorone as reported by Kishore *et al*[76]. Reaction conditions: 100 mg Ru-MgAl-HT catalyst, 7 mmol isophorone, acetonitrile 10 ml, 35 mmol TBHP, 48h.

Reaction Temperature (°C)	Conversion (%)	Ketoisophorone Selectivity (%)	Ketoisophoron Yeild (%)
40	53	100	53
50	62	100	62
60	60	100	60
70	43	100	43
80	29	76	22
100	29	52	15

Kishore *et al*[76] carried out the oxidation of α-isophorone using ruthenium supported on MgAl-hydroatalcite, acetonitrile was used as a solvent and *tert*-butyl hydroperoxide was used as an oxidant. The authors investigated the effect of solvent and found it had a significant effect on the conversion and a slight effect on the selectivity with acetonitrile the most effective for the Ru-MgAl-HT catalyst. They

also found the optimum temperature for the conversion was 60 °C (table 1.12). Further work by the same authors used copper, cobalt and iron supported on MgAl ternary hydrotalcites in acetornirile at 60 °C. The Cu-Mg-Al catalysts gave the best conversion with 62% conversion and 100% selectivity towards ketoisophorone for 7 mmol ketoisophorone in 10 ml acetonitrile with 35 mmol *tert*-butyl hydroperoxide at 60 °C for 48h. The authors observed the same patterns in temperature and solvent as had been reported previously.

1.5.4 2,6-lutidene oxidation

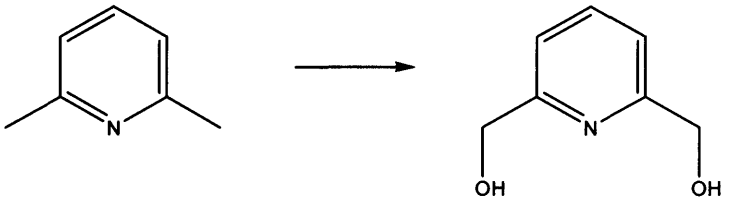

Scheme 1.8: The oxidation of 2,6-lutidene

The oxidation direct of 2,6-lutidene to 2,6-pyridinedimethanol is not been reported in the literature however previous work in the group has observed that toluene can be oxidised to benzyl alcohol using gold palladium supported on titania catalysts and the of 2,6-lutidene to 2,6-pyridinedimethanol would represent a value added process which could be useful commercially. Most reports of the formation of 2,6-pyridinedimethanol in the literature are based on the reduction of 2,6-Pyridinediacetic acid.

Similarly the oxidation of 2-picoline and 3-picoline to form 2-pyridinemetanol and 3-pyrindinemethanol respectively would be useful. The reports in the literature for this reaction again mostly focus on reductive methods of obtaining the products.

1.5.6 2,4-Dimethylnitrobenzene oxidation

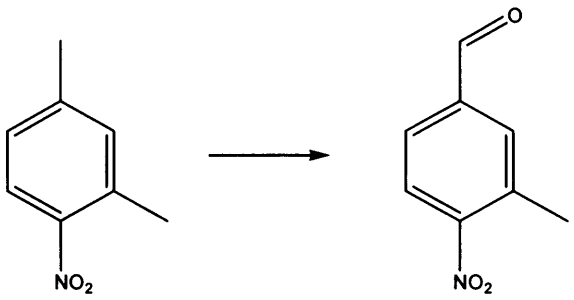

Scheme 1.9: The oxidation of **2,4-Dimethylnitrobenzene**

The catalytic oxidation of 2,4-dimethylnitrobenzene to form 3-methyl-4-nitrobenzoic acid has not reported in the literature, again a catalytic process for this oxidation would represent an industrially useful value added process. The oxidation of toluic acid using nitrourea as an oxidant has been carried out by Almog *et al*[77]. They recorded a 12% yield of 3-methyl-4-nitrobenzoic acid by adding 20 mmol of nitrourea in small portions over a period of 30 minutes to a solution of toluic acid (10 mmol) in concentrated sulfuric acid (10 ml) at 0 °C and then stirring at 25 °C for 24h. This process however would not be practical industrially due to the nature of the chemicals involved.

1.6 Aims of the Project

The objectives of the investigation are related to the advancement of the catalyst design for gold palladium bimetallic catalysts and the application of these catalysts to develop new green oxidation systems for various industrially useful oxidation targets

Objectives

1. The development of gold palladium catalysts using the solvent free oxidation of benzyl alcohol as a test reaction.

2. The application of the catalysts to the oxidation of 2,5-dimethyl furan to form furaneol under solvent free conditions using molecular oxygen as an oxidant in a stirred autoclave reactor.

3. The application of the catalysts to the oxidation of α-pinene to form verbenone under solvent free conditions using molecular oxygen as an oxidant in a stirred autoclave reactor.

4. The application of the principles established for the oxidation of 2,5-dimethyl furan and α-pinene to other similar potentially useful oxidation systems.

1.7 References

[1] J. J. Berzelius, *Edinburgh New Philosophical Journal* **1836**, *XXI*, 223

[2] www.wikipedia.com. http://en.wikipedia.org/wiki/File:CatalysisScheme.png 9/10/2009

[3] F. Moreau, G. C. Bond, A. O. Taylor, *Journal of Catalysis* **2005**, *231*, 105.

[4] M. Haruta, T. Kobayashi, H. Sano, N. Yamada, *Chemistry Letters* **1987**, 405.

[5] G. J. Hutchings, *Journal of Catalysis* **1985**, *96*, 292.

[6] S. Tsubota, M. Haruta, T. Kobayashi, A. Ueda, Y. Nakahara, *Studies in Surface Science and Catalysis* **1991**, *63*, 695.

[7] L. Prati, M. Rossi, *Journal of Catalysis* **1998**, *176*, 552.

[8] P. Landon, P. J. Collier, A. J. Papworth, C. J. Kiely, G. J. Hutchings, *Chemical Communications (Cambridge, United Kingdom)* **2002**, 2058.

[9] D. I. Enache, J. K. Edwards, P. Landon, B. Solsona-Espriu, A. F. Carley, A. A. Herzing, M. Watanabe, C. J. Kiely, D. W. Knight, G. J. Hutchings, *Science (Washington, DC, United States)* **2006**, *311*, 362.

[10] J. K. Edwards, B. E. Solsona, P. Landon, A. F. Carley, A. Herzing, C. J. Kiely, G. J. Hutchings, *J. Catal.* **2005**, *236*, 69.

[11] M. Haruta, H. Sano, T. Kobayashi, (Agency of Industrial Sciences and Technology, Japan; Japan, Ministry of International Trade and Industry). Application: US US, **1987**, p. 8 pp.

[12] M.-A. Hurtado-Juan, C. M. Y. Yeung, S. C. Tsang, *Catalysis Communications* **2008**, *9*, 1551.

[13] P. B. Walsh, *Tappi Journal* **1991**, *74*, 81.

[14] A. R. Vaino, *Journal of Organic Chemistry* **2000**, *65*, 4210.

[15] D. G. Lee, U. A. Spitzer, *Journal of Organic Chemistry* **1970**, *35*, 3589.

[16] G. J. Hutchings, *Chem. Commun. (Cambridge, U. K.)* **2008**, 1148.

[17] P. Landon, P. J. Collier, A. F. Carley, D. Chadwick, A. J. Papworth, A. Burrows, C. J. Kiely, G. J. Hutchings, *Phys. Chem. Chem. Phys.* **2003**, *5*, 1917.

[18] B. E. Solsona, J. K. Edwards, P. Landon, A. F. Carley, A. Herzing, C. J. Kiely, G. J. Hutchings, *Chem. Mater.* **2006**, *18*, 2689.

[19] R. M. Finch, N. A. Hodge, G. J. Hutchings, A. Meagher, Q. A. Pankhurst, M. R. H. Siddiqui, F. E. Wagner, R. Whyman, *Physical Chemistry Chemical Physics* **1999**, *1*, 485.

[20] J. K. Edwards, B. Solsona, P. Landon, A. F. Carley, A. Herzing, M. Watanabe, C. J. Kiely, G. J. Hutchings, *J. Mater. Chem.* **2005**, *15*, 4595.

[21] T. Ishihara, Y. Ohura, S. Yoshida, Y. Hata, H. Nishiguchi, Y. Takita, *Appl. Catal., A* **2005**, *291*, 215.

[22] G. R. Bamwenda, S. Tsubota, T. Nakamura, M. Haruta, *Catalysis Letters* **1997**, *44*, 83.

[23] G. Li, J. Edwards, A. F. Carley, G. J. Hutchings, *Catal. Commun.* **2007**, *8*, 247.

[24] G. Li, J. Edwards, A. F. Carley, G. J. Hutchings, *Catal. Today* **2007**, *122*, 361.

[25] J. K. Edwards, A. Thomas, B. E. Solsona, P. Landon, A. F. Carley, G. J. Hutchings, *Catal. Today* **2007**, *122*, 397.

[26] J. K. Edwards, A. Thomas, A. F. Carley, A. A. Herzing, C. J. Kiely, G. J. Hutchings, *Green Chem.* **2008**, *10*, 388.

[27] A. K. Sinha, S. Seelan, S. Tsubota, M. Haruta, *Topics in Catalysis* **2004**, *29*, 95.

[28] J. Chou, E. W. McFarland, *Chemical Communications (Cambridge, United Kingdom)* **2004**, 1648.

[29] M. D. Hughes, Y.-J. Xu, P. Jenkins, P. McMorn, P. Landon, D. I. Enache, A. F. Carley, G. A. Attard, G. J. Hutchings, F. King, E. H. Stitt, P. Johnston, K. Griffin, C. J. Kiely, *Nature (London, United Kingdom)* **2005**, *437*, 1132.

[30] J. A. Lopez-Sanchez, N. Dimitratos, P. Miedziak, E. Ntainjua, J. K. Edwards, D. Morgan, A. F. Carley, R. Tiruvalam, C. J. Kiely, G. J. Hutchings, *Phys. Chem. Chem. Phys.***2008**, *10*, 1921.

[31] P. Lignier, F. Morfin, L. Piccolo, J.-L. Rousset, V. Caps, *Catalysis Today* **2007**, *122*, 284.

[32] G.-j. ten Brink, I. W. C. E. Arends, R. A. Sheldon, *Science (Washington, D. C.)* **2000**, *287*, 1636.

[33] A. Stephen, K. Hashmi, G. J. Hutchings, *Angewandte Chemie, International Edition* **2006**, *45*, 7896.

[34] M. Arai, S. Nishiyama, S. Tsuruya, M. Masai, *Journal of the Chemical Society, Faraday Transactions* **1996**, *92*, 2631.

[35] V. R. Choudhary, P. A. Chaudhari, V. S. Narkhede, *Catalysis Communications* **2003**, *4*, 171.

[36] D. I. Enache, D. W. Knight, G. J. Hutchings, *Catalysis Letters* **2005**, *103*, 43.

[37] V. R. Choudhary, A. Dhar, P. Jana, R. Jha, B. S. Uphade, *Green Chemistry* **2005**, *7*, 768.

[38] V. R. Choudhary, R. Jha, P. Jana, *Green Chemistry* **2006**, *8*, 689.

[39] J. Hu, L. Chen, K. Zhu, A. Suchopar, R. Richards, *Catalysis Today* **2007**, *122*, 277.

[40] N. Dimitratos, J. A. Lopez-Sanchez, D. Morgan, A. Carley, L. Prati, G. J. Hutchings, *Catalysis Today* **2007**, *122*, 317.

[41] D. I. Enache, D. Barker, J. K. Edwards, S. H. Taylor, D. W. Knight, A. F. Carley, G. J. Hutchings, *Catalysis Today* **2007**, *122*, 407.

[42] F.-Z. Su, M. Chen, L.-C. Wang, X.-S. Huang, Y.-M. Liu, Y. Cao, H.-Y. He, K.-N. Fan, *Catalysis Communications* **2008**, *9*, 1027.

[43] J. A. Lopez-Sanchez, N. Dimitratos, P. Miedziak, E. Ntainjua, J. K. Edwards, D. Morgan, A. F. Carley, R. Tiruvalam, C. J. Kiely, G. J. Hutchings, *Physical Chemistry Chemical Physics* **2008**, *10*, 1921.

[44] G.-J. ten Brink, I. W. C. E. Arends, R. A. Sheldon, *Advanced Synthesis & Catalysis* **2002**, *344*, 355.

[45] A. Abad, P. Concepcion, A. Corma, H. Garcia, *Angewandte Chemie, International Edition* **2005**, *44*, 4066.

[46] A. Abad, C. Almela, A. Corma, H. Garcia, *Chemical Communications (Cambridge, United Kingdom)* **2006**, 3178.

[47] M. Conte, G. Budroni, J. K. Bartley, S. H. Taylor, A. F. Carley, A. Schmidt, D. M. Murphy, F. Girgsdies, T. Ressler, R. Schloegl, G. J. Hutchings, *Science (Washington, DC, United States)* **2006**, *313*, 1270.

[48] A. Abad, A. Corma, H. Garcia, *Chemistry--A European Journal* **2008**, *14*, 212.

[49] K. Kaneda, Y. Kawanishi, S. Teranishi, *Chemistry Letters* **1984**, 1481.

[50] L. Prati, A. Villa, C. Campione, P. Spontoni, *Topics in Catalysis* **2007**, *44*, 319.

[51] G.-j. ten Brink, I. W. C. E. Arends, M. Hoogenraad, G. Verspui, R. A. Sheldon, *Advanced Synthesis & Catalysis* **2003**, *345*, 1341.

[52] B. M. Adger, C. Barrett, J. Brennan, M. A. McKervey, R. W. Murray, *Journal of the Chemical Society, Chemical Communications* **1991**, 1553.

[53] J. Finlay, M. A. McKervey, H. Q. N. Gunaratne, *Tetrahedron Letters* **1998**, *39*, 5651.

[54] A. Massa, M. R. Acocella, M. De Rosa, A. Soriente, R. Villano, A. Scettri, *Tetrahedron Letters* **2003**, *44*, 835.

[55] J. Wahlen, B. Moens, D. E. De Vos, P. L. Alsters, P. A. Jacobs, *Advanced Synthesis & Catalysis* **2004**, *346*, 333.

[56] M. A. Briggs, A. H. Haines, H. F. Jones, *Journal of the Chemical Society, Perkin Transactions 1: Organic and Bio-Organic Chemistry (1972-1999)* **1985**, 795.

[57] P. A. Wender, T. P. Mucciaro, *Journal of the American Chemical Society* **1992**, *114*, 5878.

[58] R. N. Moore, C. Golumbic, G. S. Fisher, *Journal of the American Chemical Society* **1956**, *78*, 1173.

[59] M. Lajunen, A. M. P. Koskinen, *Tetrahedron Letters* **1994**, *35*, 4461.

[60] M. K. Lajunen, *Journal of Molecular Catalysis A: Chemical* **2001**, *169*, 33.

[61] P. McMorn, G. Roberts, G. J. Hutchings, *Catalysis Letters* **2000**, *67*, 203.

[62] B. A. Allal, L. El Firdoussi, S. Allaoud, A. Karim, Y. Castanet, A. Mortreux, *Journal of Molecular Catalysis A: Chemical* **2003**, *200*, 177.

[63] J. E. Ancel, N. V. Maksimchuk, I. L. Simakova, V. A. Semikolenov, *Applied Catalysis, A: General* **2004**, *272*, 109.

[64] E. P. Romanenko, E. A. Taraban, A. V. Tkachev, *Russian Chemical Bulletin* **2006**, *55*, 993.

[65] L. I. Kuznetsova, N. I. Kuznetsova, A. S. Lisitsyn, I. E. Beck, V. A. Likholobov, J. E. Ancel, *Kinetics and Catalysis* **2007**, *48*, 38.

[66] J. Chappell, Y. Yeo, S. Takahashji, (University of Kentucky Research Foundation, USA). Application: WO02006079020
WO, **2006**, p. 121 pp.

[67] C. W. Wilson, III, P. E. Shaw, *Journal of Agricultural and Food Chemistry* **1978**, *26*, 1430.

[68] J. A. R. Salvador, S. M. Silvestre, *Tetrahedron Letters* **2005**, *46*, 2581.

[69] H. Sakamaki, K.-I. Itoh, T. Taniai, S. Kitanaka, Y. Takagi, W. Chai, C. A. Horiuchi, *Journal of Molecular Catalysis B: Enzymatic* **2005**, *32*, 103.

[70] M. Furusawa, T. Hashimoto, Y. Noma, Y. Asakawa, *Chemical & Pharmaceutical Bulletin* **2005**, *53*, 1513.

[71] J. A. R. Salvador, J. H. Clark, *Green Chemistry* **2002**, *4*, 352.

[72] S. M. Silvestre, J. A. R. Salvador, *Tetrahedron* **2007**, *63*, 2439.

[73] S. B. Halligudi, N. K. Kala Raj, S. S. Deshpande, S. Gopinathan, *Journal of Molecular Catalysis A: Chemical* **2000**, *157*, 9.

[74] M. Beyrhouty, A. B. Sorokin, S. Daniele, L. G. Hubert-Pfalzgraf, *New Journal of Chemistry* **2005**, *29*, 1245.

[75] J. Mao, N. Li, H. Li, X. Hu, *Journal of Molecular Catalysis A: Chemical* **2006**, *258*, 178.

[76] D. Kishore, A. E. Rodrigues, *Catalysis Communications* **2007**, *8*, 1156.

[77] J. Almog, A. Klein, A. Sokol, Y. Sasson, D. Sonenfeld, T. Tamiri, *Tetrahedron Letters* **2006**, *47*, 8651.

Chapter Two

2. Experimental

2.1 Chemicals

The chemicals were used as received and are as follows with information of their source and purity:

Benzyl Alcohol, 98% Fluka

Water, HPLC, Aldrich

Methanol, HPLC, Aldrich

1-Octen-3-ol, 98% Fluka

2-Octen-1-ol, 97%, Aldrich

Cinnamyl alcohol, 98%, Aldrich

2,5-Dimethyl-Furan, 98% Alfa Aesar

α-Pinene, 98% Fluka

Valencene, 70% Fluka

Isophorone, 97%, Aldrich

Titania P25, Degussa

Galia, Aldrich

Carbon G60, Johnson Matthey

Cerium acetoacetate, Aldrich

Hydrogen tetrachloroaurate trihydrate, Aldrich

Palladium Chloride, Johnson Mattey

Palladium Nitrate, Strem Chemicals

Toluene, reagent grade, Aldrich

Sodium Carbonate, Aldrich

2.1.1 Definitions

$$Conversion = 100\left(\frac{Mols\_of\_Substrate\_Conveted}{Starting\_mols\_of\_Substrate}\right)$$

$$Selectivity\_to\_X = 100\left(\frac{Mols\_of\_\mathrm{Pr}oduct\_X\_Formed}{Mols\_of\_substrate\_Converted}\right)$$

$$TOF = \frac{Mols\_Substrate\_Converted \,/\, Mols\_of\_Metal}{Time(h)}$$

2.2 Catalyst Preparation.

2.2.1 Preparation of Au, Pd, Au-Pd and Au-Pd catalysts by wet impregnation

Catalysts were prepared supported on titania (P25 Degussa), graphite (Aldrich), activated carbon (AC (Aldrich Darco G60)), ceria (Aldrich, Cardiff University), Gallia (Aldrich) using a wet impregnation technique. 2.5 wt% Au/support, 5 wt% Au/support, 2.5 wt% Pd/support, 5 wt% Pd/support and a range of 2.5 wt% Au- 2.5 wt% Pd/support were prepared by impregnation of the support using aqueous solutions of palladium chloride (Johnson Matthey), $HAuCl_4.3H_2O$ (Johnson Matthey) and/or platinum chloride (Johnson Matthey). The detailed procedure for the preparation of 2g of the 2.5 wt% Au-2.5 wt% Pd/support catalyst is as follows: Palladium chloride (83.3mg) was dissolved in a stirred and heated aqueous solution (5ml) of $HAuCl_4$ (5g in 250ml water). The resultant solution was added to the support (1.9g) and the resulting slurry was dried at 80 °C for 16h. The resulting powder was ground and calcined (1g, 6 inch quartz boat) in static air at 400 °C for 3 hours at a ramp rate of 20 °C min^{-1}.

2.2.2 Preparation of Au-Pd catalysts by deposition precipitation

A stirred, heated (60 °C) slurry of titania (P25 degussa) (1.9g) in water (300ml) was adjusted to pH 8 by the dropwise addition of (1M) sodium carbonate. Palladium Nitrate (119 mg) was dissolved in a stirred and heated aqueous solution (5ml) of $HAuCl_4$ (5g in 250ml water solution) and this solution was added dropwise to the slurry with the simulations addition of sodium carbonate solution to maintain the overall pH at 8. After all the gold palladium solution had been added the slurry was maintained at pH 8 for 1.5 hours. The slurry was then filtered, washed with de-ionized water (1L). The washed solid was dried at 80 °C for 16h. The resulting powder was ground and calcined (1g, 6 inch quartz boat) in static air at 400 °C for 3 hours at a ramp rate of 20 °C min^{-1}.

2.2.3 Preparation of Au-Pd catalysts by co-precipitation analogous method

Palladium Nitrate (119 mg) was dissolved in a stirred and heated aqueous solution (5ml) of $HAuCl_4$ (5g in 250ml water) and this solution was added to a stirred, heated (60 °C) slurry of titania (P25 degussa) (1.9g) in water (300ml). Sodium carbonate (1M) was added dropwise until the solution reached pH 8. The solution was maintained at pH 8 for 1.5 hours. The slurry was then filtered, washed with de-mineralized water (1 L). The washed solid was dried at 80 °C for 16h. The resulting powder was ground and calcined (1g, 6 inch quartz boat) in static air at 400 °C for 3 hours at a ramp rate of 20 °C min^{-1}.

2.2.4 Preparation of ceria from supercritical CO_2 antisolvent precipitation ($scCeO_2$)

$scCO_2$ was pumped at 120 bar and a flow rate of 7 ml min^{-1} with the entire system held at 40 °C. A solution of $Ce(acac)_3$ in methanol (13.3 mg ml^{-1}) was pumped through a fine capillary into the precipitation vessel at a flow rate of 0.1 ml min^{-1} in co-current mode with CO_2. As the solution exited the capillary it diffused into the CO_2 causing rapid precipitation. The precursor was recovered and calcined at 400 °C for 2h (ramp rate 10 °C min^{-1}). The non-supercritical antisolvent prepared ceria ($unCeO_2$)

was prepared by calcining the unprocessed $Ce(acac)_3$ at 400 °C for 3h (ramp rate 10 °C min^{-1}).

2.3 Catalyst evaluation

2.3.1 Oxidation of benzyl alcohol – standard reaction conditions

Catalyst testing was performed using an Autoclave Engineers stainless steel autoclave (Autoclave Engineers Inline MagneDrive III) with a nominal volume of 100 ml and a maximum working pressure of 2000 psi. The vessel was charged with Benzyl alcohol (40 ml) and catalyst (25 mg). The autoclave was then purged 3 times with oxygen leaving the vessel at the desired pressure. The pressure was maintained constant throughout the experiment; as the oxygen was consumed in the reaction it was replenished. The stirrer speed was set at 1500 r.p.m. and the reaction mixture was raised to the required temperature. Samples from the reactor were taken periodically *via* a sampling pipe, ensuring that the volume purged before sampling was higher than the tube volume, and analysed by GC using a CP-Wax column.

2.3.2 Catalyst stability

To ascertain the stability of the catalysts the catalysts were tested for re-use, to obtain sufficient catalyst for stability testing the autoclave was charged with benzyl alcohol (40 ml) and catalyst (200-500 mg). The autoclave was then purged 3 times with oxygen leaving the vessel at the desired pressure. The pressure was maintained constant throughout the experiment; as the oxygen was consumed in the reaction it was replenished. The stirrer speed was set at 1500 r.p.m. and the reaction mixture was raised to the required temperature. After the reaction the reaction mixture was filtered and washed with acetone, after drying 25mg of catalyst was retested as described previously.

2.3.3 1-octen-3-ol / 2-octen-1-ol – standard reaction conditions

Catalyst testing was performed using an Autoclave Engineers stainless steel autoclave (Autoclave Engineers Inline MagneDrive III) with a nominal volume of

100 ml and a maximum working pressure of 2000 psi. The vessel was charged with 1-octen-3-ol / 2-octen-1-ol (40 ml) and catalyst (7 mg). The autoclave was then purged 3 times with oxygen leaving the vessel at the desired pressure (10 bar). The pressure was maintained constant throughout the experiment; as the oxygen was consumed in the reaction it was replenished. The stirrer speed was set at 1500 r.p.m. and the reaction mixture was raised and maintained at the required temperature (120 °C) for 24h. Samples from the reactor were taken periodically *via* a sampling pipe, ensuring that the volume purged before sampling was higher than the tube volume, and analysed by GC using a CP-Wax column.

2.3.4 Cinnamyl alcohol - standard reaction conditions

Catalyst testing was performed using an Autoclave Engineers stainless steel autoclave (Autoclave Engineers Inline MagneDrive III) with a nominal volume of 100 ml and a maximum working pressure of 2000 psi. The vessel was charged with cinnamyl alcohol (40 ml, 1M solution in toluene) and catalyst (7 mg). The autoclave was then purged 3 times with oxygen leaving the vessel at the desired pressure (10 bar). The pressure was maintained constant throughout the experiment; as the oxygen was consumed in the reaction it was replenished. The stirrer speed was set at 1500 r.p.m. and the reaction mixture was raised and maintained at the required temperature (120 °C) for 24h. Samples from the reactor were taken periodically *via* a sampling pipe, ensuring that the volume purged before sampling was higher than the tube volume, and analysed by GC using a CP-Wax column.

2.3.5 2,5-dimethyl furan – standard reaction conditions

Catalyst testing was performed using a Parr Instruments stainless steel autoclave with a nominal volume of 50 ml and a maximum working pressure of 3000 psi. The reactor was charged with 2,5-dimethyl furan and catalyst. The autoclave was then purged 3 times with oxygen leaving the vessel at the desired pressure. The pressure was maintained constant throughout the experiment; as the oxygen was consumed in the reaction it was replenished. The stirrer speed was set at 1500 r.p.m. and the reaction mixture was raised and maintained at the required temperature.

Samples were taken from the final reaction mixture and analysed by GC using a CP-Wax column.

2.3.6 α-Pinene / valenecene / isophrone – standard reaction conditions

Catalyst testing was performed using a Parr Instruments stainless steel autoclave with a nominal volume of 50 ml and a maximum working pressure of 3000 psi. The vessel was charged with α-Pinene / Valenecene / Isophrone (40 ml) and catalyst (50 mg). The autoclave was then purged 3 times with oxygen leaving the vessel at the desired pressure. The pressure was maintained constant throughout the experiment; as the oxygen was consumed in the reaction it was replenished. The stirrer speed was set at 1500 r.p.m. and the reaction mixture was raised and maintained at the required temperature (50/75/80/100 °C) for 24h. Samples from the reactor were taken periodically *via* a sampling pipe, ensuring that the volume purged before sampling was higher than the tube volume, and analysed by GC using a CP-Wax column.

2.4 Catalyst characterisation

2.4.1 BET

2.4.1.1 Background

The Brunauer, Emmet, Teller (BET) method is one of the most commonly used methods for determining the surface area of a catalyst. The theory is based on the BET equation:

$$\frac{1}{\upsilon[(P_0/P)-1} = \frac{c-1}{\upsilon_m c}\left(\frac{P}{P_0}\right) + \frac{1}{\upsilon_m c}$$

Where c is the BET constant, P is the equilibrium pressure, P_o is the saturation pressure of adsorbates at the temperature of adsorption, v is the adsopbed gas quantity and v_m is the adsorbed gas quantity of a monlayer.

The BET method determines the surface area based on the amount of gas adsorbed at a constant temperature (77 K). The amount of gas adsorbed at a given pressure can be used to calculate the number of adsorbed gas molecules that would form a monolayer on the surface of the sample. Based on the known size of the adsorbate (nitrogen) the surface area can be calculated.

2.4.1.2 Experimental

Samples were prepared for BET analysis by degassing (16h, 120 °C) then connecting to a Micromeritices Gemini 2360 Analyser automatic multi point surface area analyser. The samples were immersed in liquid nitrogen during the analysis.

2.4.2 Scanning Transmission Electron Microscopy (STEM)

2.4.2.1 Background

Transmission electron microscopy is a type of electron microscope where a beam of electrons are focused onto a sample and the transmitted part of the beam can be used to form an enlarged image of the sample. In scanning transmission electron microscopy a focussed beam of electrons is rastered across the surface of the sample to form an image. The results can be analysed by ADF (annular dark field) and EDX (energy dispersive X-ray) methods.

Energy Dispersive X-Ray (EDX) Analysis is a method for identifying the elements present during TEM. Primary electrons can cause the displacement of core shell electrons in the sample. The displaced electron is replaced by another electron from a higher shell, causing the release of an x-ray photon. This x-ray will have a wavelength that is characteristic of the species from which it is emitted, the wavelength will also be characteristic of which electron replaces the initially displaced electron, leading to several characteristic wavelengths for each element.

2.4.2.2 Experimental

Samples for characterisation by scanning transmission electron microscopy (STEM) were prepared by dispersing the catalyst powder in high-purity ethanol, then allowing a drop of the suspension to evaporate on a holey carbon film supported by a 300-mesh copper grid. Samples were then subjected to chemical microanalysis and annular dark-field imaging in a VG Systems HB603 STEM operating at 300 kV equipped with a Nion Cs corrector. The instrument was also fitted with an Oxford Instruments INCA TEM 300 system for energy-dispersive X-ray (XEDS) analysis. All STEM was carried out at Lehigh University Centre for Advanced Materials and Nanotechnology.

2.4.3 Scanning Electron Microscopy (SEM)

2.4.3.1 Background

Scanning electron microscopy uses electrons rather than light to form an image, SEM allows a greater depth of focus than optical microscopy. For this reason, SEM is able produce an image that is a good illustration of a three-dimensional sample.

A metallic filament is heated in a vacuum and generates a beam of electrons. The electron beam is focused through a series of lenses and directed towards the sample. When the electron beam hits the sample two types of electron are produced, secondary electrons and backscatter electrons. Secondary electrons are the result of the high-energy electron beam displacing loosely held surface electrons, these electrons are detected by a secondary electron detector to produce an image of the surface that relates to the topological features of the sample. Backscatter electrons are high-energy electrons from the primary beam that are scattered back out of the sample by the atomic nuclei. The intensity of the signal is dependant upon the mean atomic number of the area of interaction, the contrast of the backscatter signal gives an indication of the distribution of elements within a sample.

2.4.3.2 Experimental

SEM was performed using a Carl Zeiss EVO 40 SEM fitted with a BSD, Everhart-Thornley detector and variable pressure chamber with a tungsten source. EDX was performed using an Oxford Instruments SiLi detector. Catalysts were mounted using adhesive carbon discs.

2.4.4 X-ray Photoelectron Spectroscopy (XPS)

2.4.4.1 Background

X-ray Photoelectron Spectroscopy (XPS) can give information about elemental composition and oxidation state of a sample under study. It is a single photon in/electron out process using photons of fixed energy; these photons have a short mean free path in solids making XPS a surface sensitive technique. The photons are absorbed by an atom which leads to ionisation and emission of a core shell electron. The Kinetic energy of the emitted photoelectron is equal to the energy of the photon minus the binding energy of the electron:

$$KE = h\nu - BE$$

Each element has a characteristic binding energy leading to characteristic peaks in the spectra; the intensity of these peaks is related to the concentration of that element. The exact binding energy is dependent on the oxidation state of the element, the higher the oxidation state the higher the binding energy will be due to higher columbic interaction between the photo-emitted electron and the ion core.

The basic set up for XPS is shown in figure 2.1 and consists of an x-ray source, a high vacuum chamber containing the sample and an electron energy analyser.

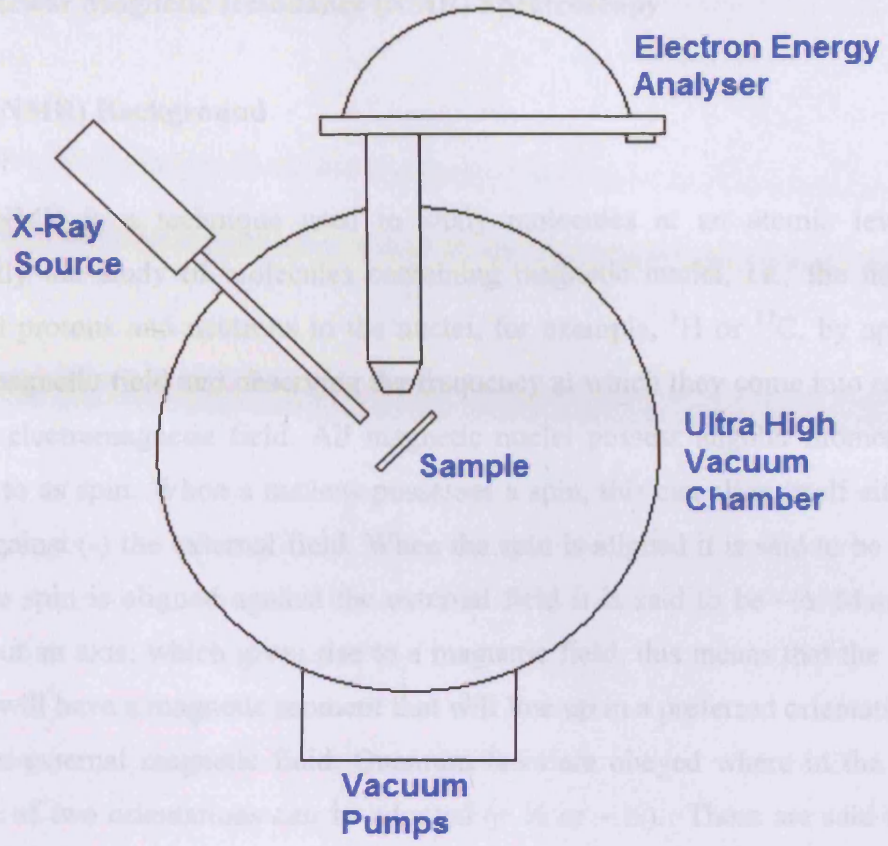

Figure 2.1: The basic set up for x-ray photoelectron spectroscopy.

2.4.4.2 Experimental

X-Ray photoelectron spectroscopy (XPS) was performed using a VG EscaLab 220i spectrometer, using a standard Al-Kα X-ray source (300 W) and an analyser pass energy of 20 eV. Samples were mounted using double-sided adhesive tape, and binding energies were referenced to the C 1s binding energy of adventitious carbon contamination, which was taken to be 284.7 eV. All XPS was carried out by the Cardiff University X-Ray Photoelectron Spectroscopy (XPS) analysis center.

2.4.5 Nuclear Magnetic Resonance (NMR) Spectroscopy

2.4.5.1 (NMR) Background

NMR is a technique used to study molecules at an atomic level, it is essentially the study of molecules containing magnetic nuclei, *i.e.,* the number of unpaired protons and neutrons in the nuclei, for example, ^{1}H or ^{13}C, by applying a strong magnetic field and observing the frequency at which they come into resonance with an electromagnetic field. All magnetic nuclei possess angular momentum, P, referred to as spin. When a nucleus possesses a spin, this can align itself either with (+) or against (-) the external field. When the spin is aligned it is said to be + ½ and when the spin is aligned against the external field it is said to be –½. Many nuclei spin about an axis, which gives rise to a magnetic field, this means that the spinning nucleus will have a magnetic moment that will line up in a preferred orientation when put in an external magnetic field. Quantum laws are obeyed where in the simplest case one of two orientations can be adopted (+ ½ or – ½). These are said to be the most and least favoured orientations that give rise to a splitting pattern (Figure 2.2).

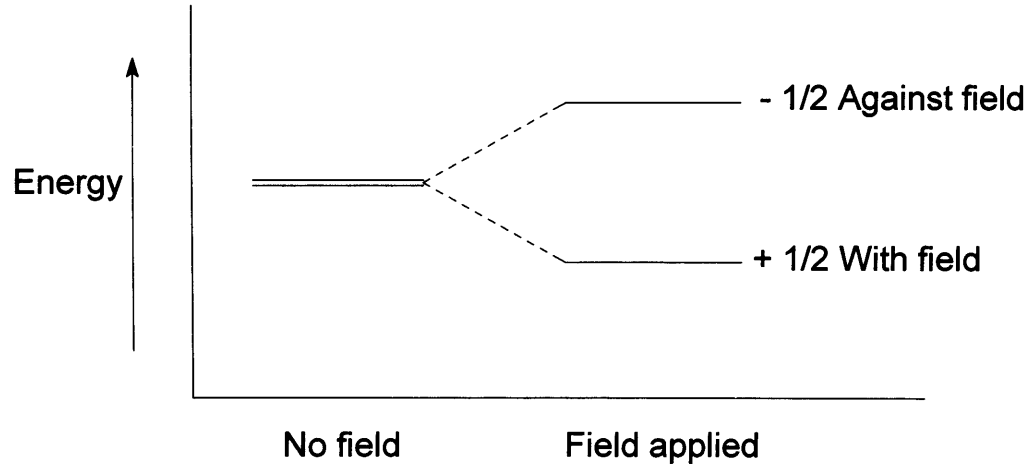

Figure 2.2: The splitting pattern between the favoured and unfavoured orientation when a nucleus is subjected to a magnetic field

Energy is distributed between the two energy levels by means of nuclear spin and the thermal motion of the molecules. A transition of the energy can be induced using radiation at the correct frequency, once this transition has occurred the spin-lattice process will again reach equilibrium with the energy being distributed amongst

the surrounding nuclei (spin-spin relaxation) or to the surroundings (spin-lattice relaxation).

The Chemical shift of a nucleus is the difference between its resonance frequency and the resonance frequency of a reference standard. The resonance frequency is dependent on the electronegativity of the surrounding atoms and shielding or deshielding caused by delocalised electrons.

Each resonance can be split into individual lines, known as the fine structure of the spectrum; this arises because each magnetic nucleus contributes to the local field experienced by other nuclei and modifies their resonance frequencies. This splitting is expressed in terms of the spin-spin coupling constant *J* which is measured in hertz (Hz).

The coupling patterns of the peaks will yield information about the number of protons that are three bonds away from the resonating group. When resonating group with n protons three bonds away from the resonating group the resonance will be split into n + 1 lines with intensity ratios predicted by Pascal's triangle.

2.4.5.2 Experimental

The ^{13}C and ^{1}H NMR spectra were obtained using a Bruker 'Avance' 400MHz DPX spectrometer, equipped with Silicon Graphics workstation running 'X win 1.3' with results reported in ppm with number of protons, multiplicity and assignment. All chemical shifts for ^{1}H NMR were recorded in deuterated chloroform (*d*-$CDCl_3$) or deuterated dimethylsulfoxide (d_6-DMSO).

2.5.6 Gas Chromatography (GC)

2.5.6.1 Background

Gas Chromatography (GC) is a method for separating and quantifying the constituents of a mixture of liquids or a solution. The compounds for analysis are

heated until they are in the gas phase in an injector and mixed with a gaseous transport medium which is carried over a column packed with an inert surface which separates the substances which are subsequently analysed by a detector (figure 2.3).

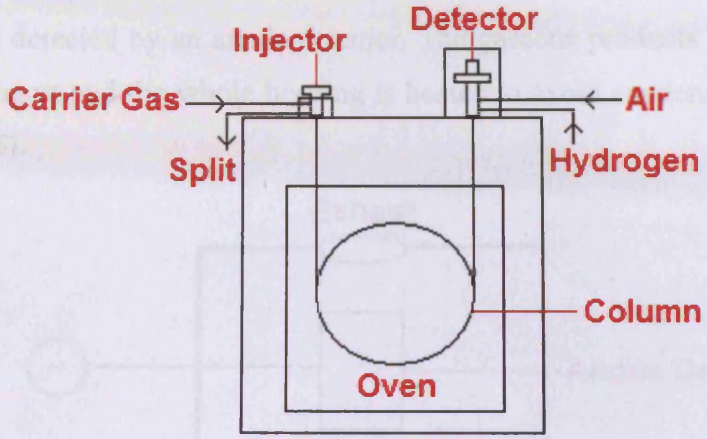

Figure 2.3: The Basic components of a GC

Most modern GC's use capillary columns which can be longer to achieve better separation without significant pressure drops, however they can only accept a low sample capacity facilitating the need for a split injector. In a split injector the sample is introduced, using a syringe, through a septum where it is heated and homogenised with the carrier gas over an inert packing. The homogenised mixture is then split into two parts using variable flow rates of the carrier gas and the split outlet (figure 2.4).

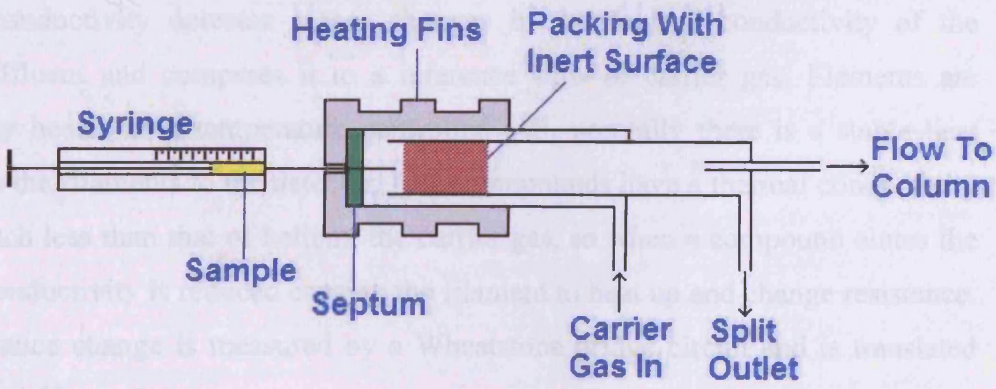

Figure 2.4: The basic components of a GC Injector.

Once the different components have been separated in the column they are quantified by a flame ionisation detector (FID). The column is directly plumbed into the FID, upon entering the detector the column effluent is mixed with air and hydrogen and burned at the jet's tip. The combustion process creates carbocations which are detected by an anode detector. The gaseous products (mainly water) leave via an exhaust and the whole housing is heated to avoid condensation in the detector (figure 2.5).

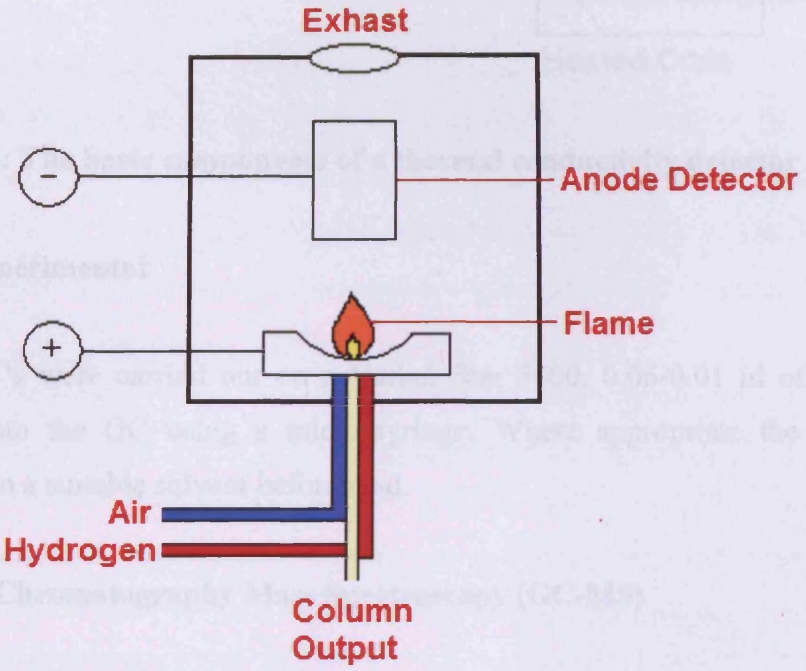

Figure 2.5: The basic components of a flame ionisation detector

Gas analysis was carried out using a thermal conductivity detector, the thermal conductivity detector senses changes in the thermal conductivity of the column effluent and compares it to a reference flow of carrier gas. Elements are electrically heated in a temperature controlled cell, normally there is a stable heat flow from the filaments to the detector. Most compounds have a thermal conductivity that is much less than that of helium, the carrier gas, so when a compound elutes the thermal conductivity is reduced causing the filament to heat up and change resistance. The resistance change is measured by a Wheatstone bridge circuit and is translated into a signal (figure 2.6).

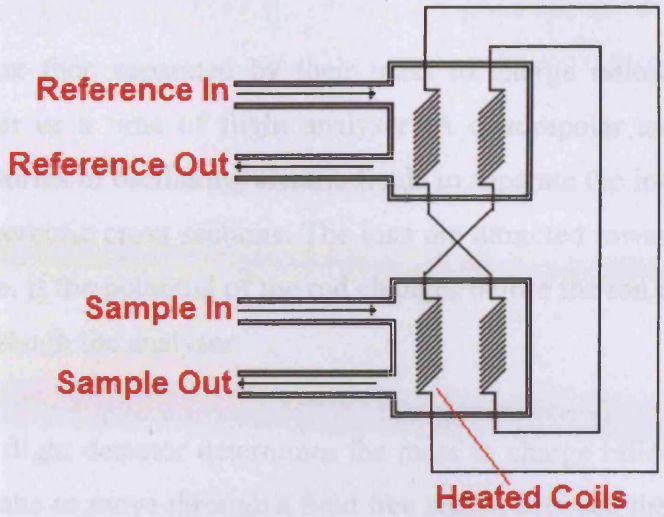

Figure 2.6: The basic components of a thermal conductivity detector

2.4.6.2 Experimental

GC's were carried out on a Varian Star 3400, 0.06-0.01 µl of sample was injected into the GC using a micro-syringe. Where appropriate the sample was dissolved in a suitable solvent beforehand.

2.4.7 Gas Chromatography Mass Spectroscopy (GC-MS)

2.4.7.1 Background

Gas chromatography mass spectroscopy is a method by which a mixture of compounds can be both separated and identified. The compounds are first separated by gas chromatography as described previously and then analysed by mass spectroscopy.

Electrons are accelerated by an electric field where they interact with the molecules separated by the GC. This interaction either leads to positive radicals due to the loss of an electron or negative radicals due to gaining an electron, positive radical species are more common. As electrons have a very small mass is similar to that of the neutral species. The molecular ion can then fragment to give ions of a smaller mass.

The ions are then separated by their mass to charge ration using either a quadrapole analyser or a time of flight analyser. A quadrapolar analyser uses the stabilities of trajectories in oscillating electric fields to separate the ions. It is made of four rods with hyperbolic cross sections. The ions are attracted towards the rod with the opposite charge, if the potential of the rod changes before the ion discharges itself the ion can pass through the analyser.

A time of flight detector determines the mass to charge ration by measuring the time that ions take to move through a field free region between the source and the detector. The lower the mass of an ion, the faster it will reach the detector. An Electrostatic reflector is a series of grids and ring reflectors that creates a retarding field that acts as an ion mirror, the reflection means that ions of the same mass to charge ratio but with different kinetic energies will reach the detector at the same time.

The separated ions can then be quantified using a faraday cup or electron multiplier. The faraday cup detects either positively or negatively charged molecules when they reach an earthed electric plate and are neutralised. The resulting flow of electrons causes a small electric current which can be recorded. The high energy molecules that hit the cup can cause a shower of secondary electrons which are also detected due to the cups shape and can amplify the signal (figure 2.7).

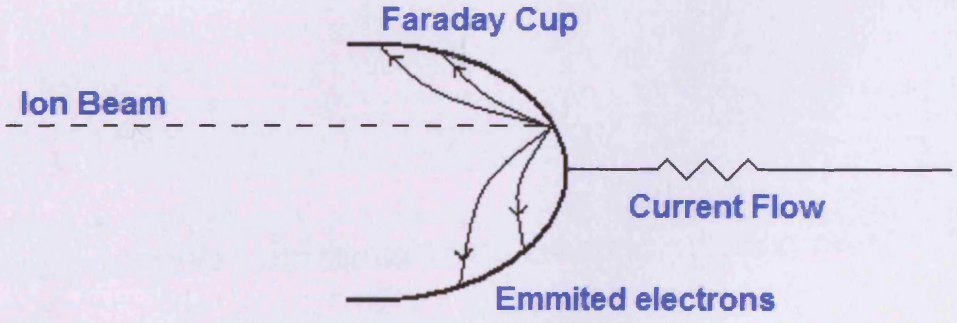

Figure 2.7: The basic set up of a faraday cup

An electron multiplier uses this principle of secondary electrons to amplify the signal. Ions are directed onto a first dynode which causes the emission of secondary

electrons which are accelerated through an electric potential so that they strike a second dynode. This process can be repeated numerous times causing an amplification of the signal up to 10^6 times (figure 2.8).

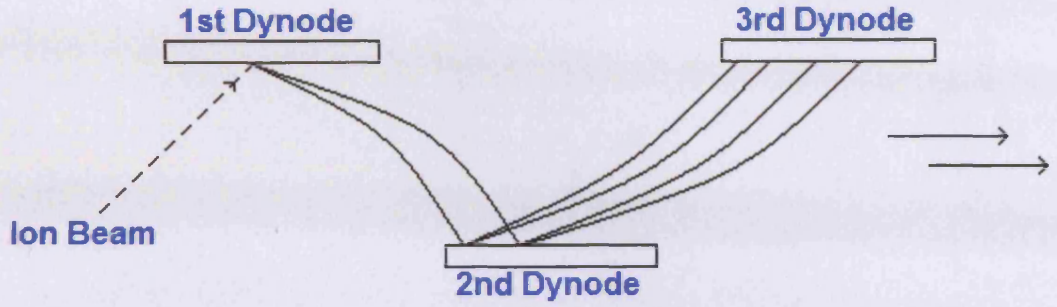

Figure 2.8: The basic principles of an electron multiplier

2.4.7.3 Experimental

GC-MS was carried out on a Walters GCT Premier GC fitter with a HP 6890N Mass spectrometer using electron impact.

Chapter Three

3. Benzyl Alcohol Oxidation

3.1 Introduction

The oxidation of primary alcohols to aldehydes is an important process both, in the laboratory and industrially, as they are valuable as both chemical intermediates and components in the perfume industry. Previous studies[1] have shown that that supported Au and Au+Pd catalysts are effective for the selective oxidation of benzyl alcohol in the liquid phase. The oxidation of benzyl alcohol can be carried out over a wide range of reaction conditions which makes it an ideal reaction for the screening of new catalysts which can subsequently be applied to different catalytic systems. The reaction scheme for benzyl alcohol is shown in scheme 3.1.

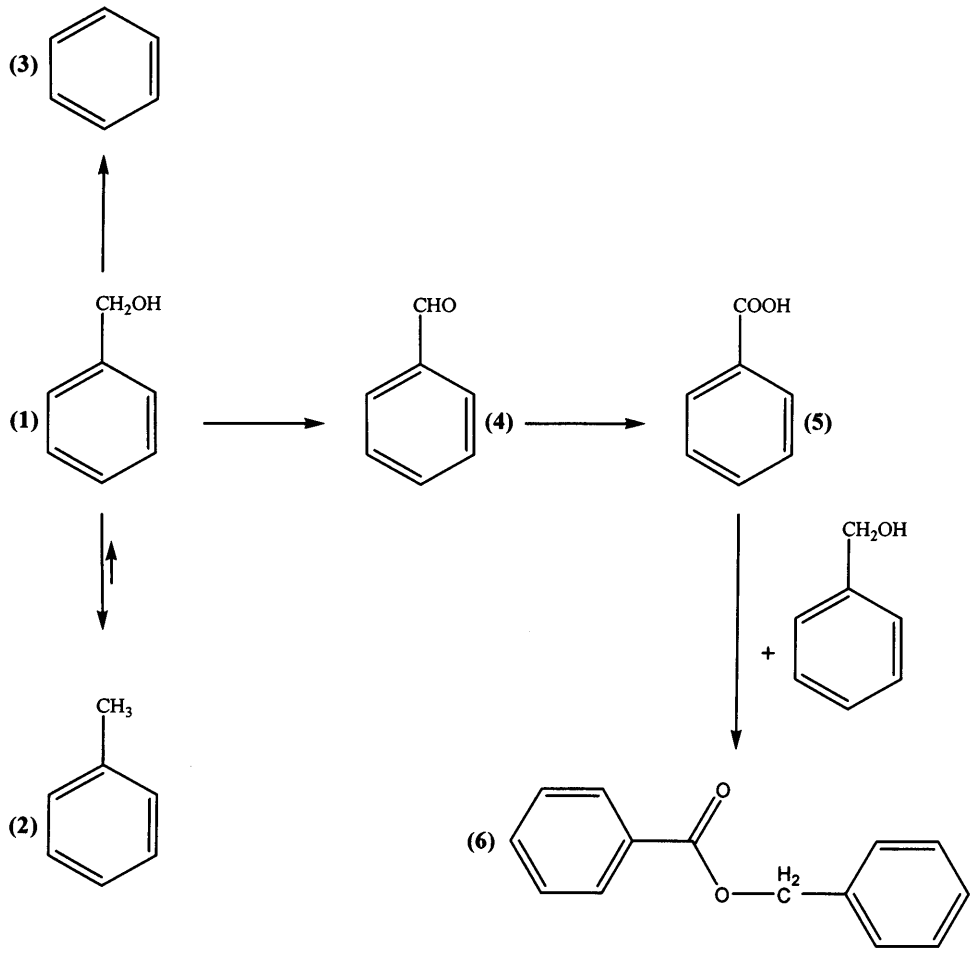

Scheme 3.1: The oxidation of benzyl alcohol; (1) benzyl alcohol, (2) Toluene, (3) Benzene, (4) Benzladehyde, (5) Benzoic acid, (6) Benzyl Benzoate.

The oxidation of benzyl alcohol will typically yield benzaldehyde as the majority product with small quantities of toluene and benzene; however, the more active catalysts can also perform the sequential oxidation to form benzoic acid, which can then react with the starting material to form benzyl benzoate. A typical GC trace is shown in figure 3.1, with the products labelled.

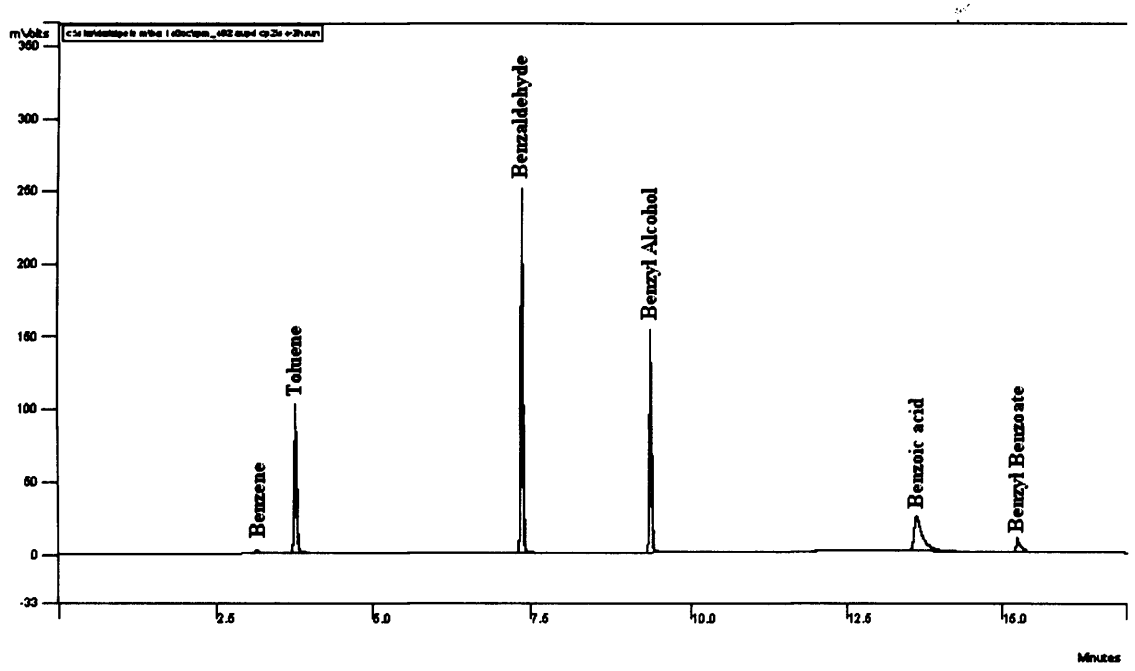

Figure 3.1: a GC trace from the oxidation of benzyl alcohol.

Gold on nanocrystalline ceria, first prepared by Corma *et al*[2], by co-precipitation, was shown to exhibit an activity two orders of magnitude greater than conventional ceria, prepared by precipitation, for the oxidation of CO. Ceria prepared by precipitation of the precursor using supercritical CO_2 as an antisolvent, followed by calcination, has been shown to give a nanocrystalline CeO_2 support that is more effective for CO oxidation, at ambient temperatures, than analogous CeO_2 prepared by simple calcination of the cerium acetate precursor[3] (scheme 3.2).

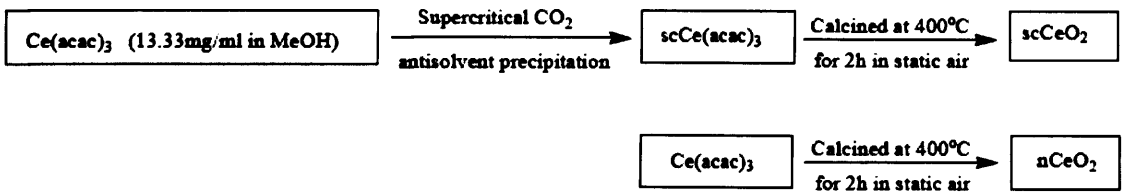

Scheme 3.2: The preparation of $ScCeO_2$ and $nCeO_2$.

Recent work by Corma and co-workers has shown that ceria supported catalysts can be effective for aldehyde[4] and alcohol oxidations[5], with high turn over numbers achieved by gold supported on ceria catalysts. A series of gold, palladium and gold + palladium catalysts supported on $nCeO_2$ (ceria prepared by calcination of the precursor that has not been subjected to antisolvent precipitation) and $ScCeO_2$ (ceria prepared by calcination of the precursor that has been subjected to antisolvent precipitation) were prepared and investigated for the oxidation of benzyl alcohol.

3.2 The oxidation of benzyl alcohol by Au+Pd catalysts prepared by non-supercritical methods.

3.2.1 The optimisation of reaction conditions

3.2.1.1 The effect of temperature

A gold and palladium bi-metallic catalyst supported on titania was prepared using the co-impregnation method (2.5%Au+2.5%Pd/TiO_{2IMP}) as described in chapter 2, and calcined at 400 °C in static air for 3 hours. This catalyst was evaluated for benzyl alcohol oxidation at various temperatures. Blank reactions were carried out at the corresponding temperatures to check for oxidation. The results are shown in table 3.1 and figures 3.2-3.5.

As the temperature of the reaction is increased, the conversion of the catalysed reaction increases; however the conversion of the un-catalysed blank reaction also increases in the temperature range of 100 °C to 140 °C the increase in the un-catalysed conversion is not significant, however at 160 °C, where the catalysed reactions shows the highest conversion the un-catalysed reaction is also significant. The selectivities towards benzaldehyde and benzoic acid were also evaluated and are shown in figure 3.6; at higher temperatures the selectivity towards benzaldehyde decreases while the selectivity towards benzoic acid increases. However, if these selectivities are considered in terms of the reaction conversion instead (figure 3.7) it can be seen that the reactions are following the same profile, independently of temperature.

Table 3.1: Conversion of benzyl alcohol and TOF after 0.5h of reaction by 2.5%Au+2.5%Pd/TiO_{2IMP} at various temperatures with 10 bar O_2 and stirred at 1500 rpm.

Temperature (°C)	Conversion @ 0.5h of Reaction (%)	TOF @ 0.5 h of Reaction (mol mol^{-1} h^{-1})
100	0.19	26
120	1.51	1295
140	4.31	3687
160	33.24	28409

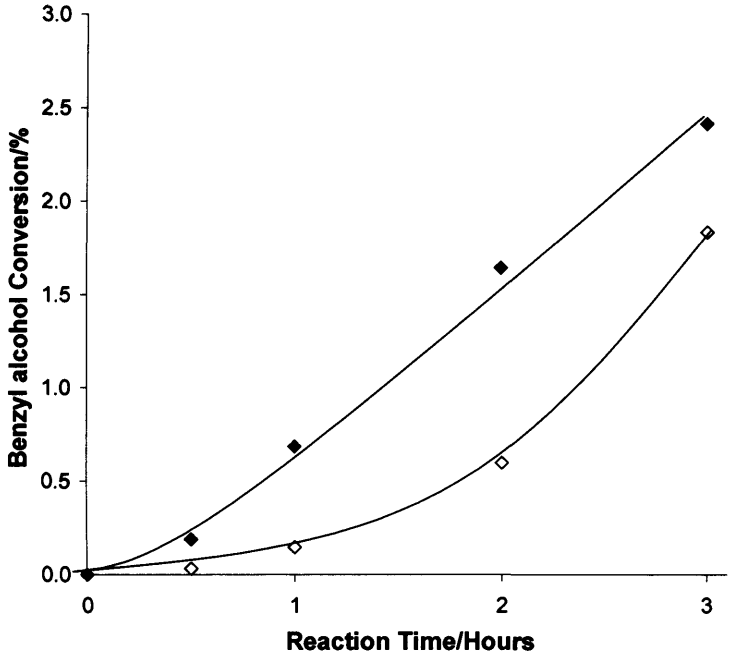

Figure 3.2: The oxidation of benzyl alcohol: blank reaction (◊) and using 25mg 2.5%Au+2.5%Pd/TiO_{2IMP} (♦) at 100 °C with 10 bar O_2, stirred at 1500 rpm.

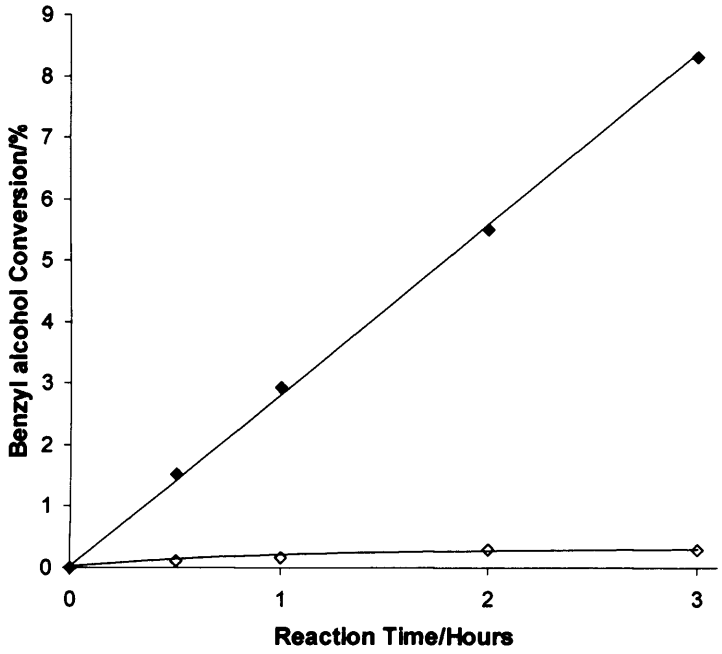

Figure 3.3: The oxidation of benzyl alcohol: blank reaction (◊) and using 25mg 2.5%Au+2.5%Pd/TiO_{2IMP} (♦) at 120 °C with 10 bar O_2, stirred at 1500 rpm.

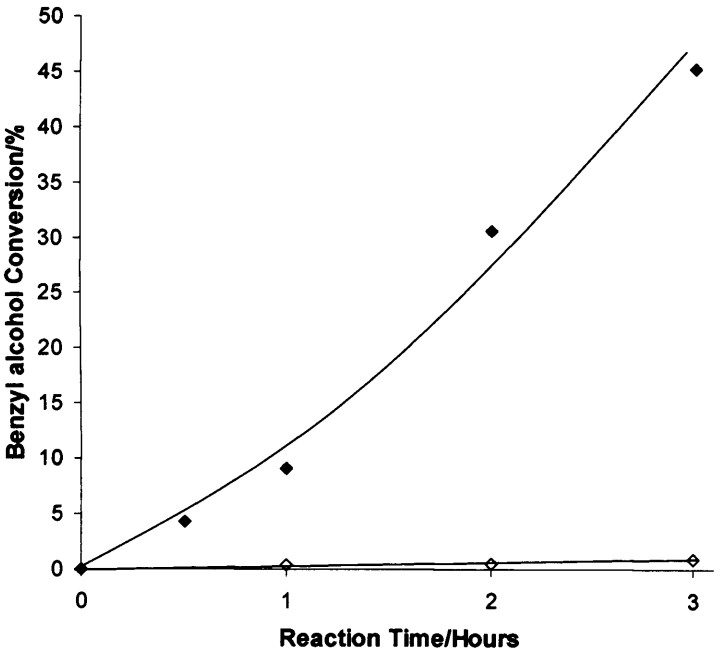

Figure 3.4: The oxidation of benzyl alcohol: blank reaction (◊) and using 25mg 2.5%Au+2.5%Pd/TiO_{2IMP} (♦) at 140 °C with 10 bar O_2, stirred at 1500 rpm.

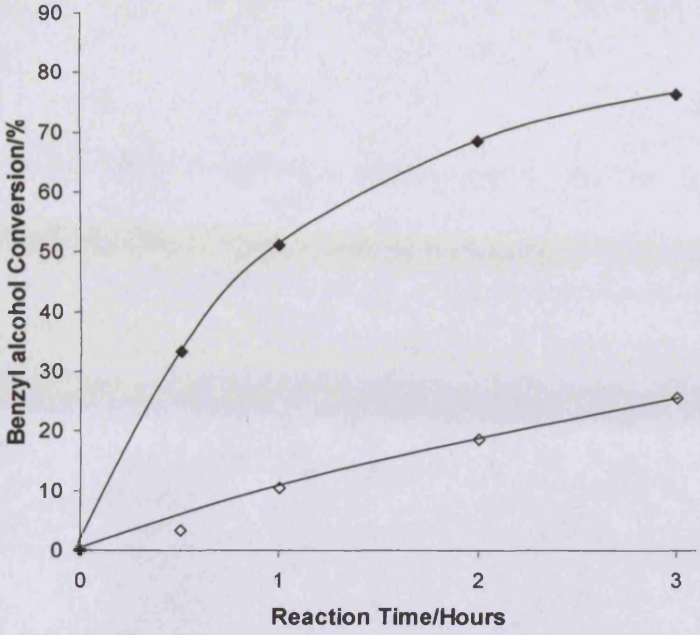

Figure 3.5: The oxidation of benzyl alcohol: blank reaction (◊) and using 25mg 2.5%Au+2.5%Pd/TiO_{2IMP} (♦) at 160 °C with 10 bar O_2, stirred at 1500 rpm.

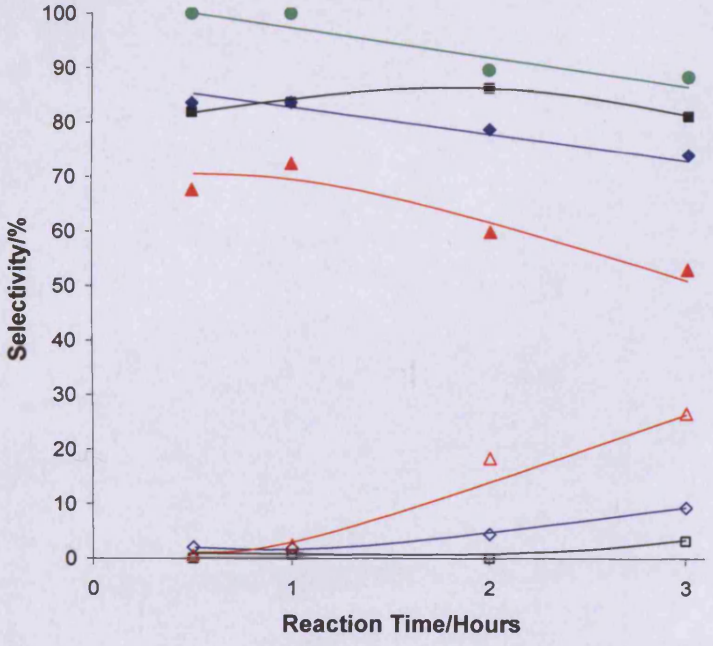

Figure 3.6: The selectivity towards benzaldehyde (closed symbols) and benzoic acid (open symbols) at 100 °C (♦), 120 °C (♦), 140 °C (♦) and 160 °C (♦).

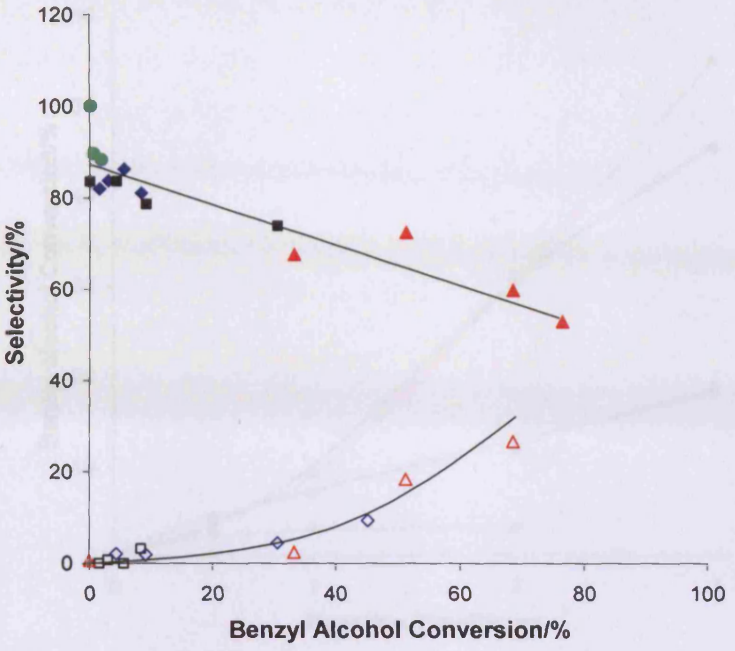

Figure 3.7: The selectivity towards benzaldehyde (closed symbols) and benzoic acid (open symbols) at 100 °C (♦), 120 °C (♦), 140 °C (♦) and 160 °C (♦) in terms of the conversion of benzyl alcohol.

3.2.1.2 The effect of the catalyst support

Following the work of Edwards *et al*[6] who used gold-palladium catalysts for the direct synthesis of hydrogen peroxide and found that catalysts supported on activated carbon are more effective than those supported on titania, and Su *et al*[7] who found gold-palladium supported on gallia to be effective for the oxidation of benzyl alcohol, oxidations of benzyl alcohol were carried out using these supports and ceria prepared by calcination of the acetyl acetate precursor.

Although the initial activity of the catalysts was very similar, as shown in table 3.2, the titania and carbon (G60) supported catalysts showed far greater activity over the extended reaction duration, figure 3.8.

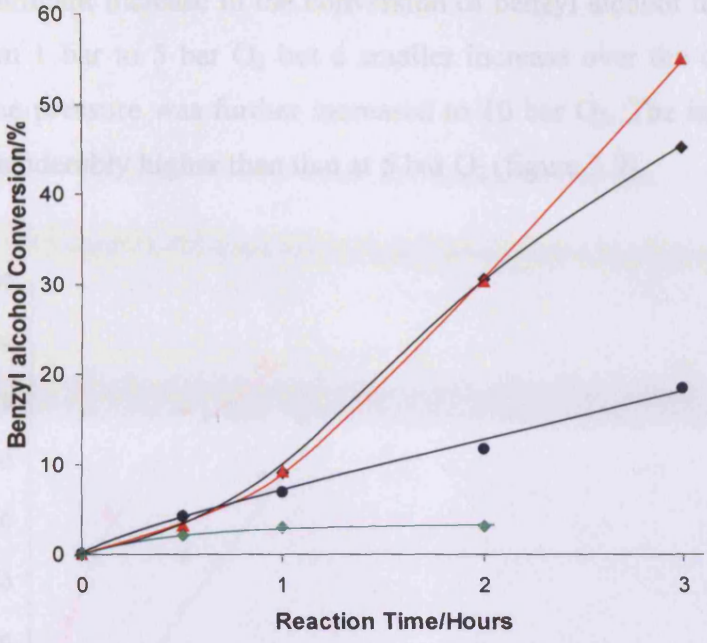

Figure 3.8: The oxidation of benzyl alcohol using 25mg 2.5%Au+2.5%Pd/TiO_{2IMP} (♦)25mg 2.5%Au+2.5%Pd/G60 (▲) 2.5%Au+2.5%Pd/CeO_2 (♦) and 2.5%Au+2.5%Pd/Ga_2O_3 (●) at 140 °C with 10 bar O_2, stirred at 1500 rpm.

Table 3.2: Conversion of benzyl alcohol and TOF after 0.5h of reaction using 2.5%Au+2.5%Pd_{IMP} on various supports at 140 °C, 10 bar O_2 and stirred at 1500 rpm; TOF based on theoretical metal content.

Support	Conversion @ 0.5h of reaction (%)	TOF @ 0.5 h of reaction (mol mol^{-1} h^{-1})
TiO_2	4.31	3687
Carbon G60	3.16	2702
Ga_2O_3	4.16	3551
CeO_2	2.12	1815

3.2.1.3 The effect of oxygen pressure

Test reactions were carried out at 160 °C, (stirring rate 1500 rpm) using 25mg 2.5%Au+2.5%Pd/TiO_{2IMP} to investigate the effect of pressure on the rate of reaction.

There was a significant increase in the conversion of benzyl alcohol upon increasing the pressure from 1 bar to 5 bar O_2 but a smaller increase over the duration of the reaction when the pressure was further increased to 10 bar O_2. The initial rate at 10 bar O_2 is still considerably higher than that at 5 bar O_2 (figure 3.9).

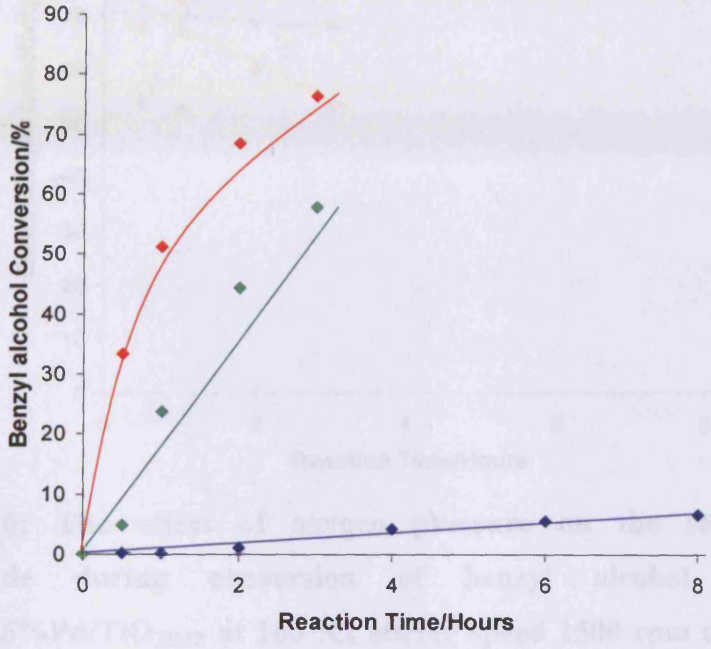

Figure 3.9: The effect of oxygen pressure on the conversion of benzyl alcohol using 25 mg 2.5%Au+2.5%Pd/TiO_{2IMP} at 160 °C, stirrer speed 1500 rpm and O_2pressure of 1 bar (♦), 5 bar (♦) and 10 bar (♦)

The selectivity towards benzaldehyde was also monitored (figure 3.10) and the highest selectivity was shown for the reaction carried out at the lowest pressure.

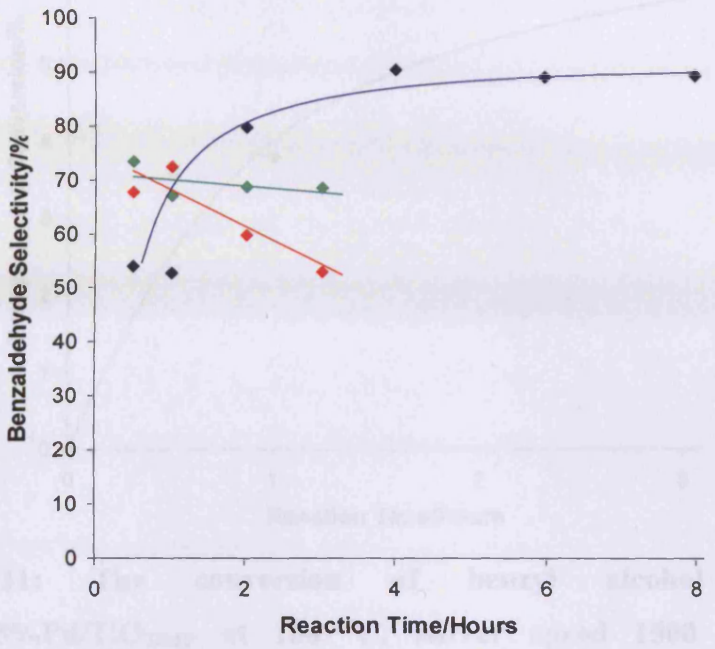

Figure 3.10: The effect of oxygen pressure on the selectivity towards benzaldehyde during conversion of benzyl alcohol using 25 mg 2.5%Au+2.5%Pd/TiO_{2IMP} at 160 °C, stirrer speed 1500 rpm and O_2 pressure 1 bar (♦), 5 bar (♦) and 10 bar (♦)

3.2.1.4 The reaction in the absence of O_2

To further investigate the effect of pressure on the reaction a test was carried out in the absence of oxygen. This reaction was carried out as described previously in chapter 2 except the oxygen was substituted by 20 bar helium.

The conversion of benzyl alcohol (figure 3.11) was considerably lower than the same reaction carried out with 10 bar O_2 (figure 3.5) and the distribution of products (figure 3.12 and 3.7) was very different. There was an almost 50% selectivity towards toluene and around 50% combined selectivity towards benzaldehyde and benzoic acid compared to a total benzaldehyde and benzoic acid selectivity of around 80% when 10 bar O_2 is used.

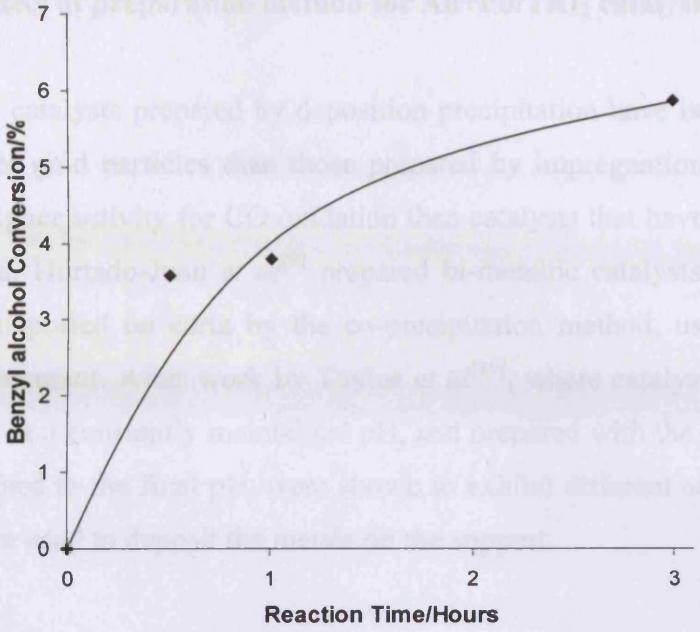

Figure 3.11: The conversion of benzyl alcohol using 25mg 2.5%Au+2.5%Pd/TiO_{2IMP} at 160 °C, stirrer speed 1500 rpm under an atmosphere of 20 bar He.

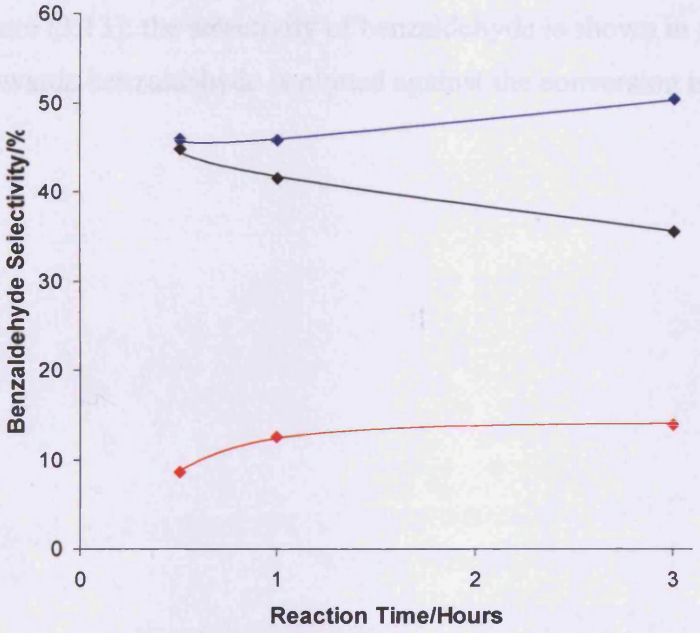

Figure 3.12: The selectivities towards the major products during the conversion of benzyl alcohol using 25mg 2.5%Au+2.5%Pd/TiO_{2IMP} at 160 °C, stirrer speed 1500 rpm under an atmosphere of 20 bar He: benzaldehyde (♦), toluene (♦) and benzoic acid (♦)

3.2.3 The effect of preparation method for Au+Pd/TiO_2 catalysts

Gold catalysts prepared by deposition precipitation have been shown to have much smaller gold particles than those prepared by impregnation[8]; these catalysts also show higher activity for CO oxidation than catalysts that have been prepared by impregnation. Hurtado-Juan *et al*[9] prepared bi-metallic catalysts comprising gold-palladium supported on ceria by the co-precipitation method, using $Pd(NO)_3$ as a palladium precursor. After work by Taylor *et al*[10], where catalysts prepared by co-precipitation at a constantly maintained pH, and prepared with the pH of the solution gradually raised to the final pH, were shown to exhibit different activities, these two methods were used to deposit the metals on the support.

3.2.3.1 Au+Pd/TiO_2 prepared by wet impregnation

To compare the activity of the deposition precipitation prepared catalysts a catalyst prepared by co-impregnation was tested. The catalyst was tested for its initial activity and the used catalyst was tested for its stability. The results of these tests are shown in figure (3.13): the selectivity of benzaldehyde is shown in figure 3.14 and the selectivity towards benzaldehyde is plotted against the conversion in figure 3.15.

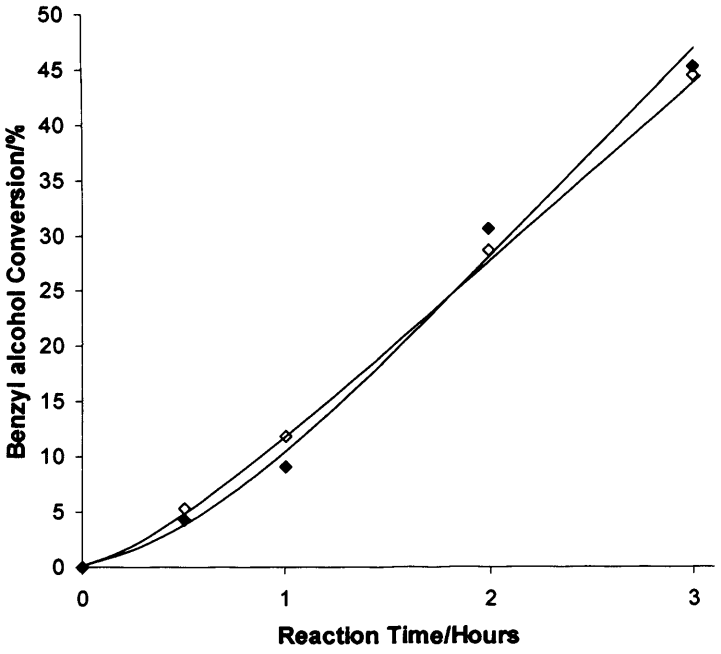

Figure 3.13: The oxidation of benzyl alcohol using 25mg 2.5%Au+2.5%Pd/TiO_2 prepared by the co-impregnation method: fresh catalyst (◊) and used catalyst (♦) at 140 °C with 10 bar O_2, stirred at 1500 rpm.

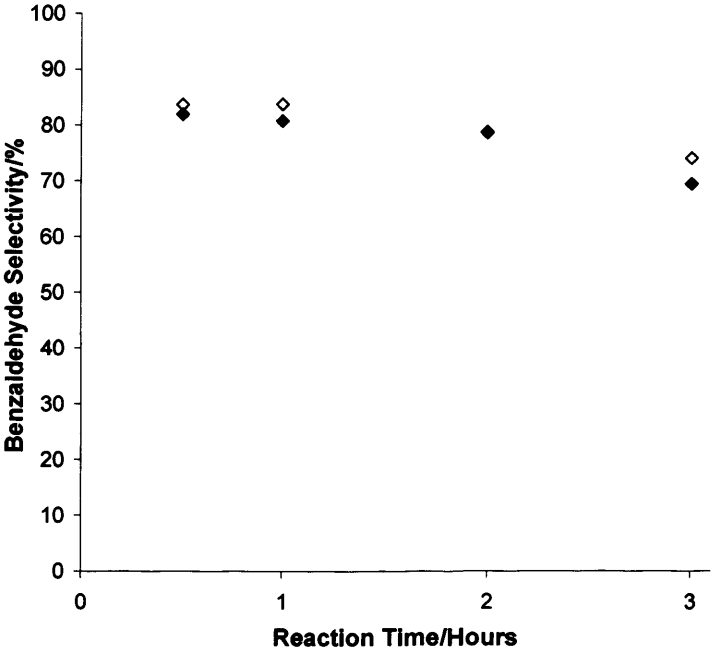

Figure 3.14: The selectivity towards benzaldehyde during the oxidation of benzyl alcohol using 25mg 2.5%Au+2.5%Pd/TiO_2 prepared by the co-impregnation method: fresh catalyst (◊) and used catalyst (♦) at 140 °C with 10 bar O_2, stirred at 1500 rpm.

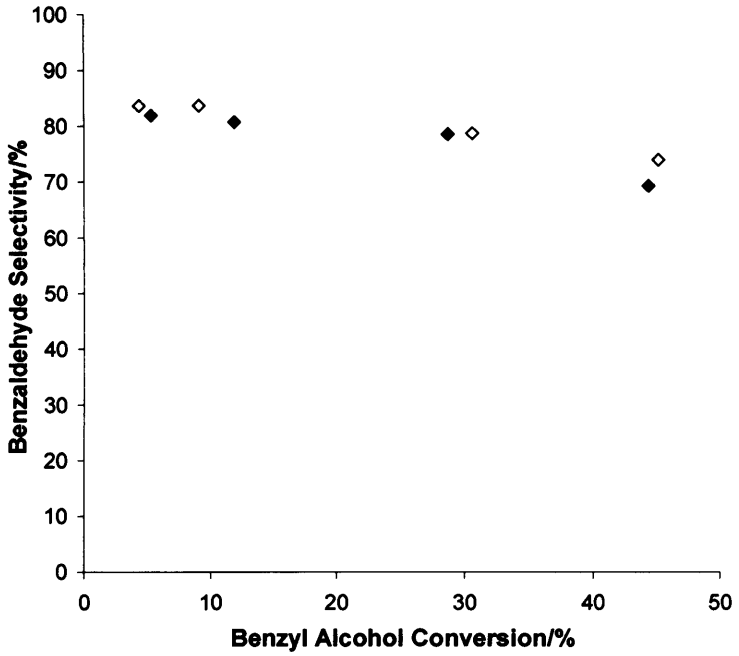

Figure 3.15: The selectivity towards benzaldehyde during the oxidation of benzyl alcohol using 25mg 2.5%Au+2.5%Pd/TiO_2 prepared by co-impregnation: fresh catalyst (◊) and used catalyst (♦) at 140 °C with 10 bar O_2, stirred at 1500 rpm, plotted against the conversion of benzyl alcohol.

3.2.3.2 Au+Pd /TiO_2 prepared by deposition precipitation at constant pH

The results from the tests of the deposition precipitation catalyst prepared at constant pH, both fresh and once-used, are shown in figure (3.16). As can be seen the activity of this catalyst is considerably higher than the activity of the catalyst prepared by co-impregnation (figure 3.13). The second use of the catalyst shows a slight drop in the activity throughout the run. The initial activity of this catalyst at 140 °C is very high and is only slightly less than the activity shown by the co-impregnation catalyst at 160 °C (figure 3.5). The selectivity towards benzaldehyde for the fresh and used catalysts is shown in figure 3.17 with the selectivities of the new and used catalyst being very similar, and the selectivity is shown in terms of the conversion in figure 3.18.

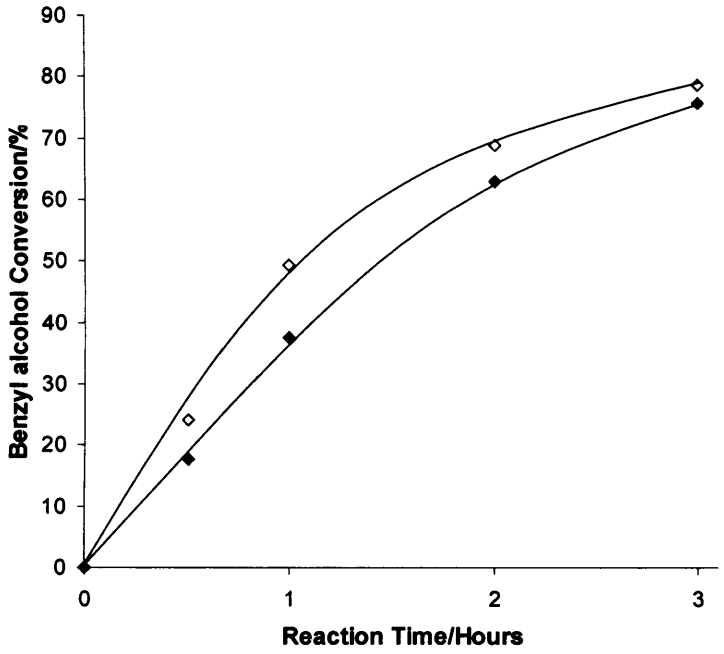

Figure 3.16: The oxidation of benzyl alcohol using 25mg 2.5%Au+2.5%Pd/TiO_2 prepared by co-deposition precipitation at constant pH: fresh catalyst (◊) and used catalyst (♦) at 140 °C with 10 bar O_2, stirred at 1500 rpm.

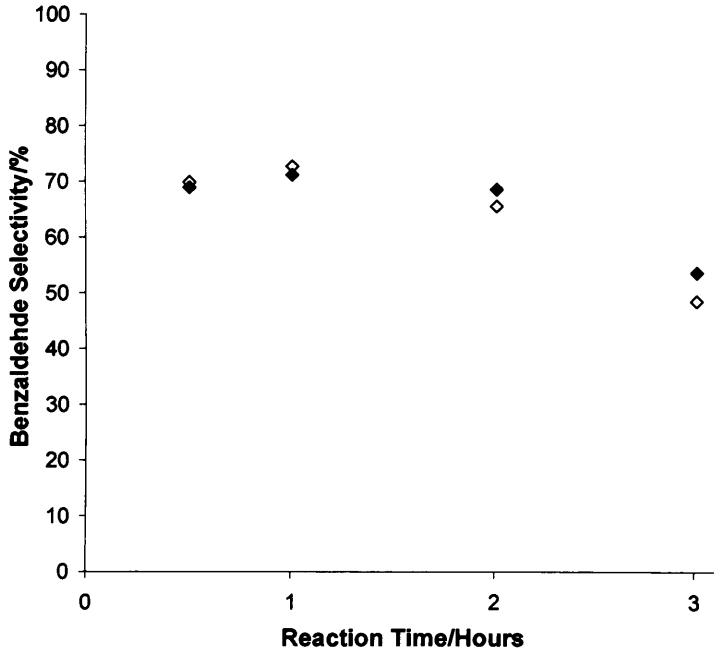

Figure 3.17: The selectivity towards benzaldehyde during the oxidation of benzyl alcohol using 25mg 2.5%Au+2.5%Pd/TiO_2 prepared by co-deposition precipitation at constant pH : fresh catalyst (◊) and used catalyst (♦) at 140 °C with 10 bar O_2, stirred at 1500 rpm.

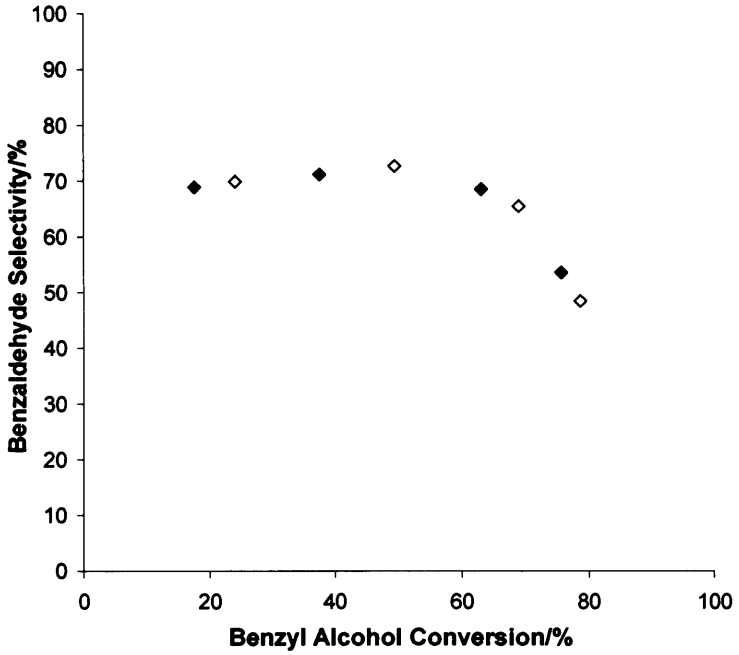

Figure 3.18: The selectivity towards benzaldehyde during the oxidation of benzyl alcohol using 25mg 2.5%Au+2.5%Pd/TiO_2 prepared by co-deposition precipitation at constant pH : fresh catalyst (◊) and used catalyst (♦) at 140 °C with 10 bar O_2, stirred at 1500 rpm, plotted against the conversion of benzyl alcohol.

3.3.3 Au+Pd/TiO_2 prepared by deposition precipitation at increasing pH.

The catalyst prepared by adding the metal precursors initially and then raising the pH to pH 8 also showed very high activity throughout the reaction run, although with slightly lower initial activity (figure 3.19). However, the final conversion of both catalysts prepared by the different deposition methods was very similar. The second use of the catalyst prepared at increasing pH however did not show the decrease in activity compared to the fresh catalyst that was apparent with the catalyst prepared at constant pH (figure 3.16). The selectivity towards benzaldehyde by the fresh and used catalysts is shown in figure 3.20 in terms of reaction time and in terms of conversion in figure 3.21.

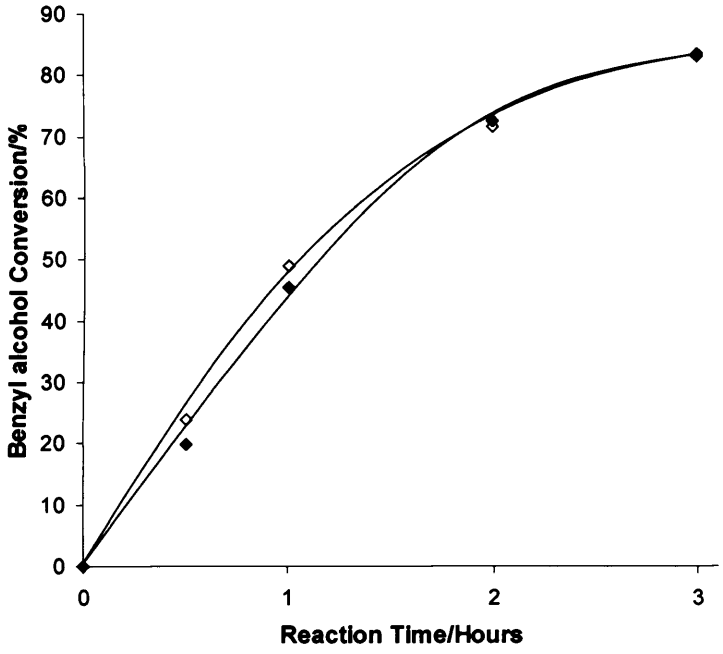

Figure 3.19: The oxidation of benzyl alcohol using 25mg 2.5%Au+2.5%Pd/TiO_2 prepared by co-deposition precipitation with increasing pH: fresh catalyst (◊) and used catalyst (♦) at 140 °C with 10 bar O_2, stirred at 1500 rpm.

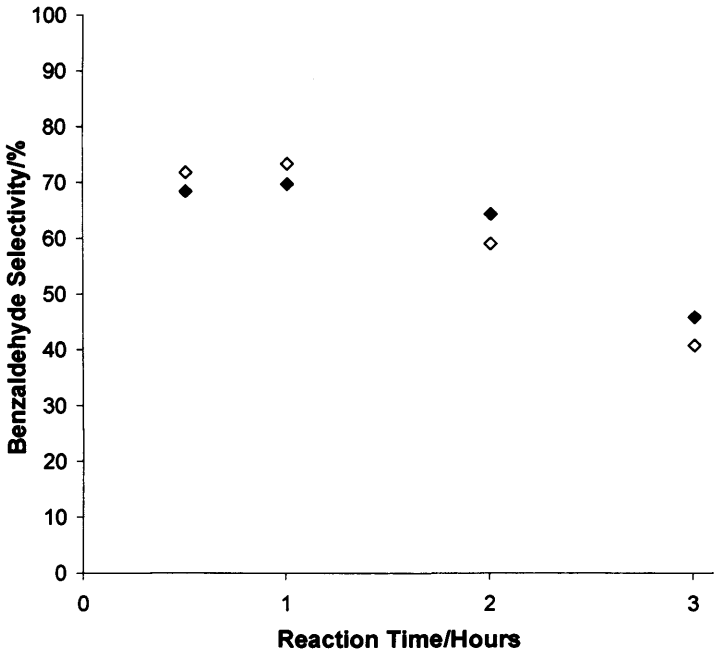

Figure 3.20: The selectivity towards benzaldehyde during the oxidation of benzyl alcohol using 25mg 2.5%Au+2.5%Pd/TiO_2 prepared by co-deposition precipitation with increasing pH: fresh catalyst (◊) and used catalyst (♦) at 140 °C with 10 bar O_2, stirred at 1500 rpm.

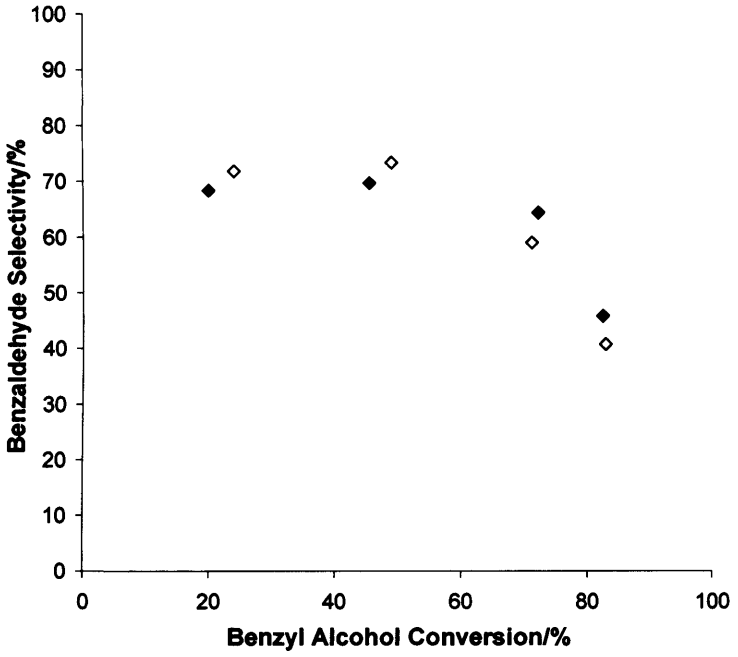

Figure 3.21: The selectivity towards benzaldehyde during the oxidation of benzyl alcohol using 25mg 2.5%Au+2.5%Pd/TiO_2 prepared by co-deposition precipitation with increasing pH : fresh catalyst (◊) and used catalyst (♦) at 140 °C with 10 bar O_2, stirred at 1500 rpm, plotted against the conversion of benzyl alcohol.

The initial activity of the deposition precipitation catalysts is shown in table 3.3; it is clear that the catalysts prepared by deposition precipitation are far more active than those prepared by co-impregnation.

Table 3.3 Conversion of benzyl alcohol and TOF (based on theoretical metal content) after 0.5h of reaction using 2.5%Au+2.5%/TiO_2 prepared by different methods: 140 °C, 10 bar O_2 and stirred at 1500 rpm.

Preparation Method	Conversion @ 0.5h of Reaction/%	TOF @ 0.5 h of Reaction (mol mol^{-1} h^{-1})
Co-Impregnation	4.31	3687
Deposition Precipitation (Constant pH)	24.12	20611
Deposition Precipitation (Increasing pH)	23.97	20482

3.2.4 Catalyst characterisation

3.2.4.1 SEM

SEM analysis was performed on the catalysts as detailed in chapter 2

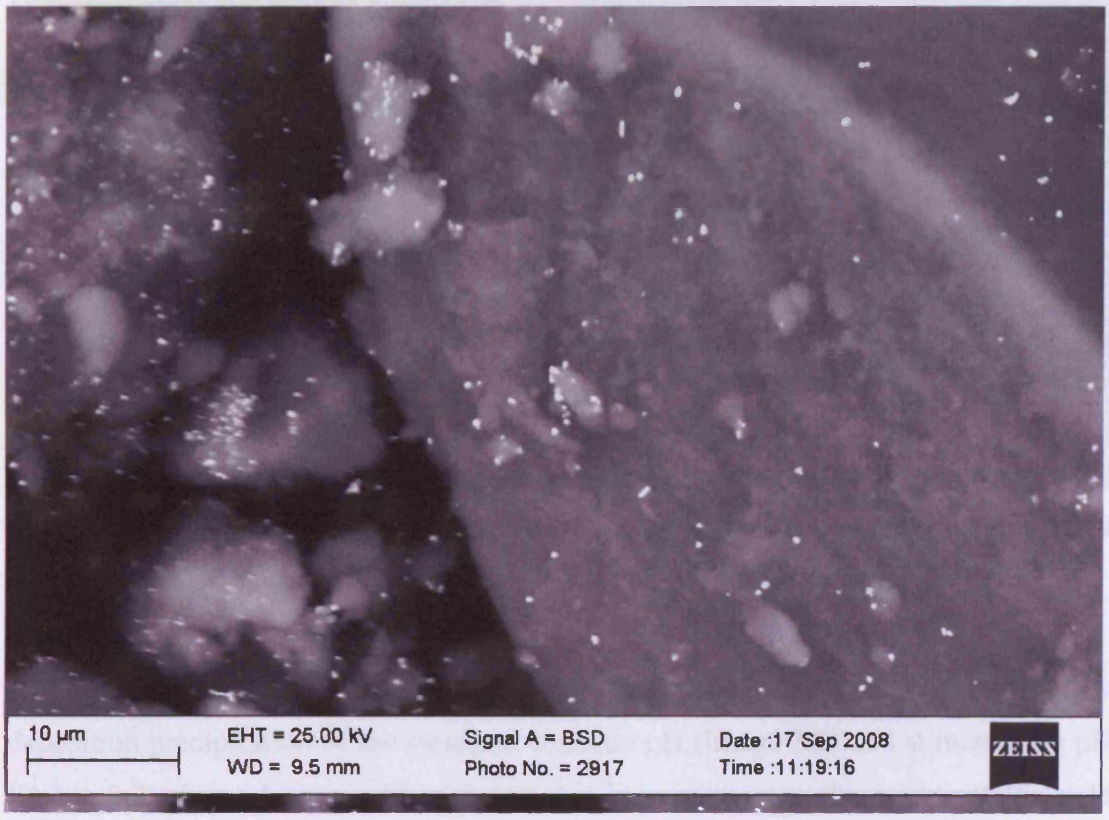

Image 3.1: An SEM image of 2.5%Au+2.5%Pd/TiO_2 prepared by co-impregnation of the metals.

The SEM image of the 2.5%Au+2.5%Pd/TiO_2 prepared by co-impregnation of the metals (image 3.1) shows large metal particles, these are characteristic of this preparation method.

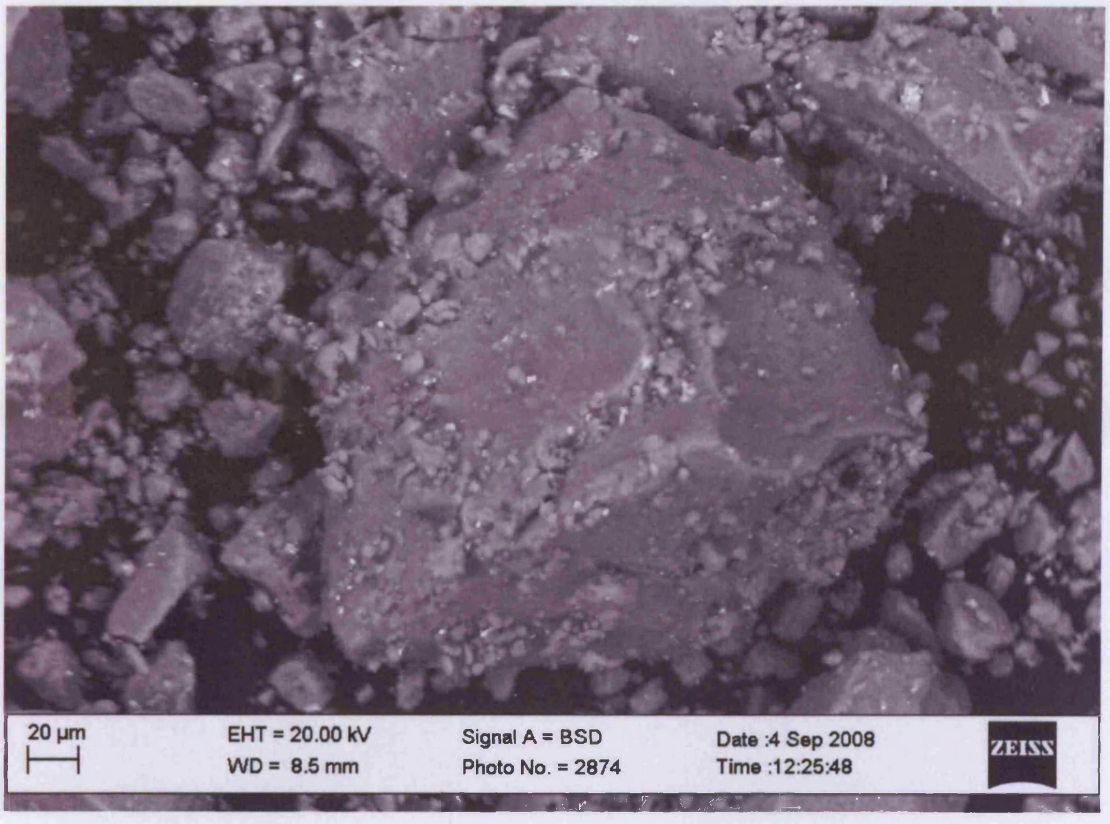

Image 3.2: An SEM image of 2.5%Au+2.5%Pd/TiO_2 prepared by deposition precipitation of the metals whilst increasing the pH of the solution.

Similarly the SEM images of the 2.5%Au+2.5%Pd/TiO_2 catalyst prepared by deposition precipitation of the metals at constant pH (image 3.2) and at increasing pH (Image 3.3) shows large metal particles; this is in contrast to the monometallic gold catalysts prepared by deposition precipitation where the gold particles are typically less than 10 nm in diameter[17].

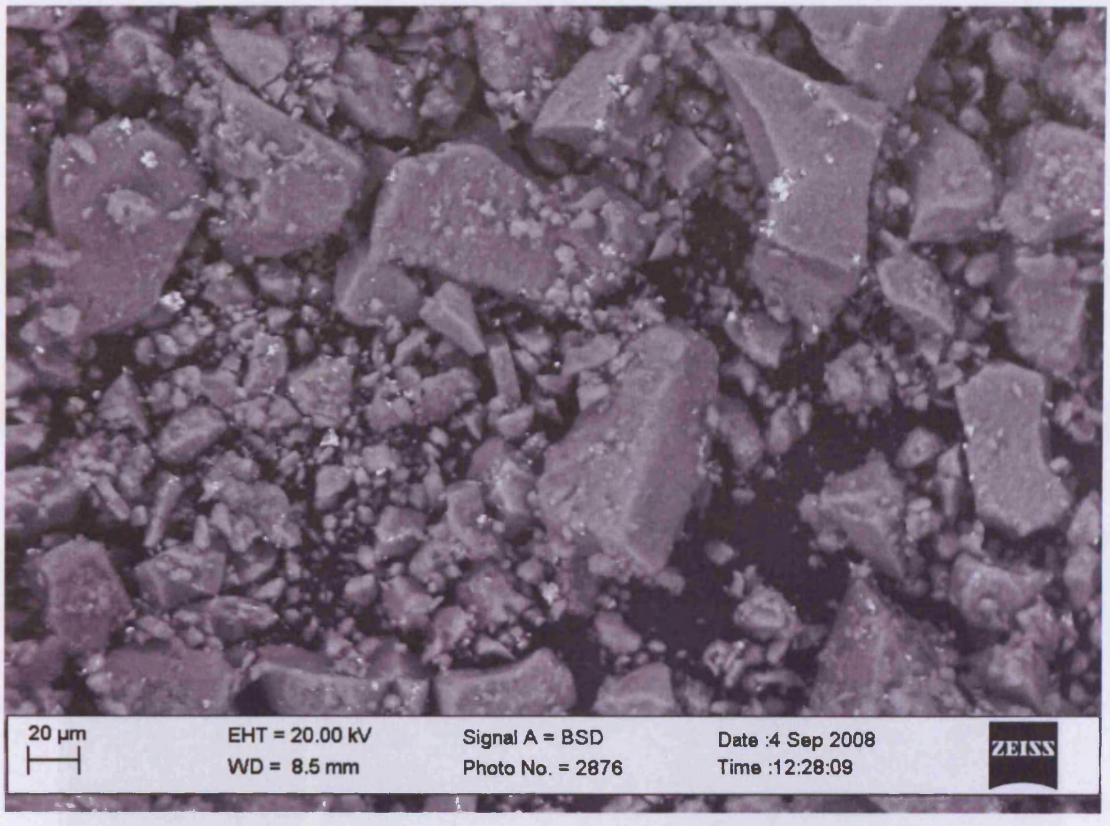

Image 3.3: An SEM image of a 2.5%Au+2.5%Pd/TiO_2 catalyst prepared by deposition precipitation of the metals whilst increasing the pH of the solution.

EDX analysis of both of the catalysts prepared using deposition precipitation showed the absence of chlorine (Figures 3.22 and 3.23) which is in contrast to the catalyst prepared by co-impregnation of the metal which the EDX analysis showed contained chlorine (figure 3.24).

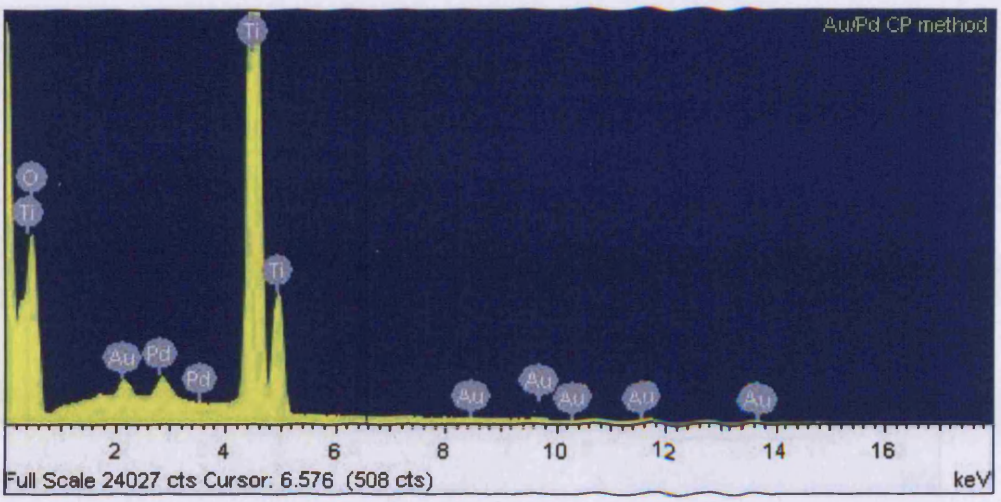

Figure 3.22: EDX analysis of a 2.5%Au+2.5%Pd/TiO_2 catalyst prepared by deposition precipitation of the metals whilst increasing the pH of the solution.

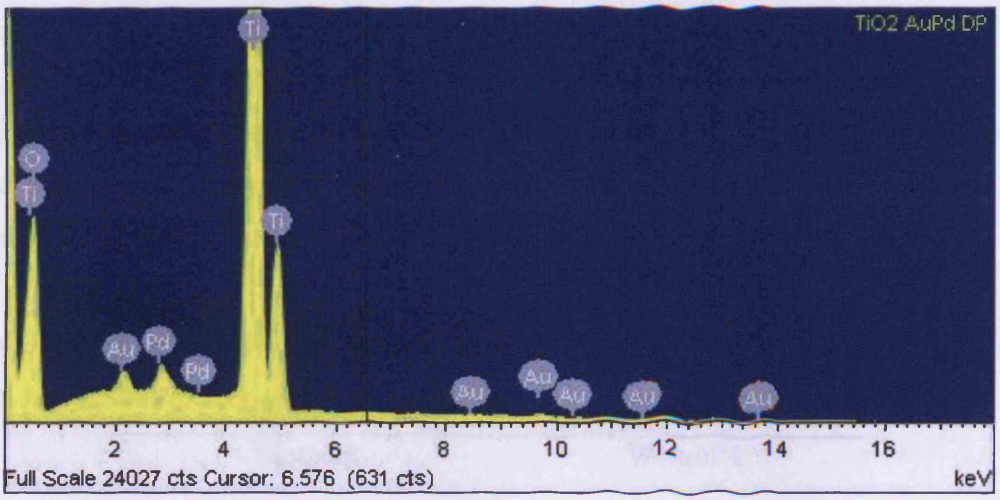

Figure 3.23: EDX analysis of a 2.5%Au+2.5%Pd/TiO_2 catalyst prepared by deposition precipitation of the metals at constant solution pH.

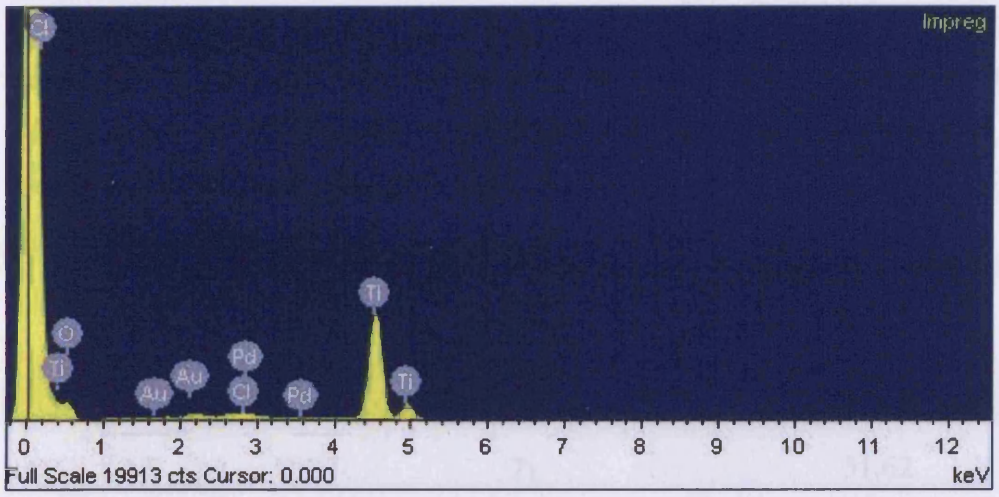

Figure 3.24: EDX analysis of a 2.5%Au+2.5%Pd/TiO_2 catalyst prepared by co-impregnation.

The EDX analysis was also able to give accurate metal loadings for the catalysts. The metal loadings for the catalysts prepared by deposition precipitation were significantly lower than both the theoretical loadings and those of the co-impregnated catalysts (tables 3.4, 3.5 and 3.6).

Table 3.4: Elemental composition derived from EDX measurements for a 2.5%Au+2.5%Pd/TiO_2 catalyst prepared by co-impregnation.

Element	Weight%
O	39.36
Ti	54.3
Pd	2.56
Au	2.66
Cl	1.23

Table 3.5: Elemental composition derived from EDX measurements for a 2.5%Au+2.5%Pd/TiO_2 catalyst prepared by deposition precipitation of the metals whilst increasing the pH of the solution.

Element	Weight%
O	45.50
Ti	51.62
Pd	1.54
Au	1.35

Table 3.6: Elemental composition derived from EDX measurements for a 2.5%Au+2.5%Pd/TiO_2 catalyst prepared by deposition precipitation of the metals at constant solution pH.

Element	Weight%
O	44.32
Ti	52.96
Pd	1.49
Au	1.23

3.2.4.2 XPS

The X-ray photoelectron survey spectra of the samples were used to derive surface elemental compositions (atom %) and these are summarised in Table 3.7.

Table 3.7: XPS derived surface elemental compositions for the Au-Pd/TiO_2 catalysts prepared by deposition-precipitation. Data are shown for the unused catalysts and also after use for benzyl alcohol oxidation

	Preparation method	No. uses	Composition atom %					Atom ratio Pd/Au*
			Pd	Au	Ti	O	Cl	
1	DP, increasing pH uncalcined	0	1.28	0.47	28.3	69.5	0.48	2.3
2	DP, increasing pH calcined	0	0.84	0.25	28.6	69.7	0.62	3.0
3	DP, increasing pH calcined	1	0.74	0.23	25.8	73.0	<0.2	2.8
4	DP, increasing pH calcined	2	0.59	0.16	24.8	74.5	<0.2	3.3
5	DP, constant pH uncalcined	0	0.86	0.18	28.2	70.4	0.32	4.4
6	DP, constant pH calcined	1	0.69	0.17	25.5	73.7	<0.2	3.5
7	DP, constant pH calcined	2	0.72	0.21	25.2	73.9	<0.2	3.0

The catalyst prepared whilst increasing the pH of the solution shows significantly higher Pd and Au loadings than the catalyst prepared at constant pH; this may arise from more efficient precipitation or a higher dispersion of the metal particles. The decrease in apparent metal content on calcination, especially for the sample prepared *via* an increasing pH, probably reflects sintering of the metal particles.

Of particular interest is the Pd:Au atom ratio, and how this value is affected by calcination and also after the catalyst has been used for benzyl alcohol oxidation. The theoretical Pd:Au ratio in the Au-Pd catalysts is 1:1 by weight, which is equivalent to an atom ratio of Pd:Au = 1.9:1. For the catalysts prepared with increasing pH the Pd:Au ratio for the uncalcined material is 2.3, not too dissimilar to the theoretical value. However after calcination this increases to 3.0 and remains close to this value after reaction with benzyl alcohol. The increase over the value

expected for homogeneous alloy particles or equally dispersed monometallic Pd and Au particles may reflect particle size changes on calcination or possibly the formation of some Au-core/Pd-shell particles, which have been observed in other systems[22]. In each case the Au(4f) XP signal may be attenuated relative to the Pd(3d) intensity, as a consequence of the low mean free path of electrons in metals which confers surface sensitivity on the XPS technique.

The O:Ti ratios in Table 3.7 are higher than the value of 2:1 expected for stoichiometric titania due to the presence of surface species such as hydroxyl and carbonate groups. No changes were observed in the peak shape or binding energy for the Ti(2p) spectra, which indicated a Ti^{4+} oxidation state throughout.

3.3 Supports prepared by precursor precipitation into a supercritical medium

3.3.1 Reactions of benzyl alcohol over Au, Pd and Au+Pd catalysts supported on $nCeO_2$ and $ScCeO_2$.

Au, Pd and Au+Pd supported on $nCeO_2$ catalysts were prepared by the co-impregnation method and 25 mg of catalyst was tested for the oxidation of benzyl alcohol for 3 hours at 140 °C, 10 bar O_2, and a stirrer speed of 1500 rpm (figure 3.25). The bi-metallic catalyst was found to have the highest conversion with the monometallic gold and palladium catalysts showing lower conversion throughout the course of the reaction. However the initial activity of the gold catalyst was higher than that of both the palladium only and gold palladium bi-metallic catalysts when calculated in terms of the TOF (figure 3.26).

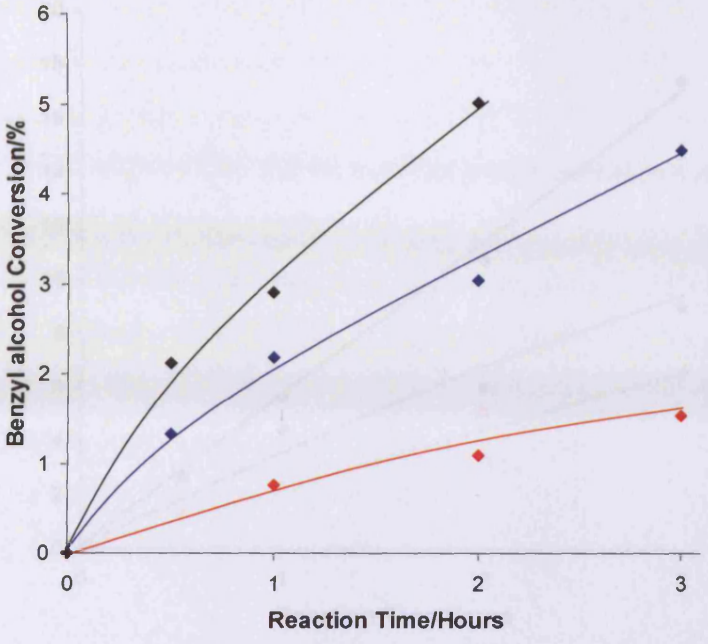

Figure 3.25: The conversion of benzyl alcohol using 2.5wt%Au+2.5wt%Pd/nCeO_2 (♦), 2.5%Au/nCeO_2 (♦) and 2.5%Pd/nCeO_2 (♦): 25mg catalyst, 140°C, 10 bar O_2 and stirrer speed of 1500 rpm.

The analogous catalysts supported on ceria prepared by the supercritical antisolvent method were also tested for benzyl alcohol oxidation. A similar pattern was observed with the highest conversion displayed by the bimetallic catalyst (figure 3.27) but with the highest initial activity shown by the gold catalyst (figure 3.26). The conversions and activities of the catalysts supported on supercritical antisolvent prepared ceria were significantly higher than those supported on the non-supercritically prepared ceria.

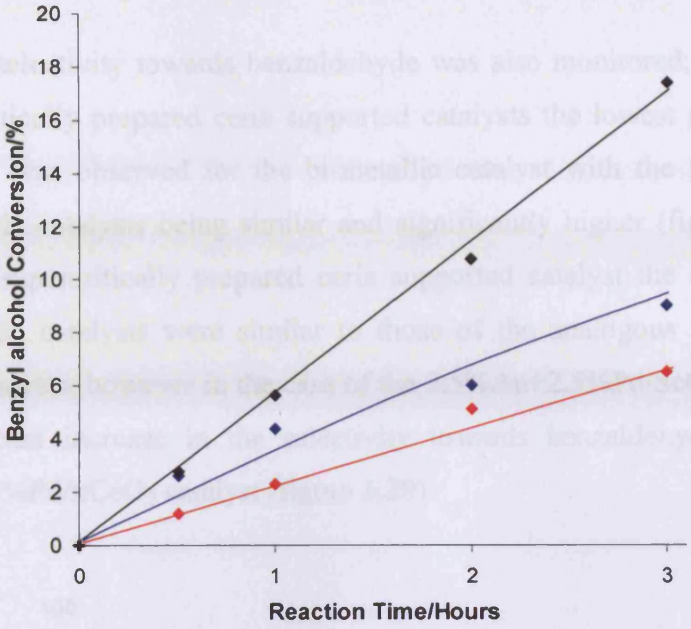

Figure 3.26: The conversion of benzyl alcohol using 2.5wt%Au+2.5wt%Pd/ScCeO$_2$ (♦), 2.5%Au/ScCeO$_2$ (♦) and 2.5%Pd/ScCeO$_2$ (♦):25mg catalyst, 140°C, 10 bar O$_2$ and stirrer speed 1500 rpm.

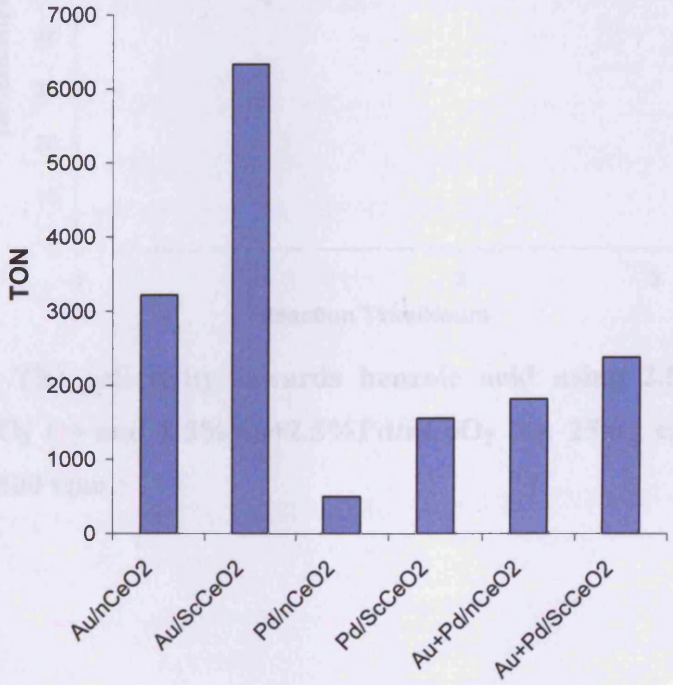

Figure 3.27: The TOF values calculated at 0.5h for the ceria supported catalysts during the oxidation of benzyl alcohol using 25mg catalyst at 140°C, 10 bar O$_2$ and stirrer speed 1500 rpm.

The selectivity towards benzaldehyde was also monitored; in the case of the non-supercritically prepared ceria supported catalysts the lowest selectivity towards benzaldehde was observed for the bi-metallic catalyst with the selectivities of the mono-metallic catalysts being similar and significantly higher (figure 3.28). In the case of the supercritically prepared ceria supported catalyst the selectivities of the mono-metallic catalysts were similar to those of the analogous non-supercritically prepared catalysts; however in the case of the 2.5%Au+2.5%Pd/$ScCeO_2$ catalyst there is a significant increase in the selectivity towards benzaldehyde relative to the 2.5%Au+2.5%Pd/$nCeO_2$ catalyst (figure 3.29).

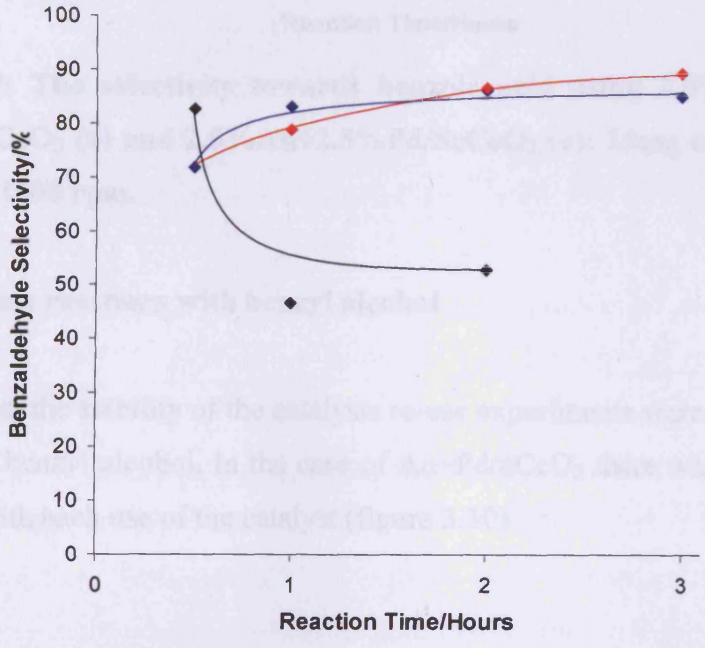

Figure 3.28: The selectivity towards benzoic acid using 2.5%Au/$nCeO_2$ (♦), 2.5%Pd/$nCeO_2$ (♦) and 2.5%Au+2.5%Pd/$nCeO_2$ (♦): 25mg catalyst, 140°C, 10 bar O_2 and 1500 rpm.

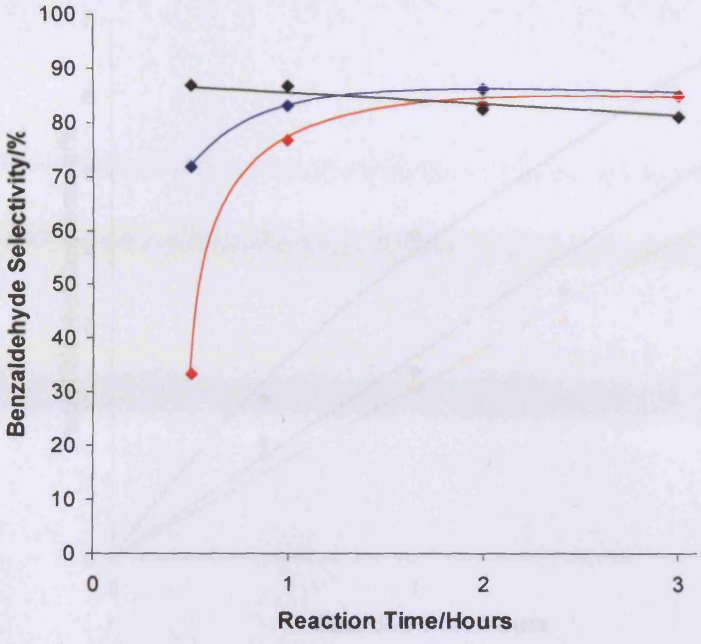

Figure 3.29: The selectivity towards benzoic acid using 2.5%Au/ScCeO$_2$ (♦), 2.5%Pd/ScCeO$_2$ (♦) and 2.5%Au+2.5%Pd/ScCeO$_2$ (♦): 25mg catalyst, 140°C, 10 bar O$_2$ and 1500 rpm.

3.3.2 Re-use reactions with benzyl alcohol

To test the stability of the catalysts re-use experiments were carried out for the oxidation of benzyl alcohol. In the case of Au+Pd/nCeO$_2$ there was a loss of activity associated with each use of the catalyst (figure 3.30).

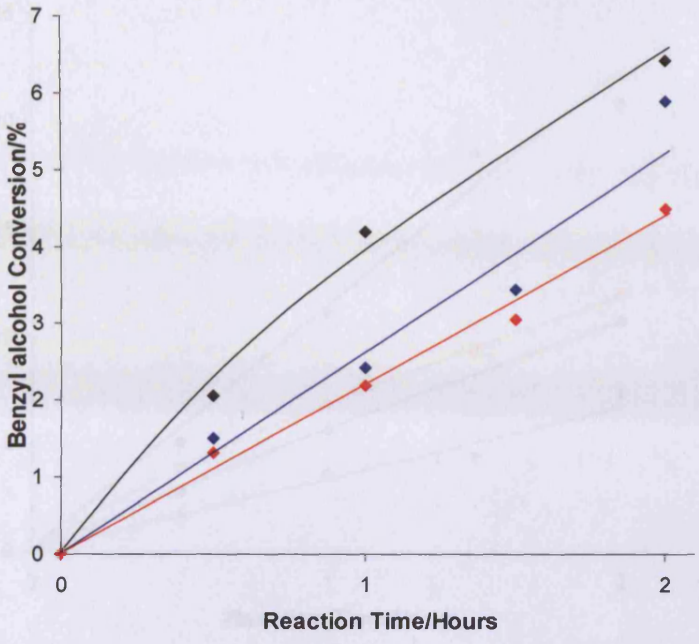

Figure 3.30: The oxidation of benzyl alcohol using a 2.5%Au + 2.5%Pd/nCeO_2 catalyst (140°C, 10 bar O_2 and 1500 rpm) using 25mg of the fresh catalyst (♦), used catalyst (♦) and twice used catalyst (♦).

The catalyst comprising gold-palladium supported on ceria prepared by the supercritical antisolvent method however, showed different behaviour. The reaction with the used catalyst showed significantly higher conversion of benzyl alcohol than the fresh catalyst. Upon further use of this catalyst however the activity of the catalyst decreased, although the twice used catalyst, surprisingly, still showed higher conversion than the fresh catalyst. There was a further decrease in conversion when the three times used catalyst was tested, with its conversion being below the level of the fresh catalyst (figure 3.31).

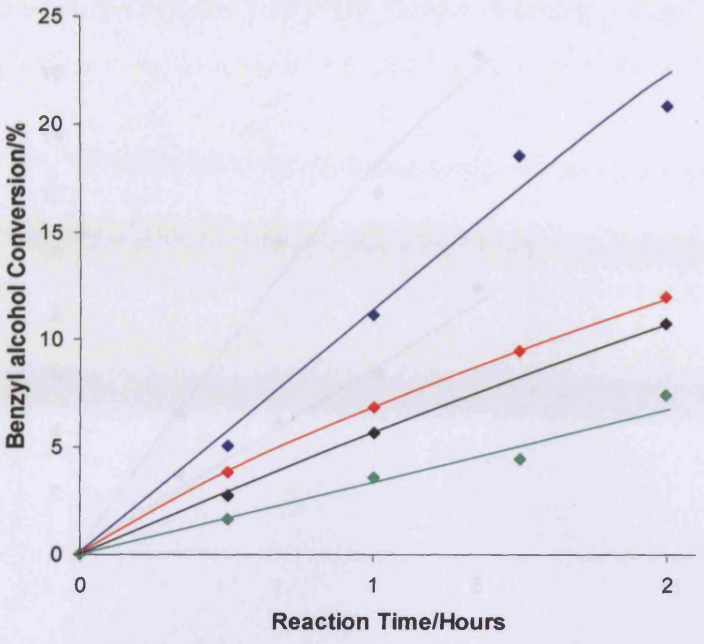

Figure 3.31: The oxidation of benzyl alcohol using a 2.5%Au + 2.5%Pd/$ScCeO_2$ catalyst (140°C, 10 bar O_2 and 1500 rpm, 25mg catalyst): fresh catalyst (♦), once used catalyst (♦), twice used catalyst (♦) and three times used catalyst (♦).

To investigate whether this is an effect of the support or the metallic elements of the catalyst, re-use tests were carried out on the gold supported on ceria prepared by supercritical antisolvent precipitation. Again there is a significant increase in the conversion of benzyl alcohol when testing the used catalyst (figure 3.32). The test was repeated with the Pd/$ScCeO_2$ catalyst with the same effect apparent (figure 3.33).

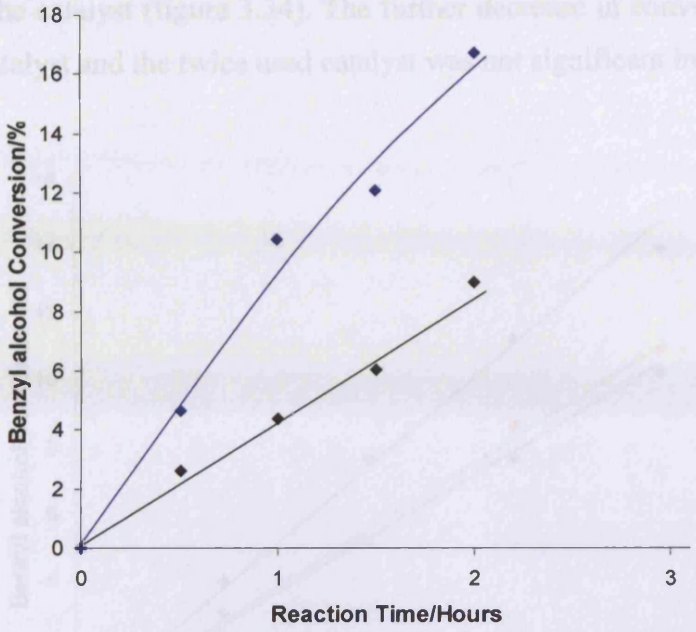

Figure 3.32: The oxidation of benzyl alcohol using 2.5%Au/$ScCeO_2$ (140°C, 10 bar O_2 and 1500 rpm, 25mg catalyst): fresh catalyst (♦) and used catalyst (♦).

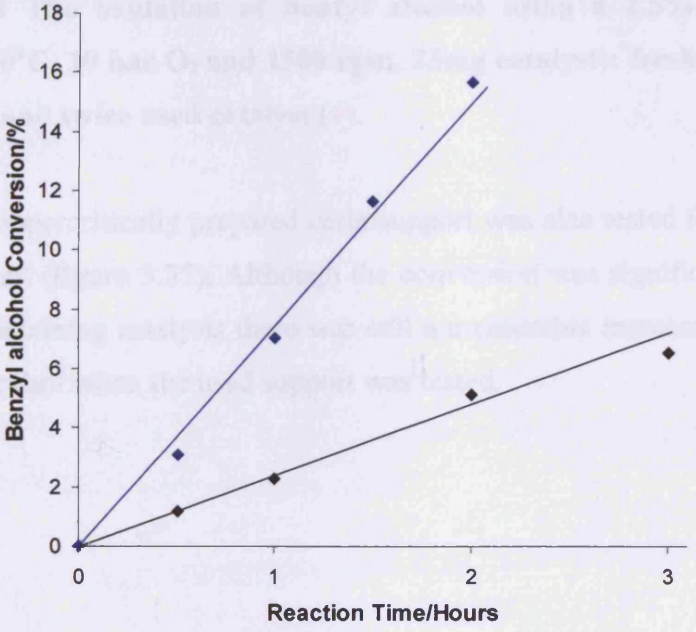

Figure 3.33: The oxidation of benzyl alcohol using 2.5%Pd/$ScCeO_2$ (140°C, 10 bar O_2 and 1500 rpm, 25mg catalyst): fresh catalyst (♦) and used catalyst (♦).

A gold palladium catalyst supported on P25 titania was also prepared to see if the effect was reproducible with a different support. In this case the fresh catalyst displayed the highest conversion with the conversion decreasing noticeably after the

first use of the catalyst (figure 3.34). The further decrease in conversion between the once used catalyst and the twice used catalyst was not significant in this case.

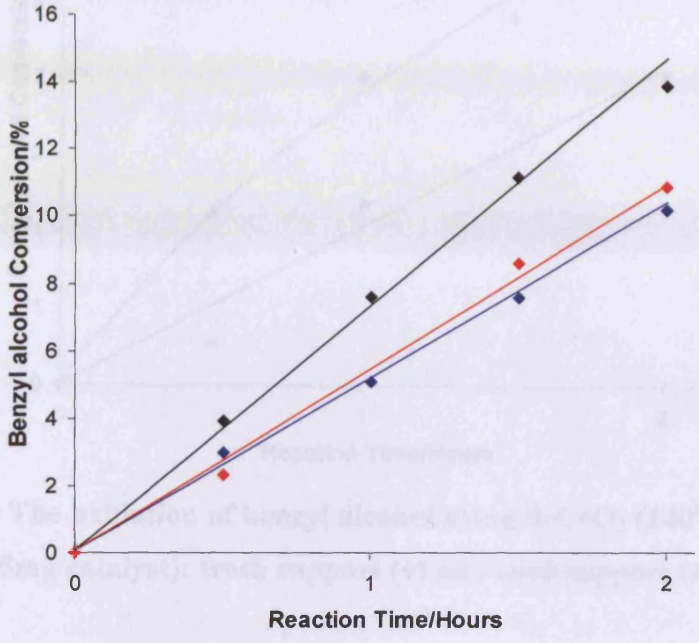

Figure 3.34 The oxidation of benzyl alcohol using a 2.5%Au+2.5%Pd/TiO_2 catalyst (140°C, 10 bar O_2 and 1500 rpm, 25mg catalyst): fresh catalyst (♦), used catalyst (♦) and twice used catalyst (♦).

The supercritically prepared ceria support was also tested for the oxidation of benzyl alcohol (figure 3.35). Although the conversion was significantly less than for the metal containing catalysts there was still a measurable increase in the conversion of benzyl alcohol when the used support was tested.

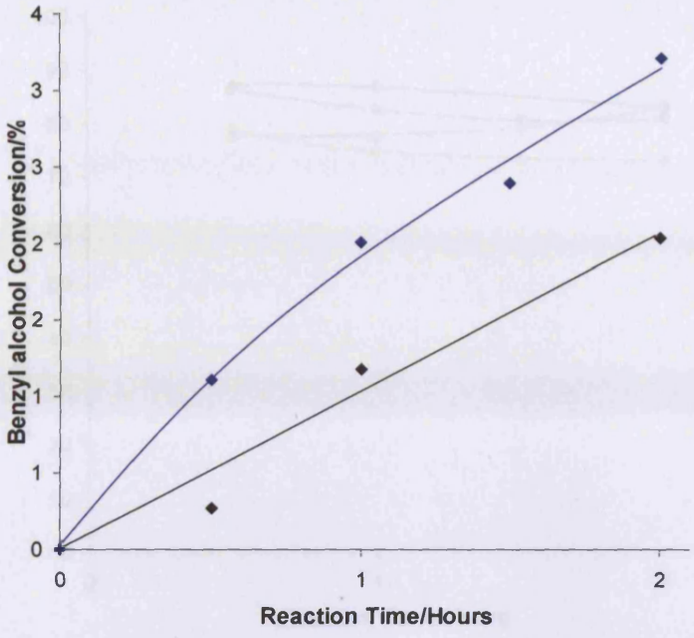

Figure 3.35: The oxidation of benzyl alcohol using $ScCeO_2$ (140°C, 10 bar O_2 and 1500 rpm, 25mg catalyst): fresh support (♦) and used support (♦).

The selectivities towards benzaldehyde during the oxidation of benzyl alcohol by gold palladium supported on ceria prepared by the supercritical antisolvent method are shown in figure 3.36. There is a small decrease in selectivity with each use of the catalyst for the first three uses, with a slight increase in the selectivity upon the fourth use (measured after 2 h reaction time). The decrease in selectivity towards benzaldehyde upon the second use of the catalyst is also seen for 2.5%Pd/$ScCeO_2$ (Figure 3.37). However, the 2.5%Au/CeO_2 showed similar selectivities for both uses of the catalyst (Figure 3.38). In the case of the gold palladium supported on non-supercritically prepared ceria the selectivity towards benzaldehyde remains similar for all three uses of the catalyst (figure 3.39).

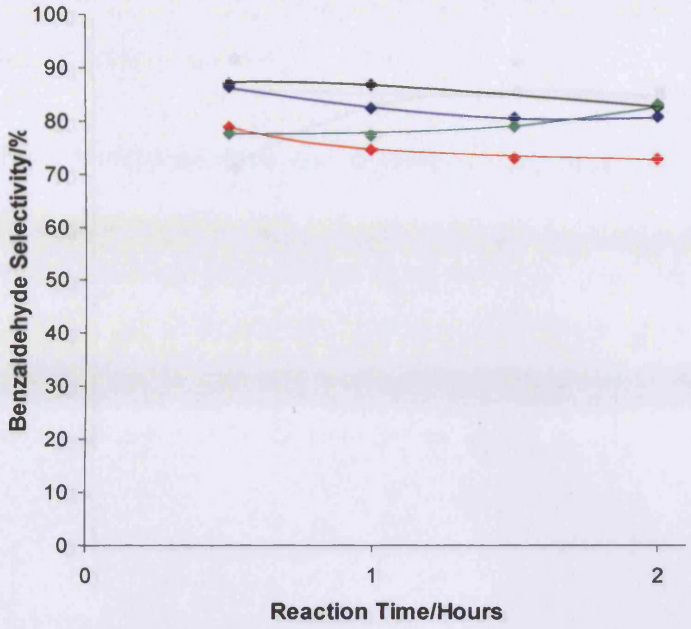

Figure 3.36: The selectivity towards benzaldehyde during the oxidation of benzyl alcohol using 2.5%Au + 2.5%Pd/ScCeO$_2$ (140^{o}C, 10 bar O$_2$ and 1500 rpm, 25mg catalyst): fresh catalyst (♦), used catalyst (♦) twice used catalyst (♦) and three times used catalyst (♦)

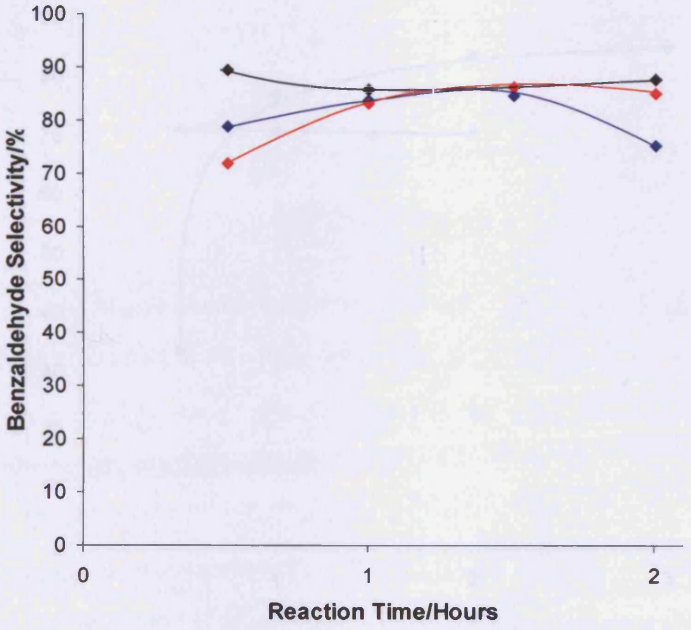

Figure 3.37: The selectivity towards benzaldehyde during the oxidation of benzyl alcohol using 2.5%Au + 2.5%Pd/nCeO$_2$ (140^{o}C, 10 bar O$_2$ and 1500 rpm, 25mg catalyst): fresh catalyst (♦), used catalyst (♦) and twice used catalyst (♦)

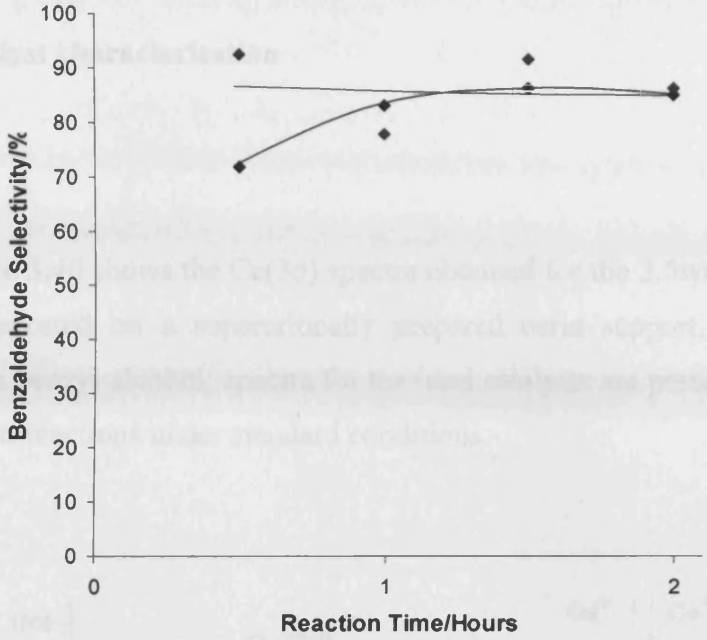

Figure 3.38: The selectivity towards benzaldehyde during the oxidation of benzyl alcohol using 2.5%Au/ScCeO$_2$ (140^{o}C, 10 bar O$_2$ and 1500 rpm, 25mg catalyst): fresh catalyst (♦) and used catalyst (♦).

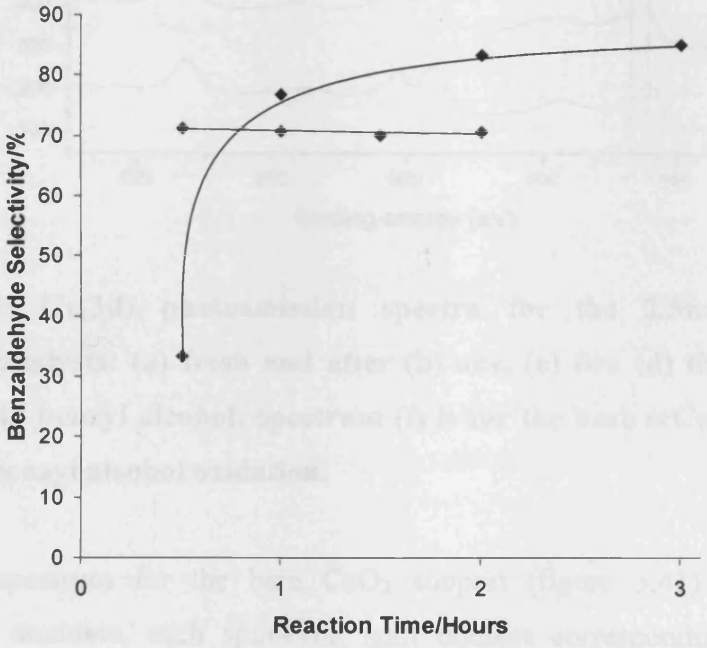

Figure 3.39: The selectivity towards benzaldehyde during the oxidation of benzyl alcohol using 2.5%Pd/ScCeO$_2$ (140^{o}C, 10 bar O$_2$ and 1500 rpm, 25mg catalyst): fresh catalyst (♦) and used catalyst (♦).

3.3.3 Catalyst characterisation

3.3.3.1 XPS

Figure 3.40 shows the Ce(3d) spectra obtained for the 2.5wt% Au+2.5wt% Pd catalysts supported on a supercritically prepared ceria support, before and after reaction with benzyl alcohol; spectra for the used catalysts are presented for one, two, three and four reactions under standard conditions.

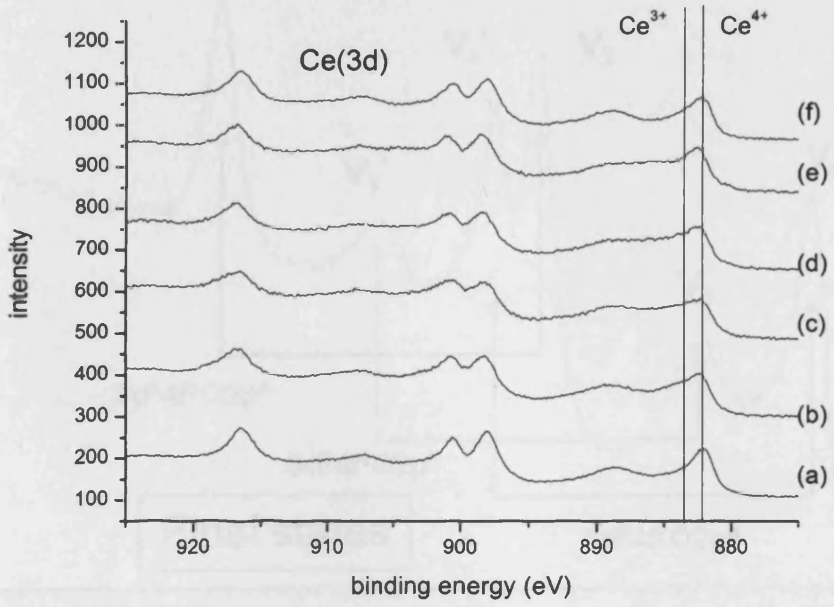

Figure 3.40: Ce(3d) photoemission spectra for the 2.5wt% Au+2.5wt% Pd/scCeO$_2$ catalysts: (a) fresh and after (b) one, (c) two (d) three and (e) four reactions with benzyl alcohol; spectrum (f) is for the bare scCeO$_2$ support after one use for benzyl alcohol oxidation.

The spectrum for the bare CeO_2 support (figure 3.41) is complex and comprises 3 doublets, each spin-orbit split doublet corresponding to a different electron distribution in the final ion state after photoemission; the different final state electronic configurations are indicated on the spectrum. The spectral profiles for the used catalysts (figure 3.40) show progressive changes, predominantly a "filling in" of

intensity around 885 eV binding energy reflecting the partial reduction of the surface of the support and the formation of Ce^{3+} species. The Ce(3d) spectra for CeO_2 and "Ce_2O_3" (a fully reduced CeO_2 sample – see Chapter 5) are compared in figure 3.42: the Ce^{3+} spectrum consists of 2 spin orbit doublets, due again to final state effects as indicated. The changes in the Ce(3d) spectra with reaction thus represent partial reduction of the support, although the support still mainly comprises CeO_2. This contrasts markedly with analogous reactions with 2-octan-1-ol, where complete reduction of the support within the XPS sampling depth is observed (Chapter 5).

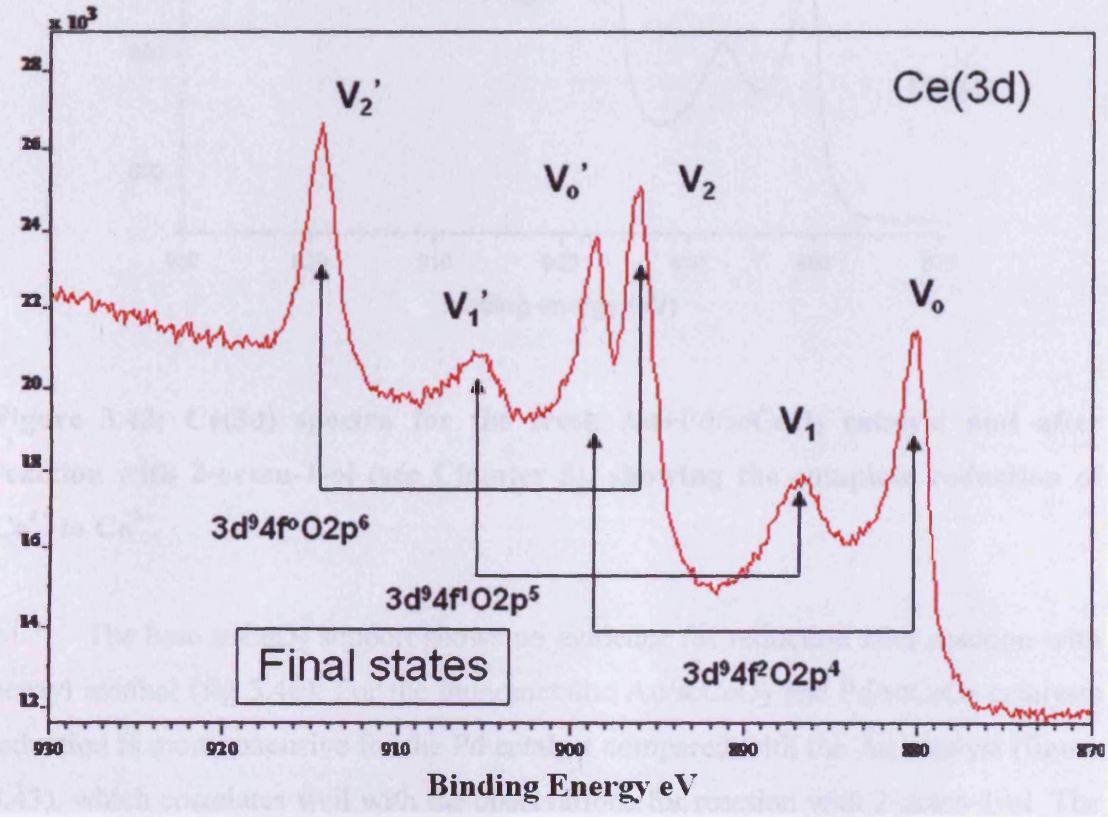

Figure 3.41: Ce(3d) spectrum from the scCeO$_2$ support, The assignments of the final state electronic structure for each of the three doublets are indicated.

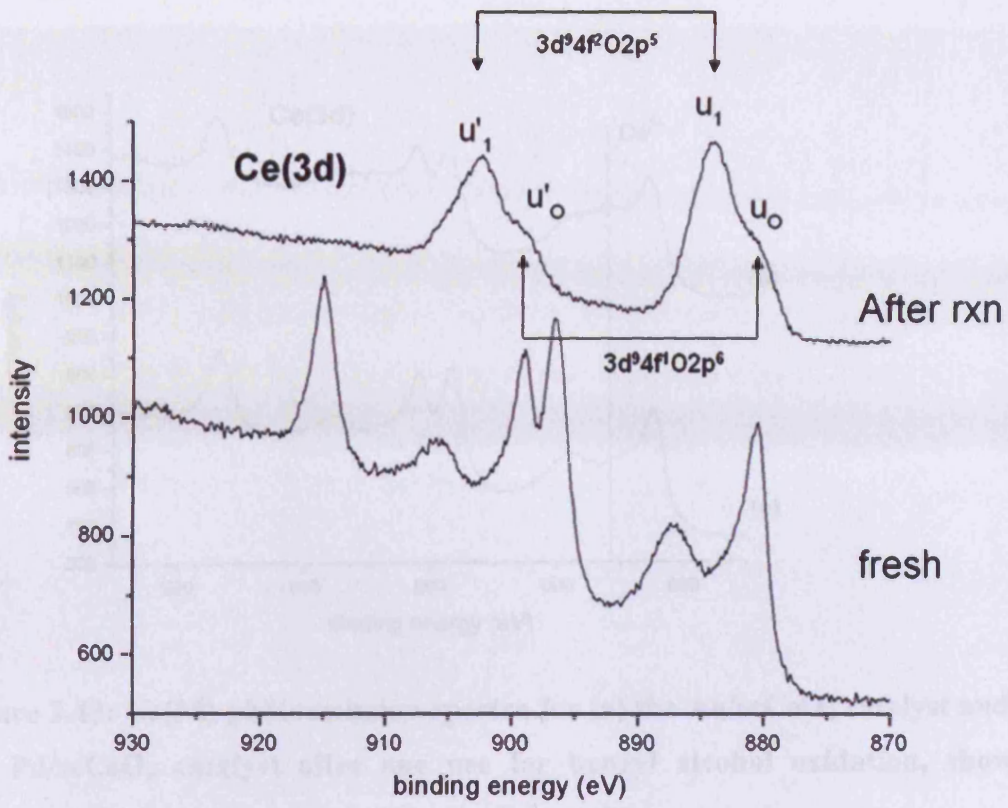

Figure 3.42: Ce(3d) spectra for the fresh Au+Pd/scCeO$_2$ catalyst and after reaction with 2-octan-1-ol (see Chapter 5), showing the complete reduction of Ce^{4+} to Ce^{3+}.

The bare scCeO$_2$ support shows no evidence for reduction after reaction with benzyl alcohol (fig 3.40). For the monometallic Au/scCeO$_2$ and Pd/scCeO$_2$ catalysts reduction is more extensive for the Pd catalyst compared with the Au catalyst (figure 3.43), which correlates well with the observations for reaction with 2-octen-1-ol. The alcohols dehydrogenate more readily on Pd sites, the hydrogen atoms spilling over to the support and leading to its reduction. Au catalysts are less active for this process.

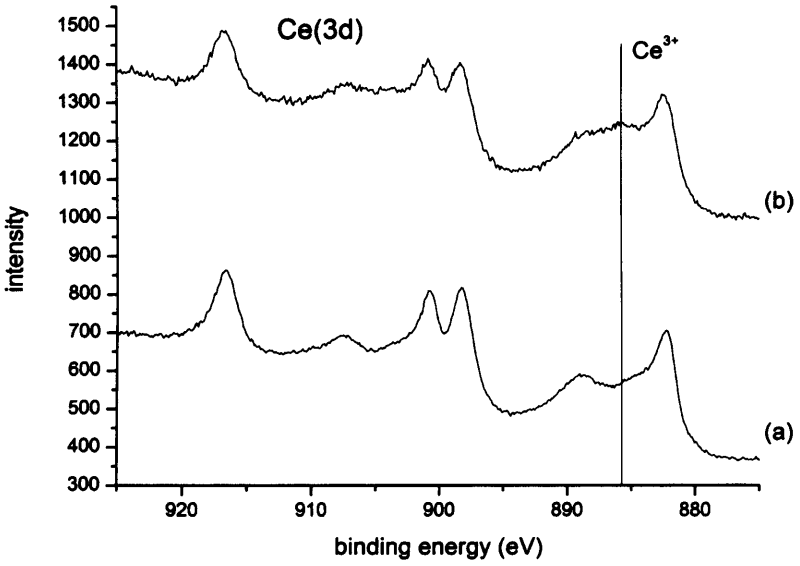

Figure 3.43: Ce(3d) photoemission spectra for (a) the Au/scCeO$_2$ catalyst and (b) the Pd/scCeO$_2$ catalyst after one use for benzyl alcohol oxidation, showing greater reduction of the support for the Pd catalyst.

A common feature of all the scCeO$_2$–supported monometallic or bimetallic catalysts is that their activities increase with re-use, at least up to two re-uses (figures 3.31-3.33). This is remarkable given the fact that extensive leaching of the metal content is observed after even one use; this is illustrated in figure 3.44 which shows the Pd(3d) spectra for the 2.5wt%+Au-2.5wt% Pd/scCeO$_2$ catalysts after increasing number of re-uses; after just one use the Pd(3d) signal is very weak, and essentially is non-existent after 4 uses; moreover, the remnant Pd species are metallic in contrast with the Pd^{2+} species present on the fresh catalyst. The Au(4f) signal is undetectable after just one use. It is clear that most of the metal content is inactive for this reaction, and moreover, the remaining metal particles after leaching are even more reactive than the original much higher loading. This surprising observation may be linked with the reduction of the support, but this is not clear. A similar effect is observed for the monometallic catalysts.

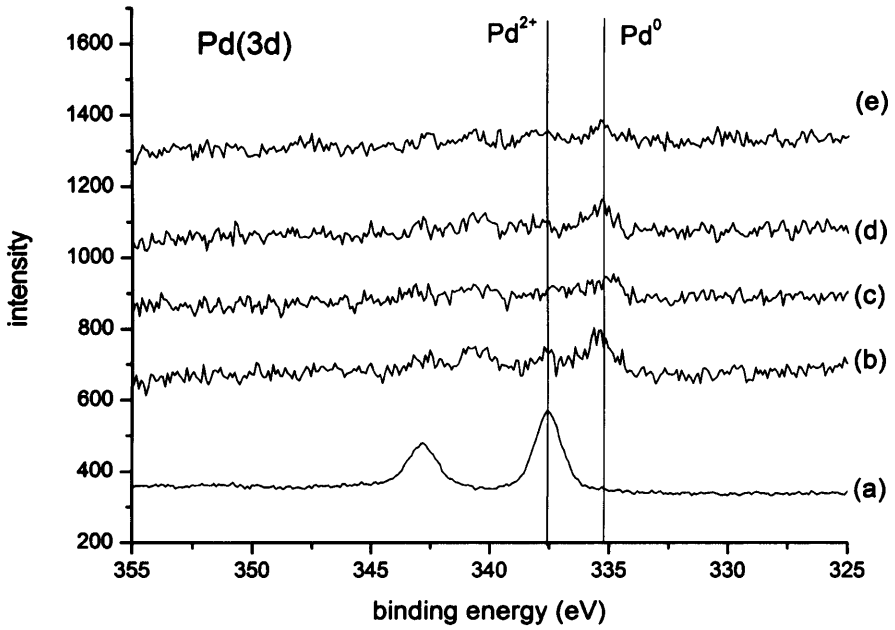

Figure 3.44: Pd(3d) photoemission spectra for the 2.5wt% Au+2.5wt% Pd/scCeO$_2$ catalysts: (a) fresh and after (b) one, (c) two (d) three and (e) four reactions with benzyl alcohol, showing the extensive leaching which occurs with catalyst use.

Quantification of the XPS data is not as straightforward as for the titania supported catalysts (section 3.2.4.2); the complex nature of the Ce(3d) spectra, and the dependence of the spectral structure on oxidation state, means that measured sensitivity factors are not reliable.

3.3.3.2 STEM

STEM analysis was performed as described in chapter 2. Image 3.4 shows TEM bright field images of 2.5%Au+2.5%Pd/nCeO$_2$; when this is compared to 2.5%Au+2.5%Pd/ScCeO$_2$ (image 3.5) the supercritically prepared supported catalyst seems to show a more spherical particle shape possibly due to the lack of surface tension in the supercritical medium when the precipitation occurs. The images of the supercritically supported catalyst after use for the oxidation of benzyl alcohol seem to show a slight breaking down of the ceria spheres (images 3.6 and 3.7)

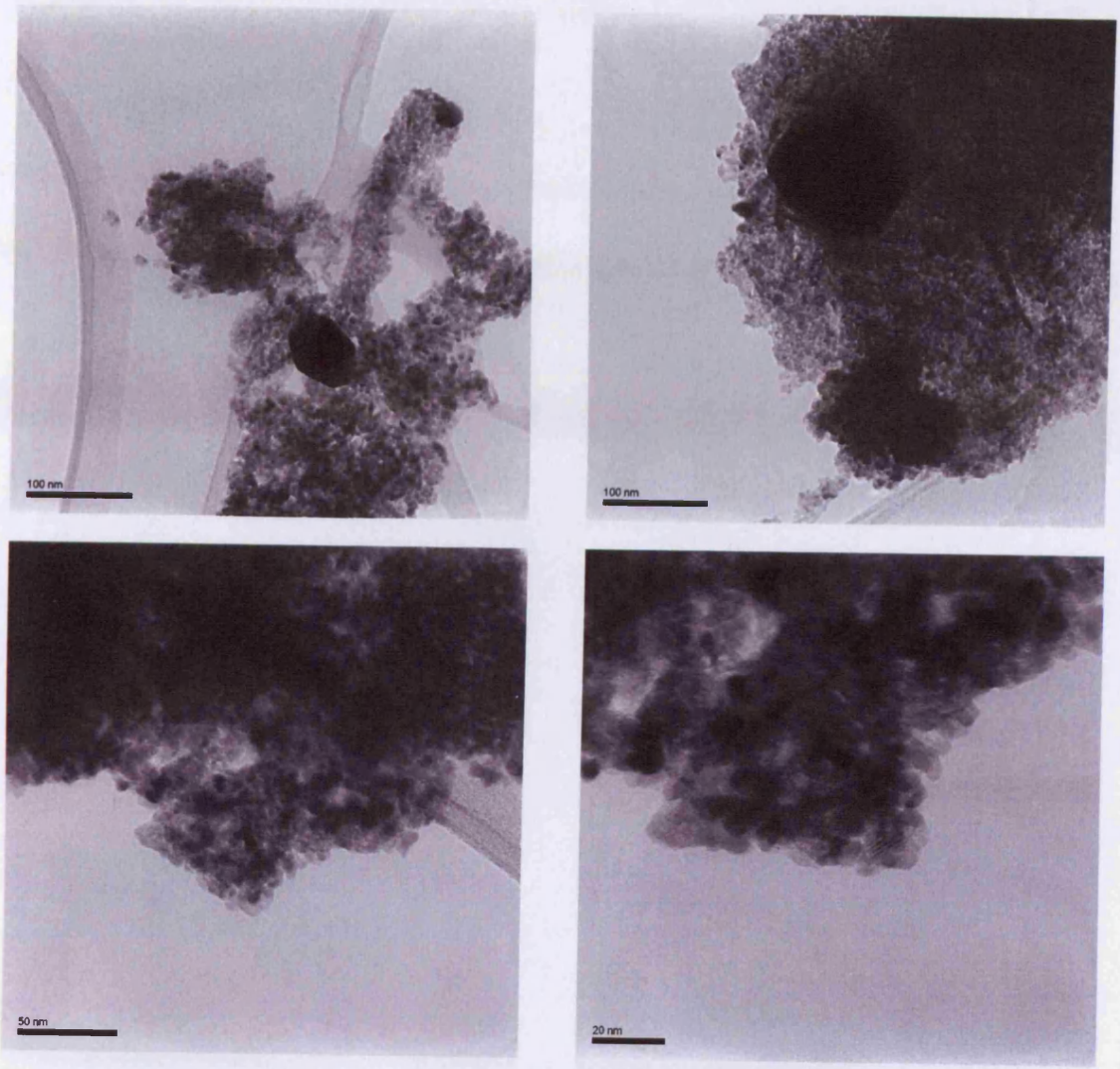

Image 3.4 TEM bright field images of 2.5%Au+2.5%Pd/unCeO$_2$.

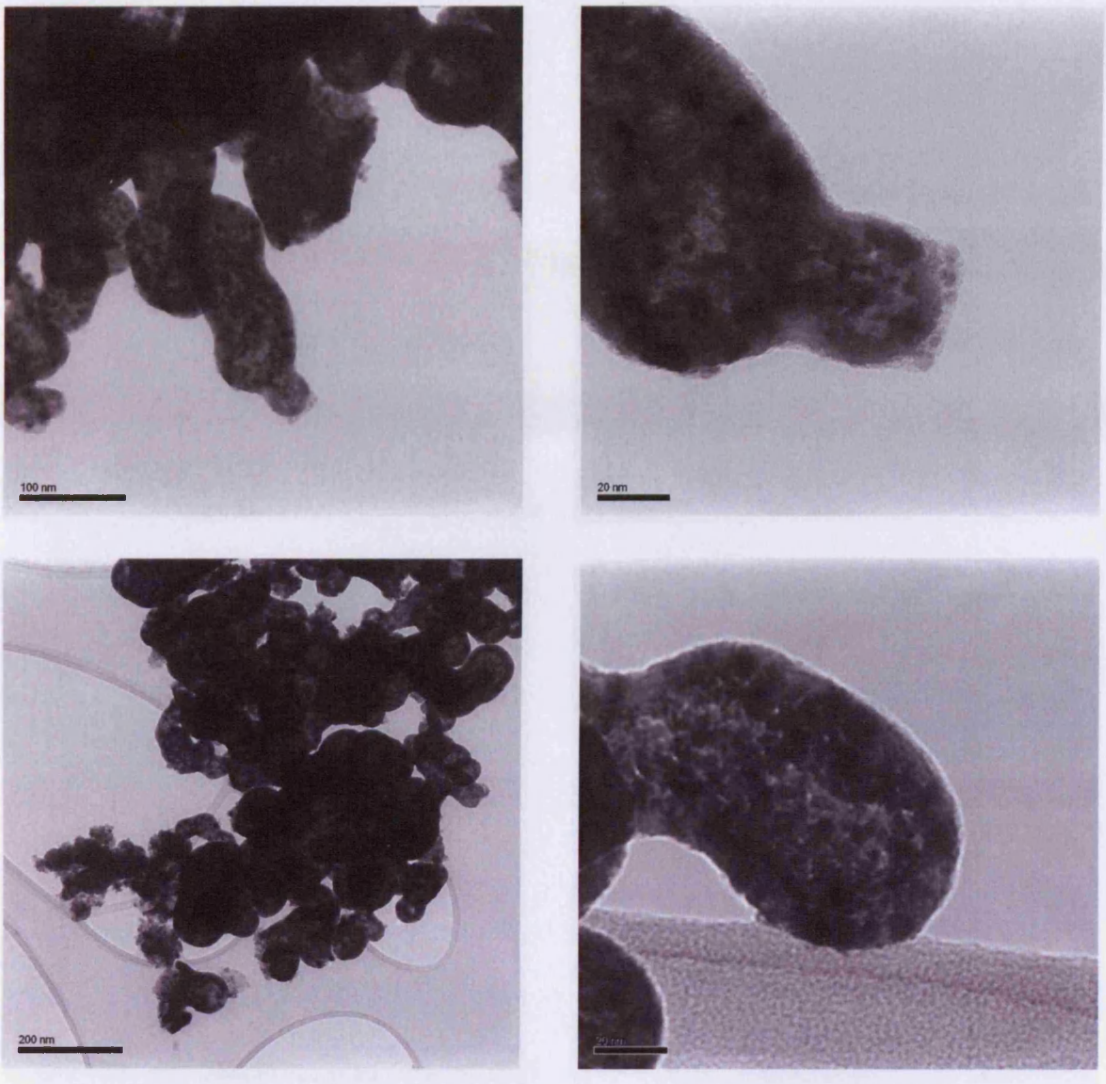

Image 3.5 TEM bright field images of 2.5%Au+2.5%Pd/$ScCeO_2$.

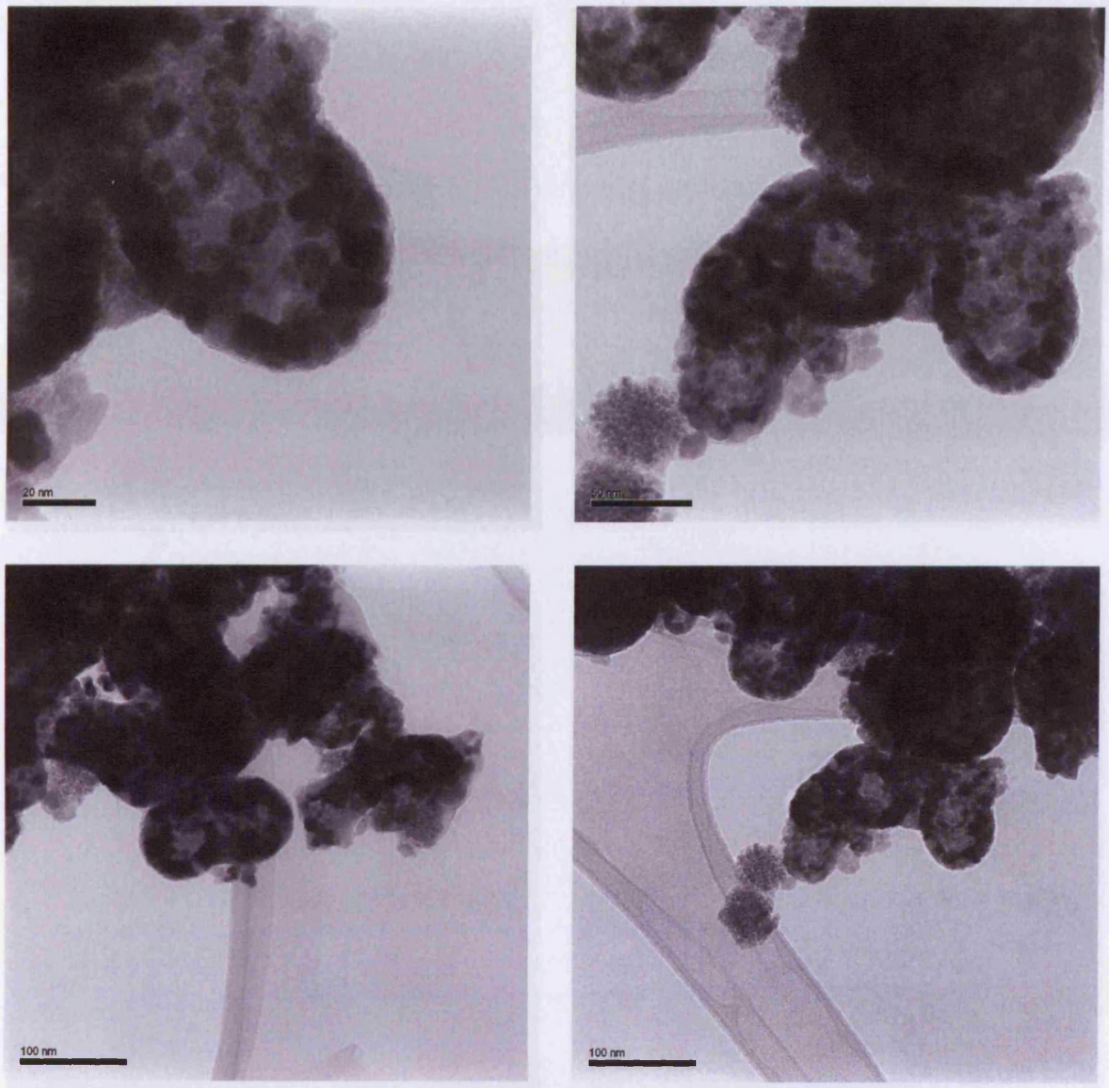

Image 3.6 TEM bright field images of 2.5%Au+2.5%Pd/$ScCeO_2$ after reaction with benzyl alcohol.

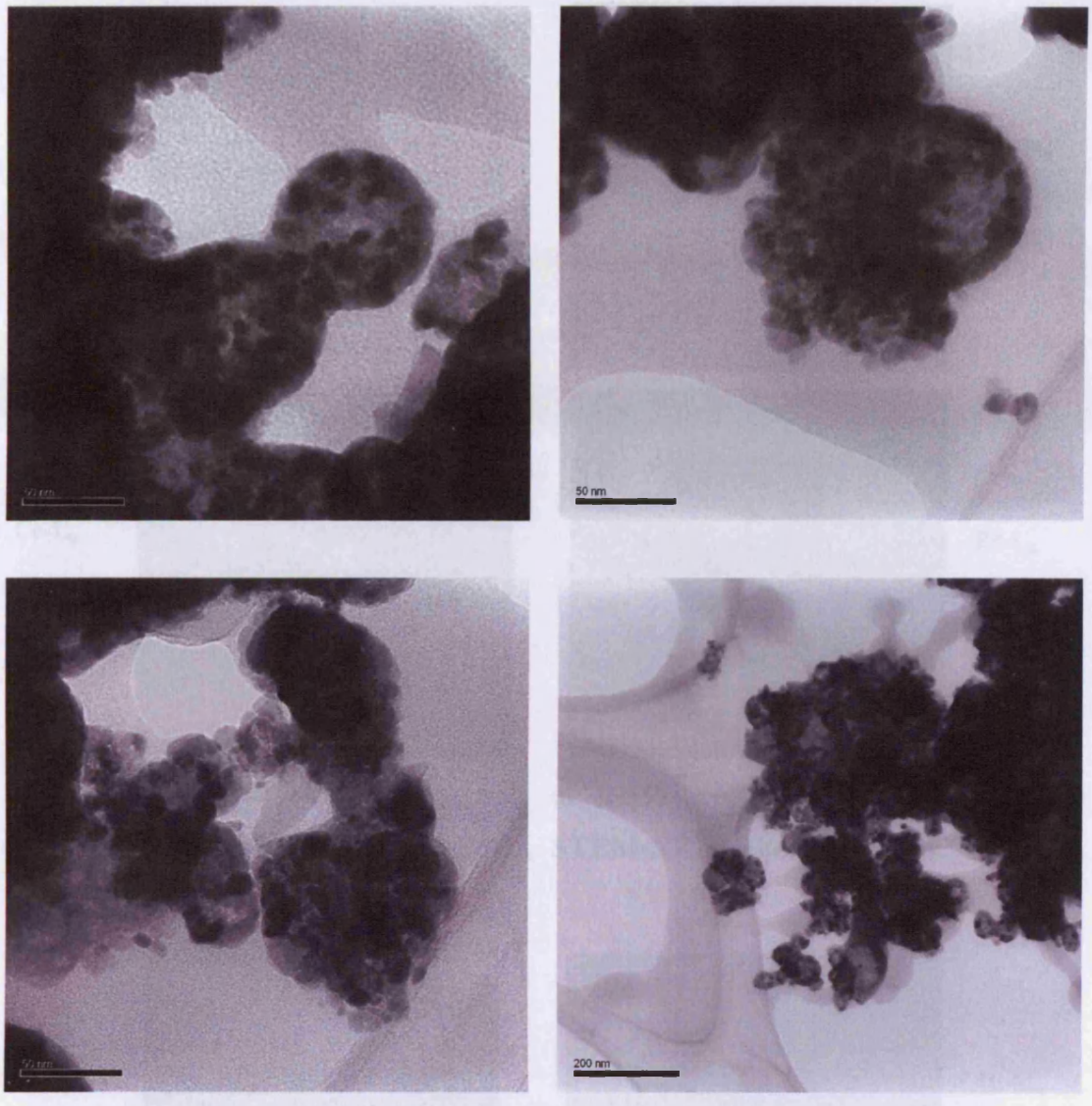

Image 3.7 TEM bright field images of 2.5%Au+2.5%Pd/$ScCeO_2$ after reaction with benzyl alcohol three times.

STEM-ADF micrographs were taken and XEDS mapping was used to identify the location of the metals. In the case of 2.5%Au+2.5%Pd/unCeO_2 (image 3.8) the gold formed large distinct particles; these particles seemed to be alloys with the palladium also forming part of the large metal particles. However the palladium content of the large particles seems to be lower than the gold content with the remaining palladium well dispersed over the surface of the support. The fresh 2.5%Au+2.5%Pd/$ScCeO_2$ catalyst (Image 3.9) in contrast, showed a high dispersion of both metals across the surface of the support; it is difficult to quantify if these particles are monometallic or alloy in nature due to this high dispersion.

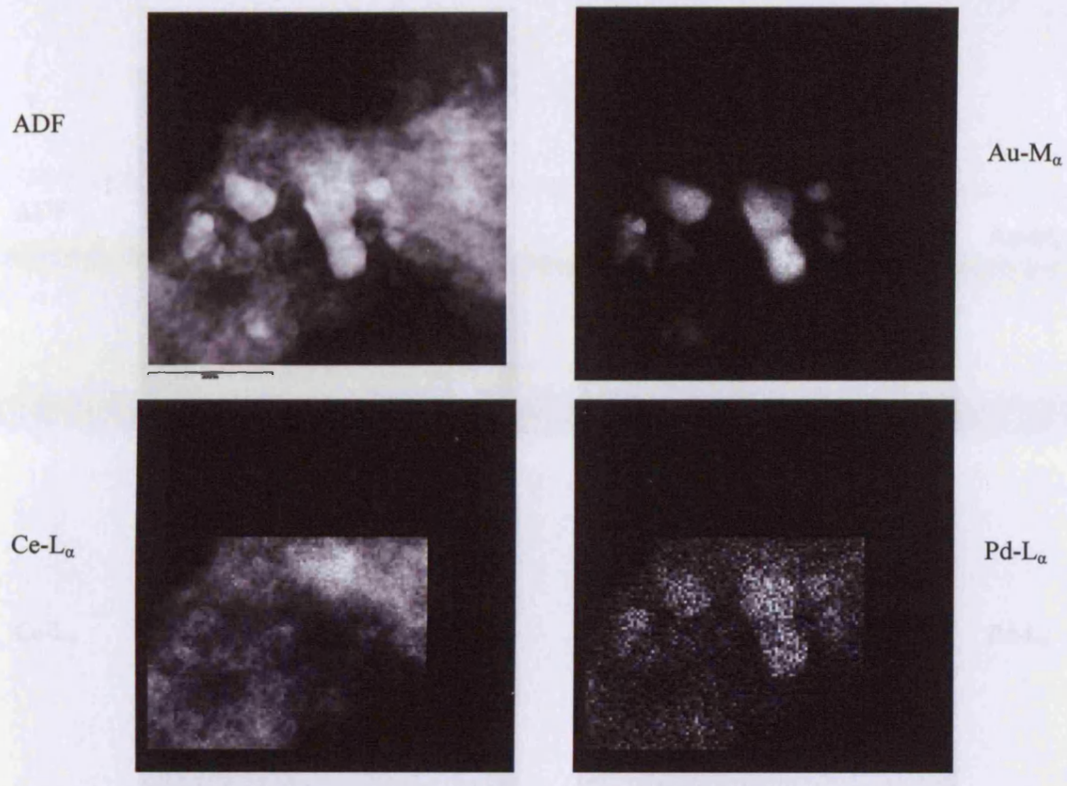

Image 3.8: STEM-ADF micrograph of 2.5%Au+2.5%Pd/unCeO$_2$ and the corresponding Au-M$_\alpha$, Ce-L$_\alpha$ and Pd-L$_\alpha$ STEM-XEDS chemical maps.

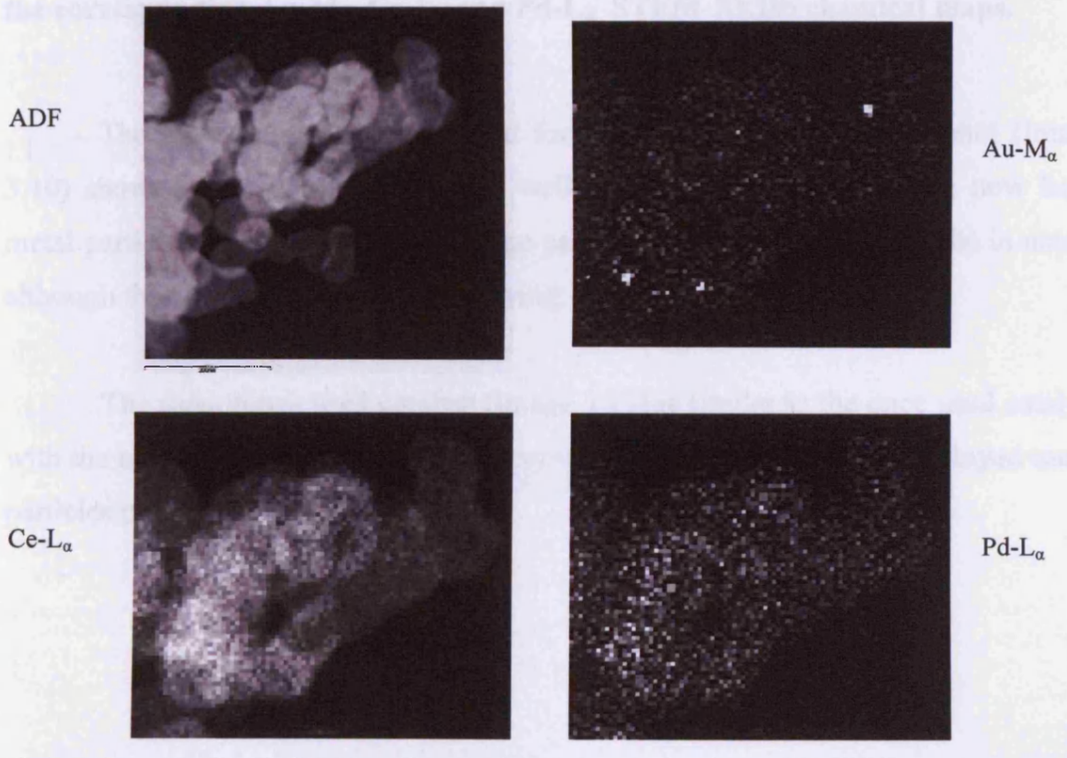

Image 3.9: STEM-ADF micrograph of fresh 2.5%Au+2.5%Pd/ScCeO$_2$ and the corresponding Au-M$_\alpha$, Ce-L$_\alpha$ and Pd-L$_\alpha$ STEM-XEDS chemical maps.

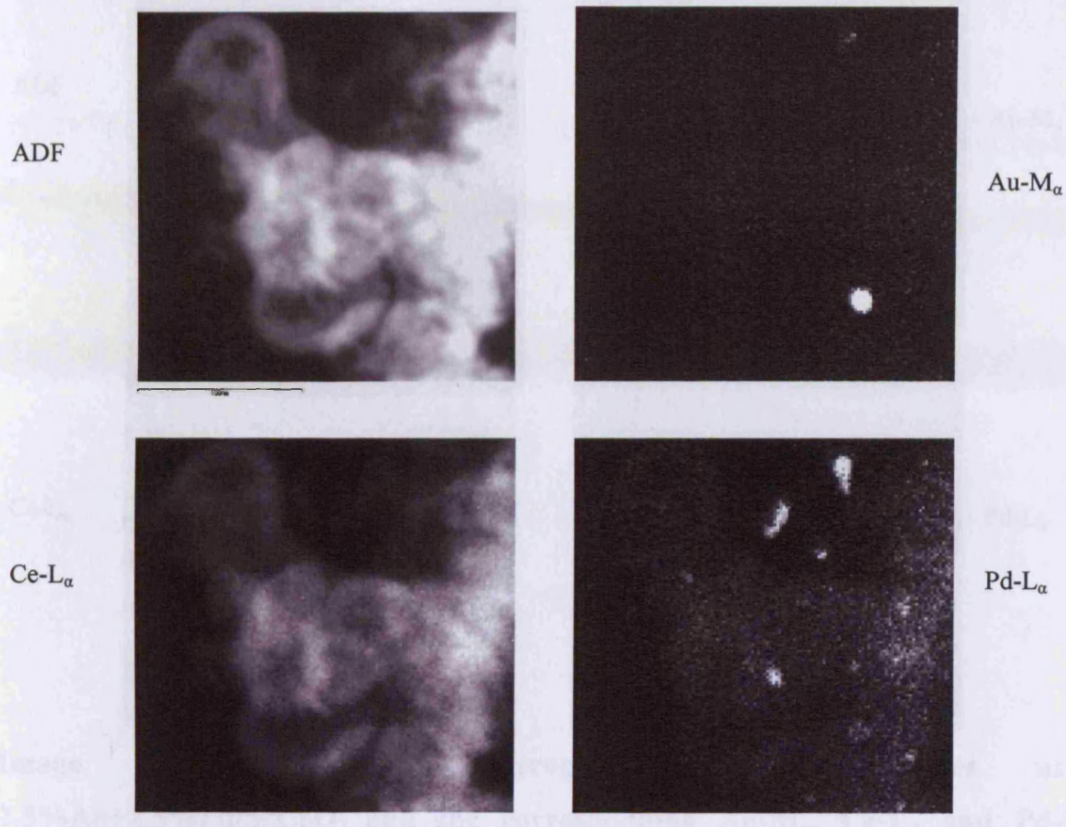

Image 3.10: STEM-ADF micrograph of once used 2.5%Au+2.5%Pd/$ScCeO_2$ and the corresponding Au-M_α, Ce-L_α and Pd-L_α STEM-XEDS chemical maps.

The catalyst that has been used for the oxidation of benzyl alcohol (Image 3.10) shows the metals generally still well dispersed however there are now large metal particles present. Most of the large particles seem to be monometallic in nature although there is some evidence of alloying.

The three times used catalyst (Image 3.11) is similar to the once used catalyst with the majority of the metals well dispersed with some larger slightly alloyed metal particles present.

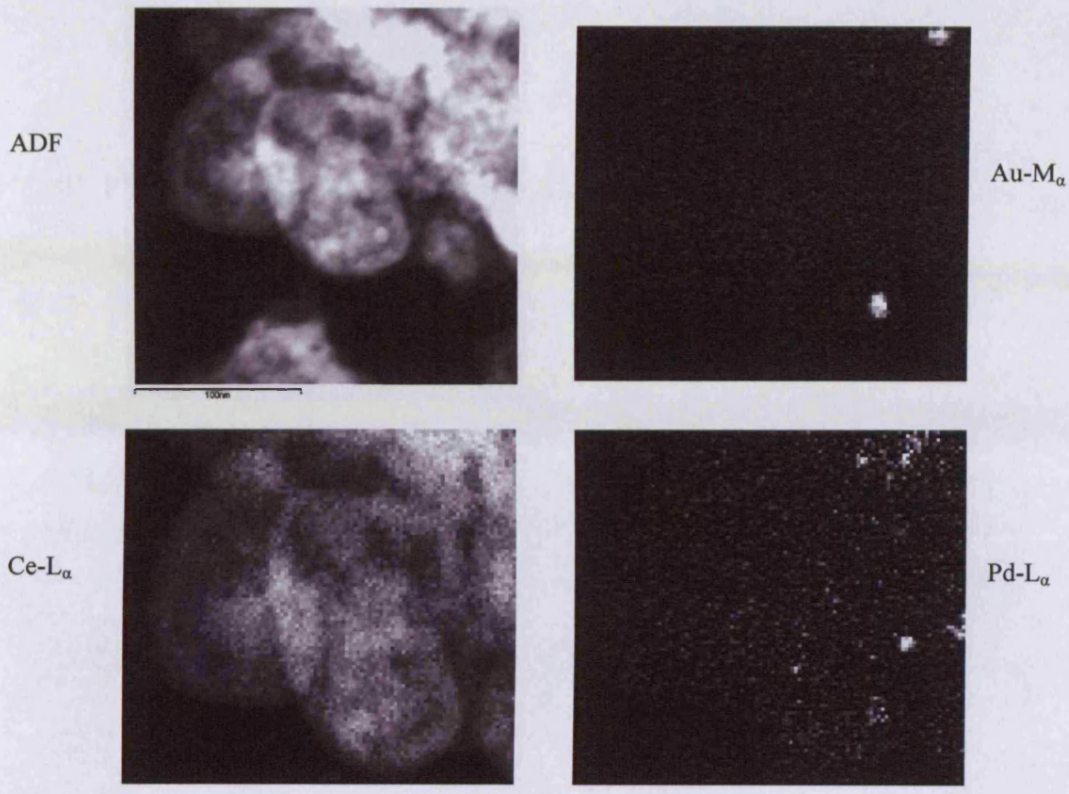

Image 3.11: STEM-ADF micrograph of three times used 2.5%Au+2.5%Pd/$ScCeO_2$ and the corresponding Au-M_α, Ce-L_α and Pd-L_α STEM-XEDS chemical maps.

3.4 Discussion

3.4.1 Optimisation of reaction conditions: The effect of temperature

The results of the investigation into the effect of temperature showed there is significant increase in activity upon increasing the temperature in the presence of a catalyst (figures 3.2-3.5); However, at the highest temperature, 160 °C, where the highest activity is exhibited, there is also significant reaction in the absence of a catalyst. Therefore for the purposes of catalyst evaluation 140 °C is considered to be the optimum temperature to highlight the differences in activity between different catalysts.

At first the selectivities of the higher temperature reactions (figure 3.6) seem inferior but the reduction in selectivity towards benzaldehyde at higher conversions is due to the sequential reaction to form benzoic acid and when the selectivities are

reviewed in the context of the conversion of benzyl alcohol (figure 3.7) they are all following the same reaction profile.

3.4.2 The effect of different supports.

In contrast to the earlier work by Cao *et al*[11] the conversion of benzyl alcohol over the carbon and titania supported catalysts were much higher than that of the gallia and the ceria supported catalysts (figure 3.8). The conversions of benzyl alcohol when using the carbon and titania catalysts were very similar, although the initial activity of the titania supported catalysts was slightly higher (table 3.2). The titania catalysts also have the advantage that the colour of the catalyst changes upon calcination, which can give a simple indication as to whether these processes have been carried out correctly.

3.4.3 The effect of pressure

The reaction at 5 bar O_2 pressure showed significantly higher conversion than that of the reaction at 1 bar O_2 pressure (figure 3.9) suggesting that the supply of oxygen to the active sites of the catalyst is the limiting factor in the reaction. While there is a change in conversion when the pressure of O_2 is further increased to 10 bar it is not as significant as the increase shown between 1 bar O_2 and 5 bar O_2, which is partially due to the reaction approaching complete benzyl alcohol conversion under these reaction conditions. The selectivities towards benzaldehyde (figure 3.10) again show the trend of the lowest selectivity being associated with the most active catalyst but when the results at similar reaction times are considered this is no longer the case.

3.4.4 The reaction in the absence of oxygen

The conversion for the reaction in the absence of oxygen is significantly lower than the analogous reaction with oxygen (figures 3.11 and 3.5). This is not surprising as oxygen is one of the reactants and the observation of any reaction is significant. When the selectivities toward the major products are considered it offers an explanation; the selectivity towards the oxygen free toluene molecule is almost 50% with the combined selectivity of the oxidised benzyl alcohol and benzoic acid

products adding up to around 50%. This suggests that in the absence of readily available oxygen the catalyst can cleave the oxygen from a benzyl alcohol molecule leaving it as toluene and allowing a different benzyl alcohol molecule to be oxidised via the usual pathway. This reaction was first proposed by Hutchings *et al*[12].

3.4.5 Superiority of the deposition precipitation preparation method

The catalysts prepared by deposition precipitation were more active for the oxidation of benzyl alcohol. The catalysts seem to be stable for reuse and the selectivities when considered in terms of the conversion are constant throughout (figures 3.13-3.21). Oxide supported gold catalysts prepared by deposition precipitation are known to be more active for the oxidation of CO than those prepared by impregnation[8]. However for the direct synthesis of hydrogen peroxide the reverse is true[13] and studies on the oxidation of benzyl alcohol by gold supported on ZSM-5[14] found the deposition precipitation prepared catalyst to be less active than the analogous impregnated catalyst. It is clear that different forms of gold are active in different reaction systems.

The advantage of the deposition precipitation method of preparing catalysts is the control over the nature of the gold species in solution which will vary with pH. The relative equilibrium concentrations of gold complexes were proposed by Nechayev *et al*[15] and are shown in figure 3.45. This suggests that at pH 8 the majority of the gold complexes will be in the chloride free $Au(OH)_4^-$ form. By substituting palladium chloride for palladium nitrate the chloride from the palladium salt is also removed from the process, as long as the catalyst is thoroughly washed after the metal complexes have been supported.

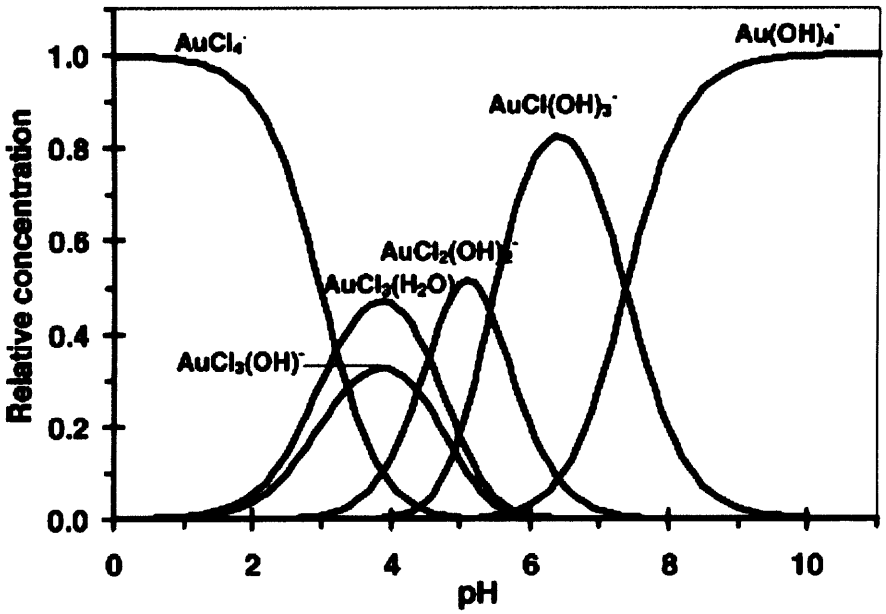

Figure 3.45: Relative equilibrium concentration of gold complexes ($[Cl^-]$ = 2.5 × 10^{-3} M) as a function of the pH of the solution, calculated with equilibrium constants reported by Nechayev *et al*[15].

The slight difference in the activities of the catalysts (figures 3.14 and 3.15) could be explained by the preparation method. In the case where the catalyst is prepared by increasing the pH of the solution the metal would be expected to precipitate sequentially whereas at constant pH the metals would be expected to precipitate simultaneously.

The SEM images (images 3.2 and 3.3) of the deposition precipitation prepared catalysts show that large metal particles are present in the catalyst, in contrast to the supported gold catalysts prepared by deposition precipitation methods where the gold particles are generally less than 10 nm. Although this would indicate that the increase in activity of these catalysts is not a function of the metal particle size the presence of large metal particles does not mean that these are exclusively the form of metal on the surface of the support, or that these large particles are the active components of the catalyst. It is possible that active small metal particles are also present on the surface of the support below the detection limit of the SEM technique.

The EDX analysis of the catalysts shows that the catalysts prepared by deposition precipitation contained no chlorine, in contrast to the catalyst prepared by

impregnation, which offers an explanation of the different activities of the catalysts. Okumura *et al*[16] found that the activity of gold catalysts, for the hydrogenation of 1,3-butadiene improved considerably when the catalysts were washed with hot water, to remove sodium and chloride ions, as part of the preparation process. EDX analysis of the catalysts also afforded accurate information on the metal loadings of these catalysts (tables 3.5 and 3.6). The metal loadings were found to be considerably lower than the theoretical loadings, which is not unexpected, Moreau *et al*[17] suggested that when the pH of the solution is higher than the isoelectric point of titania the surface of the titania will be negatively charged, resulting in repulsion of the anionic gold complex species. If the TOF values for the catalysts are recalculated in terms of the measured metal loading rather than the theoretical loading (table 3.7) the difference in activity between the two preparation methods is emphasised

Table 3.7 Conversion of benzyl alcohol and TOF based on measured metal content after 0.5h of reaction using 2.5%Au+2.5% prepared by various techniques (140 °C, 10 bar O_2 and stirred at 1500 rpm)

Preparation Method	Conversion @ 0.5h of Reaction (%)	TOF @ 0.5 h of Reaction (mol mol^{-1} h^{-1})
Co-Impregnation	4.31	3687
Deposition Precipitation (Constant pH)	24.12	36145
Deposition Precipitation (Increasing pH)	23.97	39000

3.4.6 Supercritical supports

3.4.6.1 Reactions with benzyl alcohol by Au, Pd and Au+Pd supported on $unCeO_2$ and $ScCeO_2$.

The catalysts supported on the ceria prepared using the supercritical antisolvent method proved to be more active than those supported on the analogous ceria prepared by simple calcination of the acetate precursor (figure 3.25 and 3.26). This is consistent with the results of previous studies on the oxidation on CO[3]. Previous studies by Corma et al[4] have shown a correlation between the particle size of the cerium oxide support and the activity of the catalyst. However, in this case, the

size of the ceria nanoparticles in the non-supercritically prepared support were actually smaller than those in the supercritically prepared support. The difference in activity is suggested to be a function of metal particle size. In the work carried out by Tang et al[3] STEM-ADF imaging was used to characterise the $Au/ScCeO_2$ catalyst. Only the background Au signal was detected indicating that the Au is dispersed in sub 1nm particles or as dispersed atoms. Conversely for the $unCeO_2$ catalyst STEM-ADF suggested there were large 10-40 nm Au particles present and no background Au signal detected which suggests that all the Au is present only in the larger metal clusters (Figure 3.12). The data obtained for the bi-metallic catalysts (Images 3.5 and 3.6) reflects the same trend where the non-supercritically prepared support has larger metal particles and the supercritically prepared supported catalyst has smaller more dispersed metal particles and is more active.

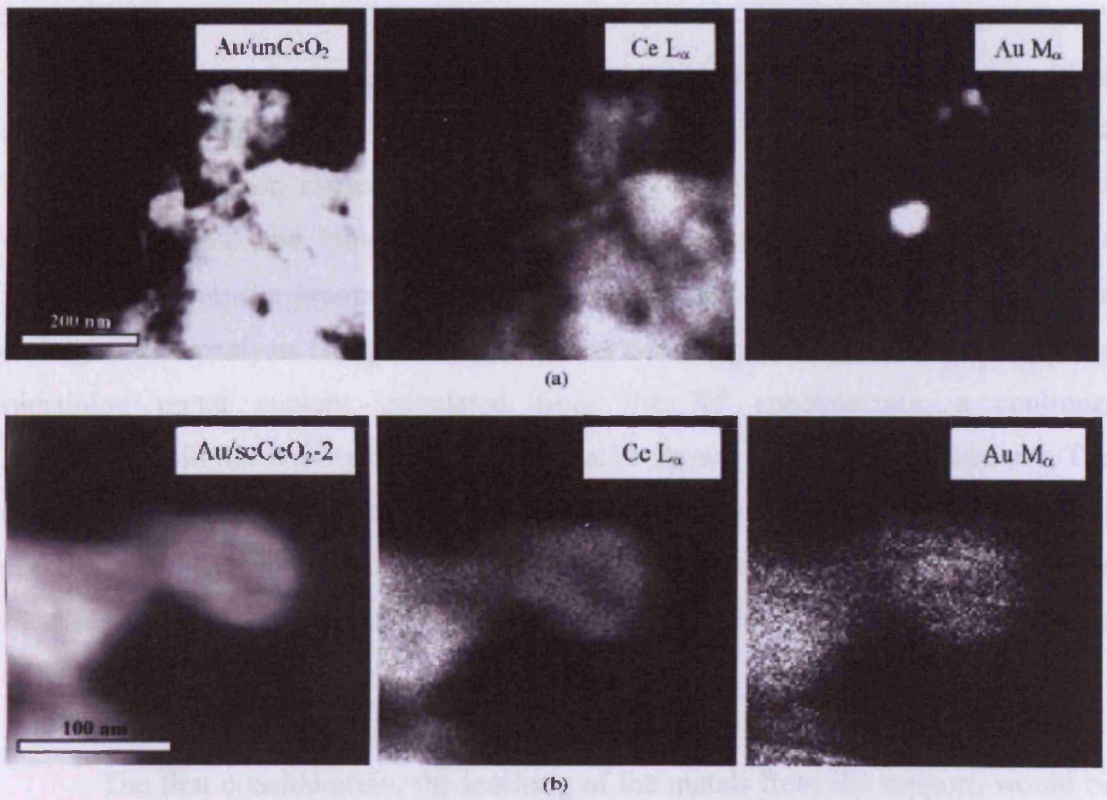

Figure 3.46: STEM-ADF micrographs (left) and STEM-XEDS spectrum images of Ce-Lα (center) and Au-Mα (right), signals of $Au/nCeO_2$ (a) and $Au/ScCeO_2$ (b).

The selectivities towards benzaldehyde for both the supercritically and non-supercritically prepared supports and different metals are similar with the exception

of gold-palladium supported on non-supercritically prepared ceria which has a notably lower selectivity. This is more than likely an anomalous result due to a slightly increased amount of benzene formed being emphasised by the low conversion of the reaction.

3.4.6.2 unCeO_2 catalysts - decrease in activity with use

The activity of the gold palladium supported on non-supercritically prepared ceria decreases with each use suggesting that these catalysts would not be suitable for industrial application. The most likely cause of this drop in activity is due to the active metal species leaching from the oxide support.

3.4.6.3 Au+Pd/ScCeO_2 catalysts - increase in activity with use

The increase in the activity of the used catalysts in the case of the supercritical catalysts is unexpected. It was initially considered that this effect is due to a homogenous reaction caused by the leaching of the metals from the catalysts, as shown by the XPS data. However if this were the case there would not be the increase in the activity on the second use, with a fresh reactant solution. Furthermore if the activity of the catalysts is expressed in terms of the TOF calculated on the basis of the remaining metal content calculated from the XP spectroscopy, a continual improvement in the activity of the catalyst can be shown for each subsequent use. The explanation for this increase in activity is not immediately obvious, but the spectroscopic data highlights three separate factors to consider: the leaching of the metals, the change in oxidation state of the cerium oxide support and the breaking down of the ceria nanoparticles.

The first consideration, the leaching of the metals from the support, would be expected to result in a less active catalyst. However a search of the literature uncovers a series of studies which have found that when gold is deliberately leached off ceria using cyanide there is no discernable change in the activity of the catalyst. In work by Flytzani-Stephanopoulos *et al*[18] gold on ceria was prepared by the deposition precipitation method, with the gold subsequently leached using a 2% NaCN solution at room temperature with the pH maintained at 12 by the addition of sodium

hydroxide. This leaching process resulted in 90% of the gold loading being removed, and STEM/EDX and XPS showed no metallic gold remaining. When these leached catalysts were tested for the water gas shift (WGS) reaction the activities were found to be the same as or a little higher than the non-leached catalyst. The catalysts were also tested for the PROX reaction, where previous work by Bond *et al*[17] has suggested that both metallic and ionic gold sites are necessary to catalyse the CO oxidation. However while the leached catalysts performed well for CO oxidation they were compared to low content gold catalysts rather than the non-leached catalysts.

This suggests that the bulk of the gold in these supported catalysts is not active and could offer an explanation as to why there is no drop in activity when the bulk of the gold has leached from the catalyst. This does however raise questions about the nature of the active form of gold and palladium, as described previously. Flytzani-Stephanopoulos *et al*[18] proposed that metallic gold was not involved in the WGS reaction; however there seems to be some disagreement in the literature with Hardacre *et al*[19] carrying out an *in situ* study into the nature of the active form of gold during the WGS reaction using EXAFS in combination with DFT studies to conclude that metallic gold is the active species. More recent work by Behm *et al*[20] has suggested that the leaching process and the subsequent calcinations and indeed the WGS reaction itself, employed in the previous work, does not leave exclusively cationic gold particles and suggested that both types of gold species contribute to the reactivity.

The active species for alcohol oxidation may be completely different from those active in the WGS reaction and the role of palladium cannot be ignored, but these studies suggest that the leaching may not lead to a drop in the activity if the leachate consists primarily of a non active form of the metal.

The change in oxidation state of the ceria (figure 3.42) is likely due to the partial reduction of cerium to form Ce_2O_3; this reaction would release half a mol of oxygen (equation 3.1)

$$2CeO_2 \rightarrow Ce_2O_3 + \tfrac{1}{2} O_2$$

Equation 3.1: The change in cerium oxidation state

This leaves oxygen vacancies which in a mechanism proposed by Corma *et al*[21] are filled by physisorption of oxygen which initiates oxygen activation. The interaction between the cerium (III) and dioxygen forms a metal peroxyl radical such as Ce-O-O·, positive gold atoms form a gold-alcoholate species and the combination of these species results in the reaction to form the ketone and the metal hydroperoxide. The cerium peroxide subsequently decomposes (figure 3.47).

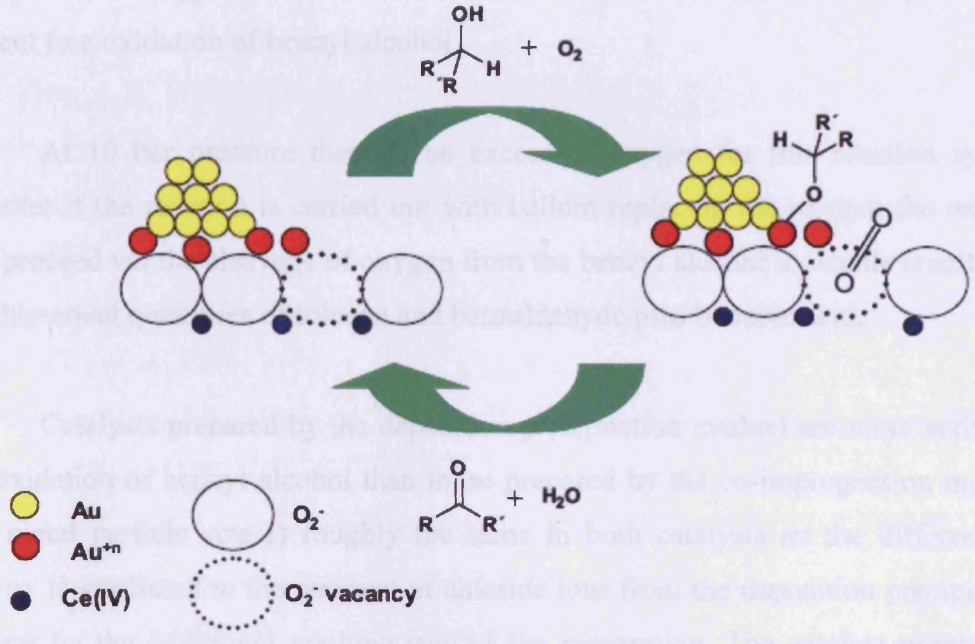

Figure 3.47: the mechanism proposed by Corma *et al*[21].

This mechanism would suggest that as the Cerium 3+ content of the support increases, the ability to uptake oxygen increases allowing a higher activity of the catalyst.

The final factor is the breaking down of the nanospheres as show by the STEM (figures 3.4.-3.7), due to the reduction of the cerium from CeO_2 to Ce_2O_3. This causes a change in density in the spheres and leads to their disruption. The cause of the increase in the activity is likely to be due to a combination of these spectroscopically and microscopically characterised features.

3.5 Conclusions

- Reaction conditions of 140°C, 10 bar O_2, 1500 rpm with 25 mg of catalyst are suitable for the testing of catalysts for the solvent free oxidation of benzyl alcohol with the maximum conversion in the shortest reaction time without reaction occurring in the absence of catalyst.

- As has been demonstrated for direct synthesis of hydrogen peroxide bimetallic gold palladium supported on carbon or titania are the most effective catalysts for the solvent free oxidation of benzyl alcohol.

- At 10 bar pressure there is an excess of oxygen for this reaction system; however if the reaction is carried out with helium replacing the oxygen the reaction will proceed *via* the cleavage of oxygen from the benzyl alcohol molecule resulting in roughly equal quantities of toluene and benzaldehyde plus benzoic acid.

- Catalysts prepared by the deposition precipitation method are more active for the oxidation of benzyl alcohol than those prepared by the co-impregnation method. The metal particle size is roughly the same in both catalysts so the difference in activity is attributed to the removal of chloride ions from the deposition precipitation catalyst by the additional washing step of the preparation. The catalyst prepared at constant pH was more stable for reuse than the catalyst prepared at increasing pH.

- Ceria supported catalyst prepared by supercritical CO_2 antisolvent precipitation are more active than those prepared by simple calcination of the $Ce(acac)_2$ precursor due to greater distribution of the metal particles on the surface.

- There is a decrease in activity, with the catalyst prepared by simple calcination of the precursor; however, for the catalyst prepared by precursor precipitation into a supercritical CO_2 antisolvent there is an increase in activity, relative to the metal content, with each use. This increase in activity is accompanied by a change in ceria oxidation state from + 4 to + 3 which leaves oxygen vacancies,

facilitating greater transport of O_2 to the active sites of the catalysts and improving activity.

3.6 References

[1] D. I. Enache, J. K. Edwards, P. Landon, B. Solsona-Espriu, A. F. Carley, A. A. Herzing, M. Watanabe, C. J. Kiely, D. W. Knight, G. J. Hutchings, *Science (Washington, DC, United States)* **2006**, *311*, 362.

[2] S. Carrettin, P. Concepcion, A. Corma, J. M. Lopez Nieto, V. F. Puntes, *Angewandte Chemie, International Edition* **2004**, *43*, 2538.

[3] Z.-R. Tang, J. K. Edwards, J. K. Bartley, S. H. Taylor, A. F. Carley, A. A. Herzing, C. J. Kiely, G. J. Hutchings, *Journal of Catalysis* **2007**, *249*, 208.

[4] A. Corma, M. E. Domine, *Chemical Communications (Cambridge, United Kingdom)* **2005**, 4042.

[5] A. Abad, C. Almela, A. Corma, H. Garcia, *Chemical Communications (Cambridge, United Kingdom)* **2006**, 3178.

[6] J. K. Edwards, A. Thomas, B. E. Solsona, P. Landon, A. F. Carley, G. J. Hutchings, *Catalysis Today* **2007**, *122*, 397.

[7] F.-Z. Su, M. Chen, L.-C. Wang, X.-S. Huang, Y.-M. Liu, Y. Cao, H.-Y. He, K.-N. Fan, *Catalysis Communications* **2008**, *9*, 1027.

[8] G. R. Bamwenda, S. Tsubota, T. Nakamura, M. Haruta, *Catalysis Letters* **1997**, *44*, 83.

[9] M.-A. Hurtado-Juan, C. M. Y. Yeung, S. C. Tsang, *Catalysis Communications* **2008**, *9*, 1551.

[10] S. Al-Sayari, A. F. Carley, S. H. Taylor, G. J. Hutchings, *Topics in Catalysis* **2007**, *44*, 123.

[11] F.-Z. Su, J. Ni, H. Sun, Y. Cao, H.-Y. He, K.-N. Fan, *Chemistry--A European Journal* **2008**, *14*, 7131.

[12] D. I. Enache, D. Barker, J. K. Edwards, S. H. Taylor, D. W. Knight, A. F. Carley, G. J. Hutchings, *Catalysis Today* **2007**, *122*, 407.

[13] J. K. Edwards, B. E. Solsona, P. Landon, A. F. Carley, A. Herzing, C. J. Kiely, G. J. Hutchings, *Journal of Catalysis* **2005**, *236*, 69.

[14] G. Li, D. I. Enache, J. Edwards, A. F. Carley, D. W. Knight, G. J. Hutchings, *Catalysis Letters* **2006**, *110*, 7.

[15] E. A. Nechaev, G. V. Zvonareva, *Geokhimiya* **1983**, 919.

[16] M. Okumura, T. Akita, M. Haruta, *Catalysis Today* **2002**, *74*, 265.

[17] F. Moreau, G. C. Bond, A. O. Taylor, *Journal of Catalysis* **2005**, *231*, 105.

[18] W. Deng, J. De Jesus, H. Saltsburg, M. Flytzani-Stephanopoulos, *Applied Catalysis, A: General* **2005**, *291*, 126.

[19] D. Tibiletti, A. Amieiro-Fonseca, R. Burch, Y. Chen, J. M. Fisher, A. Goguet, C. Hardacre, P. Hu, D. Thompsett, *Journal of Physical Chemistry B* **2005**, *109*, 22553.

[20] A. Karpenko, R. Leppelt, V. Plzak, R. J. Behm, *Journal of Catalysis* **2007**, *252*, 231.

[21] A. Abad, C. Almela, A. Corma, H. Garcia, *Tetrahedron* **2006**, *62*, 6666.

Chapter Four

Chapter 4: Alkene oxidations

4.1 Inroduction

The work carried out by Hutchings *et al*[1] on the oxidation of cyclooctene, as discussed in chapter 1 demonstrates the range of possible oxidation products arising from the oxidation of alkenes. Irrespective of the type of gold catalyst that was used the major product in the oxidation of cyclooctene was the epoxide, epoxidation of one of the double bonds on 2,5-dimethyl furan would lead to a ring opening, leaving a ene-dione product that could be further oxidised to furaneol (scheme 4.1), an aroma compound used in the perfume industry.

The minor products from the oxidation of cyclooctene have not been oxidised at the double bond, but have formed an alcohol or the ketone product, possibly in sequential steps. The ability to oxidise the carbon next to a double bond would open up the possibility to oxidise α-pinene to form verbenol and subsequently verbenone (Scheme 4.1) which is also used in the fragrance industry.

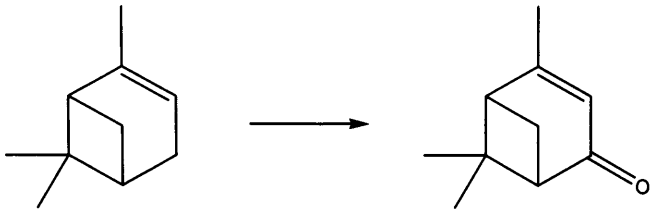

Scheme 4.1: the oxidation of α-pinene to verbenone

4.2 The oxidation of 2,5-dimethyl furan by Au/Au+Pd catalysts

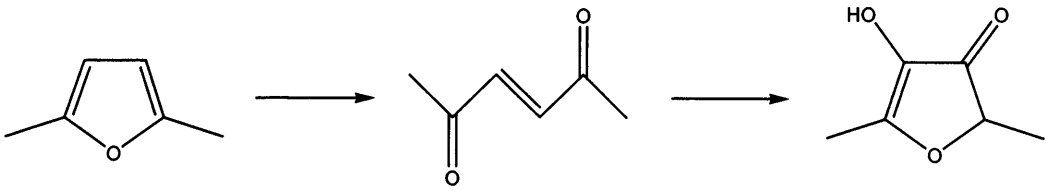

Scheme 4.2 the oxidation of 2,5-dimethylfuran

4.2.1 The effect Temperature

Initial attempts to oxidise 2,5-dimethylfuran were carried out at low temperature, either ambient or cooled by ice, under these conditions, the conversion of 2,5-dimethyl furan was very low after 2h. When the temperature was raised to 50 °C there was some conversion after 2h, however when the temperature was further raised to 75 °C there is almost complete conversion of the 2,5-dimethylfuran (figure 4.1). A reaction was attempted at 100 °C, however when 85 °C was reached reaction runaway occurred.

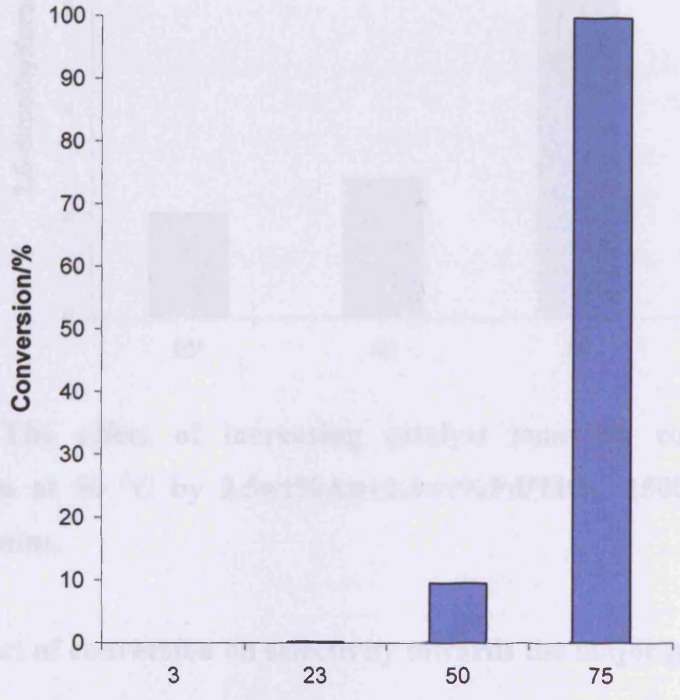

Figure 4.1: The effect of temperature on the conversion of 2,5-dimethylfuran during the oxidation by 40 mg 2.5wt%Au+2.5wt%Pd/TiO_2, 1500 r.p.m. at different temperatures.

4.2.2 The effect of catalyst mass

To check for mass transport limitations, the quantity of catalyst was varied, 20, 40 and 80 mg of catalyst were tested at 50 °C, there is a slight increase in conversion between the 20 mg and 40 mg reactions however the conversion for the reaction with 20 mg of catalyst was measured after 240 minutes while the reaction with 40 mg of

catalyst was measured after 120 minutes. There is a significant increase in conversion when 80 mg of catalyst was used in comparison with 40 mg (figure 4.2).

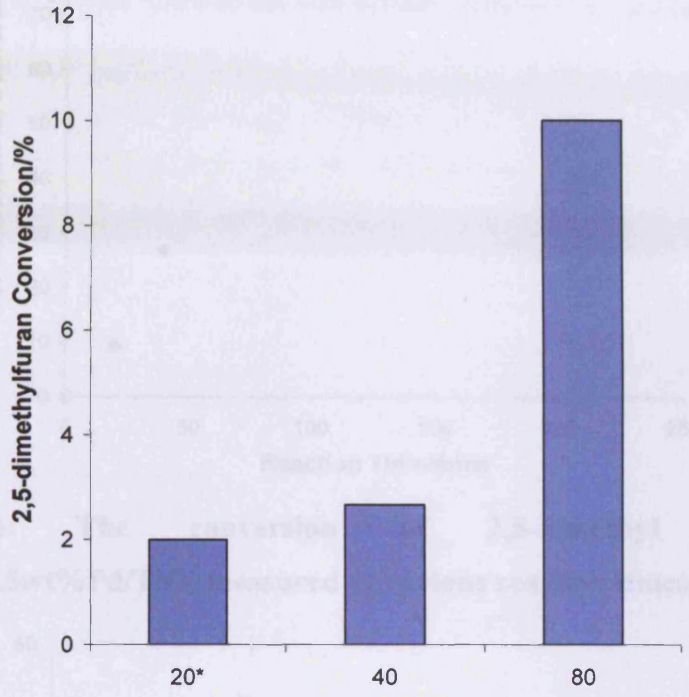

Figure 4.2: The effect of increasing catalyst mass on conversion of 2,5-dimethylfuran at 50 °C by 2.5wt%Au+2.5wt%Pd/TiO_2, 1500 r.p.m after 120 mins, *=240 mins.

4.2.3 The effect of conversion on selectivity towards the major products.

The conversion of 2,5-dimethylfuran at 75 °C at various reaction times is shown in figure 4.3, under these reaction conditions the conversion of 2,5-dimethyl furan is almost complete after 100 mins. The selectivities towards the major products are shown in figure 4.4, at low conversion there is selectivity towards one major product, however as the reaction progresses the selectivity towards this major product decreases, simultaneously the selectivity towards a second product increases suggesting there is a sequential reaction occurring. The first major product formed was identified by ^{13}C NMR as hex-3-ene-2,5-dione.

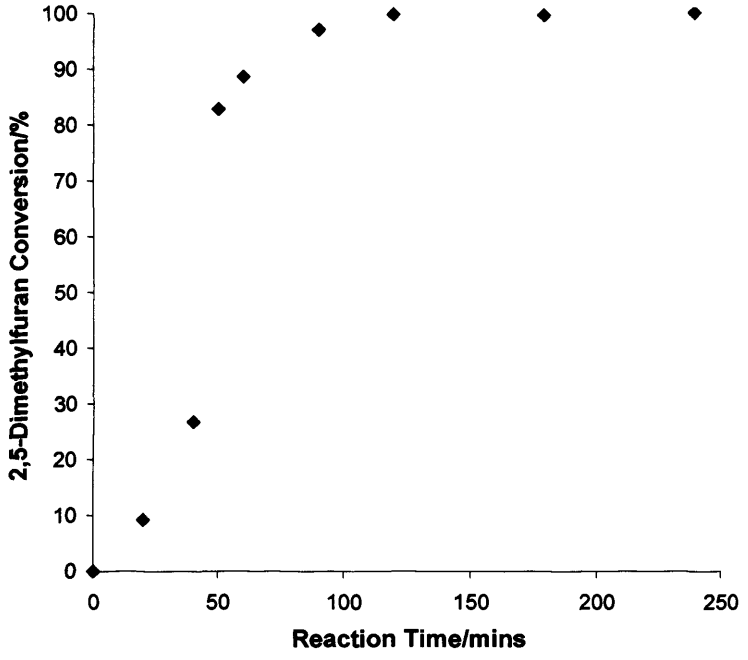

Figure 4.3: The conversion of 2,5-dimethyl furan using 2.5wt%Au+2.5wt%Pd/TiO_2 measured at various reaction times.

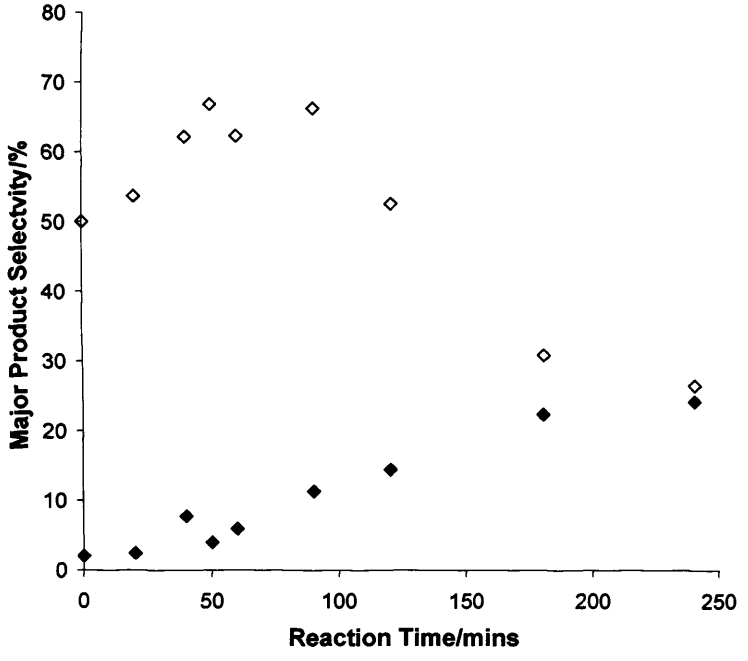

Figure 4.4: The selectivity towards the major products during the oxidation of 2,5-dimethyl furan using 2.5wt%Au+2.5wt%Pd/TiO_2. Hex-3-ene-2,5-dione (open symbols and 4-oxopent-2-enoic acid (closed symbols).

4.2.4 The effect of Catalyst support

After work by Yi Jun *et al*[2] on the oxidation of cyclohexene, where gold supported on carbon was used to oxidise cyclohexene to 1,2-Cyclohexanediol, carbon was investigated as a support for the oxidation of 2,5-dimethylfuran. Initially the carbon catalyst was prepared to be analogous to the catalyst supported on titania. Under these conditions the initial activity of the carbon supported catalyst was higher whereas the titania supported catalyst seemed to have an initial induction time but displayed greater activity over sustained reaction runs (figure 4.5).

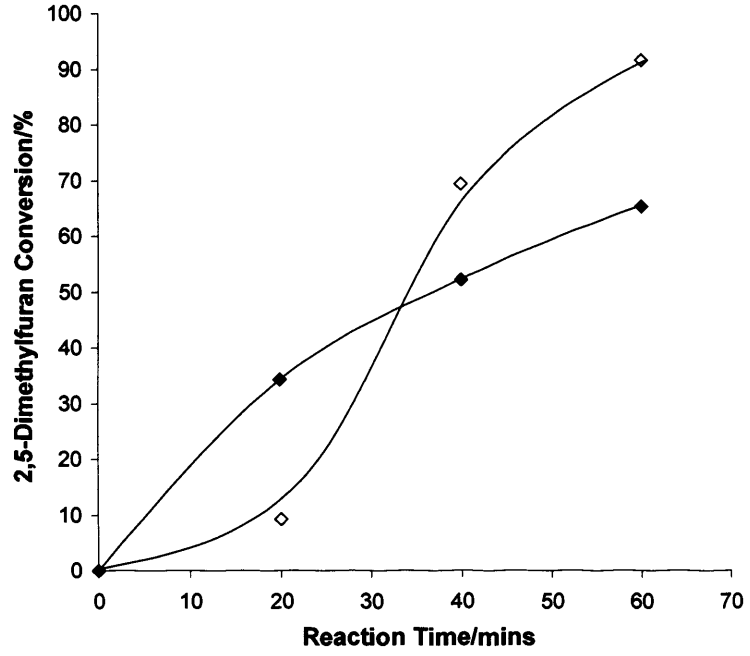

Figure 4.5: The oxidation of 2,5-dimethylfuran by 80 mg 2.5wt%Au+2.5wt%Pd supported on titania (◊) and graphite (♦) at 75 °C, 300psi O_2 and 1500 rpm.

The selectivities towards hex-3-ene-2,5-dione (figure 4.6) of the two catalysts are similar and are reflective of the reaction profile shown previously (figure 4.3) with the lowest selectivity at each point being associated with the catalyst that shows the highest conversion.

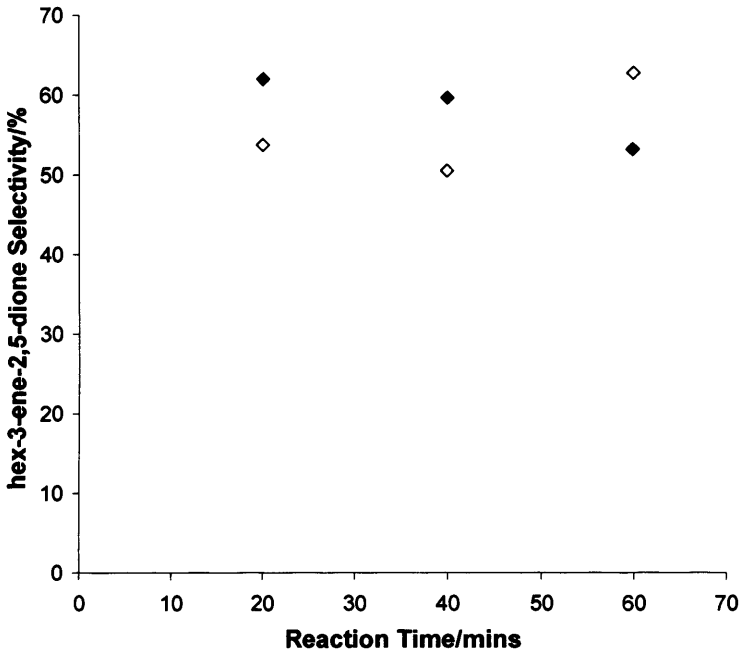

Figure 4.6: The Selectivity towards hex-3-ene-2,5-dione during the oxidation of 2,5-dimethylfuran by 80 mg 2.5wt%Au +2.5wt%Pd supported on titania (♦) and graphite (◊) at 75 °C, 300psi O_2 and 1500 rpm.

The gold supported on carbon catalyst analogous to those prepared by Yi Jun *et al*[2], was also prepared and tested for the oxidation of 2,5-dimethly furan, as with the bi-metallic catalyst the carbon supported catalyst showed higher initial activity but over the course of the reaction the titania supported catalyst proved to be more active (figure 4.7). In this case the selectivities towards the major products ware similar for both supports (figure 4.8).

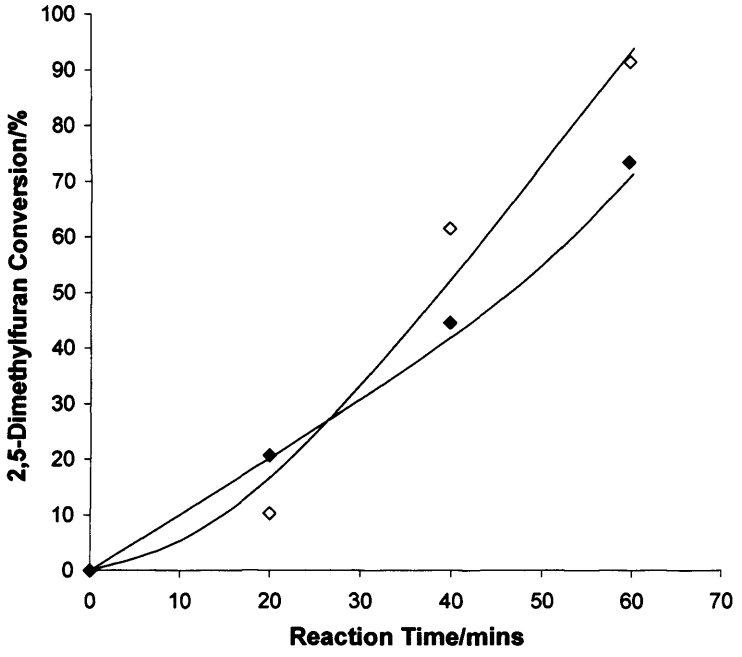

Figure 4.7: The oxidation of 2,5-dimethylfuran by 80 mg 2.5wt%Au supported on titania (◊) and graphite (♦) at 75 °C, 300psi O_2 and 1500 rpm.

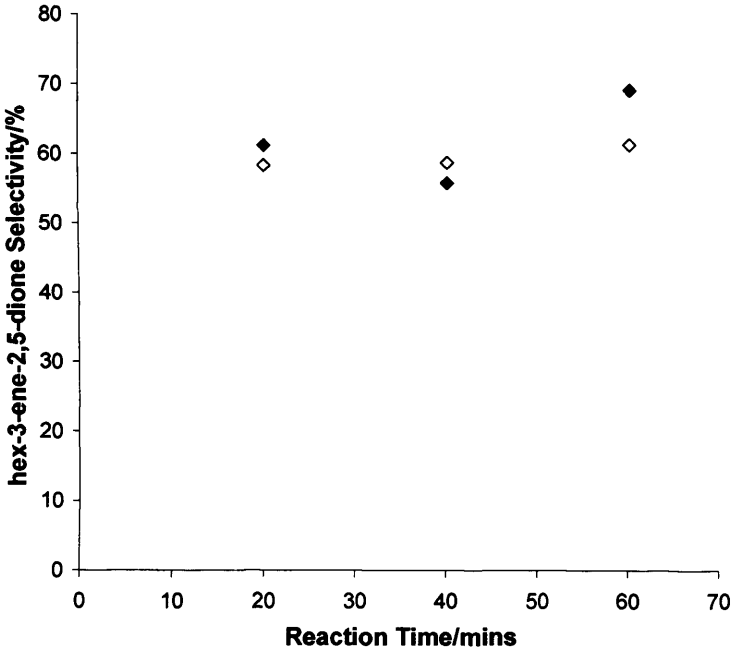

Figure 4.8: The Selectivity towards hex-3-ene-2,5-dione during the oxidation of 2,5-dimethylfuran by 80 mg 2.5wt%Au supported on titania (♦) and graphite (◊) at 75 °C, 300psi O_2 and 1500 rpm.

4.2.5 The effect of radical initiator

To investigate whether the higher initial activity of the carbon supported catalysts was due to greater ability to generate radical species the reactions with the gold catalysts were repeated with tertiarybutyl hydro peroxide (TBHP) added to the reaction (figure 4.9). For both the gold catalyst and the gold-palladium catalyst supported on both titania and graphite, there was a significant increase in the initial activity (figures 4.9 to 4.11). The selectivity towards hex-3-one-2,5-dione was similar for all the catalysts independently of the addition of TBHP (figures 4.12-4.14).

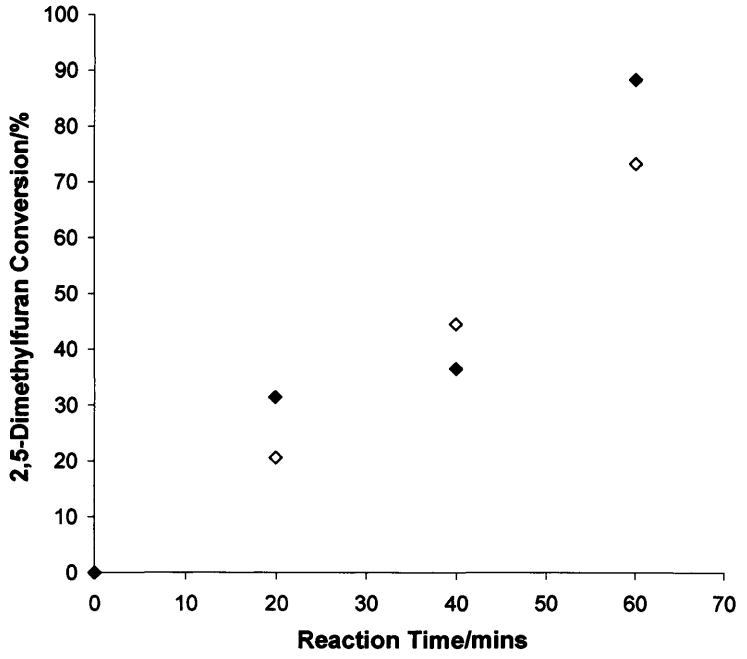

Figure 4.9: The oxidation of 2,5-dimethylfuran by 80 mg 2.5wt%Au supported on graphite (◊) and with the addition of TBHP (0.116 cm^3) (♦) at 75 °C, 300psi O_2 and 1500 rpm.

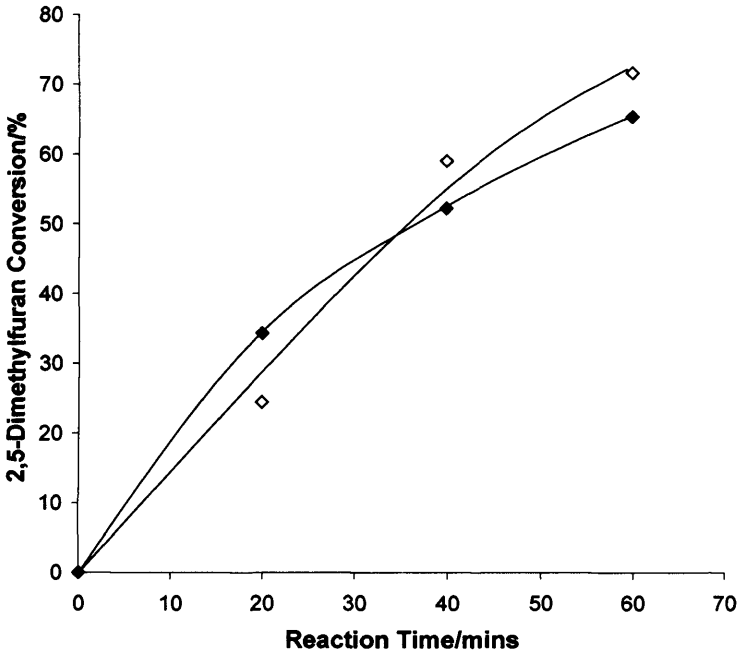

Figure 4.10: The oxidation of 2,5-dimethylfuran by 80 mg 2.5wt%Au+2.5wt%Pd supported on graphite (◊) and with the addition of TBHP (0.116 cm^3) (♦) at 75 °C, 300psi O_2 and 1500 rpm.

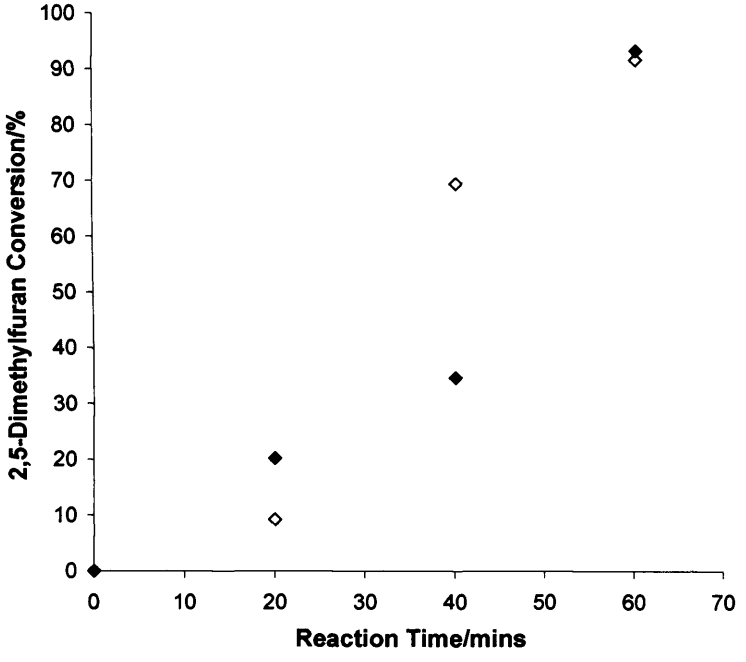

Figure 4.11: The oxidation of 2,5-dimethylfuran by 80 mg 2.5wt%Au+2.5wt%Pd supported on titania (◊) and with the addition of TBHP (0.116 cm^3) (♦) at 75 °C, 300psi O_2 and 1500 rpm.

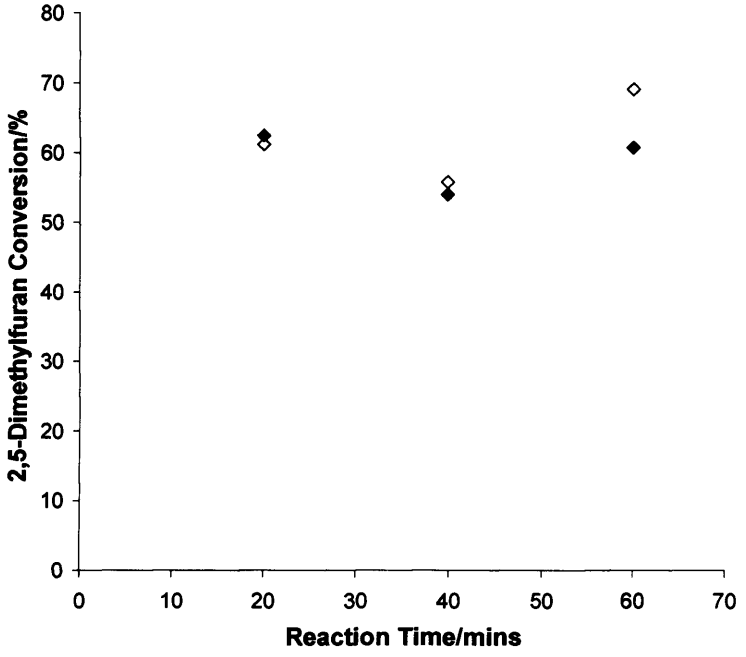

Figure 4.12: The Selectivity towards hex-3-ene-2,5-dione during the oxidation of 2,5-dimethylfuran by 80 mg 2.5wt%Au supported on graphite (♦)and with the addition of TBHP (0.116 cm^3) (◊) at 75 °C, 300psi O_2 and 1500 rpm.

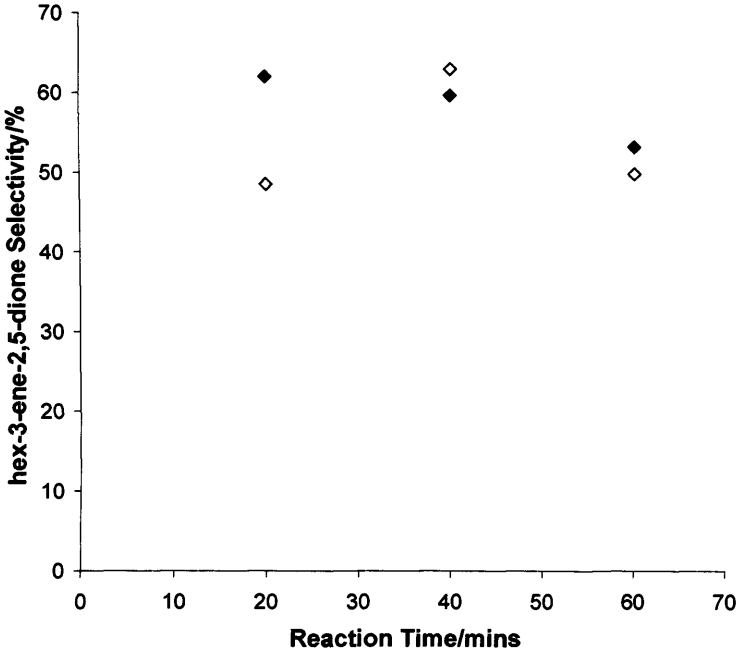

Figure 4.13: The Selectivity towards hex-3-ene-2,5-dione during the oxidation of 2,5-dimethylfuran by 80 mg 2.5wt%Au+2.5wt%Pd supported on graphite (♦) and with the addition of TBHP (0.116 cm^3) (◊) at 75 °C, 300psi O_2 and 1500 rpm.

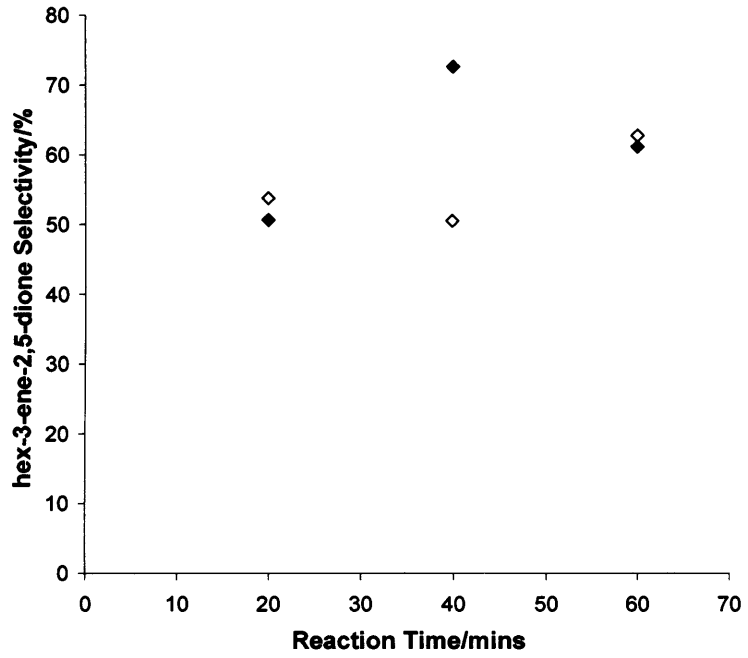

Figure 4.14: The Selectivity towards hex-3-ene-2,5-dione during the oxidation of 2,5-dimethylfuran by 80 mg 2.5wt%Au+2.5wt%Pd supported on titania (◊) and with the addition of TBHP (0.116 cm^3) (♦) at 75 °C, 300psi O_2 and 1500 rpm.

4.2.6 The effect of pressure

Using the previously optimised reaction conditions, with 80 mg 2.5wt%Au+2.5wt%Pd/TiO_2, the effect of O_2 pressure was investigated. The temperature for this reaction was restricted to 50 °C as the reactions at 75 °C were deemed to be operating at to close to the temperature where the reaction runaway occurs (85 °C). The effect of increasing the pressure from 10 bar to 20 bar and subsequently 30 bar seemed negligible on the conversion of 2,5-dimethylfuran (figure 4.15), however the selectivity towards hex-3-ene-2,5-dione seemed to decrease as the pressure increased (figure 4.16). This led to a longer reaction being carried out at 1 bar O_2 pressure, under these conditions the conversion of 2,5-dimethylfuran was almost complete after 24h (figure 4.17) and the selectivity towards hex-3-ene-2,5-dione was consistently the highest displayed under any of the reaction conditions (figure 4.18).

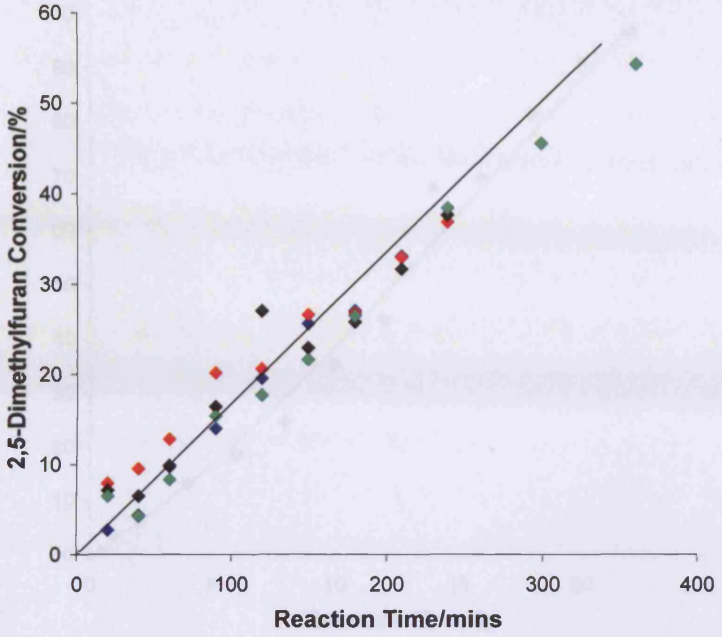

Figure 4.15: The effect of O_2 pressure on the oxidation of 2,5-dimethylfuran by 2.5wt%Au+2.5wt%Pd/graphite at 50 °C, 1500 rpm, by 80mg of catalyst at 5 bar (♦), 10 bar (♦), 20 bar (♦) and 30 bar (♦).

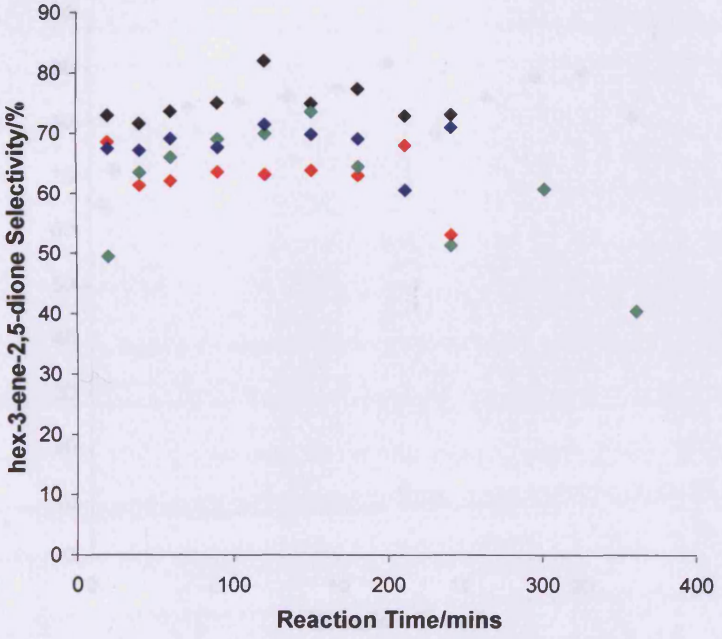

Figure 4.16: The effect of O_2 pressure on the selectivity towards hex-3-ene-2,5-dione during the oxidation of 2,5-dimethylfuran by 2.5wt%Au+2.5wt%Pd/graphite at 50 °C, 1500 rpm, by 80mg of catalyst at 5 bar (♦), 10 bar (♦), 20 bar (♦) and 30 bar (♦).

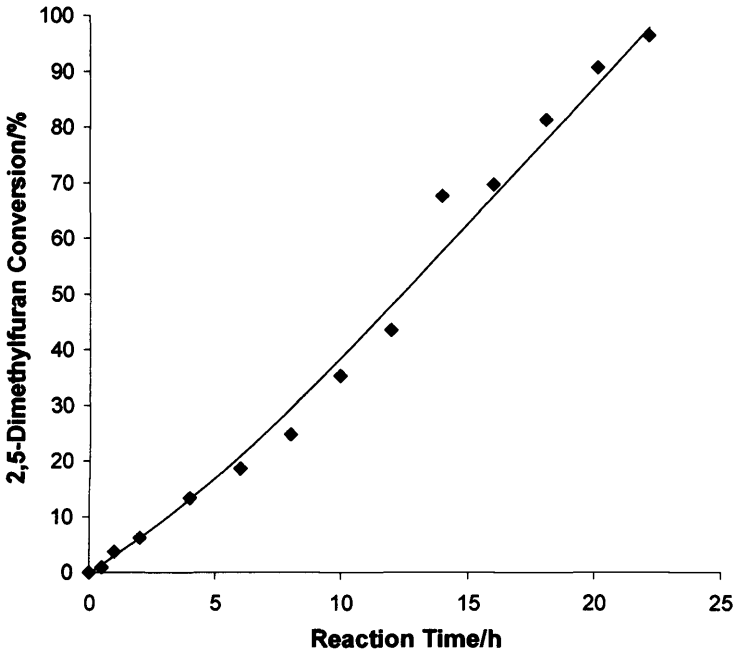

Figure 4.17: The conversion of 2,5-dimethylfuran by 2.5wt%Au+2.5wt%Pd/graphite at 50 °C, 1500 rpm, by 80mg of catalyst at 1 bar O_2.

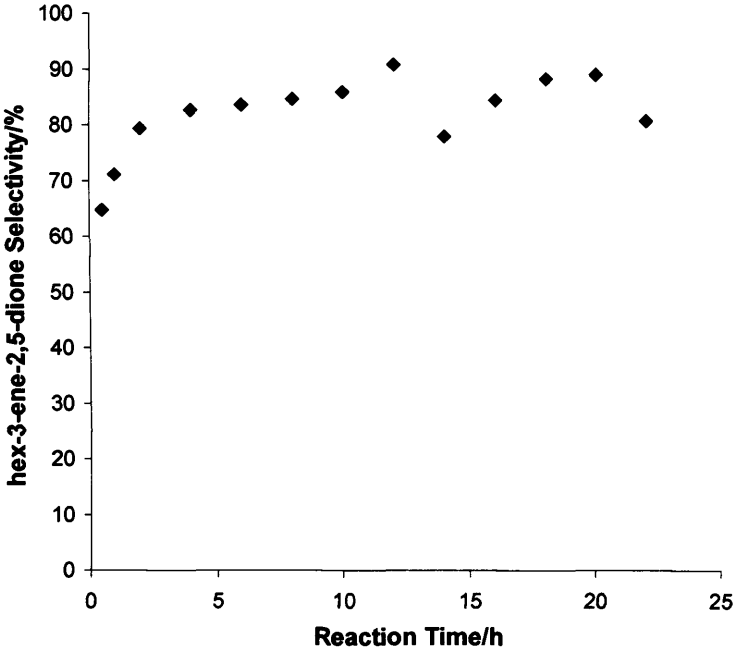

Figure 4.18: The selectivity towards hex-3-ene-2,5-dione during the oxidation of 2,5-dimethylfuran by 2.5wt%Au+2.5wt%Pd/graphite at 50 °C, 1500 rpm, by 80mg of catalyst at 1 bar O_2.

With the reaction at 1 bar O_2 giving high selectivity towards hex-3-ene-2,5-dione this reaction was used to provide the starting material for further studies into the second stage of the oxidation reaction to try and achieve conversion to the desired target material.

Supported sulphuric and phosphoric acid resin were added to the reaction mix to try and provide acid groups to catalyse the second stage of the sequential oxidation, however these did not change the reaction products.

TBHP was added to the hex-3-ene-2,5-dione to attempt to start a radically initiated reaction however when the temperature of the reaction was raised to the desired level (50 °C) reaction runaway occurred, probably due to a polymerisation reaction. To try and prevent this reaction further oxidations were attempted in the presence of solvents (acetone and ethanol) however after reaction runs of 4h at 75 °C and 6h at 50 °C no further reaction occurred.

4.3 The oxidation of α-pinene/2,6,6-trimethylbicyclo[3.1.1]hept-2-ene

4.3.1 The effect of temperature

Oxidation reactions at ambient and 50 °C using 50 mg 2.5wt%Au+2.5wt%Pd/TiO_2 were carried out with 10 bar O_2 and 1500 r.p.m stirring. For reactions up to 4 hours in duration there was no conversion of α-pinene. However when the reaction conditions that had proved successful for the oxidation of 2,5-dimethylfuran were applied an oxidation reaction occurred, the major products from this reaction were identified by GC-MS as verbenol and verbanone and confirmed by comparison of the retention times to those of GC standards.

4.3.2 Reactions with different catalysts.

The performance of the 2.5wt%Au+2.5wt%Pd/TiO_2 catalyst was compared to that of 5wt%Au/TiO_2 and 2.5wt%Au+2.5wt%Pd/CeO_2 the conversion of α-pinene for all three catalysts were remarkably similar (figure 4.19). The selectivities towards

verbanol and verbenone (figures 4.20 and 4.21), however, showed distinct differences with the different catalysts.

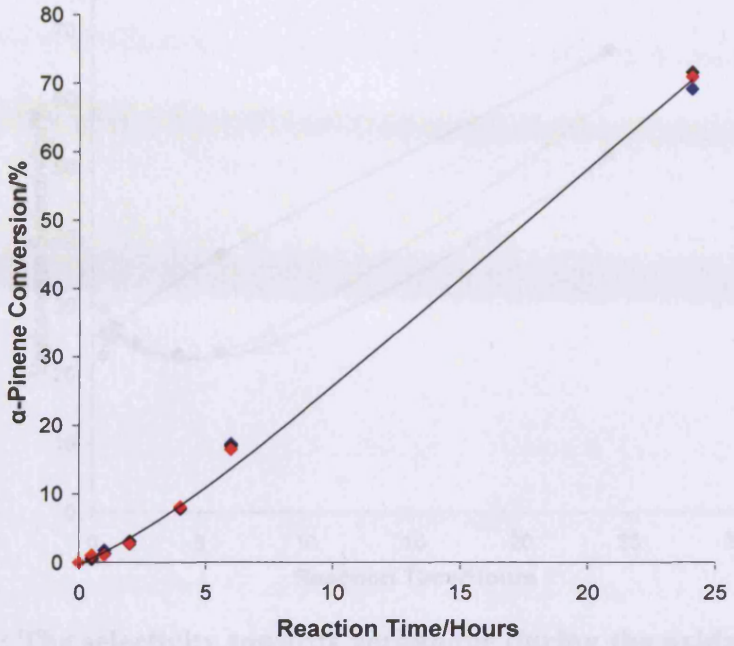

Figure 4.19: the oxidation of α-pinene at 75 °C, 10 bar O_2, 1500 r.p.m by 50 mg 2.5wt%Au + 2.5wt%Pd/CeO_2 (♦), 5wt%Au/TiO_2 (♦) and 2.5wt%Au + 2.5wt%Pd/TiO_2 (♦).

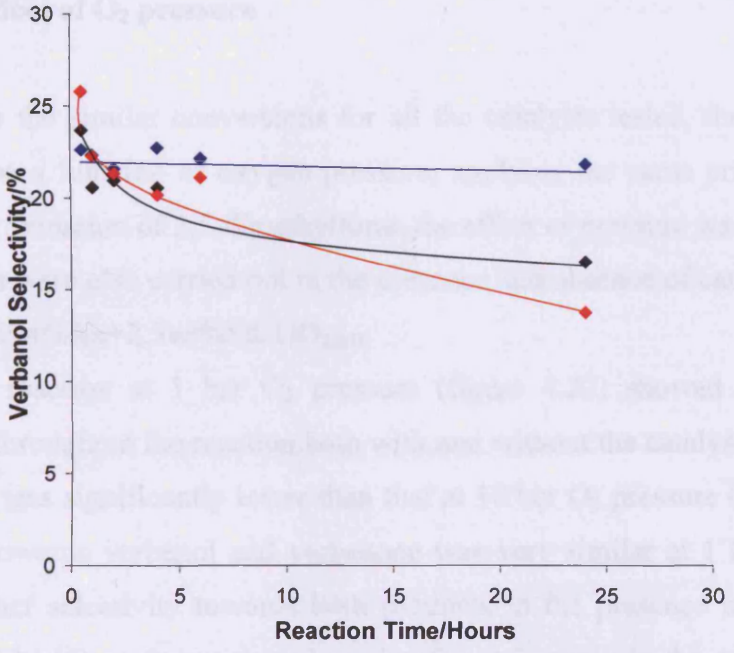

Figure (4.20): The selectivity towards verbanol during the oxidation of α-pinene at 75 °C, 10 bar O_2, 1500 r.p.m by 50 mg 2.5wt%Au + 2.5wt%Pd/CeO_2 (♦), 5wt%Au/TiO_2 (♦) and 2.5wt%Au + 2.5wt%Pd/TiO_2 (♦).

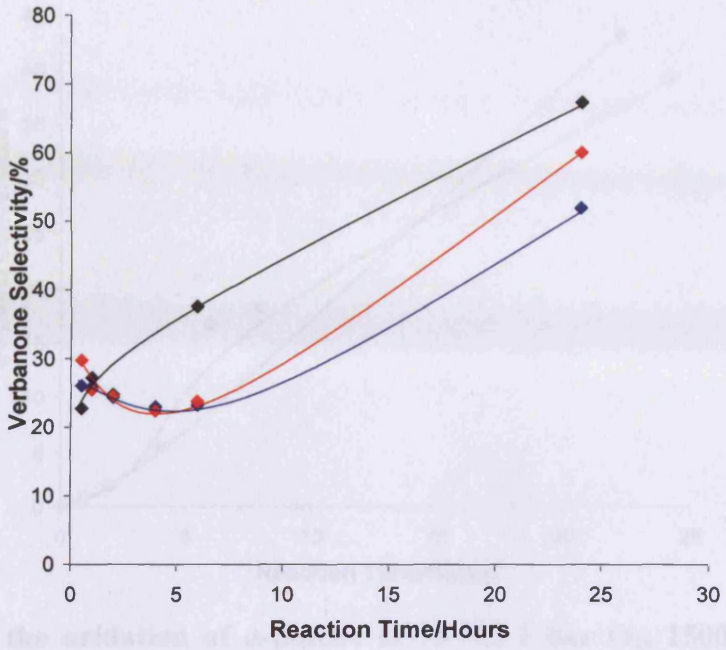

Figure 4.21: The selectivity towards verbanone during the oxidation of α-pinene at 75 °C, 10 bar O_2, 1500 r.p.m by 50 mg 2.5wt%Au + 2.5wt%Pd/CeO_2 (♦), 5wt%Au/TiO_2 (♦) and 2.5wt%Au + 2.5wt%Pd/TiO_2 (♦).

4.3.3 The effect of O_2 pressure

After the similar conversions for all the catalysts tested, the conversion was thought to be a function of oxygen pressure, applying the same principles as in the work on the oxidation of 2,5-dimethylfuran the effect of pressure was investigated but the reactions were also carried out in the presence and absence of catalyst, the catalyst used was 2.5wt%Au+2.5wt%Pd/TiO_{2IMP}

The reaction at 1 bar O_2 pressure (figure 4.22) showed similar α-pinene conversion throughout the reaction both with and without the catalyst. The conversion of α-pinene was significantly lower than that at 10 bar O_2 pressure (figure 4.24). The selectivity towards verbenol and verbenone was very similar at 1 bar pressure with slightly higher selectivity towards both products in the presence of catalyst (figure 4.23). At 10 bar O_2 pressure there is a significant increase in the selectivity towards verbenone, this seems to correspond to the higher conversion of the reaction. The presence of catalyst at this pressure seems to lead to slightly higher conversion of the α-pinene and the selectivity towards both main products is increased (figure 4.25).

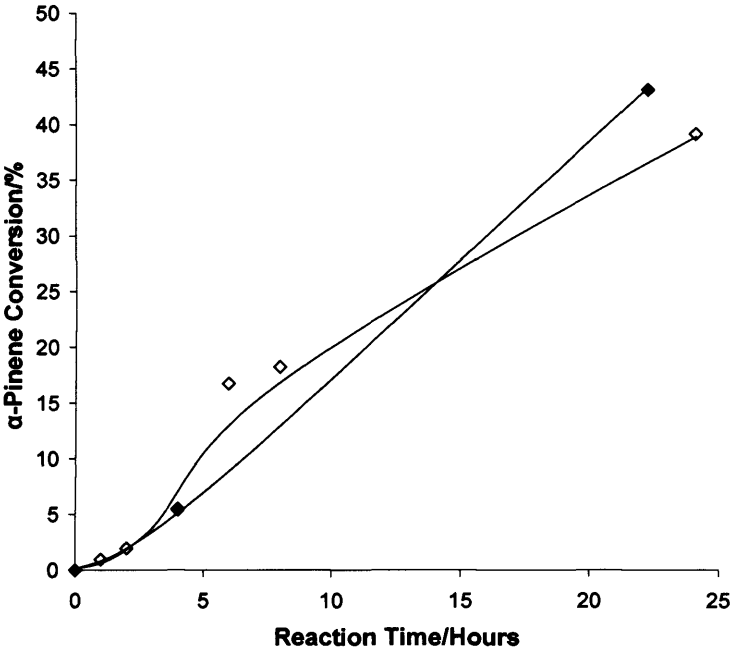

Figure 4.22: the oxidation of α-pinene at 75 °C, 1 bar O_2, 1500 r.p.m , blank reaction (♦) and with 50mg 2.5wt%Au + 2.5wt%Pd/TiO_2 (◊).

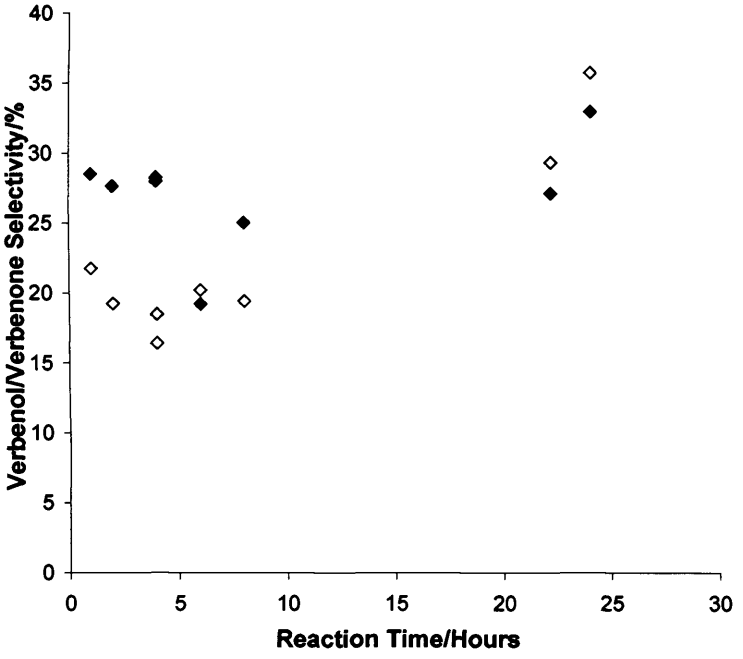

Figure 4.23: The selectivity towards the major products during the oxidation of α-pinene at 75 °C, 1 bar O_2, 1500 r.p.m , blank reaction (♦) with 50mg 2.5wt%Au + 2.5wt%Pd/TiO_2 (♦) verbenol (closed symbols) and verbenene (open symbols).

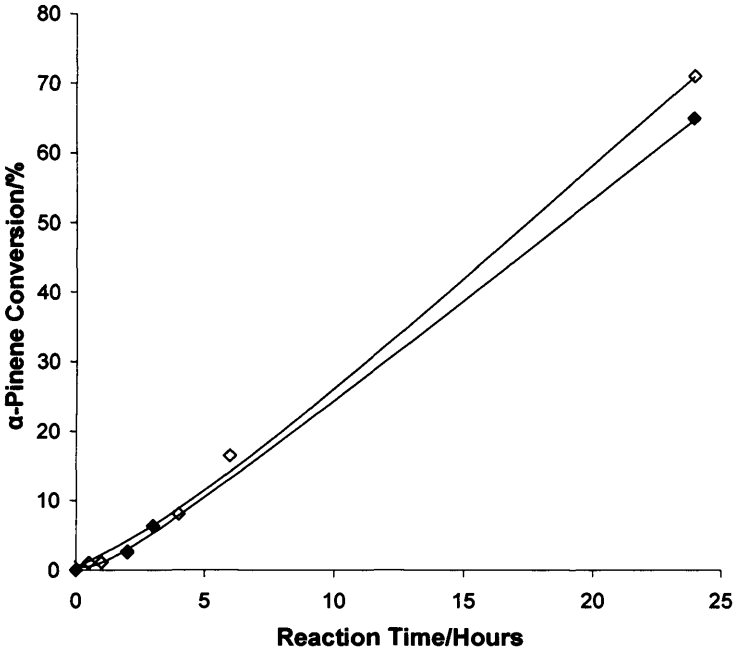

Figure 4.24: the oxidation of α-pinene at 75 °C, 10 bar O_2, 1500 r.p.m, blank reaction (♦) and with 50mg 2.5wt%Au + 2.5wt%Pd/TiO_2 (◊).

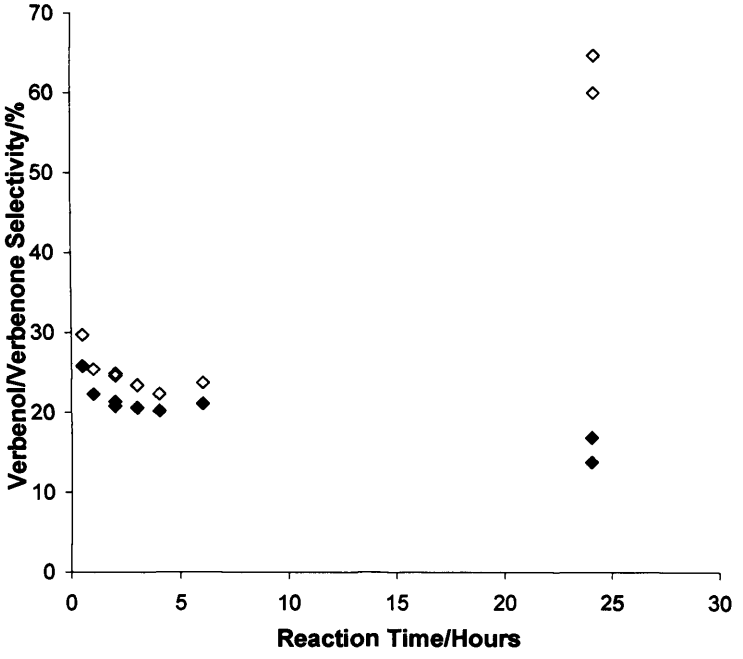

Figure 4.25: The selectivity towards the major products during the oxidation of α-pinene at 75 °C, 10 bar O_2, 1500 r.p.m , blank reaction (♦) with 50mg 2.5wt%Au + 2.5wt%Pd/TiO_2 (♦) verbenol (closed symbols) and verbenone (open symbols).

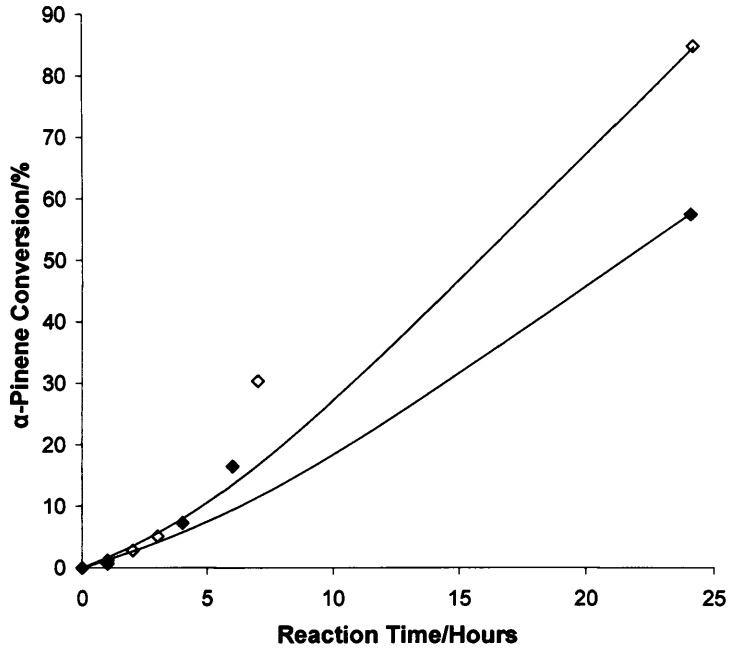

Figure 4.26: the oxidation of α-pinene at 75 °C, 20 bar O_2, 1500 r.p.m , blank reaction (♦) and with 50mg 2.5wt%Au + 2.5wt%Pd/TiO_2 (◊).

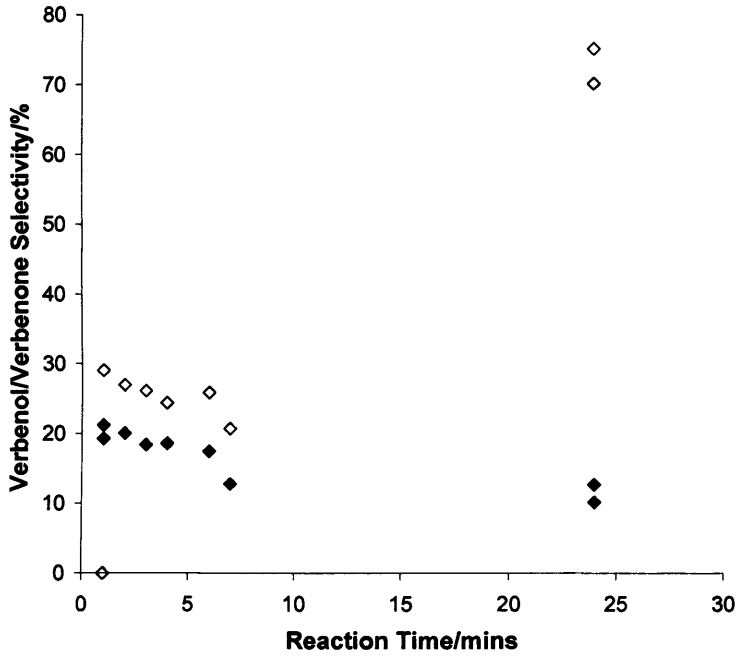

Figure (4.27): The selectivity towards the major products during the oxidation of α-pinene at 75 °C, 20 bar O_2, 1500 r.p.m , blank reaction (♦) with 50mg 2.5wt%Au + 2.5wt%Pd/TiO_2 (♦) verbenol (closed symbols) and verbenone (open symbols).

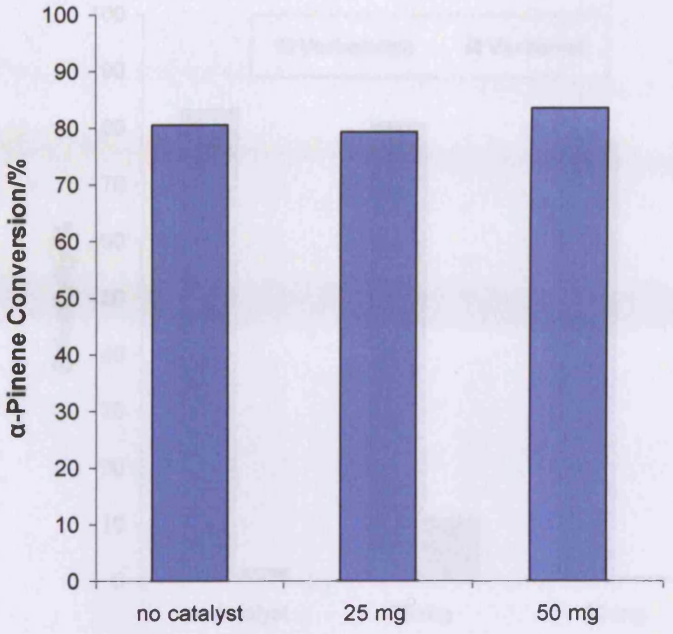

Figure 4.28: the oxidation of α-pinene at 75 °C, 30 bar O_2, 1500 r.p.m , blank reaction and with 25/50mg 2.5wt%Au + 2.5wt%Pd/TiO_2.

The reaction at 20 bar O_2 pressure showed greater conversion of α-pinene, it also showed the greatest selectivity towards verbenone (figures 4.26 and 4.27).

The reaction carried out at 30 bar O_2 pressure showed the highest conversion of α-pinene with around 80% conversion in the absence of a catalyst (figure 4.28), there was a slight improvement on the conversion upon the addition of 50 mg of 2.5wt%Au+2.5wt%Pd/TiO_2 however in this case the selectivity towards verbanone was greatest for the reaction without a catalyst. With the addition of 25 mg of catalyst the total selectivity towards verbenol and verbanone was the highest of any reaction at around 90%, however with 50 mg of catalyst the verbenol peak was significantly smaller (figure 4.29) and the selectivity towards verbanone was lower than that observed for the blank reaction.

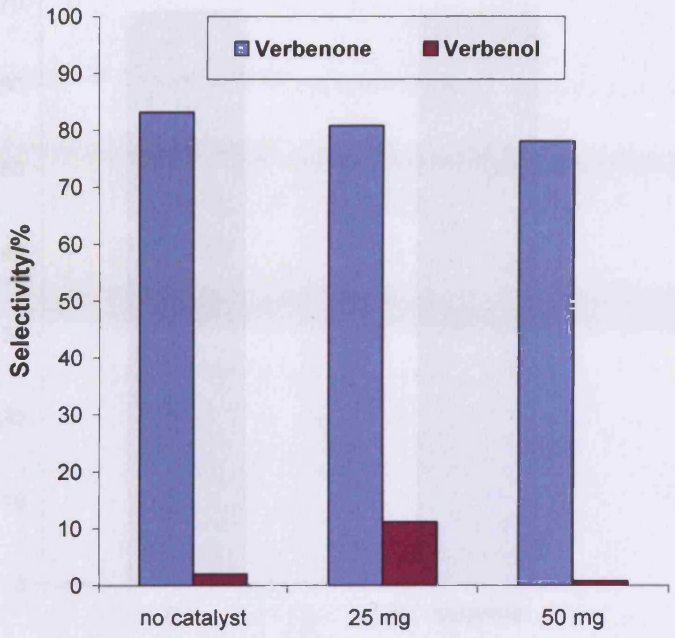

Figure 4.29: The selectivity towards the major products during the oxidation of α-pinene at 75 °C, 30 bar O_2, 1500 r.p.m , blank reaction and with 25/50mg 2.5wt%Au + 2.5wt%Pd/TiO_2.

4.3.4 The reaction of pure α-pinene

As there was significant oxidation of the α-pinene in the absence of catalyst a purer form of α-pinene was obtained to test if any of the impurities in the pinene was acting as catalyst. The reaction was carried out at 30 bar in the absence of catalyst, the conversion of both forms of α-pinene was very similar (figure 4.30).

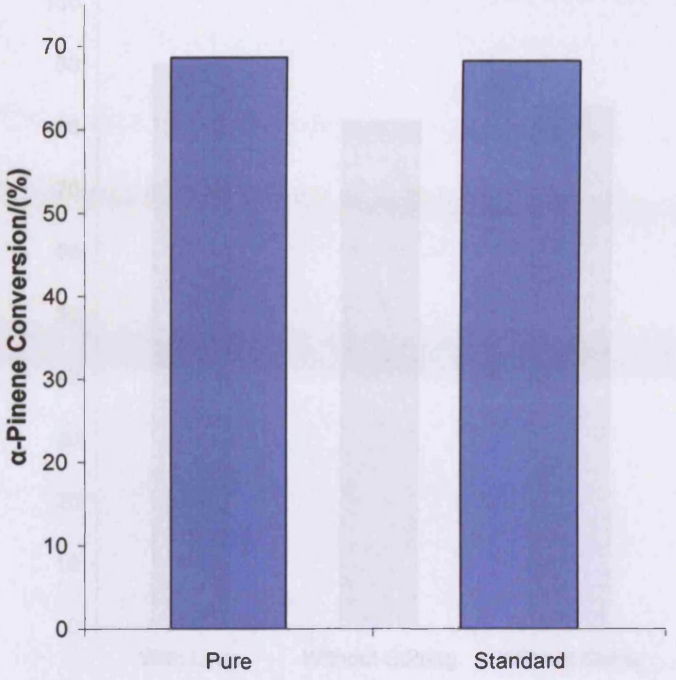

Figure 4.30: the conversion of standard α-pinene and pure α-pinene at 75 °C 10 bar O_2 pressure (♦) with 50mg 2.5wt%Au + 2.5wt%Pd/TiO_2 catalyst after 20h

4.3.5 The use of a reactor liner

Furthermore to test if the reaction was catalysed by walls of the autoclave a reaction was carried out at 30 bar O_2 pressure with a Teflon liner in the autoclave, without stirring and with the stirrer removed. In these cases the conversion of α-pinene was higher than the non-lined reactions and was similar in all three cases (figure 4.31).

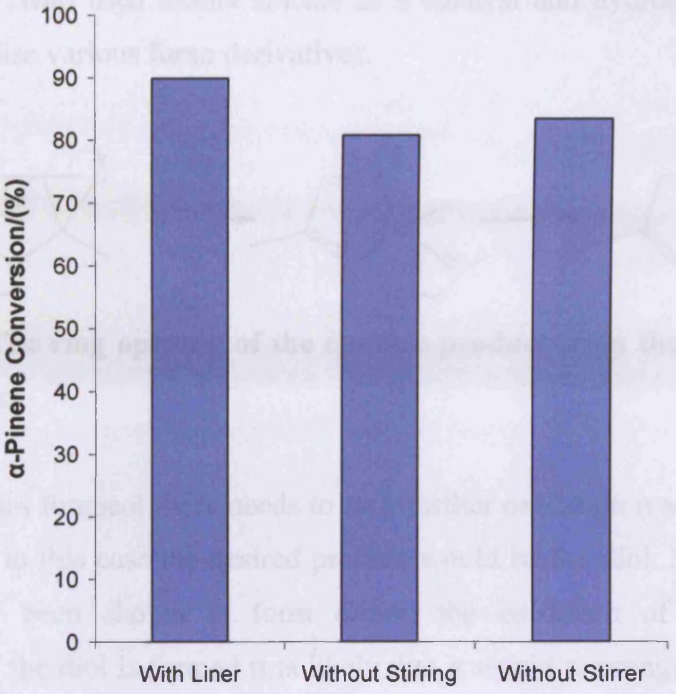

Figure 4.31: the conversion of α-pinene when the autoclave has a Teflon liner, no stirring and the stirrer removed.

4.4 Discussion:

4.4.1 2,5-dimethyl furan

4.4.1.1 The effect of conversion on the selectivities of the major products

The conversion of 2,5-dimethyl furan increased with the temperature of the reaction (figure 4.1) and the selectivity towards hex-3-ene-2,5-dione remained constant. Above 85 °C reaction runaway occurred, possibly due to a polymerisation reaction of the hex-3-ene-2,5-dione which would be susceptible to a Michael addition type polymerisation process.

The formation of hex-3-ene-2,5-dione could occur if the initial oxidation reaction leads to the epoxidation of one of the double bonds in the furan system (Scheme 4.3). The epoxidation of cyclohexene by supported gold catalysts is a known reaction[2] and the epoxidation mechanism for this ring opening has been suggested by

Whalen *et al*[3] who used titania silicate as a catalyst and hydrogen peroxide as an oxidant to oxidise various furan derivatives.

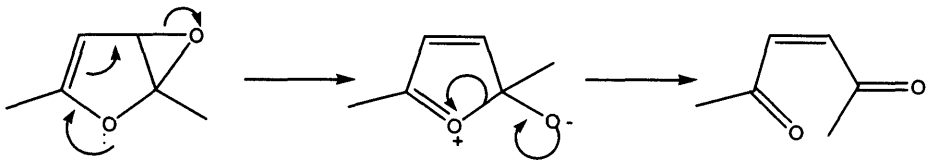

Scheme 4.3: The ring opening of the epoxide product from the oxidation of 2,5-dimehtyl furan

To obtain furaneol there needs to be a further oxidation reaction of the hex-3-ene-2,5-dione, in this case the desired product would be the diol. Small quantities of the diol have been shown to form during the oxidation of cyclohexene and cyclooctene. If the diol is formed it is likely that it would rearrange to form furaneol. The transformation from 3,4-dihydroxyhexane-2,5-dione to furaneol has been reported previously[5].

4.4.1.2 The effect of catalyst mass

The conversion of the 2,5-dimethyl furan increases upon the addition of a greater amount of catalyst (figure 4.2), the increase in conversion upon adding 40 mg of catalysts compared with 20 mg is not significant but it must be noted that the reaction with 20 mg of catalyst was run for twice the time. There is a significant increase in conversion upon further increasing the catalysts mass to 80 mg, this suggests there is no mass transport limitation problems under these conditions.

4.4.1.3 Identification of the second major product

Due to the tendency of reaction runaway to occur under the conditions originally used for this reaction it has proved difficult to identify the second major product observed when the reaction is carried out at 75 °C (figure 4.4) GC-MS data has suggested 4-oxopent-2-enoic acid, however further characterisation would be required to confirm this.

4.4.1.4 The effect of Support

The use of different supports for the oxidation of 2,5-dimethylfuran seems to affect the reaction profile, when a graphite support is used the initial conversion of the furan seems to be greater than when a titania support is used (figure 4.5). Throughout the course of the reaction the catalysts supported on titania showed the greatest conversion. The differences between the catalysts on different supports could be due to the ability to generate radical species. To this end several reactions were carried out with the addition of a radical generator, tertiarybutylhydroperoxide (TBHP). The addition of TBHP led to an increase in the initial reaction rate of the reaction with all the different catalysts (figures 4.9 to 4.11), however the conversion of 2,5-dimethyl furan over longer reaction runs with and without the initiator was relatively similar and the selectivities towards hex-3-ene-2,5-dione were similar in all cases (figures 4.12-4.14).

4.4.1.5 The effect of Pressure

The oxygen pressure does not seem to have a significant effect on the conversion of 2,5-dimethyl furan (figure 4.15), reactions with O_2 pressure of between 5 and 30 bar all showed similar conversion, however the selectivity towards hex-3-ene-2.5-dione was greatest for the reaction at the lowest pressure. A further reaction conducted at 1 bar O_2 pressure showed less conversion of 2,5-dimethyl furan (figure 4.17) but a significant increase in the selectivity towards hex-3-ene-2,5-dione (figure 4.18). The oxidation reactions carried out at higher temperatures (figure 4.4) would suggest that there is a sequential reaction occurring with the hex-3-ene-2,5-dione being further oxidised to form a secondary product. Under lower temperature and lower O_2 pressure reaction conditions however this secondary oxidation may not take place leading to an increase in the selectivity of the hex-3-ene-2,5-dione.

The attempts to further oxidise the hex-3-ene-2,5-dione to form furaneol proved unsuccessful probably due to a polymerisation reaction occurring when there is no solvent present in the reaction. The gold palladium catalysts used have been demonstrated to work in the presence of solvents[4] so the failure to further oxidise the

hex-3-ene-2,5-dione could be due to the low temperature enforced on the reaction due to the need to prevent reaction runaway.

4.4.2 α-pinene

4.4.2.1 The use of various catalysts

The results of the tests with various catalysts suggest that the catalyst does not play a part in the reaction (figure 4.19), this is an unexpected result studies by Casuscelli *et al*[5] have carried out the oxidation of α-pinene at similar temperature but using hydrogen peroxide instead of molecular oxygen as the oxidant and did not observe a reaction in the absence of catalyst. The reaction was also carried out using magnetic stirring and the additional agitation provided by a mechanical stirrer and the high pressure O_2 may be responsible for the autoxidation. While the type of catalyst did not appear to affect the conversion of the α-pinene there was an observable difference in the product distribution with the different catalysts with the bimetallic catalysts showing the greatest selectivity towards the desired verbenone product (figure 4.21).

The formation of verbenol and verbenone from α-pinene could be due to a radical mechanism, an example of which has been proposed by Casuscelli *et al*[5] and is shown in Scheme 4.4. This mechanism would give equal quantities of verbenol and verbenone, in the early stages of the reaction this appears to be the case, however as the reaction continues the verbenone product is strongly favoured suggesting a further reaction is taking place which could be the conversion of verbenol into verbenone.

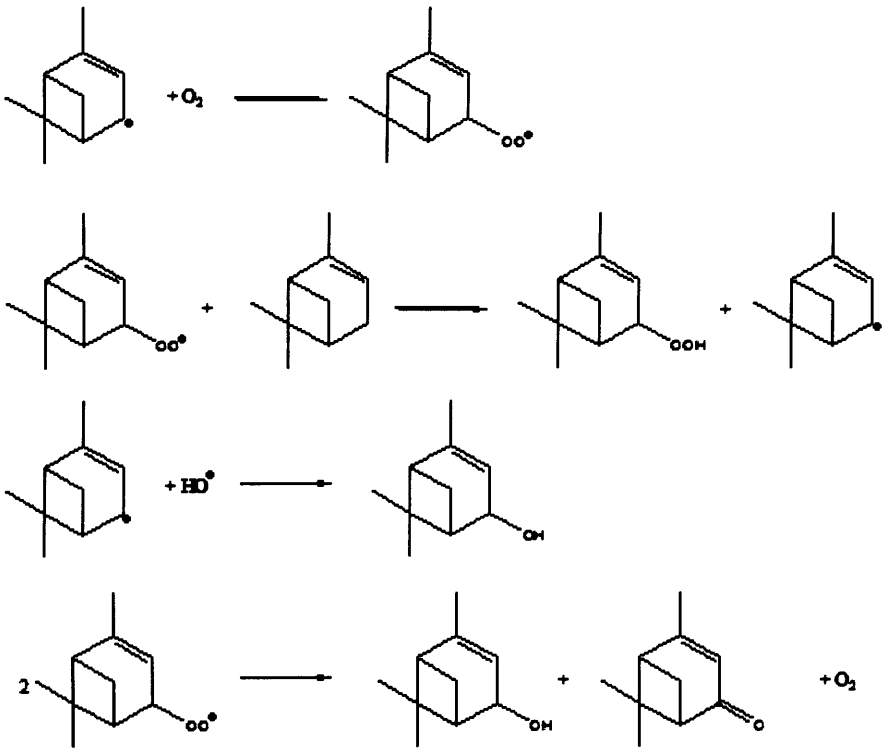

Scheme 4.4: radical mechanism for the formation of verbenol and vernbenone from α-pinene as proposed by Casuscelli *et al*[6].

4.4.2.2 The effect of pressure

As the catalyst was not having an effect on the conversion of α-pinene reactions were carried out at different O_2 pressures. Due to the differences observed in the selectivities these reactions were carried out with and without catalyst present. The reaction carried out at 1 bar O_2 pressure (figure 4.22) showed lower conversion of α-pinene than the reaction carried out at 10 bar O_2 pressure (figure 4.24). The conversion of α-pinene was similar with and without the catalysts. The selectivity was lower at 1 bar O_2 pressure (figure 4.23) but this is more likely to be a function of the conversion. This pattern is repeated as the pressure is increased to 20 and 30 bar respectively, the reactions at 20 (figure 4.26) and 30 (figure 4.28) bar show a slight increase in the conversion when the catalyst is present but it is not a significant increase. The selectivity towards verbenone also seems to increase with the pressure of the O_2. The selectivities towards the major products do not appear to be influenced by the presence of catalyst at elevated pressures (figure 4.29).

Wen *et* al[7] found that the walls of their stainless steel reactor acted as a catalyst for the oxidation of cyclohexane, to test whether this was the case for α-pinene a Teflon liner was used (figure 4.31) in the autoclave. The conversion of α-pinene was even greater than without the liner, this could be due to the fact that the liner reduces the volume of the autoclave by about 33%, the molar quantity of α-pinene that was converted could be similar. Furthermore tests where there was no stirring were also carried out and it was found that this made no difference to the conversion and a test with the stirrer removed also showed similar conversion suggesting that the reaction is not catalysed by the stainless steel of the autoclave.

As the catalyst did not seem to be influencing the reaction pure α-pinene was tested under the same reaction conditions, in case the oxidation reaction was catalysed by an impurity in the α-pinene. The conversion after 24h was very similar to the as purchased α-pinene (figure 4.30) this indicates that the reaction is not catalysed by the impurities in the pinene.

4.5 Conclusions

4.5.1 The oxidation of 2,5-dimethyl furan

- The ring opening oxidation of 2,5-dimethylfuran to yield hex-3-ene-2,5-dione was carried out using various catalysts, probably via the epoxidation of one of the furan double bonds. Attempts to further oxidation of hex-3-ene-2,5-dione to form furaneol proved unsuccessful with reaction runaway occurring when solvent free reactions were attempted.

- The ring opening reaction was carried out with the highest conversion at 75 °C, however this temperature was found to be too close to the temperature at which reaction runaway occurs and longer reactions carried out at 50 °C are considered a safer alternative.

- The use of carbon as a support seemed to lead to a higher initial conversion of 2,5-dimethyl furan when compared to catalysts using titania as a support. Over

the duration of the reaction however the catalysts supported on titania displayed the greater conversion.

- The use of a radical initiator lead to an increase in the initial conversion but had little effect on the conversion over the duration of the reaction, under the reaction conditions the radical initiator would have a very short half life and therefore would be consumed rapidly.

- The highest selectivity towards hex-3-ene-2,5-dione was achieved at the lowest pressure of oxygen tested, this suggests that higher pressure leads to the formation of other side products which is potentially desirable as further oxidation is required to form furaneol but as furaneol was not one of the other products formed it is undesirable in this case.

4.5.2 The oxidation of α-pinene

- The oxidation of α-pinene to form verbenone was successfully carried out with good conversion and selectivity, however the conversion appears to be independent of the presence of a catalyst.

- The oxygen pressure had a large effect on the conversion of α-pinene with the highest pressure leading to the highest conversion. The presence of catalysts at various pressures seems to have an effect on the selectivity towards verbenone but a regular pattern was not established.

- The use of a purer form of α-pinene did not lead to a reduction in its conversion under the standard reaction conditions suggesting that the reaction is not catalysed by impurities in the starting material

- When a reactor liner was used the conversion of α-pinene was slightly higher under standard reaction conditions suggesting the walls of the reactor did not catalyse this reaction. The increase in the conversion is thought to be due to the reduction in volume associated with the use of a liner.

4.6 References

[1] A. Stephen, K. Hashmi, G. J. Hutchings, *Angewandte Chemie, International Edition* **2006**, *45*, 7896.

[2] M. D. Hughes, Y.-J. Xu, P. Jenkins, P. McMorn, P. Landon, D. I. Enache, A. F. Carley, G. A. Attard, G. J. Hutchings, F. King, E. H. Stitt, P. Johnston, K. Griffin, C. J. Kiely, *Nature (London, United Kingdom)* **2005**, *437*, 1132.

[3] J. Wahlen, B. Moens, D. E. De Vos, P. L. Alsters, P. A. Jacobs, *Advanced Synthesis & Catalysis* **2004**, *346*, 333.

[4] N. Dimitratos, A. Villa, D. Wang, F. Porta, D. Su, L. Prati, *Journal of Catalysis* **2006**, *244*, 113.

[5] M. A. Briggs, A. H. Haines, H. F. Jones, *Journal of the Chemical Society, Perkin Transactions 1: Organic and Bio-Organic Chemistry (1972-1999)* **1985**, 795.

[6] S. G. Casuscelli, G. A. Eimer, A. Canepa, A. C. Heredia, C. E. Poncio, M. E. Crivello, C. F. Perez, A. Aguilar, E. R. Herrero, *Catalysis Today* **2008**, *133-135*, 678.

[7] Y. Wen, O. E. Potter, T. Sridhar, *Chemical Engineering Science* **1997**, *52*, 4593.

Chapter Five

Chapter 5: Application of established catalysts and principles to other oxidation systems.

5.1 Introduction

Having successfully used gold-palladium catalysts for the oxidation of α-pinene, there are several other oxidation systems where the addition of a ketone group next to a double bond would represent a value added process that could be a viable industriall process. To this end the oxidation of valencene and isophorone were attempted under the conditions established for the α-pinene system.

The co-impregnation prepared bi-metallic catalyst has also been used, by the Hutchings group for the oxidation of toluene to benzyl alcohol, the oxidation of a methyl group, to form an alcohol, on an pyridine ring is an analogous reaction that would be useful for 2,6-lutidene, 2-picoline and 3-picoline to yield value added products. Furthermore previous work in the group has shown that ortho and meta-xylene can be selectively oxidised on one of the methyl groups, the selective oxidation of one of the methyl groups on 2,4-dimethylnitrobenzene would be an industrially useful process.

5.2 The oxidation of valencene/ (*1R,7R,8aS*)-1,2,3,5,6,7,8,8a- Octahydro-1,8a-dimethyl-7- (1-methylethenyl)naphthalene

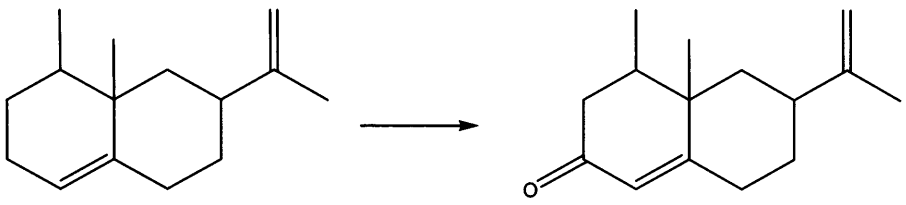

Scheme 5.1: the oxidation of valencene to nootkatone

The oxidation of valencene to form nootkatone (scheme 5.1) was carried out under the standard reaction conditions established for the α-pinene system; the reaction was carried out at 80 °C with 50 mg 2.5wt%Au+2.5wt%Pd/TiO_2. The catalyst proved to be able to oxidise valencene under these reaction conditions and after a period of 72h the conversion of valencene had reached almost 100 % (figure

5.1). The selectivity towards nootkatone, identified by comparison of GC retention time with a known standard, was around 50% throughout the reaction (figure 5.2).

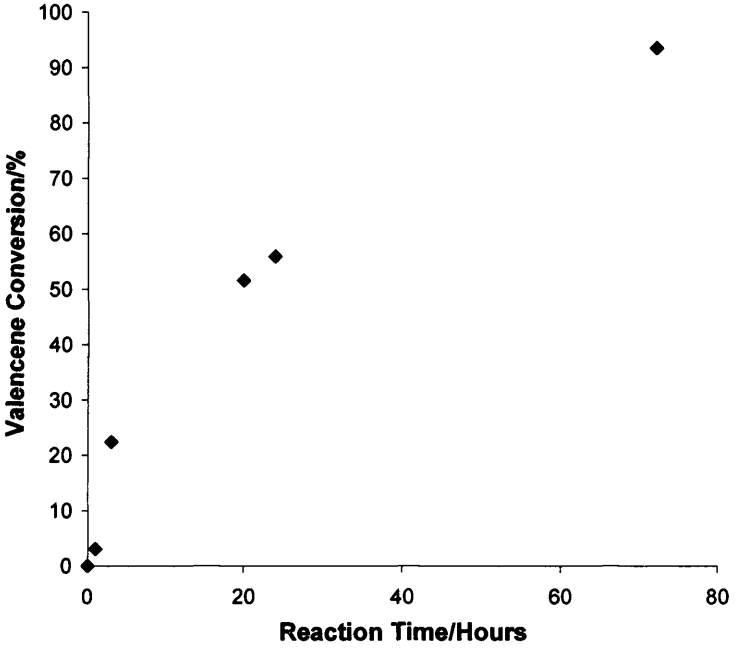

Figure 5.1: The conversion of valencene using 50 mg 2.5wt%Au + 2.5wt%Pd/TiO_2 at 80 °C and 1500 r.p.m.

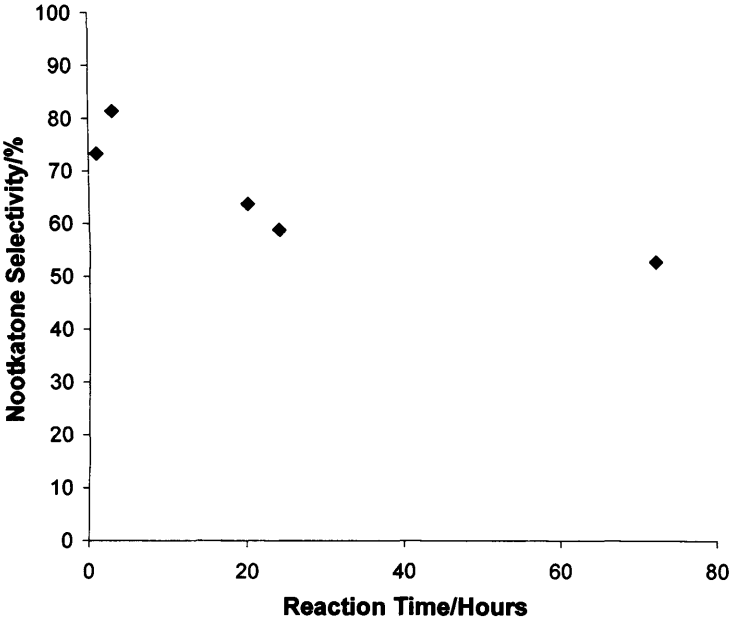

Figure 5.2: The selectivity towards nookkatone during the oxidation of valencene using 50 mg 2.5wt%Au+2.5wt%Pd/TiO_2 at 80 °C and 1500 r.p.m.

5.3: The oxidation of Ispohorone (3,5,5-Trimethyl-2-Cyclohexene-1-one)

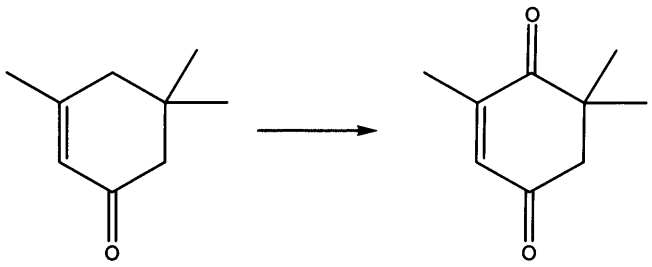

Scheme 2: the oxidation of isophorone to 4-oxoisophorone

The oxidation of isophorone to 4-oxoisophorone was also attempted using 50 mg 2.5wt%Au+2.5wt%Pd/TiO_2 prepared by the co-impregnation method and then subsequently, 2.5wt%Au+2.5wt%Pd/TiO_2 prepared by the deposition precipitation method (the more active catalyst for benzyl alcohol oxidation), and the standard reaction conditions established for the α-pinene system. Under these conditions there was around 30% conversion after 24h (figure 5.3) and a selectivity towards 2-oxoisophorone, identified by comparison of retention time to that of a known standard, of around 50% (figure 5.4).

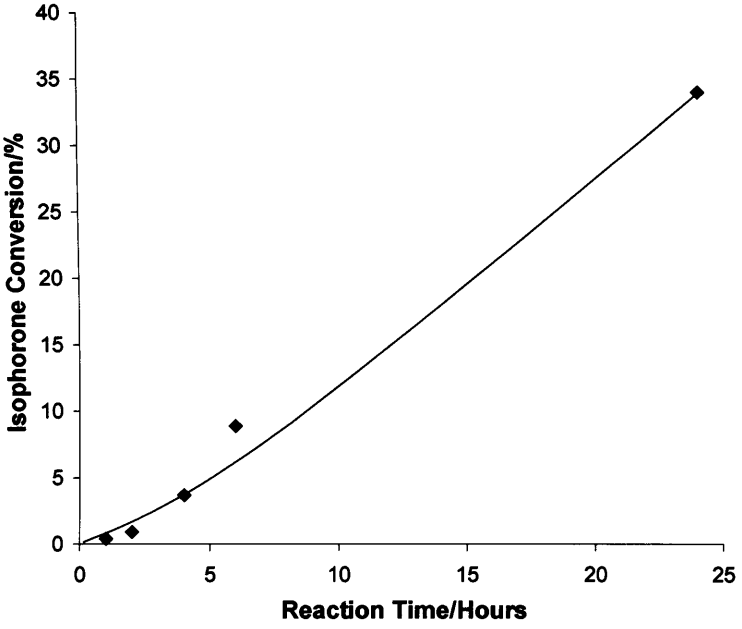

Figure 5.3: The oxidation of isophorone at 75 °C, 1500 r.p.m. with 10 bar O_2, using a 2.5wt%Au+2.5wt%Pd/TiO_2 catalyst prepared by the deposition precipitation method.

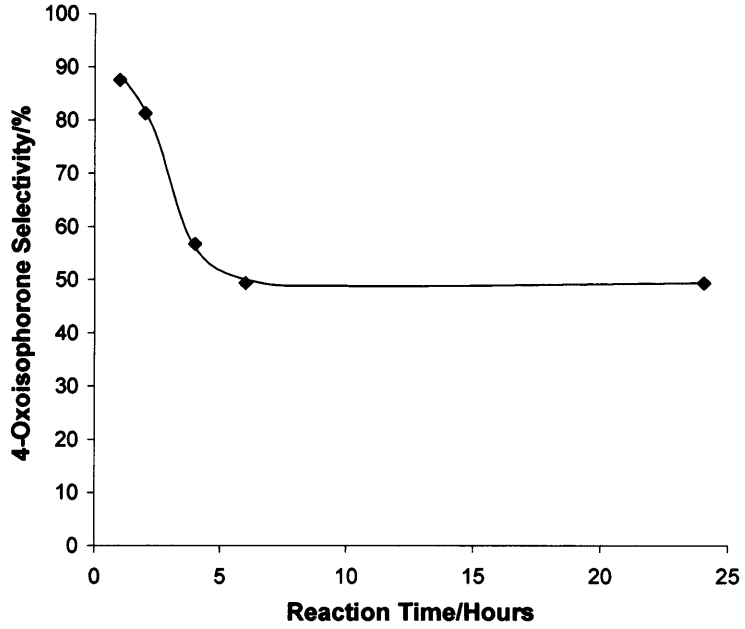

Figure 5.4; The selectivity towards 4-oxoisophorone during the oxidation of isophorone at 75 °C, 1500 r.p.m. with 10 bar O_2, using a 2.5wt%Au+2.5wt%Pd/TiO_2 catalyst prepared by the deposition precipitation method.

5.4 The oxidation of 2,6-dimethylpyridine (2,6-Lutidine)

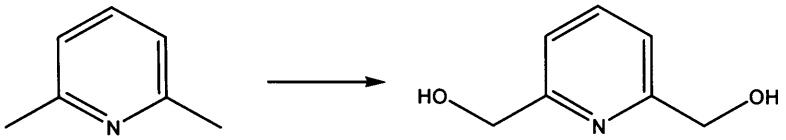

Scheme 5.3 The oxidation of 2,6-lutidene to 2,6-pyridinedimethanol

The oxidation of 2,6-lutidne to 2,6-pyridinedimethanol by 2.5wt%Au+2.5wt%Pd/TiO_2 was attempted at several different temperatures, when no reaction was apparent at 100 °C, 2,6-lutidene was tested to see if it acted as a poison for the 2.5wt%Au+2.5wt%Pd/TiO_2 catalyst. Using the method described in chapter 2, a stiochiometric amount of lutidine was added to a benzyl alcohol reaction carried out under the standard conditions described in chapter 2. With the addition of the lutidene the oxidation of benzyl alcohol was severely restricted (figure 5.5) suggesting that 2.5wt%Au+2.5wt%Pd/TiO_2 cannot be used as a catalyst for this system.

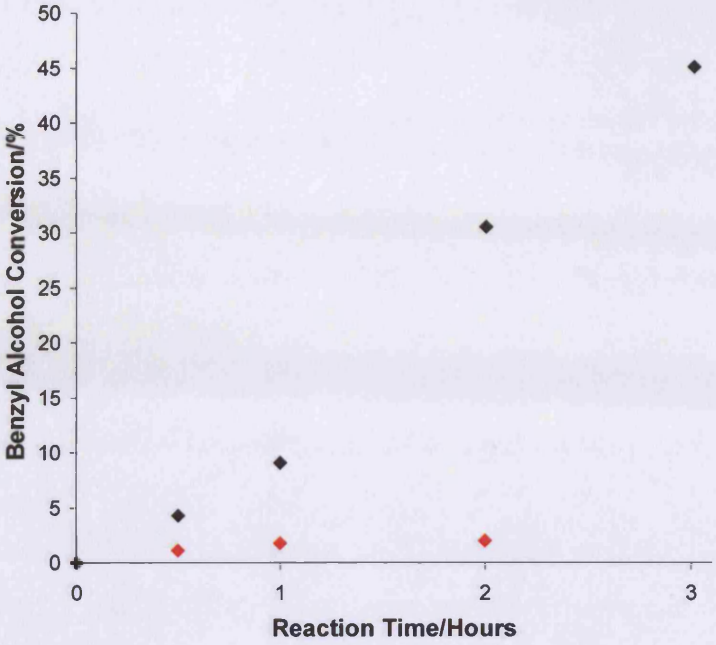

Figure 5.5: The oxidation of benzyl alcohol by 25mg 2.5wt%Au+2.5wt%Pd/TiO_2 at 140°C, 10 bar O_2 and 1500 r.p.m. (♦) and with the addition of a stoichometric amount of 2,6-lutidene (♦).

5.5: The oxidation of 2-Picoline and 3-picoline

Scheme 5.4: The oxidation of 2-picoline (red) and 3-picoline (blue) to form 2-pyridinemetanol (red) and 3-pyrindinemethanol (blue).

After attempts to oxidise 2-picoline and 3-picoline at 100 °C using 2.5wt%Au+2.5wt%Pd/TiO_2 at 10 bar O_2 and 1500 r.p.m proved unsuccessful and due to their similarities to the 2,6-lutidene system, these substrates were also tested for poisoning using the method outlined in chapter 2. The addition of either 2-picoline or 3-picoline showed a similar effect on the conversion of benzyl alcohol as shown with the addition of 2,6-lutidene (figure 5.5) proving 2.5wt%Au+2.5wt%Pd/TiO_2 is also unsuitable for these oxidations.

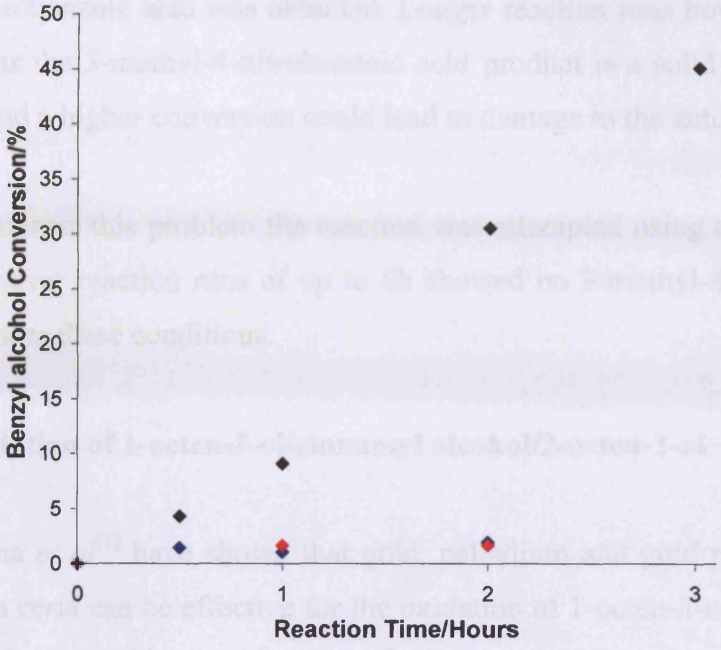

Figure 5.6: The oxidation of benzyl alcohol by 25mg 2.5wt%Au+2.5wt%Pd/TiO_2 at 140°C, 10 bar O_2 and 1500 r.p.m. (♦), with the addition of a stoichometric amount of 2-picoline (♦) and 3-picoline (♦).

5.6: The oxidation of 2,4-Dimethyl-1-Nitrobenzene/2,4-Dimethylnitrobenzene

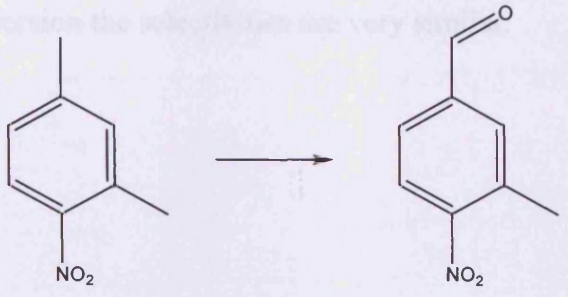

Scheme 5.5 The oxidation of 4-nitro-xylene to 3-methyl-4-nitrobenzoic acid

Previous studies within the group have shown that toluene can be oxidised using gold-palladium catalysts at temperatures above 160 °C. The same principles were applied to the oxidation of 4-nitoro-xylene. Reactions were carried out at 180 °C with 25 mg 2.5%Au+2.5%Pd/TiO_2 prepared by the deposition precipitation method. The reaction mixture was filtered and washed with $CHCl_3$ and the product identified to be 3-methyl-4-nitrobenzoic acid by NMR. After 4h of reaction a 2.7% yield of 3-

methyl-4-nitrobenzoic acid was obtained. Longer reaction runs however could not be carried out as the 3-methyl-4-nitrobenzoic acid product is a solid under the reaction conditions and a higher conversion could lead to damage to the autoclave equipment.

To counter this problem the reaction was attempted using chlorobenzene as a solvent; however reaction runs of up to 6h showed no 3-methyl-4-nitrobenzoic acid formation under these conditions.

5.7 The oxidation of 1-octen-3-ol/cinnamyl alcohol/2-octen-1-ol

Corma *et al*[1] have shown that gold, palladium and gold palladium catalysts supported on ceria can be effective for the oxidation of 1-octen-3-ol, 2-octen-1-ol and cinnamyl alcohol. The oxidation of 1-octen-3-ol was carried out using 2.5wt%Au+2.5wt%Pd/nCeO_2 and 2.5wt%Au+2.5wt%Pd/ScCeO_2 at 120°C at 1 bar O_2 pressure and 1500 r.p.m stirring (figure 5.7). The catalyst supported on the supercritically prepared ceria (ScCeO_2) proved to be more active for this reaction than that supported on ceria made conventionally (nCeO_2). In the initial stages of the reaction the catalysts supported on non-supercritically prepared ceria appeared to be more selective to the corresponding ketone (figure 5.8); however when the reaction is considered at isoconversion the selectivities are very similar.

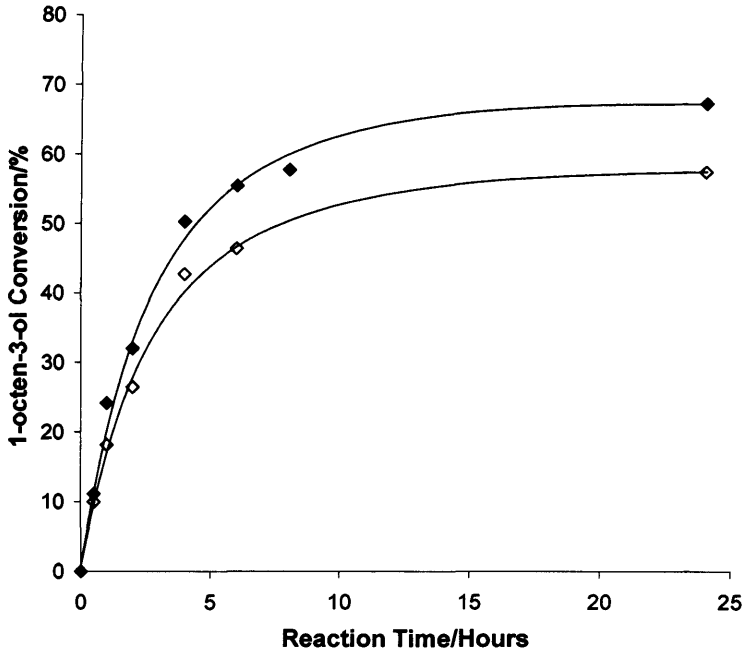

Figure 5.7: The oxidation of 1-octen-3-ol by 2.5wt%Au+2.5wt%Pd/nCeO$_2$ (◊) and 2.5wt%Au+2.5wt%Pd/ScCeO$_2$ (♦) at 120 °C at 1 bar O$_2$ pressure and a stirrer speed of 1500 r.p.m.

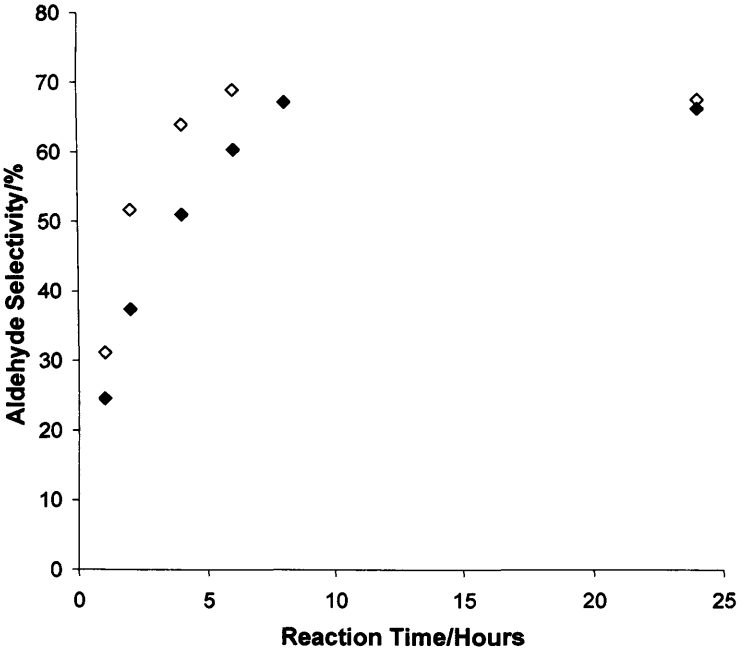

Figure 5.8: The ketone selectivity during the oxidation of 1-octen-3-ol by 2.5wt%Au+2.5wt%Pd/nCeO$_2$ (◊) and 2.5wt%Au+2.5wt%Pd/ScCeO$_2$ (♦) at 120 °C at 1 bar O$_2$ pressure and a stirrer speed of 1500 r.p.m.

Furthermore, the oxidation of 1-octen-3-ol was also carried out using 2.5%Au/$ScCeO_2$ and 2.5%Pd/$ScCeO_2$ (figure 5.9). In this case the gold mono-metallic catalyst showed the highest conversion of these catalysts. The bi-metallic catalyst however was found to be the most selective towards the ketone (figure 5.10). When the catalyst activity is considered in terms of TOF, the gold catalyst was shown to have the highest initial activity (table 5.1).

The same set of catalysts was also used for the oxidation of a 1M solution of cinnamyl alcohol in toluene. In this case the bi-metallic catalysts showed the greatest conversion (figure 5.11) and highest selectivity towards the aldehyde (figure 5.12). The highest initial activity was again recorded for the gold monometallic catalyst (table 5.2).

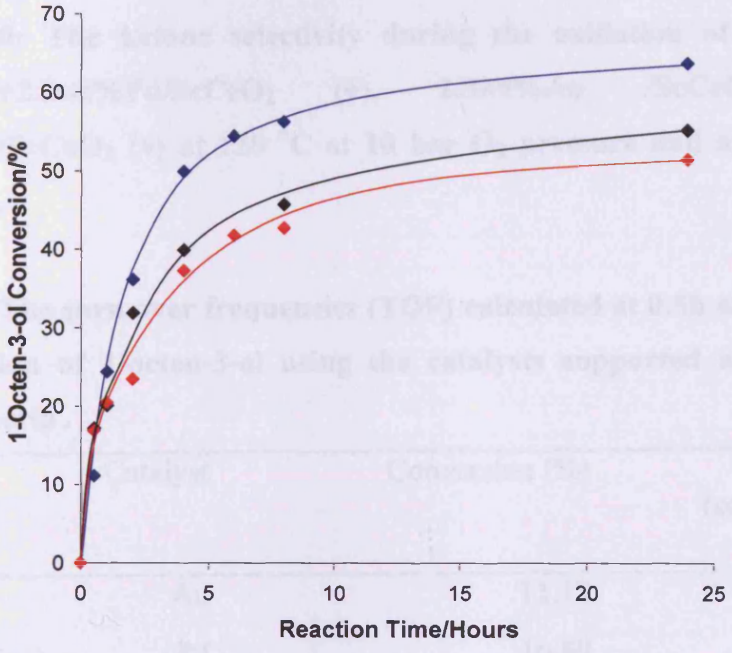

Figure 5.9: The oxidation of 1-octen-3-ol by 2.5wt%Au+2.5wt%Pd/$ScCeO_2$ (♦), 2.5wt%Au /$ScCeO_2$ (♦) and 2.5wt%Au/$ScCeO_2$ (♦) at 120 °C at 10 bar O_2 pressure and a stirrer speed of 1500 r.p.m.

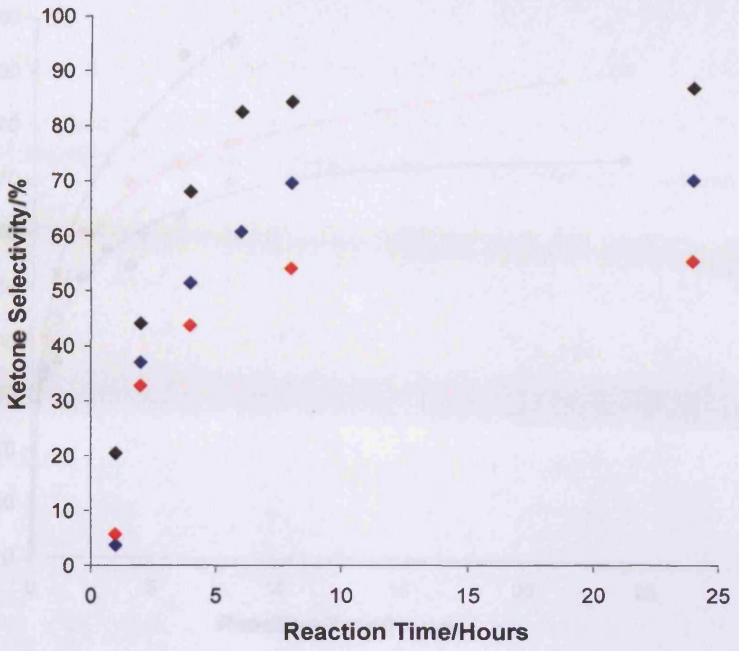

Figure 5.10: The ketone selectivity during the oxidation of 1-octen-3-ol by 2.5wt%Au+2.5wt%Pd/$ScCeO_2$ (♦), 2.5wt%Au /$ScCeO_2$ (♦) and 2.5wt%Au/$ScCeO_2$ (♦) at 120 °C at 10 bar O_2 pressure and a stirrer speed of 1500 r.p.m.

Table 5.1: The turn over frequencies (TOF) calculated at 0.5h of reaction during the oxidation of 1-octen-3-ol using the catalysts supported on supercritically prepared ceria .

Catalyst	Conversion (%)	TOF (calculated at 0.5h of reaction)
Au	11.12	64819
Pd	16.89	54519
Au+Pd	17.19	34535

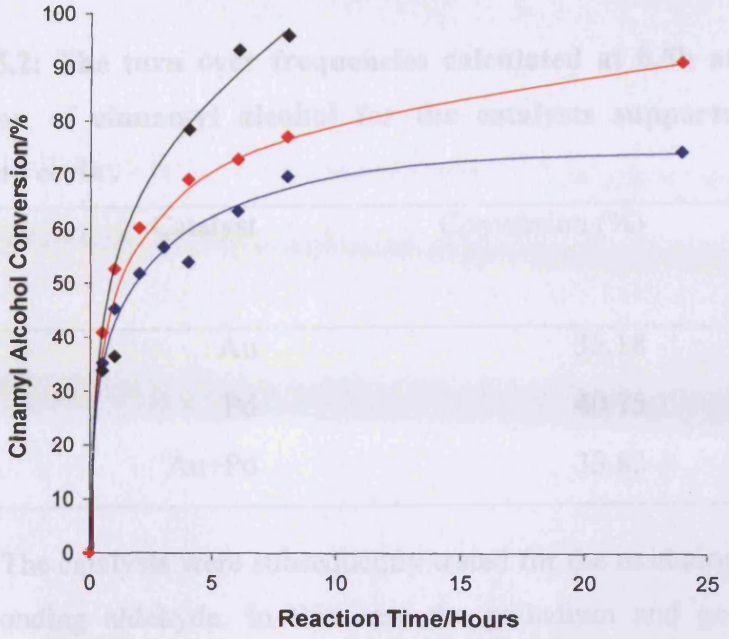

Figure 5.11: The oxidation of 1M cinnamyl alcohol in toluene by 2.5wt%Au+2.5wt%Pd/$ScCeO_2$ (♦), 2.5wt%Au /$ScCeO_2$ (♦) and 2.5wt%Au/$ScCeO_2$ (♦) at 120 °C at 10 bar O_2 pressure and a stirrer speed of 1500 r.p.m.

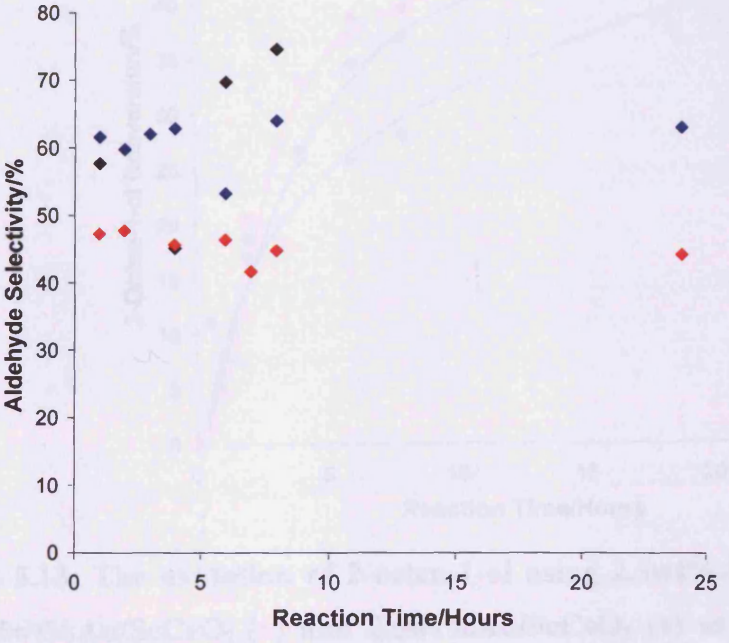

Figure 5.12: The aldehyde selectivity during the oxidation of 1M cinnamyl alcohol in toluene by 2.5wt%Au+2.5wt%Pd/$ScCeO_2$ (♦), 2.5wt%Au /$ScCeO_2$ (♦) and 2.5wt%Au/$ScCeO_2$ (♦) at 120 °C at 10 bar O_2 pressure and a stirrer speed of 1500 r.p.m.

Table 5.2: The turn over frequencies calculated at 0.5h of reaction during the oxidation of cinnamyl alcohol for the catalysts supported on supercritically prepared ceria .

Catalyst	Conversion (%)	TOF (calculated at 0.5h of reaction)
Au	35.18	31677
Pd	40.75	19825
Au+Pd	33.83	10685

The catalysts were subsequently tested for the oxidation of 2-octen-1-ol to the corresponding aldehyde. In this case the palladium and gold palladium catalysts showed similar conversions, slightly higher than the gold catalyst (figure 5.13); the gold catalysts did, however, show the highest selectivity towards the aldehyde (figure 5.14) and the highest initial activity in terms of the TOF (table 5.3).

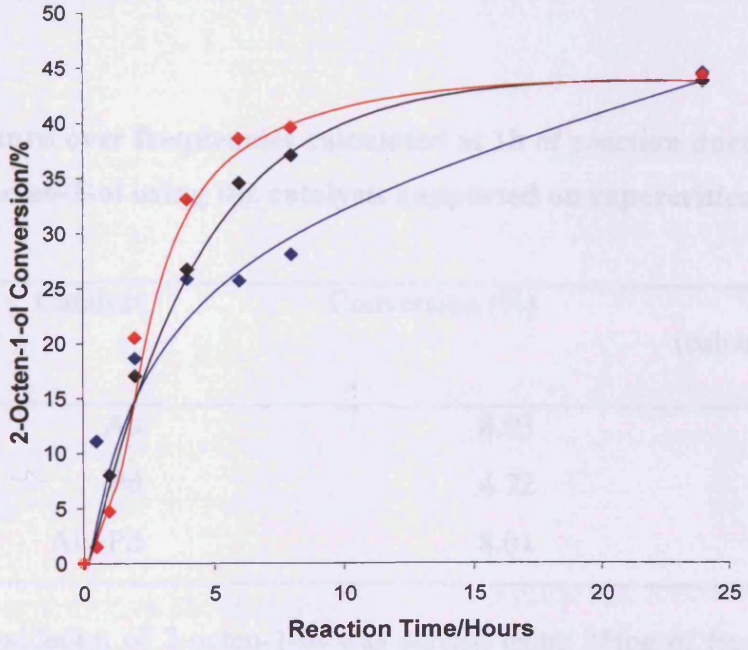

Figure 5.13: The oxidation of 2-octen-1-ol using 2.5wt%Au+2.5wt%Pd/$ScCeO_2$ (♦), 2.5wt%Au/$ScCeO_2$ (♦) and 2.5wt%Au/$ScCeO_2$ (♦) at 120 °C at 10 bar O_2 pressure and a stirrer speed of 1500 r.p.m.

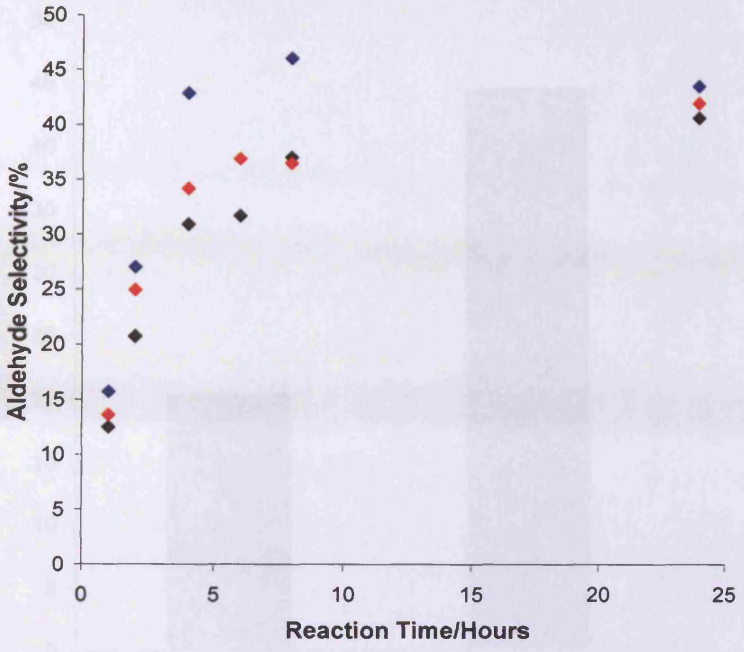

Figure 5.14: The aldehyde selectivity during the oxidation of 2-octen-1-ol using 2.5wt%Au+2.5wt%Pd/$ScCeO_2$ (♦), 2.5wt%Au/$ScCeO_2$ (♦) and 2.5wt%Au/$ScCeO_2$ (♦) at 120 °C at 10 bar O_2 pressure and a stirrer speed of 1500 r.p.m.

Table 5.3: The turn over frequencies calculated at 1h of reaction during the oxidation of 2-octen-1-ol using the catalysts supported on supercritically prepared ceria

Catalyst	Conversion (%)	TOF (calculated at 1h of reaction)
Au	8.03	23711
Pd	4.72	8338
Au+Pd	8.01	7549

Further oxidation of 2-octen-1-ol was carried using 25mg of fresh and once-used 2.5%Au+2.5%Pd/$ScCeO_2$; after 4h of reaction the used catalyst had converted significantly more of the 2-octen-1-ol (figure5.15).

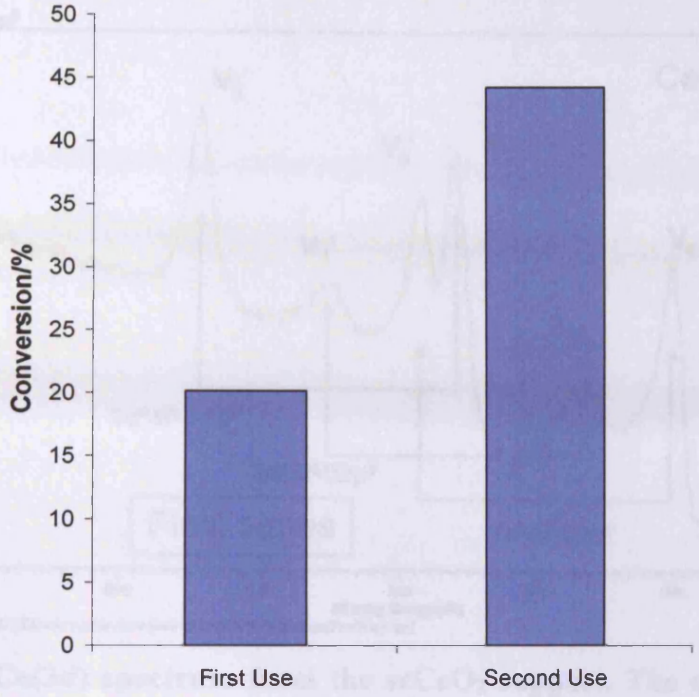

Figure 5.15: The conversion of 2-octen-1-ol using 25 mg of fresh and once-used 2.5wt%Au+2.5wt%Pd/ScCeO$_2$.

5.7 XPS

The Ce(3d) spectrum of the scCeO$_2$ support is shown in Figure 5.16. The complex spectral envelope consists of 3 doublets, each corresponding to a different final state electronic structure as indicated on the figure. This spectrum is characteristic of pure ceria[2]. The Ce(3d) spectrum of the Au-Pd/CeO$_2$ catalyst used for 2-octan-1-ol oxidation shows significant reduction of the ceria support compared with the catalyst before use (Figure 5.17).

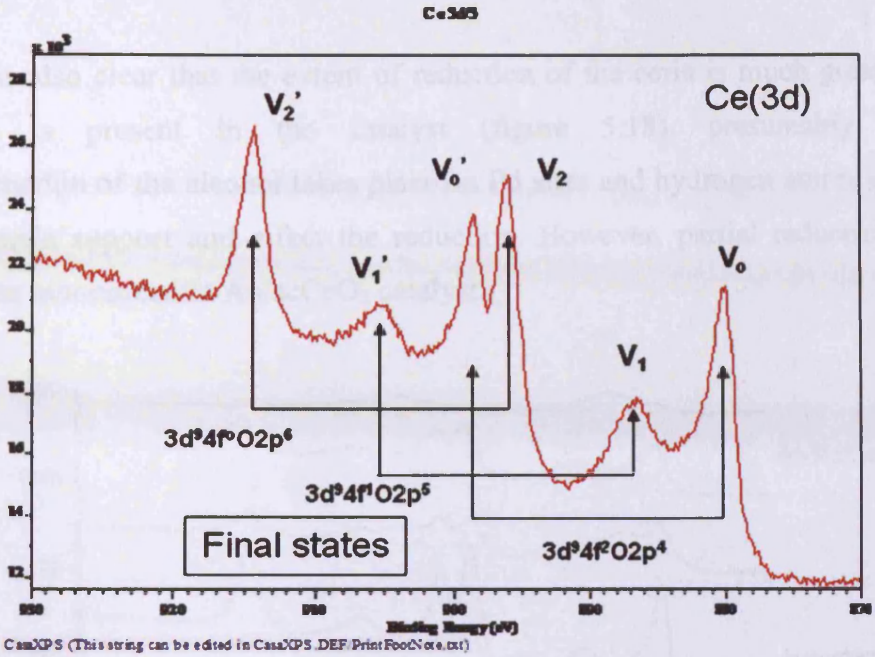

Figure 5.16: Ce(3d) spectrum from the scCeO$_2$ support, The assignment of the final state electronic structure for each of the three doublets is indicated

This reduction is much more extensive than that previously noted when these catalysts are used for the oxidation of benzyl alcohol (chapter 3) and, indeed, the cerium is completely reduced from Ce^{4+} to Ce^{3+} within the sampling depth of XPS (ca 25 Å).

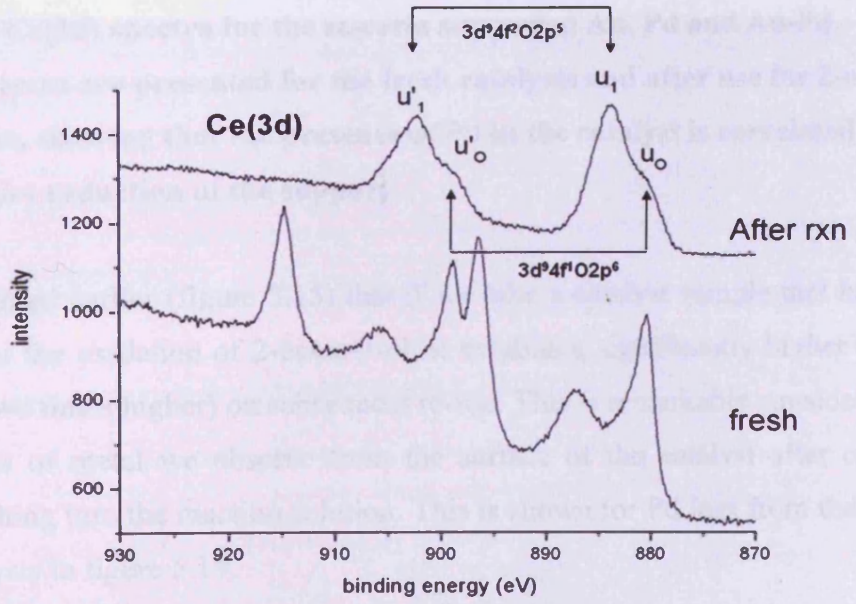

Figure 5.17: Ce(3d) spectra for the fresh Au-Pd/scCeO$_2$ catalyst and after reaction with 2-octan-1-ol, showing the complete reduction of Ce^{4+} to Ce^{3+}.

It is also clear that the extent of reduction of the ceria is much greater when palladium is present in the catalyst (figure 5.18), presumably because dehydrogenation of the alcohol takes place on Pd sites and hydrogen atoms spill over onto the ceria support and effect the reduction. However, partial reduction occurs even for the monometallic $Au/scCeO_2$ catalyst.

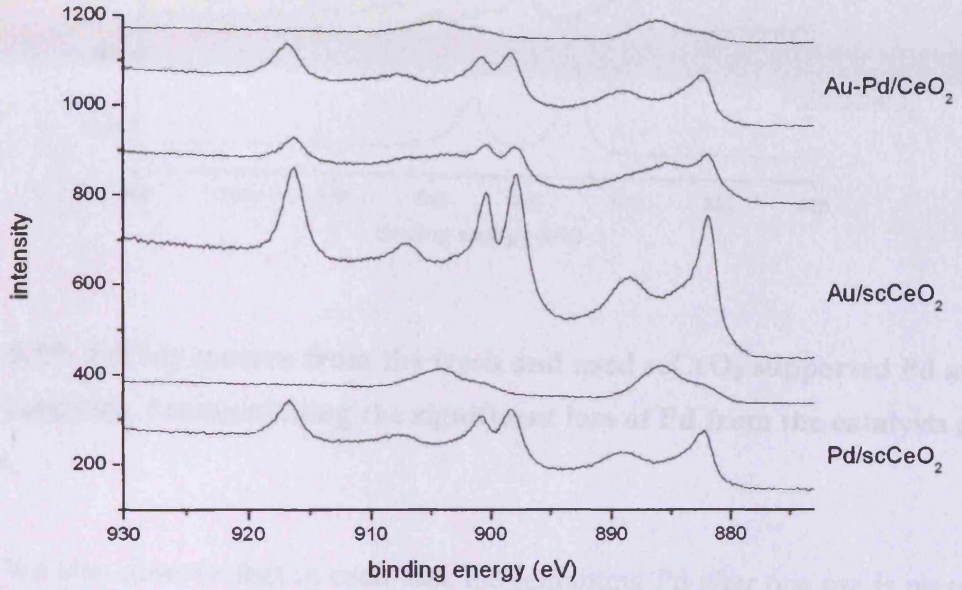

Figure 5.18: Ce(3d) spectra for the sc-ceria supported Au, Pd and Au-Pd catalysts; spectra are presented for the fresh catalysts and after use for 2-octan-1-ol oxidation, showing that the presence of Pd in the catalyst is correlated with more extensive reduction of the support.

We noted earlier (figure 5.15) that if we take a catalyst sample that has been used once for the oxidation of 2-octen-1-ol, it exhibits a significantly higher activity (more than two times higher) on subsequent re-use. This is remarkable considering the dramatic loss of metal we observe from the surface of the catalyst after one use, through leaching into the reaction solution. This is shown for Pd loss from the Pd and Au-Pd catalysts in figure 5.19.

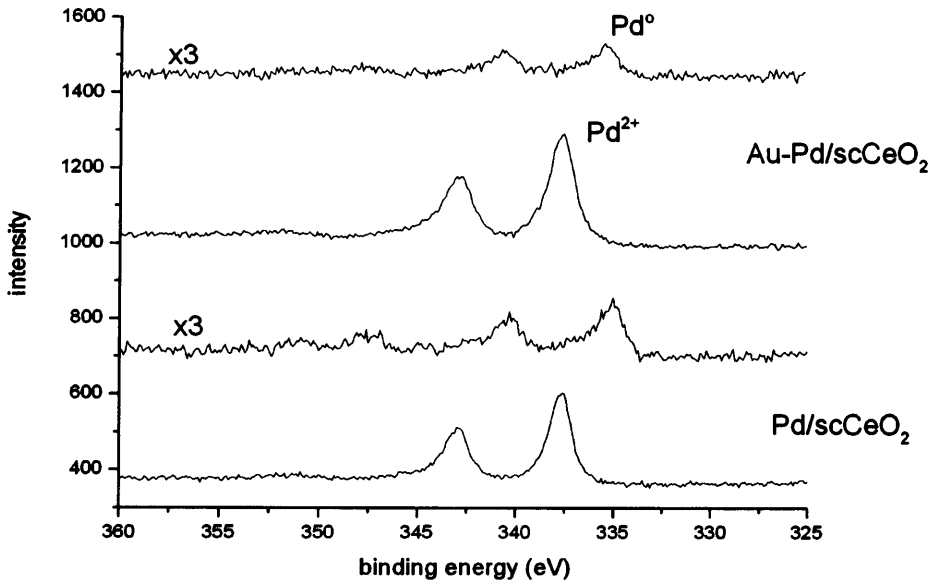

Figure 5.19: Pd(3d) spectra from the fresh and used $scCeO_2$ supported Pd and Au-Pd catalysts, demonstrating the significant loss of Pd from the catalysts after one use.

We also observe that in each case the remaining Pd after one use is present as metallic Pd, in contrast to the fresh catalysts where the palladium is present as Pd^{2+}. Similar levels of leaching of Au are observed for the Au and Au-Pd catalysts. Clearly, most of the metal deposited on the original catalyst is not involved in the catalytic reaction, and furthermore the small amount of metal remaining after first use is even more effective than the original loading, resulting in an enormous increase in TOF from 1466 for the fresh catalyst to 3225 for the once used catalyst based on no metal leaching from the catalyst.

5.8 STEM

STEM analysis was performed as described in chapter 2. Image 5.1 shows the fresh 2.5wt%Au+2.5wt%Pd/$ScCeO_2$ catalyst and image 5.2 shows the catalyst after it has been used for 2-octen-1-ol oxidation. As was noted from the XPS results the most extensive reduction of the support was observed during the oxidation of 2-octen-1-ol. As with the TEM described in chapter 3 where the catalyst was used for benzyl

alcohol oxidation there seems to be a breaking down of the ceria spheres after use for 2-octen-1-ol oxidation.

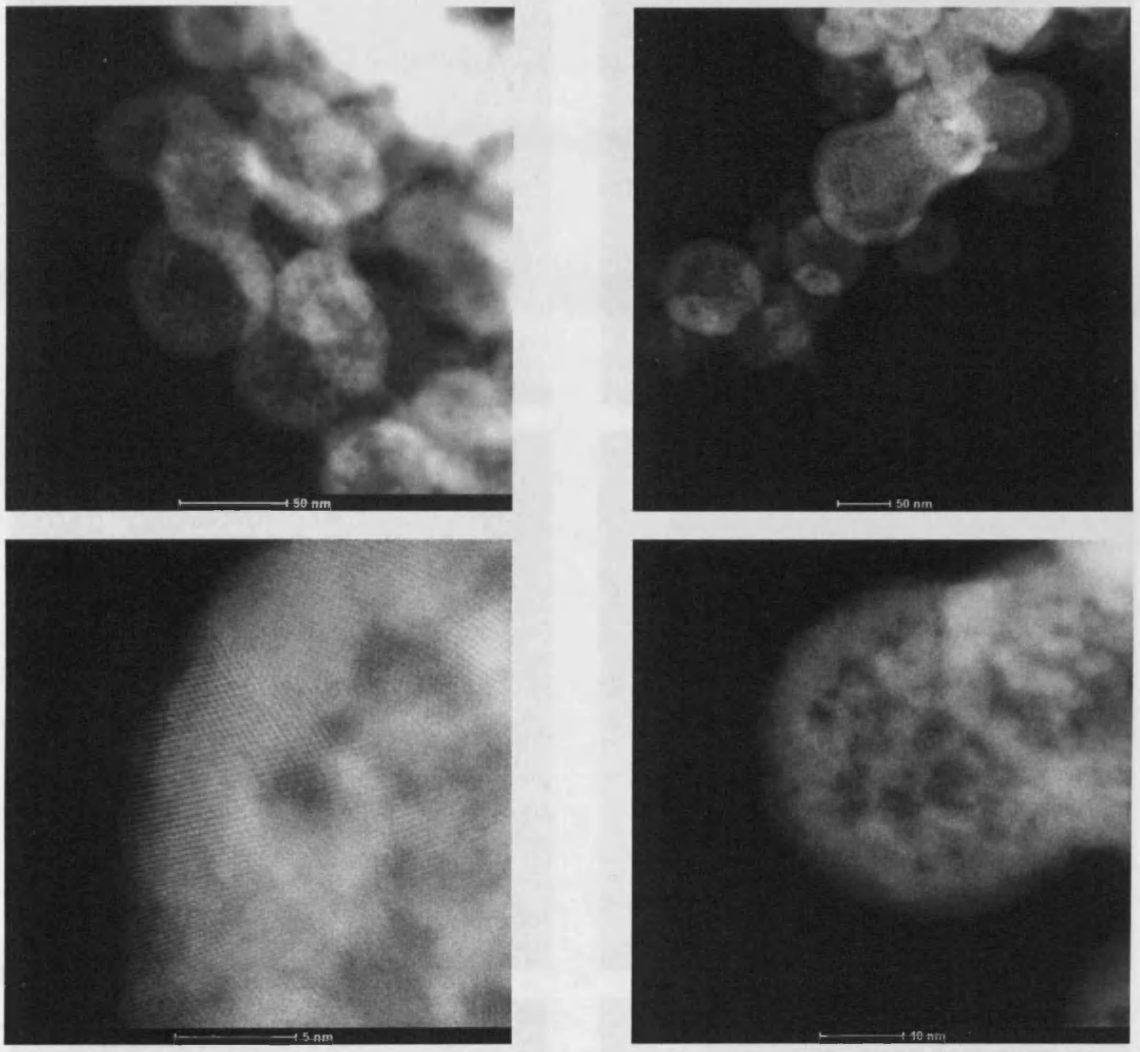

Image 5.1: TEM images of fresh 2.5wt%Au+2.5wt%Pd/$ScCeO_2$

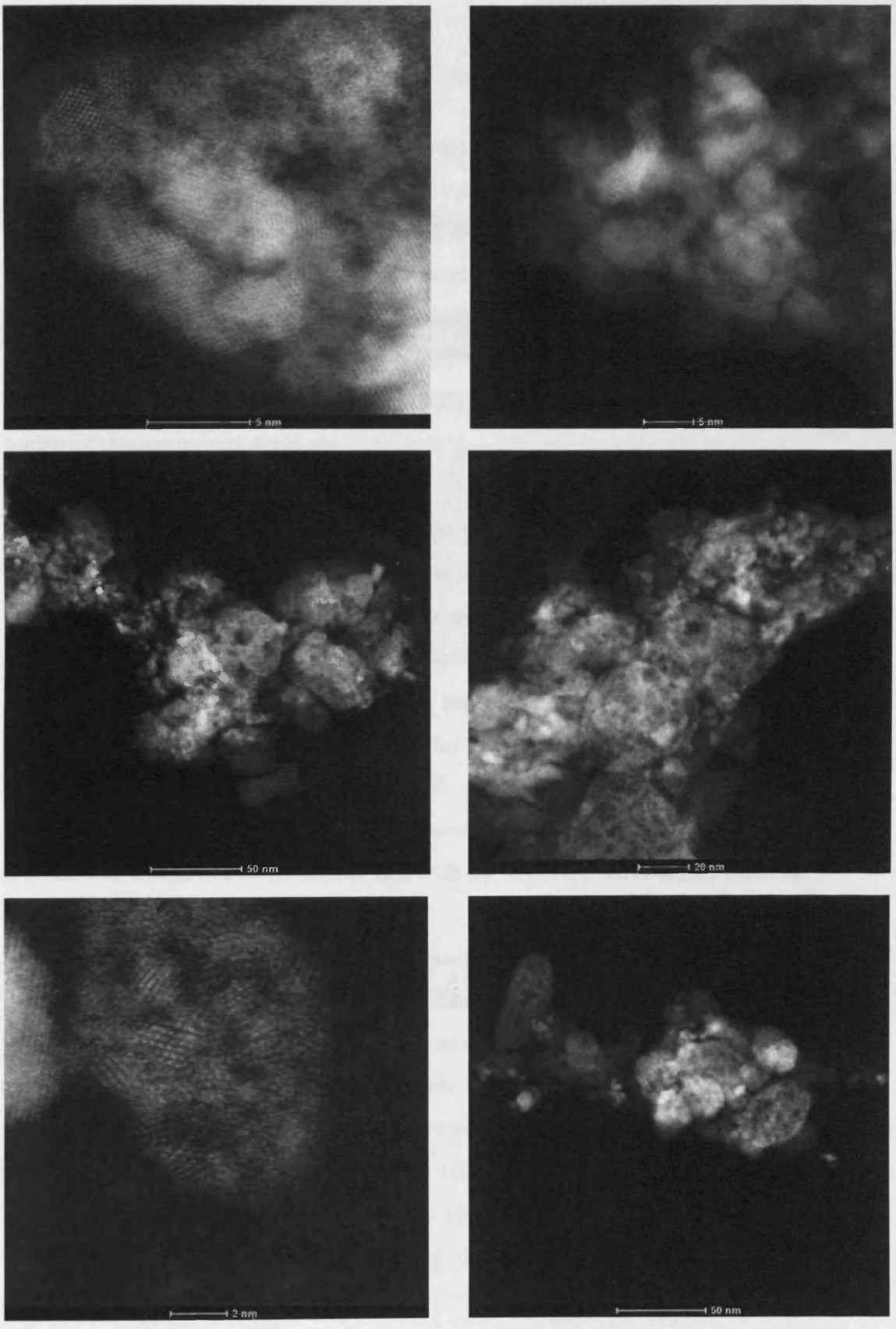

Image 5.2: TEM images of 2.5wt%Au+2.5wt%Pd/$ScCeO_2$ after use for 2-octen-1-ol oxidation.

5.10 Discussion

5.10.1 The oxidations of valencene and isophorone

The 2.5wt%Au+2.5wt%Pd/TiO_2 catalyst appears to be active for the oxidation of valencene to nootkatone (figure 5.1) using reaction conditions similar to those described previously for the oxidation of α-pinene. The oxidation of valencene was carried out at a slightly higher temperature than for α-pinene and required a considerably longer reaction time (72h compared to 24h for α-pinene). The selectivity towards the desired product, nootkatone, 50% after 72h, (figure 5.2) was less than that achieved for the oxidation of α-pinene (80% after 24h) but this could be improved by tuning of the reaction conditions.

Theses results, in terms of conversion and selectivity do not compare favourably with those reported in the literature with Furusawa *et al*[3] reporting 100% conversion and 100% selectivity towards nootkatone using enzymes to perform the biotranformation. However this reaction took 25 days to convert 20 mg of valencene. A homogeneously catalysed process was reported by Salvador *et al*[4] using a cobalt based catalyst with the authors obtaining nootkatone in a 38% yield, again this process was carried out on the small scale (16 mg valencene) with acetonitrile as a solvent presenting practical and environmental problems in terms of an industrial process that would not be as significant with the reported solvent free process.

Similarly the utilisation of the α-pinene reaction conditions to the oxidation of isophorone achieved reasonable results. The reaction was carried out at 100 °C as there was no reaction observed at 75 °C, and at 120 °C the reaction proceeded in the absence of catalyst with multiple products being formed. However at 100 °C there was reasonable conversion of the isophorone after 24h (figure 5.3) and a selectivity towards 4-oxoisophorone of about 50% (figure 5.4). In this case it is known that increasing the reaction temperature leads to a loss of selectivity[5] so the selectivity could possibly be improved by reducing the temperature and carrying out longer reaction runs.

5.10.2 The oxidations of 2,6-lutidene, 2-picoline and 3-picoline

Attempts to oxidise 2,6-lutidine, 2-picoline and 3-picoline proved unsuccessful at the temperature ranges used in this study, with no conversion observed when the reaction mixtures were analysed by GC. Della Pina et al[6] have shown that a pyridine derivative can be oxidised to the n-oxide form under less harsh conditions than those attempted in this study. It is possible that the n-oxide is formed and this is binding to the metal. The doped benzyl alcohol tests that were carried out (Figures 5.5 and 5.6) confirm that these ligands are acting as poisons of the gold palladium catalyst. Furthermore in work by Venugopal *et al*[7] the addition of 2,6-lutidine to the gas stream acted as a poison during oxidation of CO (figure 5.20)

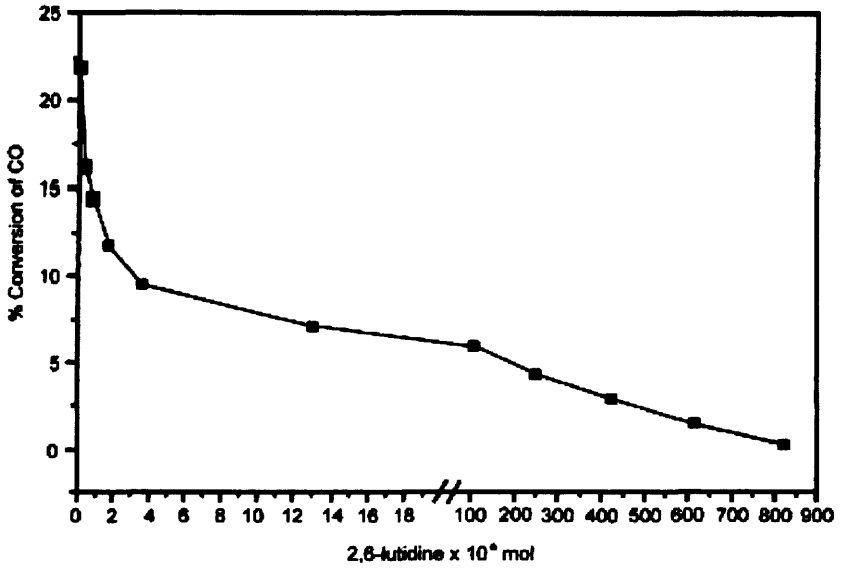

Figure 5.20: Effect of addition of 2,6-dimethylpyridine to the feed on the water–gas shift activity of 3 wt.% Au/Fe_2O_3 catalyst[6]

5.10.3 The oxidation of 2,4-dimethylnitrobenzene

The oxidation of 2,4-dimethylnitrobenzene to 3-methyl-4-nitrobenzoic acid is another good example of the application of the 2.5wt%Au+2.5wt%Pd/TiO_2 catalysts, the problem with this reaction however is the nature of the product formed, because of it's high melting point (216-218 °C) the product will be a solid under reaction conditions, while this considerably eases separation of the products the reactions cannot be run for long periods of time as this will lead to large quantities of solid being formed which could damage the autoclave equipment. To combat this

problem a suitable solvent could be used, tests were carried out using chlorobenzene as a solvent, however no reaction occurred. A search of the literature suggests that acetic acid could be a suitable solvent for this system.

5.10.4 The oxidation of 1-octen-3-ol/cinnamyl alcohol/2-octen-1-ol

The supercritically prepared ceria supported catalysts proved useful for the oxidation of 1-octen-3-ol, as was the case with benzyl alcohol in chapter 3 there was a significant improvement in the reactivity of the catalyst compared to the catalyst supported on ceria prepared by calcination of the acetate (figure 5.7). The TOF's for this oxidation are also very high (table 5.1) although direct comparison with the work carried out by Corma *et al*[1] is not possible due to the different nature of the reaction conditions used. The XPS of the used catalysts shows a reduction in the oxidation state of the ceria similar to that observed for the oxidation of benzyl alcohol described in chapter 3.

In the case of cinnamyl alcohol there was a very high initial activity associated with these catalysts (figure 5.11). The reported TOF by Corma *et al*[1], 538 h^{-1} is considerably lower than the observed TOF of 31577 h^{-1} (Table 5.2) although it must be noted that the experiments by Corma *et al*[1] were carried out at a lower oxygen pressure and a considerably higher metal/substrate ratio and it is not noted what time the calculation of TOF was based upon making comparison subjective at best. The oxidation of cinnamyl alcohol also demonstrates that these oxide supported gold palladium catalysts can work in the presence of solvent a fact previously shown by Su *et al*[8] who used gold supported on gallia could be used to oxidise a range of alcohols including benzyl alcohol using mesitylene as a solvent and Dimitrstos *et al*[9] who used gold palladium alloyed catalysts supported on carbon for the oxidation of benzyl alcohol with both water and toluene as solvents, but is in contrast the results observed for the oxidation of 2,4-dimethylnitrobenzene and, the previously described in chapter 4, oxidation of hex-3ene-2,5-dione where the addition of a solvent seemed to prevent the oxidation taking place.

The oxidation of 2-octen-1-ol provides interesting data, as with the other two alcohols described in this chapter the TOF is very high (table 5.3), further providing evidence that these are excellent catalysts for the oxidation of these systems, but also the XPS shows that there is near total reduction of the ceria from 4+ to 3+. This reduction is much more extensive than that shown for benzyl alcohol, described in chapter 3 and indeed for the other alcohols described in this chapter. The TEM images of the used catalyst seem to show the breaking down of the ceria spheres (image 2) which is though to be associated with the change in the oxidation state of the ceria and this breaking down seems to be more extensive than was the case for the benzyl alcohol oxidation. As was the case for the oxidation of benzyl alcohol, the used catalyst showed a much greater activity than the fresh catalyst. If this is a function of the oxidation state of the ceria the catalyst that has been almost completely reduced by the oxidation of 2-octen-1-ol should be active for the oxidation of benzyl alcohol.

5.11 Conclusions

- The optimum reaction conditions established for the oxidation of α-pinene have been adapted and applied to various other reaction systems with good results obtained for the oxidation of valencene and isophorone. With the fine tuning of the reaction conditions greater conversion and selectivity should be attainable.

- Attempts to oxidise 2,6-lutidene, 2-picoline and 3-picoline proved unsuccessful. Furthermore when the oxidation of benzyl alcohol was carried out with stoichiometric amounts of these compounds added to the starting material all three compounds were found to act as poisons to the catalyst.

- Initial reactions of 2,4-dimethylnitrobenzene have shown the oxidation using gold catalysts to form 3-methyl-4-nitrobenzoic acid is possible at low yields. The extent of the reaction however was limited by the melting point of the product and a more complete reaction could be carried out if a suitable solvent system is established.

- The oxidations of cinnamyl alcohol, 2-octen-1-ol and 1-octen-3-ol demonstrate the advantage of using ceria prepared by the supercritical antisolvent precipitation method when compared to ceria prepared by simple calcination with high TOF's observed for these reactions.

- An increase in activity, similar to that described in chapter 3 for the oxidation of benzyl alcohol, was observed when used catalysts were tested. The increase in activity was dramatic for the catalyst used for 2-octen-1-ol oxidation. This catalyst was shown, by XPS, to undergo almost complete reduction of the surface ceria and the STEM imaging shows significant breaking down of the ceria spheres.

5.12 Refernces

[1] A. Abad, C. Almela, A. Corma, H. Garcia, *Chemical Communications (Cambridge, United Kingdom)* **2006**, 3178.

[2] J. Rebellato, M. M. Natile, A. Glisenti, *Applied Catalysis, A: General* **2008**, *339*, 108.

[3] M. Furusawa, T. Hashimoto, Y. Noma, Y. Asakawa, *Chemical & Pharmaceutical Bulletin* **2005**, *53*, 1513.

[4] J. A. R. Salvador, J. H. Clark, *Green Chemistry* **2002**, *4*, 352.

[5] D. Kishore, A. E. Rodrigues, *Catalysis Communications* **2007**, *8*, 1156.

[6] C. Della Pina, E. Falletta, M. Rossi, *Topics in Catalysis* **2007**, *44*, 325.

[7] A. Venugopal, M. S. Scurrell, *Applied Catalysis, A: General* **2004**, *258*, 241.

[8] F.-Z. Su, M. Chen, L.-C. Wang, X.-S. Huang, Y.-M. Liu, Y. Cao, H.-Y. He, K.-N. Fan, *Catalysis Communications* **2008**, *9*, 1027.

[9] N. Dimitratos, A. Villa, D. Wang, F. Porta, D. Su, L. Prati, *Journal of Catalysis* **2006**, *244*, 113.

Chapter Six

6. General Discussion, Conclusions and Future Work

6.1 General discussion and conclusions

Gold and gold palladium bimetallic catalysts have been used to carry out a range of oxidations using various substrates and reaction conditions. Benzyl alcohol oxidation, a test reaction used to assess the performance of catalysts has been used to establish a set of reaction conditions for quick assessment of catalysts without significant blank reactions occurring.

The oxidation of benzyl alcohol has also allowed the further development of gold catalysts. As outlined in chapter one the development of gold catalysts has been a continual process focusing on several different reactions, with sometimes contradictory results obtained for different processes. Focusing on alcohol oxidations the preparation method for bimetallic catalysts has been shown to be as significant, in terms of the activity of the catalysts as it is known to be for monometallic catalysts. The bimetallic catalysts prepared by the deposition precipitation method were significantly more active than those prepared by the impregnation methodology. Preliminary tests on the hydrogen peroxide oxidation system indicate there is about a 50% improvement in the productivity of the hydrogen peroxide when compared with the catalyst prepared by the impregnation method. The origin of this improvement in activity could be explained by several factors:

1: Smaller metal particles.

2: The nature of the metal particles

3: The washing process removing chloride ions which may otherwise act as a poison.

The simple explanation is that deposition precipitation preparation method gives smaller metal particles as is the case for monometallic catalysts[1]. However when the catalyst is viewed using SEM the metal particles still seem large, but there might be smaller metal particles also present that are smaller than the detection limit of the microscope and are highly active. As discussed in chapter 3 the nature of the

active gold species is much debated and it is possible that the majority of metal on a catalyst merely plays a spectator role in the reactions. The nature of the metal particles is also likely to be different due to the different preparation method. For hydrogen peroxide formation the most active catalysts reported to date, are those supported on carbon, which form a homogeneous alloy. The titania bimetallic catalysts prepared by impregnation are known to form a core shell structure[2]. It is also possible that the catalysts prepared by the deposition precipitation method do not form alloys at all. STEM analysis of the catalysts should provide an indication of the nature of the metal species and help to answer these questions.

The third factor, the poisoning of the impregnation prepared catalysts by chloride ions is an interesting possibility, there are reports of chloride ions poisoning gold catalysts in the literature[3] and the EDX analysis of the catalysts confirms the absence of chlorine. The field of catalyst poisons, with respect to gold catalysts, however is not well documented, as was discussed in chapter 5, where 2,6-lutidne, 2-picoline and 3-picoline were found to act as poisons to these catalysts, this seems to be an area where further research would be worthwhile as this could lead to better understanding of how these catalysts work and subsequently the development of better catalysts.

Several supports were investigated during this work and the different activity of a catalyst with identical metal loadings on different support requires consideration. While it has been suggested that different supports will have different iso-electric points leading to different surface charge during the reaction, this does not offer an explanation to why there is a difference between non-supercritically and supercritically prepared ceria supported catalysts. The supercritical antisolvent precipitation process tends to lead to homogeneous ceria spheres with a lower surface area than the calcination prepared ceria[4] however the metal also tends to be distributed in smaller particles and this is though to explain the higher activity of the catalyst. The increase in the activity of the catalyst, as discussed in chapter 3 is harder to explain, especially as there is significant leaching of the metals, raising further questions about the nature of the activity of these catalysts as discussed previously. It would be interesting to see if this improvement in activity can be attributed to the preparation method or that ceria was chosen as the support.

The oxidation of 2,5-dimethylfuran did not yield the intended product furaneol, however the first step of the reaction, the opening of the ring, possibly *via* the epoxidation of one of the double bonds, was carried out selectively yielding hex-3-ene-2,5-dione. This reaction was carried out most successfully at lower temperatures and lower pressure with a selectivity of abound 90% achieved. Achieving the best selectivity for this ring opening reaction by the use of mild conditions is not surprising when the reactivity of the formed product is considered; under forcing conditions it is likely that it will react further and form a variety of products. To further understand this it would be useful to investigate the reaction of hex-3-ene-2,5-dione under reaction conditions however under these conditions reaction runaway occurs. To achieve the oxidation of hex-3-ene-2,5-dione the use of different solvents could be investigated. Previous work by this research group has found a significant solvent effect on the products from the oxidation of cyclohexene[4] and if the same principles were applied to hex-3-ene-2,5-dione the desired product could be attained while the solvent would negate the runaway problem.

In contrast to the oxidation of 2,5-dimethylfuran the oxidation of α-pinene occurred with the best selectivity at higher oxygen pressures and it is noted that the catalyst does not seem to have a significant effect on the reaction under optimised conditions. Previous work had reported the blank reaction taking place but always less significantly than the reaction in the presence of catalyst[5, 6]. With less favourable conditions the catalyst seems to give an increase in the selectivity towards verbenone however this is not observed under the optimised conditions. Again investigating the reaction of the product, verbenone, under the reaction conditions would be useful to provide an insight to the reaction mechanism.

The application of the optimised reaction conditions from the α-pinene system to valencene and isophorone showed that this reaction system could be feasible for a range of similar oxidation processes and while the selectivity to the desired product was not high (around 50% in both cases) these reactions both have the potential to provide the desired products in good yield with the appropriate tuning of the reaction conditions.

The use of gold as a catalyst has increased dramatically over the last 30 years, from virtually nonexistent to a key topic in modern catalysis, the focus on gold as a catalyst has generally been for several key reactions, as discussed in chapter 1, however the results discussed in chapter 5, for the various reaction systems, shows the diverse nature of gold as a catalyst with the potential to play a significant role in a large range of oxidation reactions in the future.

6.2 Future Work

6.2.1 Benzyl alcohol Oxidation: The further development of the catalyst:

- The deposition precipitation catalysts were prepared at pH 8, however the relative equilibrium constants at this pH would suggest that the gold will partially be present as $AuCl(OH)_3$ (figure 3.45), a catalyst prepared with the deposition carried out at pH 9 may give higher activity without the large gold particles forming.

- Investigating whether a similar improvement in reactivity occurs for gold palladium catalysts supported on supercritically prepared titania would give an indication into the origin of this effect for supercritically prepared ceria supported catalysts.

- An investigation into various poisons of gold catalysts, both the testing of pyridine based compounds and the reintroduction of chloride ions into a deposition precipitation prepared catalyst would lead to a better understanding of gold catalysts.

- The use of a catalyst that has been used for 2-octen-1-ol oxidation. The catalyst used for 2-octen-1-ol oxidation exhibited almost total surface reduction of the ceria. If this reduction is responsible for the increase in activity this catalyst should be significantly more active than a catalyst that has been used for benzyl alcohol with similar metal loading

6.2.2 The oxidation of 2,5-dimethyl furan

- The investigation of different radical initiators. The addition of a second batch of radical initiator into the reaction mix after the formation of hex-3-ene-2,5-dione lead to reaction runaway. However a radical initiator with a longer half life at the reaction temperature might be able to initiate the second oxidation step of the reaction.

- The use of various solvents for the oxidation of hex-3-ene-2,5-dione, the solvent would prevent reaction runaway occurring and could lead to the desired oxidation product following the methods reported by Hughes *et al*[4].

6.2.3 The oxidation of α-pinene

- The reduction of the reaction temperature for the oxidation of α-pinene, the reports in the literature suggest that a lower temperature of reaction will lead to better selectivity of verbenone over a longer reaction period[8].

- The investigation of the oxidation of verbenol and verbenone under the reaction conditions used for the oxidation of α-pinene. These reactions will give an indication of the reaction pathway and could lead to further optimisation of the conditions.

6.2.4 The oxidations of valencene and isophorone

- Further experiments to investigate the effects of pressure, temperature, reaction time and catalyst mass; to try and increase the yield of the desired products.

- The use of different catalysts for these reactions

- Investigate the stability of the products from these systems under reaction conditions to gain knowledge of the reaction pathway.

6.2.5 The oxidation of 2,4-Dimethylnitrobenzene

- Find a suitable solvent for the oxidation of 2,4-Dimethylnitrobenzene so that the reaction can be run until completion and the selectivities of the major products can be calculated.

- Carry out the solvent free oxidation in a reactor that can operate at higher temperatures which would allow the reaction to be run until completion.

6.3 References

[1] P. Landon, P. J. Collier, A. J. Papworth, C. J. Kiely, G. J. Hutchings, *Chemical Communications (Cambridge, United Kingdom)* **2002**, 2058.

[2] J. K. Edwards, A. F. Carley, A. A. Herzing, C. J. Kiely, G. J. Hutchings, *Faraday Discussions* **2008**, *138*, 225.

[3] M. Okumura, T. Akita, M. Haruta, *Catalysis Today* **2002**, *74*, 265.

[4] Z.-R. Tang, J. K. Edwards, J. K. Bartley, S. H. Taylor, A. F. Carley, A. A. Herzing, C. J. Kiely, G. J. Hutchings, *Journal of Catalysis* **2007**, *249*, 208.

[5] M. D. Hughes, Y.-J. Xu, P. Jenkins, P. McMorn, P. Landon, D. I. Enache, A. F. Carley, G. A. Attard, G. J. Hutchings, F. King, E. H. Stitt, P. Johnston, K. Griffin, C. J. Kiely, *Nature (London, United Kingdom)* **2005**, *437*, 1132.

[6] N. V. Maksimchuk, M. S. Melgunov, Y. A. Chesalov, J. Mrowiec-Bialon, A. B. Jarzebski, O. A. Kholdeeva, *Journal of Catalysis* **2007**, *246*, 241.

[7] P. McMorn, G. Roberts, G. J. Hutchings, *Catalysis Letters* **2000**, *67*, 203.

[8] E. A. Nechaev, G. V. Zvonareva, *Geokhimiya* **1983**, 919.

[9] N. V. Maksimchuk, M. S. Melgunov, J. Mrowiec-Bialon, A. B. Jarzebski, O. A. Kholdeeva, *Journal of Catalysis* **2005**, *235*, 175.

Chapter Seven

7 Appendix

7.1 GC Calibration Curves

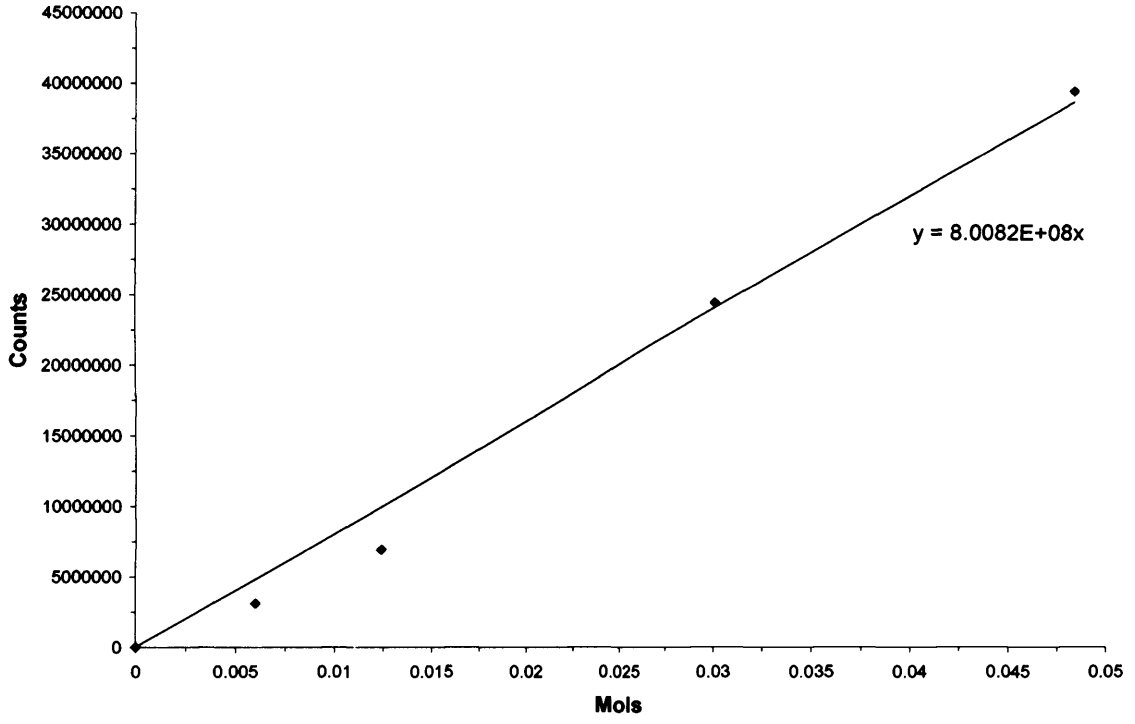

Figure 7.1 The GC calibration curve for benzyl alcohol.

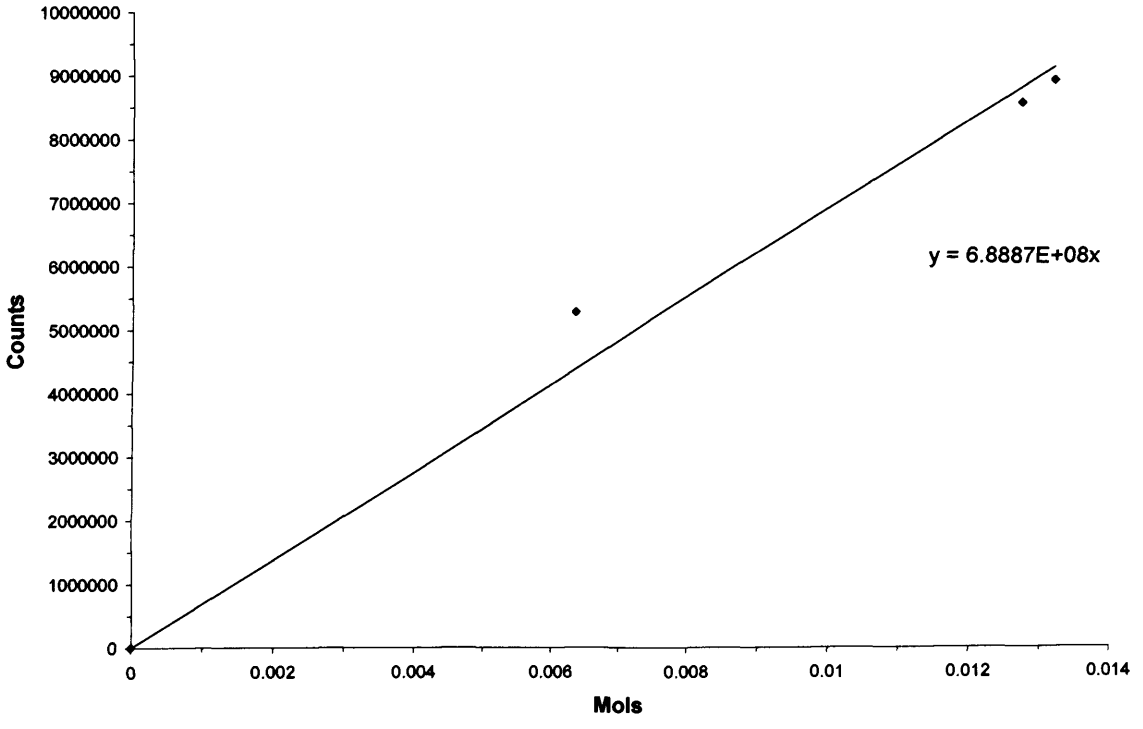

Figure 7.2 The GC calibration curve for benzaldehyde.

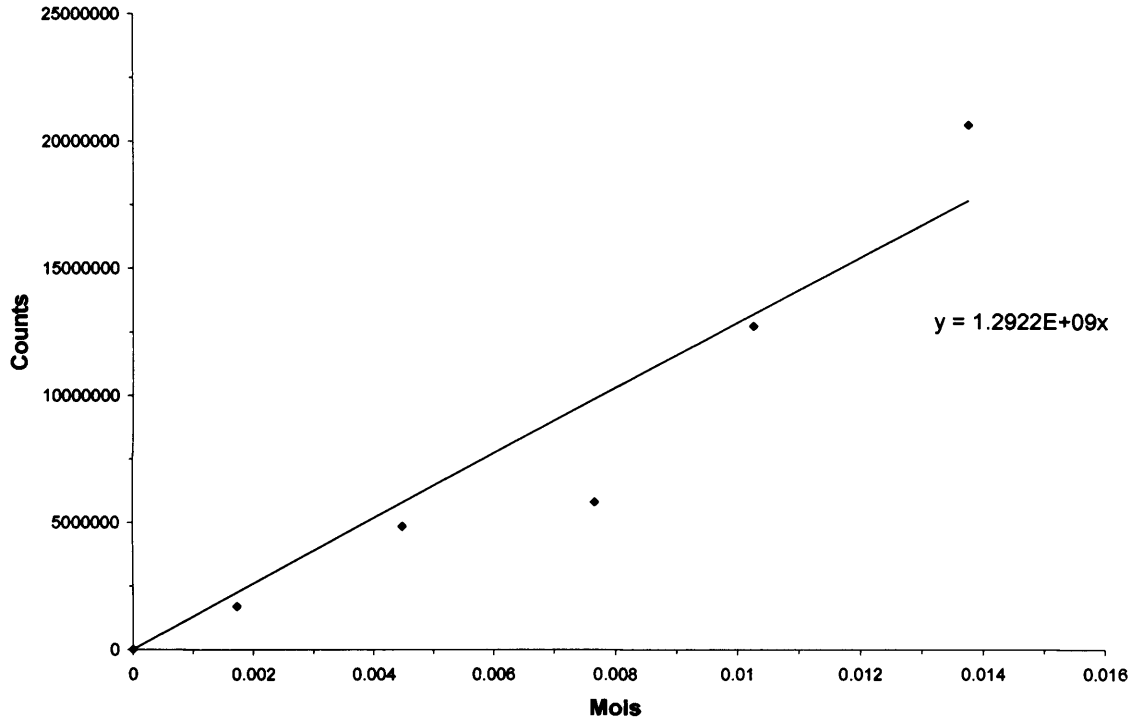

Figure 7.3 The GC calibration curve for benzylbenzoate.

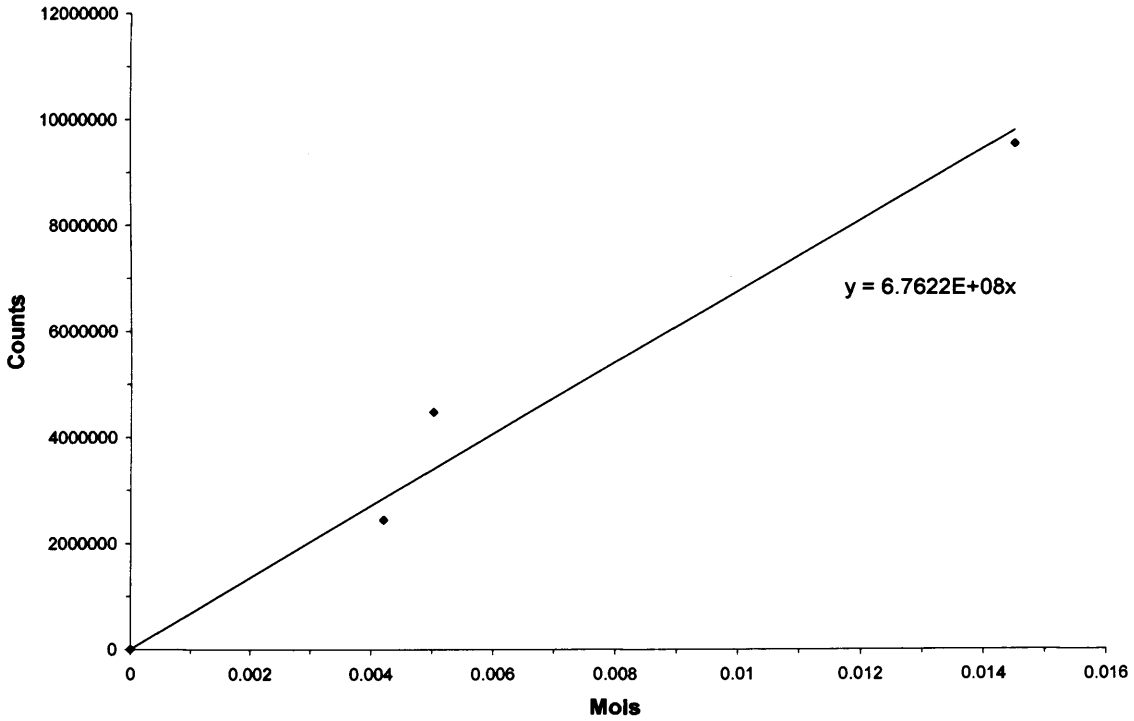

Figure 7.4 The GC calibration curve for toluene.

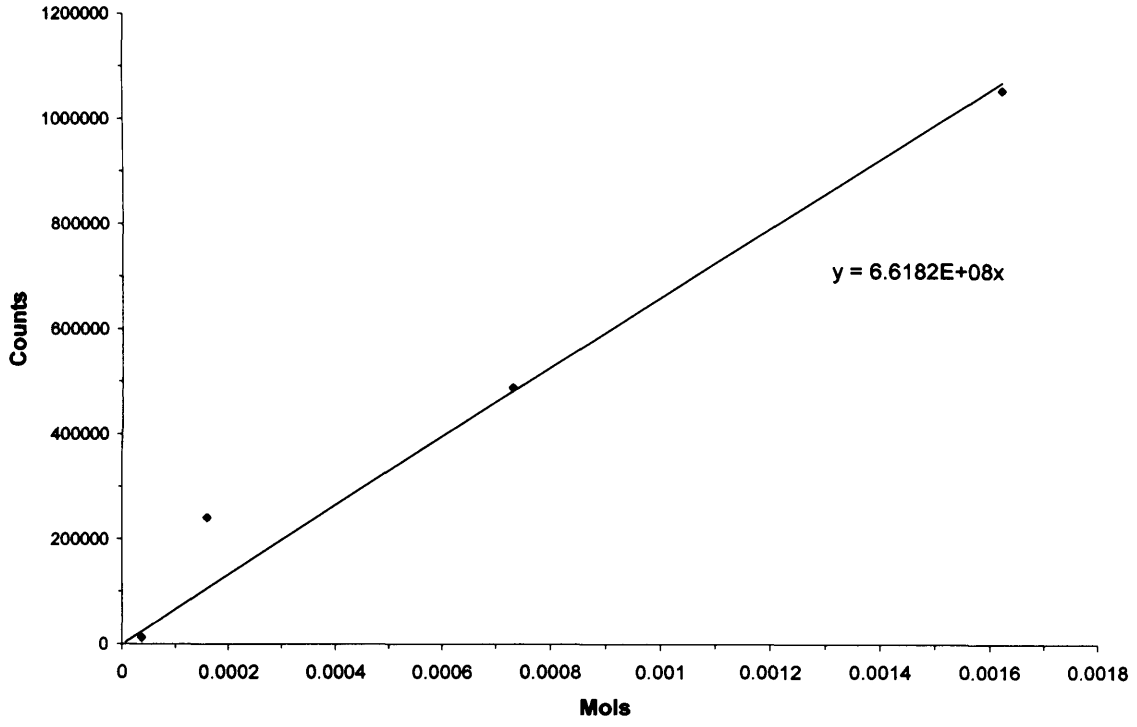

Figure 7.5 The GC calibration curve for benzoic acid.

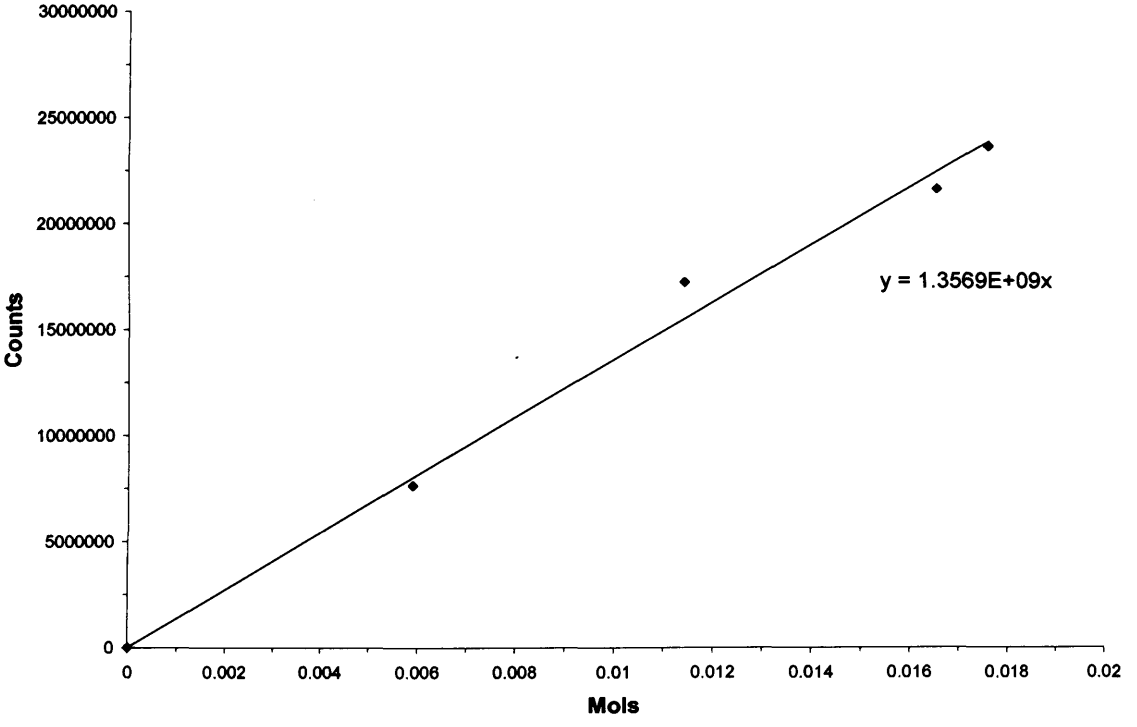

Figure 7.6 The GC calibration curve for α-pinene.

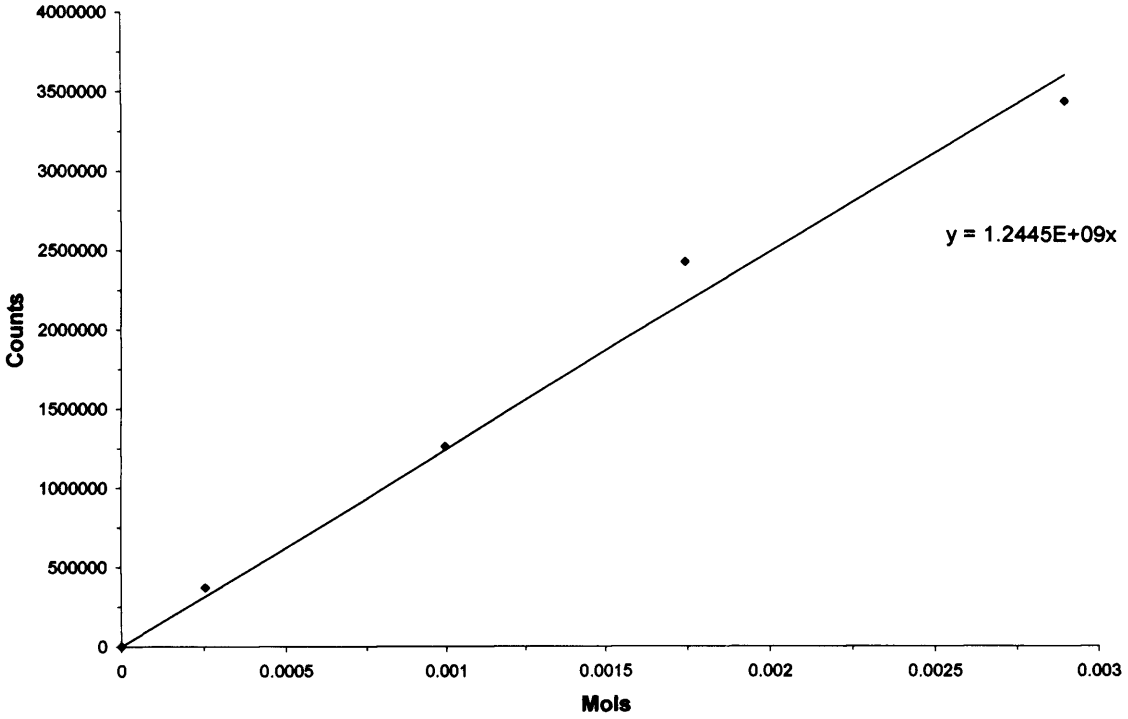

Figure 7.7 The GC calibration curve for verbenol

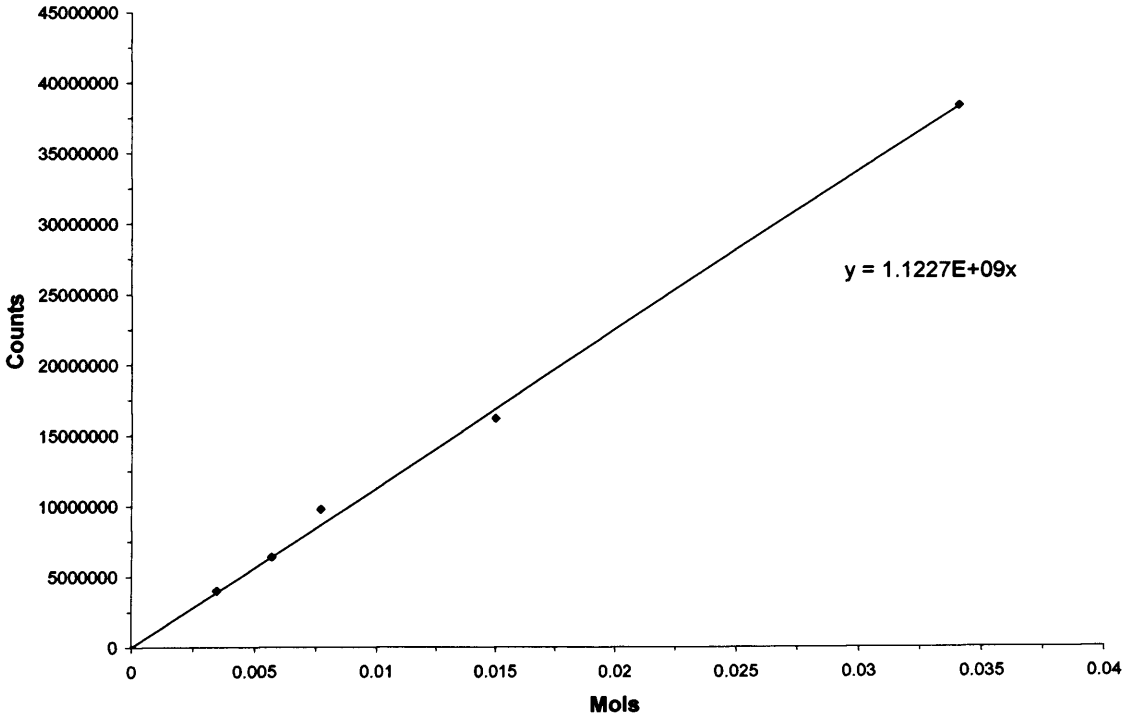

Figure 7.8 The GC calibration curve for verbenone

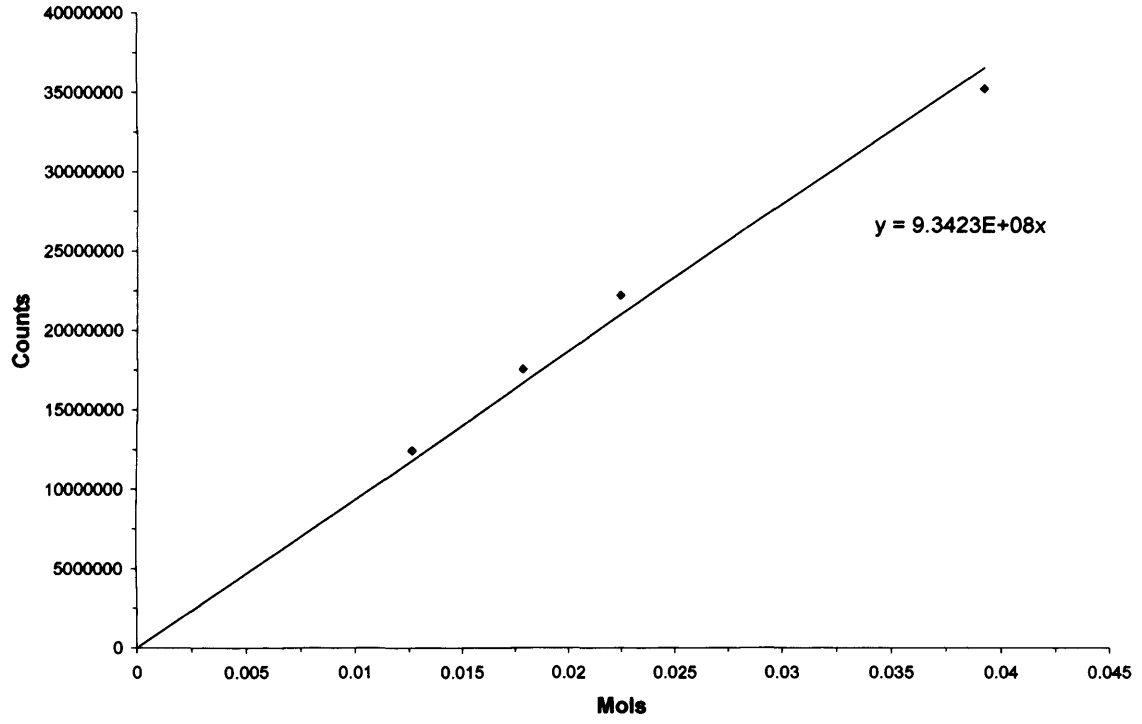

Figure 7.9 The GC calibration curve for isophorone

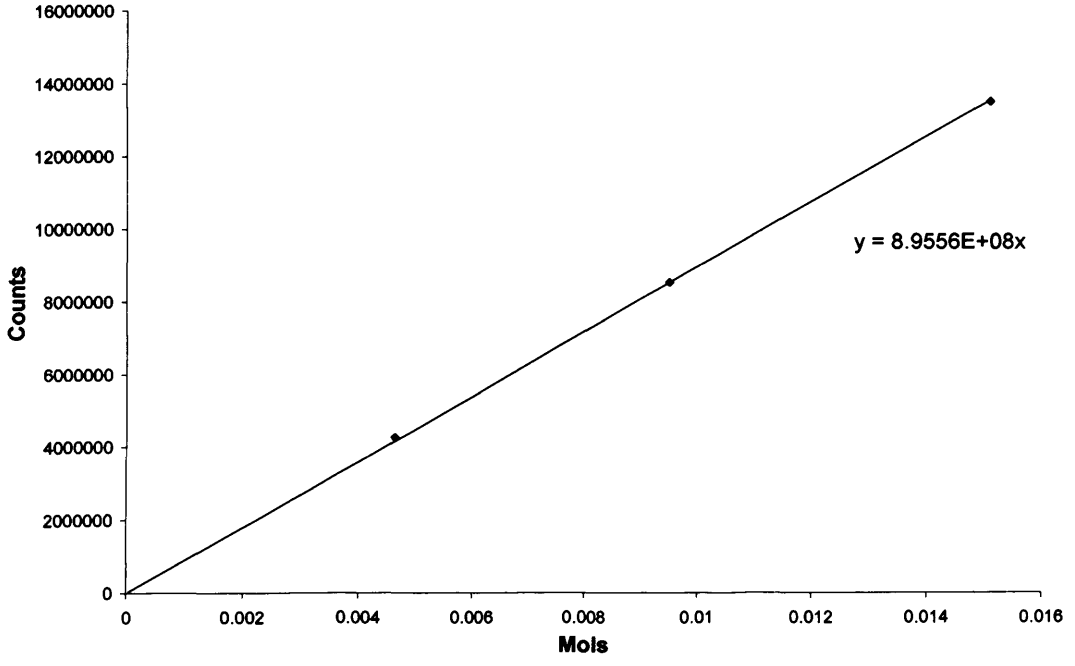

Figure 7.10 The GC calibration curve keto-isophorone

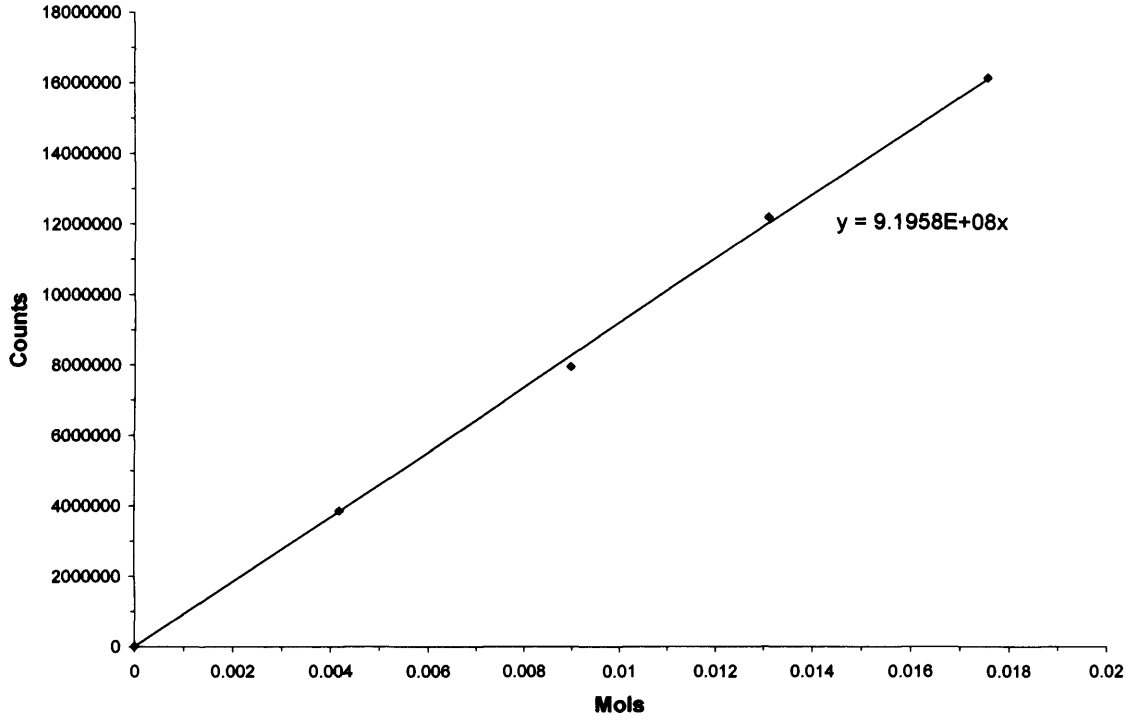

Figure 7.11 The GC calibration curve for 1-octen-3-ol

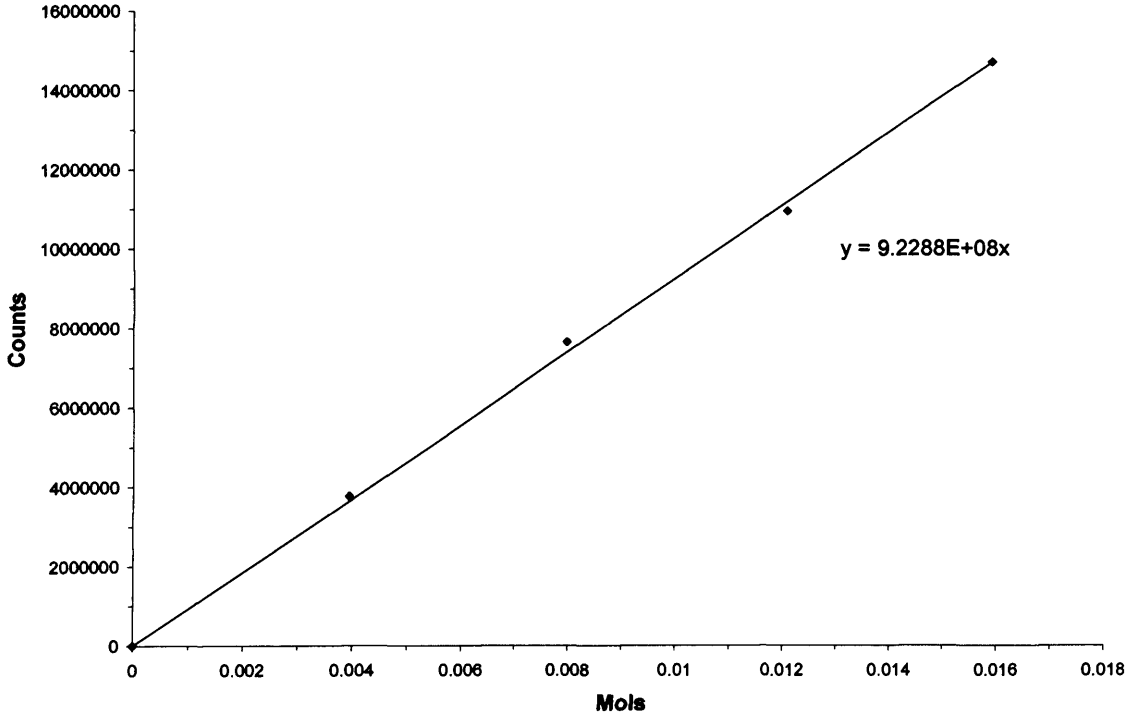

Figure 7.12 The GC calibration curve for 2-octen-1-ol

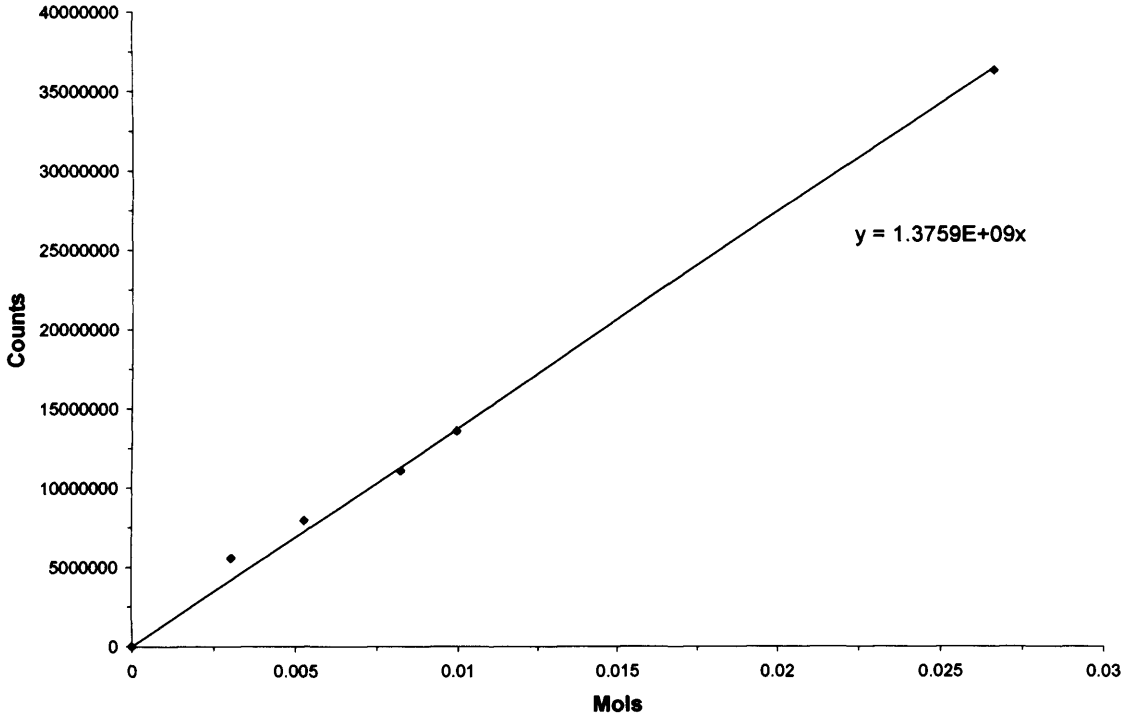

Figure 7.13 The GC calibration curve for valencene

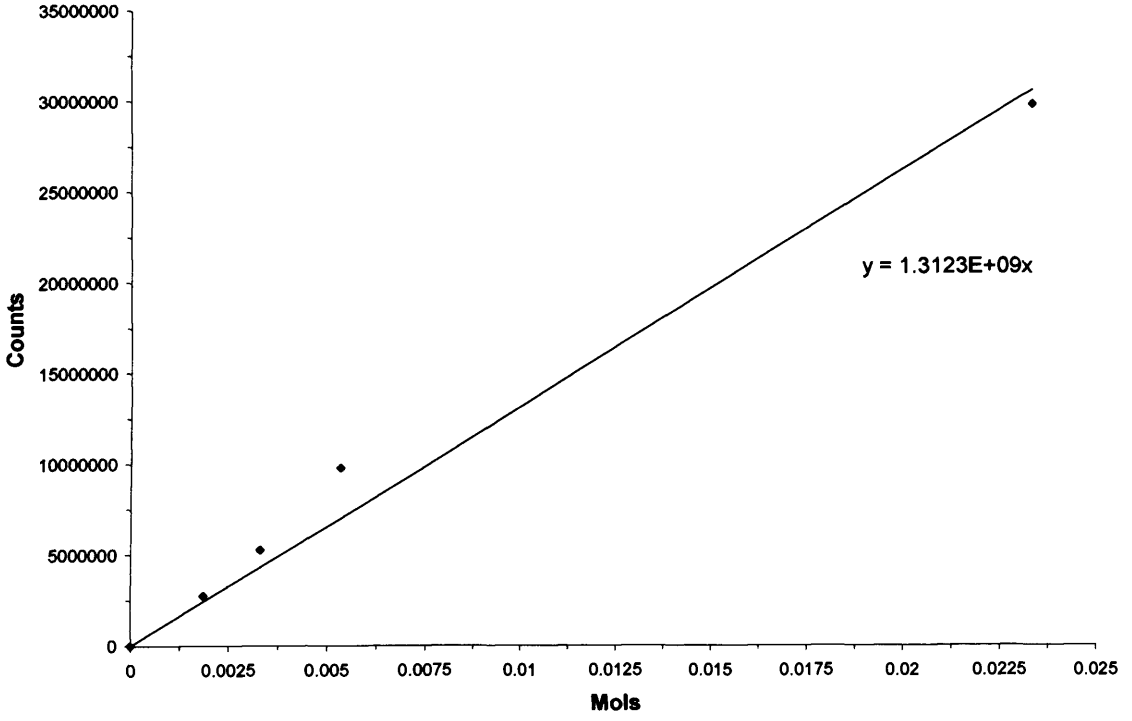

Figure 7.14 The GC calibration curve for Nootkatone